2009-9

Synthesis, Characterisation and Anti-Candida Activity of Inorganic and Organic Derivatives of 1,10-Phenanthroline

Ruth Cogan
Technological University Dublin

Synthesis, Characterisation and Anti-*Candida* Activity of Inorganic and Organic Derivatives of 1,10-Phenanthroline

A THESIS SUBMITTED TO THE DUBLIN INSTITUTE OF TECHNOLOGY IN FULFILMENT OF THE REQUIREMENTS FOR THE DEGREE OF

MASTER OF PHILOSOPHY

Ruth Cogan B.Sc.

School of Food Science and Environmental Health
Dublin Institute of Technology,
Marlborough St.,
Dublin 1

September 2009

Research Supervisors: Prof. Michael M. Devereux
Dr. Denis O' Shea

Abstract

This thesis reports results in three areas: (i) the synthesis, characterisation and biological activity of simple metal salts incorporating 1,10-phenanthroline (phen) and 1,10-phenanthroline-5,6-dione (phendione) ligands, (ii) the synthesis, characterisation and biological activity of three different organic derivatives of phendione, and (iii) the synthesis or attempted synthesis, characterisation and biological activity of phendione-amino acid conjugates.

A range of metals nitrate, chloride, sulphate and acetate (metal = Cu^{2+}, Co^{2+}, Zn^{2+}, Mn^{2+}) complexes incorporating the chelating phen and phendione ligands were synthesized and characterised. The anti-*Candida* activity of these complexes were studied and a range of these complexes were found to exhibit moderate to excellent activity.

A range of aldehydes were reacted with phendione to yield novel 1,10-pheanthroline derivatives. The anti-*Candida* activity of these derivatives were examined. Two of the four compounds produced were used to generate a range of manganese(II) (nitrate, chloride and acetate) and copper(II) (nitrate) complexes. The anti-*Candida* activity of these metal complexes were also examined. The X-ray crystal structure of $[Co(phendione)(H_2O)_4](NO_3)_2.H_2O$ was determined.

A novel L-tyrosine methyl ester compound incorporating phendione was generated and characterised. The X-ray crystal structure of PhenTyrOMe.CH_3OH was determined. The anti-*Candida* activity of this compound was found to be excellent. Attempts to react the methyl and ethyl ester of a range of other amino acids with phendione were unsuccessful, as were attempted reactions of seven simple amino acids with phendione.

Declaration

I certify that this thesis, which I now submit for examination for the award of MPhil, is entirely my own work and has not been taken from the work of others and to the extent that such work has been cited and acknowledged within the text of my work.

This thesis was prepared according to the regulations for postgraduate study by research of the Dublin Institute of Technology and has not been submitted in whole or in part for an award in any other Institute or University.

The work reported on in this thesis conforms to the principles and requirements of the Institute's guidelines for ethics in research.

The Institute has permission to keep, to lend or to copy this thesis in whole or in part, on condition that any such use of the material of the thesis is dully acknowledged.

Signature Ruth Cogan Date Sept 2009.

Ruth Cogan

Dedicated to my Mother

Julie Cogan

Acknowledgements

I would like to sincerely thank my supervisors Prof. Michael Devereux and Dr. Denis O' Shea for there excellent guidance, patient supervision and encouragement throughout the course of my research. I wish to thank Dr. Gary Henehan (Head of School, Department of Food Science and Environmental Health, Dublin Institute of Technology, Cathal Brugha St.) for his support over the last number of years. A Strand 1 grant from Dublin Institute of Technology is gratefully acknowledged.

I would also like to thank Dr. Sarah Rawe in DIT Kevin St., for her tremendous help by sharing her knowledge and expertise in the area of NMR. Also thanks to Prof. Vickie McKee for carrying out the crystallography work and Mr. Adam Coburn for undertaking all my compounds for microanalysis.

I'd like to thank all the academic and technical staff and porter staff in DIT Cathal Brugha St., especially Mr. Noel Grace and also thanks to Mr. Martin Kitson (technical staff, DIT, Kevin St.). Many thanks to the postgrads past and present that have made the last few years so interesting and enjoyable.

Finally, I would like to extend my most sincere thanks and gratitude to my parents, Thomas and Julie, for their unfailing support throughout my college years and also a special thanks to my brother Paul, sister Gillian and James.

Symbols and Abbreviations

acy	acyclovir
AIDS	Acquired immune deficiency syndrome
Aβ	Amyloid-Beta
5-NH_2-phen	5-amine-1,10-phenathroline
Å	Angstrom (10^{-10} m)
approx.	approximately
Ar	aromatic
$bdoaH_2$	benzene-1,2-dioxyacetic acid
Bipy	2,2'-bipyridyl
$mbpibH_2.6H_2O$	1,3-bis([1,10] phenanthroline-[5,6-d]-imidazol-2-yl) benzene
^{13}C NMR	carbon 13 NMR
C. albicans	*Candida albicans*
calc	calculated
cm	centimeter
δ	chemical shift in ppm
ca.	circa
norb	cis-5-norborene-endo-2,3-dicarboxylic acid
Cisplatin	cis-diaminedichloroplatinum(II)
Conc.	Concentration
coord.	coordinated

J	coupling constant in Hz
$cdoaH_2$	coumarin-6,7-dioxyacetic acid
CN	cyanide
°	Degrees
°C	degree Celsius
d_6 – DMSO	deuterated DMSO
DNA	deoxyribonucleic acid
dmp	2,9-dimethyl-1,10-phenanthroline
dnb	3,5-dinitrobenzoic acid
DMSO	dimethylsulphoxide
DMF	dimethylforamide
$DPBN.3H_2O$	4-(2,3-Dihydro-1H-1,3,7,8-tetraazacyclopenta-[I]-phenanthrene-2-yl)-Benzonitrile
dpy	di-pyrido[3,2-f:2',3'-h]quinoxaline
dppz	dipyrido[3,2-a:2',3'-c]phenazine
dpq-QX	dipyrido[3,2-f:2',3'-h]quinoxaline[2,3-b]quinoxaline ring
Me_2phen/2,9-DMP	2,9-dimethyl-1,10-phenathroline
5,6-dmp	5,6-dimethyl-1,10-phenanthroline
4,7-Me_2phen	4,7-dimethyl-1,10-phenanthroline
Ph_2phen	4,7-diphenyl-1,10-phenanthroline
2dmpeda	2,2-dimethylpentanedioic acid
3dmpeda	3,3-dimethylpentadioic acid
d	doublet

dd	doublet of doublets
dt	doublet of triplets
μ_{eff}(B.M.)	effective magnetic moment (Bohr magneton)
EtOH	ethanol
mfmp.$4H_2O$	2-(3-formylphenyl)imidazo[4,5-f]-[1,10]phenanthroline
fum	fumeric acid
g	gram
>	greater than
Hz	Hertz
HSV	Herpes Simplex Virus
N_2H_4	hydrazine
HCl	hydrochloric acid
Imda	iminodiacetic acid
IR	infra-red
IC	inhibitory concentration
LLCT	Inter-ligand charge transfer transition
isophH_2	isophthalic acid
J	Joules

K	Kelvin
mnt	maleonitriledithiolate
$MgSO_4$	magnesium sulphate
m.p.	melting point
m-subsituted	meta-substituted
5Mphen	5-methyl-1,10-phenanthroline
4-MecdoaH_2	4-methylcoumarin-6,7-dioxyacetic acid
MeOH	methanol
CH_2Cl_2	methylene chloride
MLCT	metal to ligand charge transfer
µM	micromolar
µg/ml	microgram per millilitre
mmol	milli-moles
min	minutes
MIC	minimum inhibitory concentration
m	moles
M	Molar
m	multiplet
nm	nanometer
A-498	neoplastic renal cell line
Hep G2	neoplastic hepatic cell line

5-NO_2-phen	5-nitro-1,10-phenanthroline
HNO_3	nitric acid
nda	nonanedioic acid
HK-2	non-neoplastic renal cell line
Chang	non-neoplastic hepatic cell line
NMR	nuclear magnetic resonance
Nuc	nucleophile
oda	octanedioic acid
hnc	4-oxy-3-nitro-coumarin
p-substituted	para-substituted
ppm	parts per million
$PdCl_2$	palladium chloride
%	percentage
IO_4^-	periodate ion
pen	penciclovir
Phen	1,10-phenanthroline
Phendione /pdon	1,10-phenanthroline-5,6-dione
phendiamine	1,10-phenanthroline-5,6-diamine
phanquinone	4,7-phenanthroline-5,6-dione
1,7-phen	1,7-phenanthroline
4,7-phen	4,7-phenanthroline
H_2pdol	1,10-Phenanthroline-5,6-diol

phH_2	phthalic acid
Phol	phenol
PBS	phosphate buffered saline
PC12 cells	pheochromocytoma cells
$Pt(PPh_3)_4$	platinum tetra(triphenylphosphine)
KBr	potassium bromide
^1H NMR	proton NMR
PCIP	2-(2-pyridinecarbox)imidazo[4,5f][1,10]phenanthroline
q	quartet
R.T.	room temperature
SDA	sabouraud dextrose agar
$salH_2$	salicylic acid
s	singlet
NaOH	sodium hydroxide
Na_2CO_3	sodium carbonate
$NaHCO_3$	sodium bicarbonate
H_2SO_4	sulphuric acid
Sym, asym	symmetric and asymmetric, respectively

$_{L}$-tarH_2	$_{L}$-tartaric acid
typ	2,2';6',2"-terpyridine
TMF	trimethylformamide
tda	thiodiacetat (2-) ion
td	triplet of doublets
TCC	2,3,5-triphenyltetrazolium chloride
PPh_3	triphenylphosphine
uncoord.	uncoordinated
H_2O	water

MEDICINAL DEFINITIONS

AIDS: Acquired immune deficiency syndrome or acquired immunodeficiency syndrome (AIDS) is a disease of the human immune system caused by the human immunodeficiency virus (HIV).

Aspergillosis: Aspergillosis is the name given to a wide variety of diseases caused by fungi of the genus Aspergillus.

Alzheimer's disease (AD): Is senile Dementia of the Alzheimer Type (SDAT) or simply Alzheimer's, is the most common form of dementia.

Apoptosis: Is the process of programmed cell death that may occur in multicellular organisms.

Ames testing: The Ames test is a biological assay to assess the mutagenic potential of chemical compounds.

Bacteriostatic: For example - Bacteriostatic antibiotics limit the growth of bacteria by interfering with bacterial protein production, DNA replication, or other aspects of bacterial cellular metabolism

Cancer: Is a class of diseases in which a group of cells display uncontrolled growth (division beyond the normal limits), invasion (intrusion on and destruction of adjacent tissues), and sometimes metastasis (spread to other locations in the body via lymph or blood). These three malignant properties of cancers differentiate them from benign tumors, which are self-limited, and do not invade or metastasize.

Candida albicans: Is a diploid fungus (a form of yeast) and a causal agent of opportunistic oral and genital infections in humans.

Cell culture: Is the process by which cells are grown under controlled conditions. In practice the term "cell culture" has come to refer to the culturing of cells derived from multicellular eukaryotes, especially animal cells.

Central nervous system: Is the part of the nervous system that functions to coordinate the activity of all parts of the bodies of bilaterian animals—that is, all animals more advanced than sponges or jellyfish.

Cisplatin [cis-diaminedichloroplatinum(II)]: Is a platinum-based chemotherapy drug used to treat various types of cancers, including sarcomas, some carcinomas (e.g. small cell lung cancer, and ovarian cancer), lymphomas, and germ cell tumors.

Cytochromes: In general are membrane-bound hemoproteins that contain heme groups and carry out electron transport.

Doxorubicin: Is a chemotherapy drug that is given as a treatment for many different types of cancer.

DNA: Deoxyribonucleic acid (DNA) is a nucleic acid that contains the genetic instructions used in the development and functioning of all known living organisms and some viruses. The main role of DNA molecules is the long-term storage of information.

Ergosterol: Is a sterol and is a biological precursor (a provitamin) to vitamin D_2. Ergosterol is a component of fungal cell membranes, serving the same function that cholesterol serves in animal cells. The presence of ergosterol in fungal cell membranes coupled with its absence in animal cell membranes makes it a useful target for antifungal drugs.

The **human gastrointestinal tract (GI tract)**: Is the system of organs within humans that takes in food, digests it to extract energy and nutrients, and expels the remaining matter. The major functions of the gastrointestinal tract are ingestion, digestion, absorption, and defecation.

Gram-positive bacteria: are those that are stained dark blue or violet by Gram staining. This is in contrast to Gram-negative bacteria, which cannot retain the crystal violet stain, instead taking up the counterstain and appearing red or pink. Gram-positive organisms are able to retain the crystal violet stain because of the high amount of peptidoglycan in the cell wall. Gram-positive cell walls typically lack the outer membrane found in Gram-negative bacteria.

Gram-negative bacteria: are those bacteria that do not retain crystal violet dye in the Gram staining protocol. In a Gram stain test, a counterstain is added after the crystal violet, coloring all Gram-negative bacteria with a red or pink color. The test itself is useful in classifying two distinct types of bacteria based on the structural differences of their cell walls. On the other hand, Gram-positive bacteria will retain the crystal violet dye when washed in a decolorizing solution.

Herpes Simplex Virus: Is a virus which cause infections in humans.

Hepatic cell line: liver cell line

Immunocompromised patients: Immune deficiency is a state in which the immune system's ability to fight infectious disease is compromised or entirely absent. Most cases

of immunodeficiency are acquired ("secondary") but some people are born with defects in the immune system, or primary immunodeficiency.

Ketoconazole: Is a synthetic antifungal drug used to prevent and treat skin and fungal infections, especially in immunocompromised patients such as those with AIDS.

Leukemia: Is a cancer of the blood or bone marrow and is characterized by an abnormal proliferation (production by multiplication) of blood cells, usually white blood cells (leukocytes).

Myeloid: The term myeloid suggests an origin in the bone marrow or spinal cord, or a resemblance to the marrow or spinal cord.

Mitochondrial: In cell biology, a **mitochondrion** is a membrane-enclosed organelle found in most eukaryotic cells.

Nephrotoxicity: Is a poisonous effect of some substances, both toxic chemicals and medication, on the kidney.

Neoplasm: Is an abnormal mass of tissue as a result of neoplasia.

PC12 cells (Rats PC12 pheochromocytoma cells): Is a cell line derived from a pheochromocytoma of the rat adrenal medulla. PC12 cells stop dividing and terminally differentiate when treated with nerve growth factor. This makes PC12 cells useful as a model system for neuronal differentiation.

Sterols: are an important class of organic molecules. They occur naturally in plants, animals and fungi, with the most familiar type of animal sterol being cholesterol, which has been shown to contribute to high blood pressure and heart disease.

2,3,5-triphenyltetrazolium chloride (TTC): Is a redox indicator used to differentiate between metabolically active and inactive tissues.

A **tumor**: Is the name for a swelling or lesion formed by an abnormal growth of cells (termed neoplastic). Tumor is not synonymous with cancer. A tumor can be benign, pre-malignant or malignant, whereas cancer is by definition malignant

Testicular cancer: Is cancer that develops in the testicles, a part of the male reproductive system.

TABLE OF CONTENTS

FIGURES:

TABLES:

INTRODUCTION

I. 1 INORGANIC ANTI-FUNGAL AGENTS

I.1.1 Introduction

Fungal infections have recently emerged as a growing threat to human health especially in patients with weakened or compromised immune systems[1]. Infections are often associated with complex disease entities, for example candidiasis in AIDS patients, aspergillosis in bone marrow or organ transplant patients. The yeast *Candida albicans* is considered to be the most opportunistic pathogen as it presents itself in immunocompromised patients, and over 75 % of women suffer from vaginal candidosis at some stage in their lifetime. *Candida* infections are diverse in their manifestations, varying from superficial skin problems, chronic infection of the nails, mouth, throat or vagina to frequently fatal systemic diseases that involve the lungs, heart, gastrointestinal tract, central nervous system and other organs. These infections are considered to be opportunistic in nature since some aspect of the host's defence system is impaired in some way.

The problems associated with the state-of-the-art systematic anti-fungal polyene and azole drugs (resistance and unwanted side effects) have resulted in a search for possible alternative anti-fungal agents. The strategy for the development of new anti-*Candida* agents must involve compounds which act on the *Candida* via an alternative mode of action to that of the current, purely organic, therapeutics. Due to the possibility of a difference in mode of anti-fungal activity, metal-base drugs may represent a novel group of anti-mycotic agents which could have potential applications as pharmaceuticals.

I.1.2 Phenanthrolines and their derivatives as anti-fungals

Recently, in this laboratory it has been shown that the chelating ligand 1,10-phenanthroline (phen) {Figure 1(a)} and certain types of its derivatives such as the compound 1,10-phenanthroline-5,6-dione (phendione) {Figure 1(b)} represent a novel class of anti-fungal agents. Metal free phen has shown anti-fungal activity at concentrations of between 2–5 μg/ml [2] and this activity is even greater for phendione[3, 4].

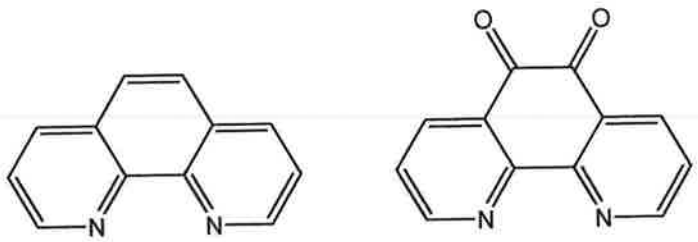

(a) (b)

Figure 1: The structure of (a) 1,10-phenanthroline and (b) 1,10-phenanthroline-5,6-dione

I.1.3 Biological activity of phenanthroline and its metal complexes

Phen, bipyridine (bipy) (Figure 2) and their substituted derivatives, both in the metal-free state and as ligands coordinated to transition metals, disturb the functioning of a wide variety of biological systems[5]. When the metal-free N,N'-chelating bases are found to be bioactive it is usually assumed that the sequestering of trace metals is involved, and that the resulting metal complexes are the active species[6].

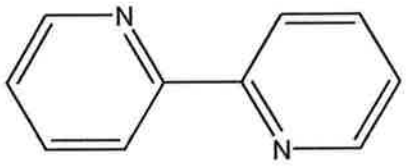

Figure 2: Structure of 2,2-bipyridine (bipy)[5]

The *in-vitro* anti-bacterial action of phen has been demonstrated on several species of bacteria. Whereas phenanthroline metal complexes can be bacteriostatic and bacteriocidal towards many Gram-positive bacteria, they are relatively ineffective against Gram-negative organisms[6].

Whereas *m*- and *p*- substituted phenanthrolines were less effective than phen at preventing fungal growth, 2,9-dimethyl-1,10-phenanthroline (Me_2phen) was the most potent inhibitor. Recent *in-vitro* studies have shown that although bipy and its metal complexes did not suppress the growth of clinical isolates of *Candida* species, dilute aqueous solutions of phen and its Cu^{2+} and Mn^{2+} complexes were extremely toxic to the cells[6,7,8].

The synthesis of platinum complexes containing an aromatic di-imine phen or Me_2phen and anti-viral acyclovir (acy) guanosine–type ligand {Figure 3(a)} or penciclovir (pen) {(Figure 3(b)} has been reported by Margiotta et al[9].

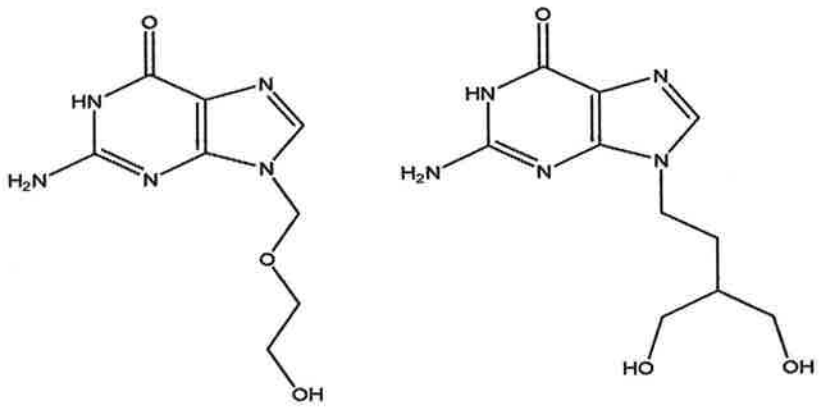

(a) (b)

Figure 3: Structure of acyclovir (a) and penciclovir (b)[9]

Phen and Me_2phen were used in the synthesis of these complexes for their ability to yield stable platinum complexes and creating the possibility of DNA intercalation of the aromatic segment of either ligand. Once synthesized, complexes $[Pt(Me_2phen)(acy)_2]I_2$ **(1)**, $[Pt(Me_2phen)(pen)_2](NO_3)_2$ **(2)**, $[Pt(phen)(acy)_2](NO_3)_2$ **(3)** and $[Pt(phen)(pen)_2](NO_3)_2$ **(4)** were analysed for anti-viral activity against different strains of Herpes Simplex Virus (HSV). As shown in Table 1, the anti-viral activity of complexes **(1 & 3)** and **(2 & 4)** were investigated against different strains of HSV in E_6SM cell cultures and were compared to parent compounds acy and pen[9].

Table 1: Anti-viral activity of complexes **1, 2, 3** and **4** against different strains of HSV in E_6SM cell cultures[9]

Complex	MIC (μM)			
	HSV-1 (KOS)	HSV-2 (G)	HSV-1 TK⁻ KOS-ACV^r	HSV-1 TK⁻ VMW1837
Acyclovir	0.341	0.341	213	2.84
Penciclovir	0.379	0.126	78.9	0.63
1	0.346	0.0693	>72	0.577
2	0.371	0.124	>15	0.371
3	0.67	0.134	>84	2.02
4	0.38	0.38	80	1.91

As shown in Table 1, complex **1** exhibits slightly better activity than reference acy at 0.341 μM against HSV-1 (KOS) whereas complex **3** shows slightly worse activity at 0.67 μM. The presence of the phen ligand had a range of effects on the anti-viral properties of the complexes tested.

It has previously been shown that a range of carboxylate and dicarboxylate complexes incorporating transition metal centres and the N,N'- donor ligand phen are potent *in-vitro* inhibitors of the growth of *Candida albicans*[10].

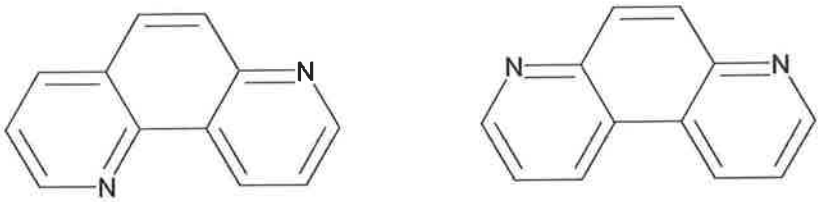

(a) (b)

Figure 4: The structures of (a) 1,7- phenanthroline; (b) 4,7-phenanthroline

Experiments with 1,7-phenanthroline and 4,7-phenanthroline {Figures 4(a) and 4(b)} demonstrated that ligands without chelating ability appeared to form less potent anti-fungal agents than those incorporating the chelating phen.

Table 2 compares the performance of the highly active metal-free phen ligand and the inactive metal-free 1,7- and 4,7-phenanthroline ligands. Furthermore, Cu^{2+} and Mn^{2+} complexes of 1,7-phen displayed only marginal activity[6].

Table 2: Anti-*Candida* activity of $[M(phen)_n](CH_3CO_2)_2$, $[M(1,7\text{-phen})n](CH_3CO_2)_2$, ($M = Mn^{2+}$, Cu^{2+}) and metal free phenanthroline ligands[6]

Complexes	**% Cell Kill 20 µg/ml**
$[Mn(phen)_2](CH_3CO_2)_2].4H_2O$	98
$[Cu(phen)(CH_3CO_2)_2].H_2O$	92
$[Mn(1,7\text{-phen})_2(CH_3CO_2)_2]$	17
$[Cu(1,7\text{-phen})(CH_3CO_2)_2].2H_2O$	11
1,7-phen	1
4,7-phen	7
phen	100

As shown in Table 2, both the uncoordinated 1,7-phen and its metal complexes were found to be ineffective against the pathogen. Both phen complexes exhibit discrete anti-*Candida* activity causing 98 % and 92 % inhibition of cell kill at 20 µg/ml. Significantly the "metal free" phen itself shows the greatest activity causing 100 % cell kill at a concentration of 20 µg/ml[10].

Although all of the phenanthroline isomers can coordinate to a metal centre, phen is the only ligand capable of actually chelating the metal and forming an extremely stable metal-phen entity in solution. Also when phen is replaced by the structurally similar N,N'-donor ligand bipy (Figure 2) complexes devoid of anti-*Candida* activity are obtained[10].

Recently, Devereux et al.[11] have shown that a range of cobalt, copper, manganese and silver complexes containing a carboxylic acid and the N,N'-donor ligand phen inhibit the growth of *Candida albicans* with potency comparable to the state-of-the-art commercial azole or polyene drugs[11]. Early studies have revealed that phen complexes prove to have a difference in the mode of action to the prescription drugs.

The synthesis and structural characterization of four novel Mn^{2+} complexes derived from 2,2-dimethylpentanedioic acid (2dmpeda) and 3,3-dimethylpentanedioic acid (3dmepda) incorporating either phen or bipy has been reported by Devereux et al[11]. Reaction of 2dmpeda and 3dmepda with $Mn(CH_3COO)_2.4H_2O$ yielded the complexes $[Mn(2dmpeda)].1.5H_2O$ and $[Mn(3dmepda)].H_2O$ and the reaction of $[Mn(2dmpeda)].1.5H_2O$ with bipy or phen resulted in the formation of $[Mn(2dmepda)_2(bipy)].H_2O$ and [Mn(2dmepda)(phen)]. Similar reactions generated complexes $[Mn_2(3dmepda)_2(bipy)_3].5H_2O$ and $[Mn(3dmepda)(phen)_2].7.25H_2O$[11].

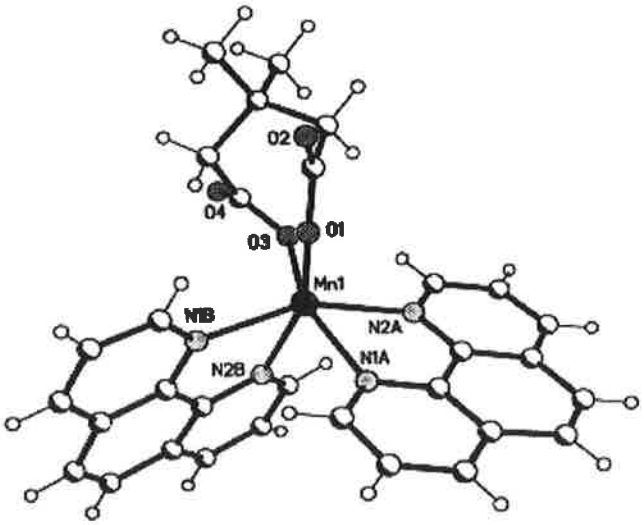

Figure 5: X-Ray crystal structure of $[Mn(3dmepda)(phen)_2]$[11]

In $[Mn(3dmepda)(phen)_2].7.25H_2O$ the Mn atom is ligated by four nitrogen atoms from the two chelating phen molecules and two oxygen atoms one from each of the carboxylate moieties of the $3dmepda^{2-}$ ligands (Figure 5)[11].

The anti-fungal activity of all of the novel complexes was compared to that of the commercial azole drug Ketoconazole (Table 3)[11].

Table 3: Anti-fungal activity of Mn^{2+} complexes of 2dmpeda and 3dmepda tested at different concentrations [11]

Test Compound	% Cell Kill		
	10 µg/ml	5 µg/ml	2.5 µg/ml
Control	0	0	0
Ketoconazole	75	74	53
$[Mn(2dmpeda)].1.5H_2O$	0	-	-
$[Mn(3dmepda)].H_2O$	0	-	-
$[Mn(2dmepda)_2(bipy)].H_2O$	3	-	-
[Mn(2dmepda)(phen)]	68	57	40
$[Mn_2(3dmepda)_2(bipy)_3].5H_2O$	5	-	-
$[Mn(3dmepda)(phen)_2].7.25H_2O$	70	84	28
2dmpeda	0	-	-
3dmepda	0	-	-
phen	89	86	78
bipy	0	-	-

As shown in Table 3, both the uncoordinated bipy and its metal complexes were found to be ineffective against the pathogen. Both phen complexes exhibit discrete anti-*Candida* activity causing 68 % and 70 % inhibition of cell growth at 10 µg/ml falling to 40 % and 28 % respectively at 2.5 µg/ml. Significantly the "metal free" phen itself shows the greatest activity causing 89 % inhibition of cell growth at a concentration of 10 µg/ml. The efficacy of both phen complexes were comparable to the azole drug Ketoconazole at 10 µg/ml and as the concentration lowered the anti-fungal activity of the phen complexes decreased significantly in comparison to the Ketoconazole drug[11].

In 1999, this research group reported the fugitoxic activity for a range of Co^{2+}, Mn^{2+} and Cu^{2+} species containing the carboxylate ligands, octanedioic acid (oda), nonanedioic

acid (nda), salicylic acid ($salH_2$) and *cis*-5-norborene-endo-2,3-dicarboxylic acid (norb) along with phen[12].

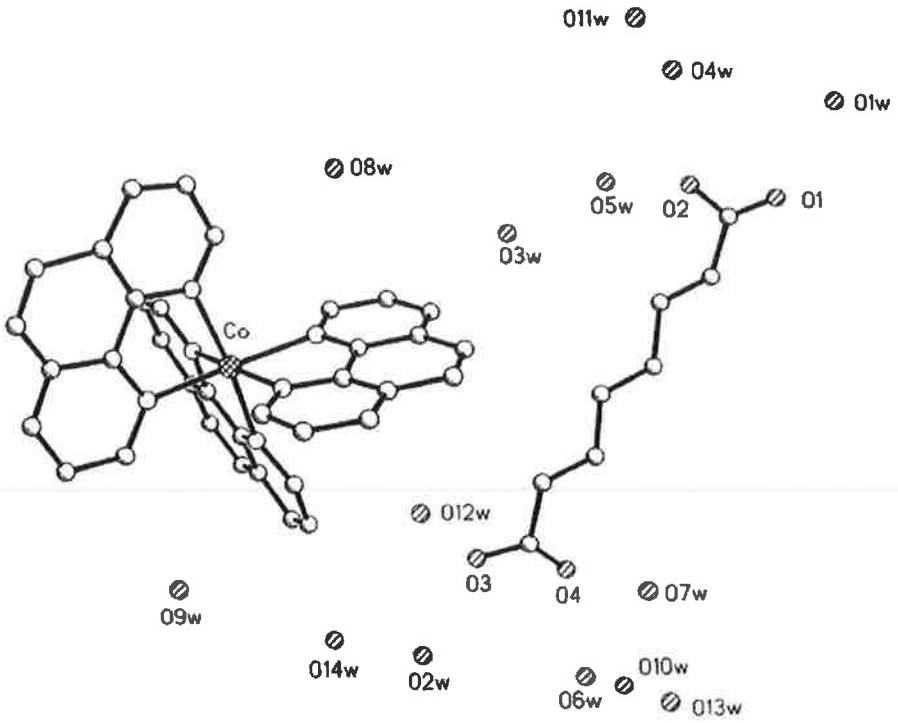

Figure 6: X-Ray crystal structure of $[Co(phen)_3].oda.14H_2O$[12]

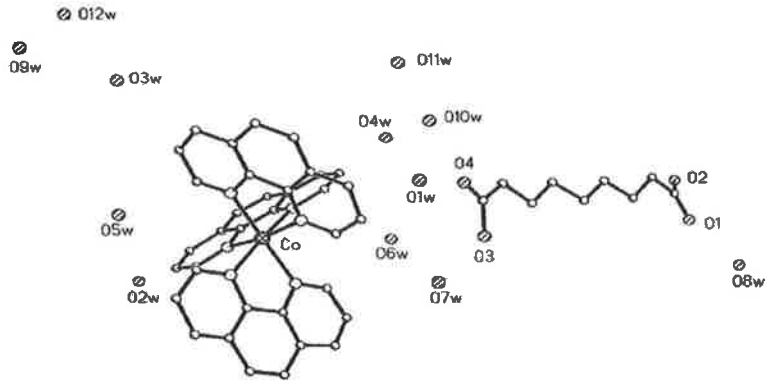

Figure 7: X-Ray crystal structure of $[Co(phen)_3].nda.11.5H_2O$[12]

The cobalt(II) complexes $[Co(phen)_3].oda.14H_2O$ (Figure 6) and $[Co(phen)_3].nda.11.5H_2O$ (Figure 7) along with cobalt(II) acid complexes $[Co(oda)].3H_2O$ and $[Co(nda)].4H_2O$, free acids $odaH_2$ and $ndaH_2$ and metal free phen were tested for their ability to inhibit the growth of three clinical isolates of *Candida albicans* (Table 4)[12].

Table 4: Anti-fungal activity of Co^{2+} complexes of $odaH_2$, $ndaH_2$ and metal free phen tested at a concentration of 20 ug/ml[12]

Test Complex	% Cell Kill		
	Isolate 1	Isolate 2	Isolate 3
Control	0	0	0
$odaH_2$	0	2	7
$ndaH_2$	0	12	13
phen	88	86	85
$[Co(oda)].3H_2O$	44	42	40
$[Co(nda)].4H_2O$	47	32	41
$[Co(phen)_3].oda.14H_2O$	62	60	55
$[Co(phen)_3].nda.11.5H_2O$	55	64	46

As shown in Table 4, the carboxylate ligands, oda and nda, as expected showed little or no anti-*Candida* activity in isolates 1-3. $[Co(oda)].3H_2O$ and $[Co(nda)].4H_2O$ showed moderate activity against all three isolates. $[Co(phen)_3].oda.14H_2O$ and $[Co(phen)_3].nda.11.5H_2O$ showed a marked improvement of anti-*Candida* activity on these compounds. Significantly, the "metal free" phen itself showed the greatest activity causing 88 % inhibition of cell growth in isolate[12].

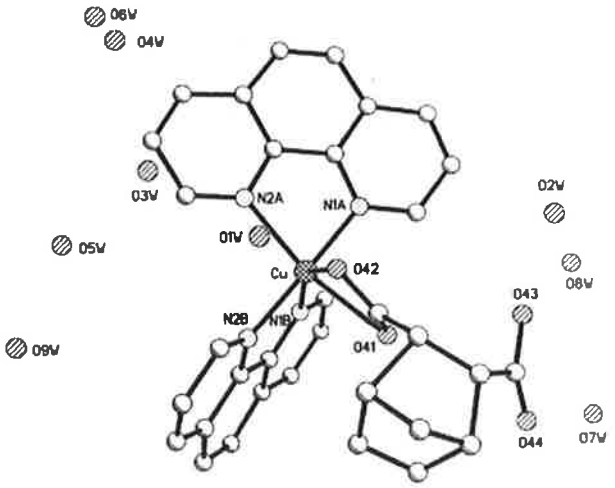

Figure 8: X-Ray crystal structure of $[Cu(phen)_2(norb)].6.5H_2O$ [8]

$[Cu(phen)_2(norb)].6.5H_2O$ (Figure 8) along with its free ligands, were tested for their anti-*Candida* activity against three isolates of *Candida albicans* (Table 5). Of the free ligands only phen showed very high anti-*Candida* activity, while norb showed limited activity. When the activity of $[Cu(norb)].H_2O$ was tested, slight improvement was shown. $[Cu(phen)_2(norb)].6.5H_2O$ was shown to exhibit remarkable anti-*Candida* activity against all three isolates[8].

When $[Cu(sal)(bipy)]C_2H_5OH.H_2O$ along with its free ligands, was tested for anti-*Candida* activity against the three isolates of *Candida albicans* (Table 5), salicylic acid showed limited anti-microbial activity, $[Cu(salH)_2(H_2O)_2].0.5H_2O$ showed a slight improvement, while $[Cu(sal)(bipy)]C_2H_5OH.H_2O$ showed no increase in activity from that of the free ligand[8].

Table 5: Anti-fungal activity of compounds tested at a concentration of 20 µg/ml [8]

Test Complex	% Cell Kill		
	Isolate 1	Isolate 2	Isolate 3
Control	0	0	0
$NorbH_2$	18	0	2
$SalH_2$	7	0	2
phen	88	86	85
bipy	15	20	0
$[Cu(norb)].H_2O$	34	21	15
$[Cu(phen)_2(norb)].6.5H_2O$	88	75	85
$[Cu(salH)_2(H_2O)_2].0.5H_2O$	6	0	5
$[Cu(sal)(bipy)]C_2H_5OH.H_2O$	14	0	14

Fungitoxicity investigations of Mn^{2+} fumarate complexes incorporating phen and bipy were reported by this group in 2000[13]. Of the complexes tested the bipy complex $[Mn(fum)(bipy)(H_2O)]_n$ (Figure 9) was inactive while, $[Mn(phen)_2(H_2O)_2](fum).4H_2O$ (Figure 10) showed significant activity at 10 µg/ml and all the rest are shown in Table 6[13].

Table 6: Anti-fungal activity of compounds tested at a concentration of 10 µg/ml[13]

Test Complex	% Cell Kill
Control	0
Fumeric acid	0
phen	77
bipy	0
[Mn(fum)]	2
$[Mn(fum)(bipy)(H_2O)]_n$	0
$[Mn(phen)_2(H_2O)_2](fum).4H_2O$	67

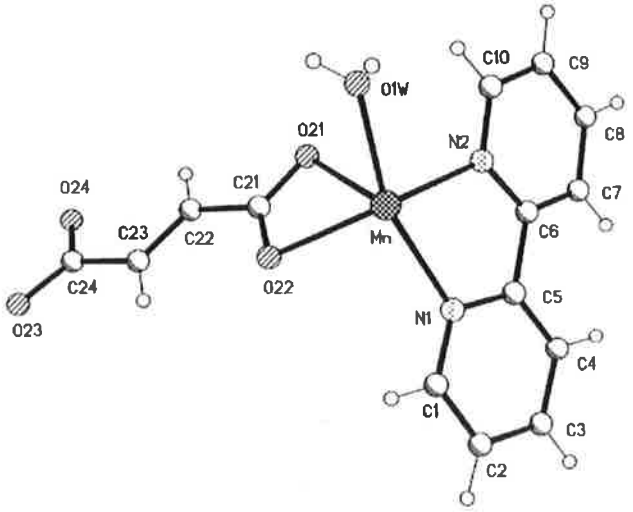

Figure 9: The X-Ray crystal structure of $[Mn(fum)(bipy)(H_2O)]_n$[13]

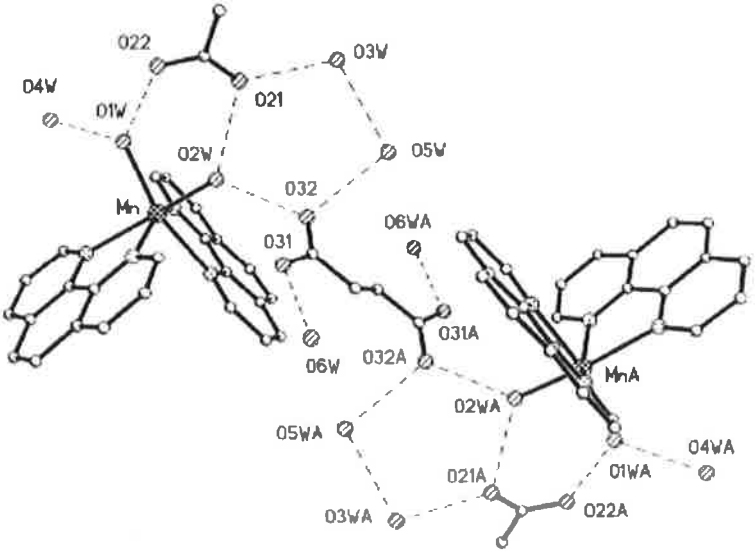

Figure 10: Structure of $[Mn(phen)_2(H_2O)_2](fum).4H_2O$ with hydrogen bonding indicated[13]

Creaven et al.[14] reported synthesis and structural characterization of two novel coumarin-based ligands, coumarin-6,7-dioxyacetic acid ($cdoaH_2$) and 4-methylcoumarin-6,7-dioxyacetic acid (4-$MecdoaH_2$). Reaction of $cdoaH_2$ and

4-MecdoaH_2 with copper(II) acetate yielded complexes [Cu(cdoa)$(H_2O)_2$].1.5H_2O and [Cu(4-Mecdoa)$(H_2O)_2$]. By reacting complexes [Cu(cdoa)$(H_2O)_2$].1.5H_2O and [Cu(4-Mecdoa)$(H_2O)_2$] with phen in ethanol, [Cu(cdoa)$(phen)_2$].8.8H_2O and [Cu(4-Mecdoa)$(phen)_2$].13H_2O were synthesized[14].

The X-ray crystal structure of both [Cu(cdoa)$(phen)_2$].8.8H_2O and [Cu(4-Mecdoa)$(phen)_2$].13H_2O confirmed that the Cu atom is ligated by four nitrogen atoms from the two chelating phen molecules and one oxygen atom from a single carboxylate oxygen of the dicarboxylate ligand (Figures 11 and 12)[14].

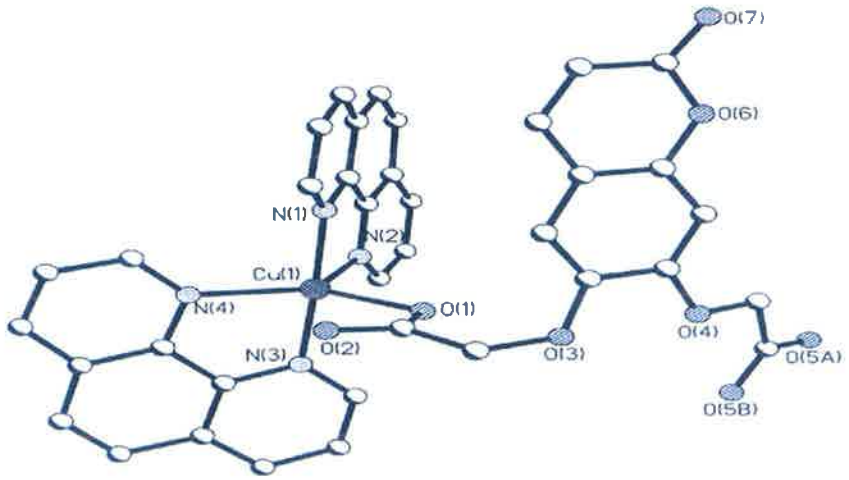

Figure 11: X-Ray crystal structure of [Cu(cdoa)$(phen)_2$].8.8H_2O[14]

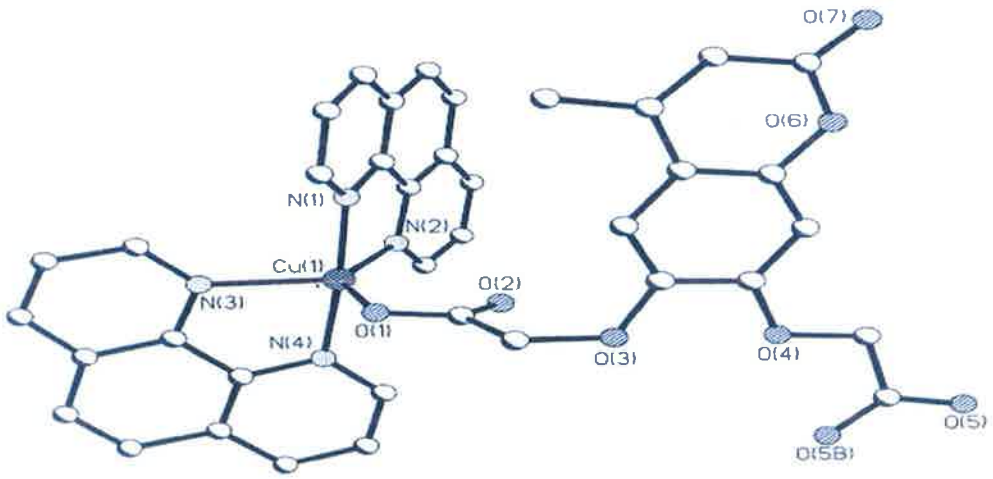

Figure 12: X-Ray crystal structure of $[Cu(4\text{-Mecdoa})(phen)_2].13H_2O$[14]

The anti-*Candida* activity of all complexes was assessed as shown in Table 7.

Table 7: Anti-*Candida* activity of test compounds[14]

Test Compound	MIC_{80} (μM)
$cdoaH_2$	87.74
4-$MecdoaH_2$	98.5
$[Cu(cdoa)(H_2O)_2].1.5H_2O$	>500
$[Cu(4\text{-Mecdoa})(H_2O)_2]$	>500
$[Cu(cdoa)(phen)_2].8.8H_2O$	22.2
$[Cu(4\text{-Mecdoa})(phen)_2].13H_2O$	42.7
Phen	16.7

As shown in Table 7[14], phen - containing Cu^{2+} complexes $[Cu(cdoa)(phen)_2].8.8H_2O$ and $[Cu(4\text{-Mecdoa})(phen)_2].13H_2O$ were found to have significantly lower MIC_{80} values than the metal free ligands $cdoaH_2$ and 4-$MecdoaH_2$ but are not as active as metal-free phen which shows the best activity at 16.7 μM. Furthermore, when the fungal

cells were exposed to complexes $[Cu(cdoa)(phen)_2].8.8H_2O$ and $[Cu(4\text{-}Mecdoa)(phen)_2].13H_2O$ certain biological activity occurred as respiration was inhibited, levels of ergosterol in the membrane were reduced and the cytochrome content was changed. From these findings, it was suggested that the anti-fungal effect of these complexes is due to the disruption of mitochondrial function[14].

Devereux et al[15]. reported the synthesis and structural characterization of three novel Mn^{2+} complexes derived from either phthalic or isophthalic acid and incorporating the phen ligand. Mn^{2+} acetate reacted smoothly with phthalic acid (phH_2) to produce $[Mn(ph)].0.5H_2O$. Reaction of $[Mn(ph)].0.5H_2O$ with phen in ethanol yielded $[Mn(ph)(phen)].2H_2O$ and $[Mn(ph)(phen)_2(H_2O)].4H_2O$. In $[Mn(ph)(phen)_2(H_2O)].4H_2O$ (Figure 13) the two phen ligands are co-ordinated to the manganese atom in a bidentate mode, while the phthalate anion is bound to the metal through only one carboxylate oxygen, by with one bound water molecule[15].

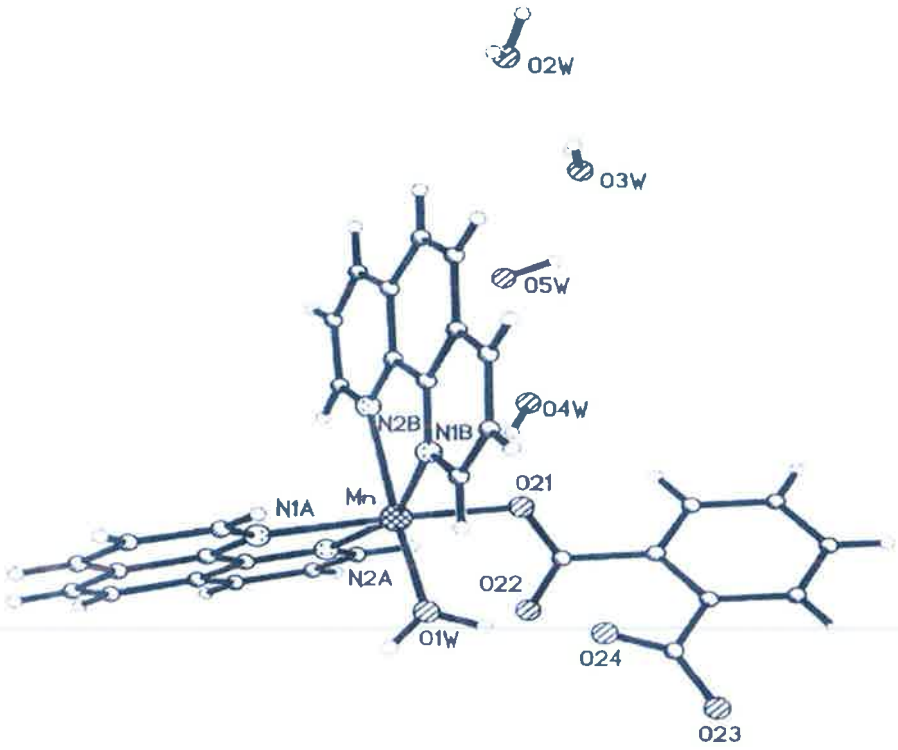

Figure 13: X-Ray crystal structure of $[Mn(ph)(phen)_2(H_2O)].4H_2O$[15]

Reaction of isophthalic acid ($isophH_2$) with Mn^{2+} acetate resulted in the formation of $[Mn(isoph).2H_2O]$. The addition of the N,N'-donor ligands phen or bipy to $[Mn(isoph)].2H_2O$ led to the formation of $[Mn_2(isoph)_2(phen)_3].4H_2O$, $[Mn(phen)_2(H_2O)_2]_2(isoph)_2(phen).12H_2O$ and $\{[Mn(isoph)(bipy)]_4.2.75bipy\}_n$. As shown in Figure 14, $[Mn(phen)_2(H_2O)_2]_2(isoph)_2(phen).12H_2O$ consists of two independent $[Mn(phen)_2(H_2O)_2]^{2+}$ cations, two independent isophthalate anions $[isoph]^-$, a non-coordinated phenanthroline molecule and twelve uncoordinated lattice water molecules. As for $\{[Mn(isoph)(bipy)]_4.2.75bipy\}_n$ (Figure 15) each manganese ion is coordinated to one bipy group, one bidentate carboxylate group and two further oxygen donors, one from each of two 1,3-carboxylate bridges[15].

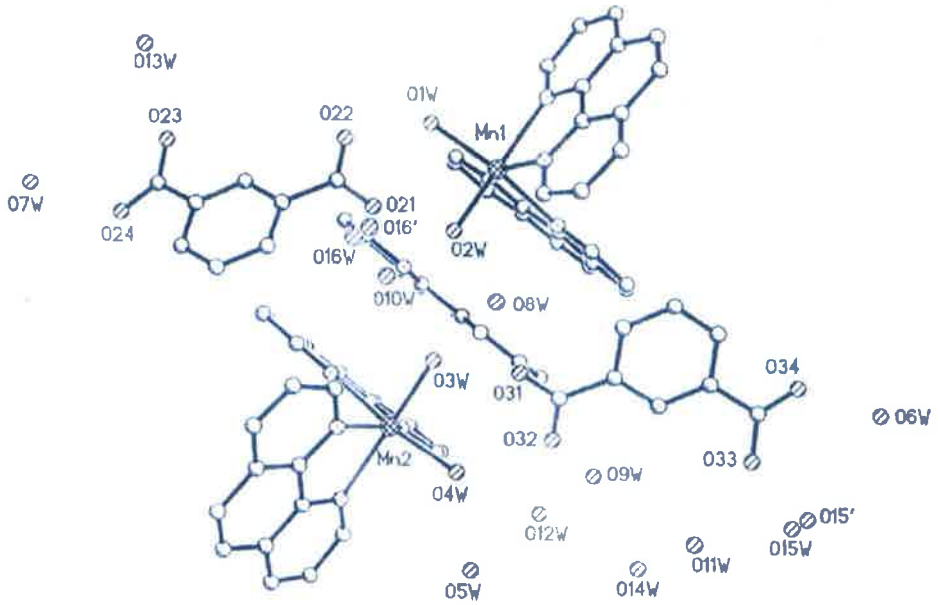

Figure 14: X-Ray crystal structure of $[Mn(phen)_2(H_2O)_2]_2(isoph)_2(phen).12H_2O$[15]

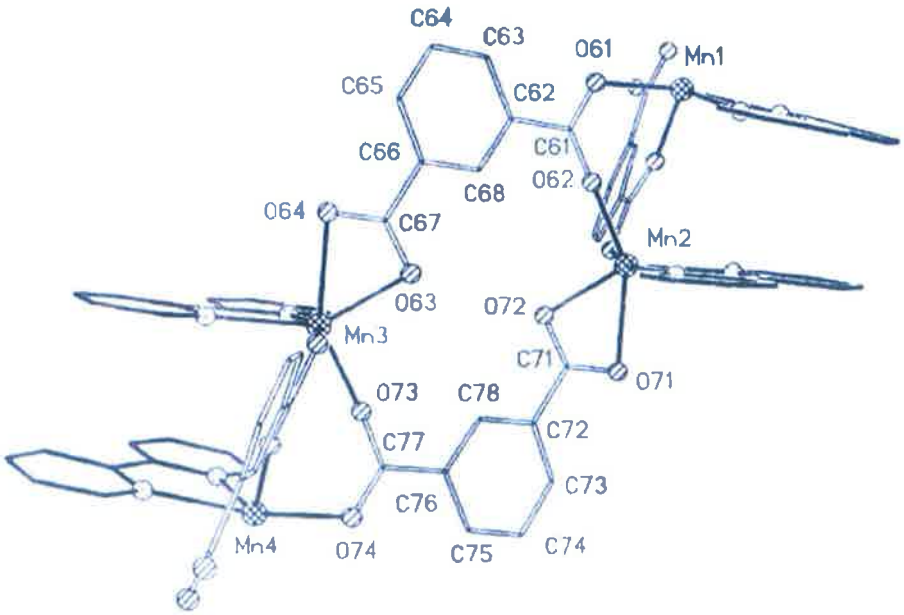

Figure 15: The structure of $[Mn(isoph)(bipy)]_4$ component of complex $\{[Mn(isoph)(bipy)]_4.2.75bipy\}_n$[15]

All novel complexes, metal free ligands and simple manganese salts were tested for their ability to inhibit the growth of *Candida albicans* at a concentration of 10 ug/ml as shown in Table 8.

Table 8: Anti-*Candida* activity of complexes $[Mn(ph)].0.5H_2O$, $[Mn(ph)(phen)].2H_2O$, $[Mn(ph)(phen)_2(H_2O)].4H_2O$, $[Mn(isoph)].2H_2O$, $[Mn_2(isoph)_2(phen)_3].4H_2O$, $[Mn(phen)_2(H_2O)_2]_2(isoph)_2(phen).12H_2O$, $\{[Mn(isoph)(bipy)]_4.2.75bipy\}_n$ and their starting materials[15]

Test Compound	% Cell Kill
	10 ug/ml
Control	0
Phthalic acid	0
Isophthalic acid	0
phen	77
bipy	0
$[Mn(ph)].0.5H_2O$	0
$[Mn(ph)(phen)].2H_2O$	81
$[Mn(ph)(phen)_2(H_2O)].4H_2O$	70
$[Mn(isoph)].2H_2O$	0
$[Mn_2(isoph)_2(phen)_3].4H_2O$	74
$[Mn(phen)_2(H_2O)_2]_2(isoph)_2(phen)].12H_2O$	72
$\{[Mn(isoph)(bipy)]_4.2.75bipy\}_n$	10

"Metal free" phen showed very high anti-*Candida* activity and was surpassed by the activity of the phthalate phen complex $[Mn(ph)(phen)].2H_2O$.

In conclusion, it would appear that phthalic acid and isophthalic acid whether coordinated or uncoordinated to manganese do not posses any anti-*Candida* properties. The N,N'- donor ligand bipyridine does not improve the activity of the isophthalate

complex. The phen molecule is a potent anti-*Candida* agent and upon reaction with the phthalate and isophthalate complexes it yielded compounds with comparable fungitoxic activity.

In 1999, McCann et al.[16] reported the synthesis and structural characterization of three novel Co^{2+}, Mn^{2+} and Cu^{2+} complexes derived from benzene-1,2-dioxyacetic acid ($bdoaH_2$) and incorporating the phen ligand. $[Co(CH_3CO_2)_2].4H_2O$ reacts with $bdoaH_2$ to give the Co^{2+} complexes $[Co(bdoa)(H_2O)_3].H_2O$ **(1a)** and $[Co(bdoa)(H_2O)_3].3.5H_2O$ **(1b)** (Figure 16)[16].

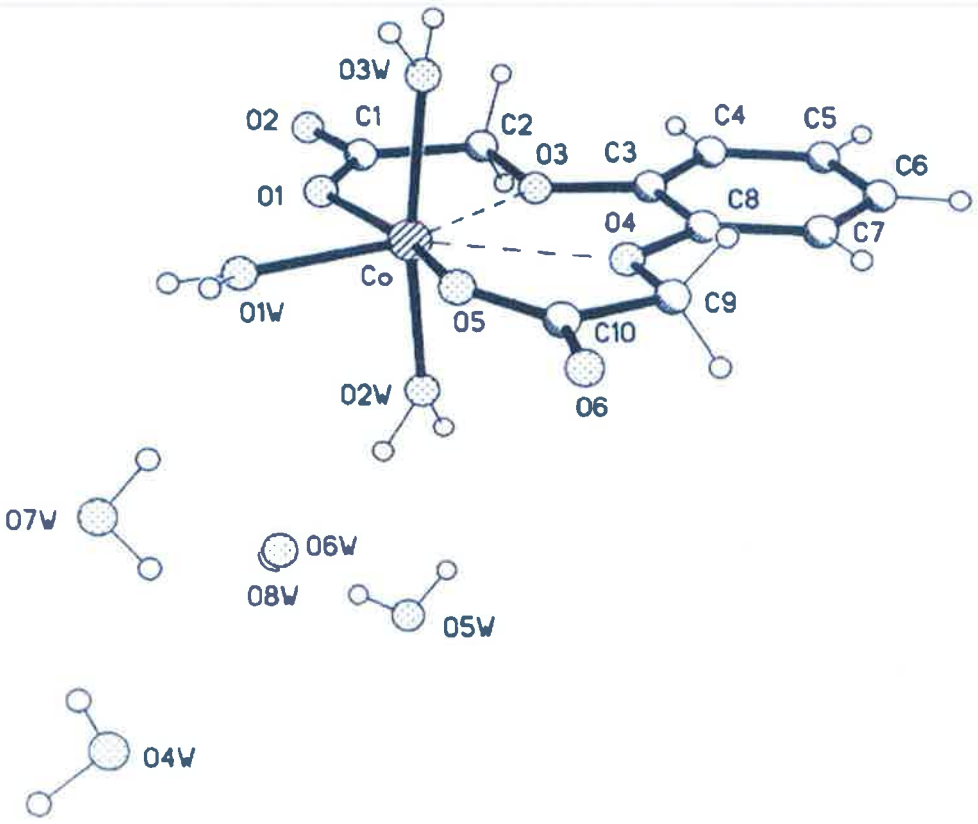

Figure 16: X-Ray crystal structure of $[Co(bdoa)(H_2O)_3].3.5H_2O$ (1b)[16]

Reaction of $[Co(bdoa)(H_2O)_3].H_2O$ **(1a)** with phen produced $[Co(phen)_3]bdoa.10H_2O$ **(2a)** and $\{[Co(phen)_3](bdoa)\}_2.24H_2O$ **(2b)** (Figure 17). The Mn^{2+} and Cu^{2+} complexes $[Mn(bdoa)(phen)_2].H_2O$ **(3)**, $[Cu_2(bdoa)(phen)_4]bdoa.13H_2O$ **(4)** and $[Cu_2(bdoa)(bipy)_4]bdoa.8.6H_2O$ **(5)** were also synthesized[16].

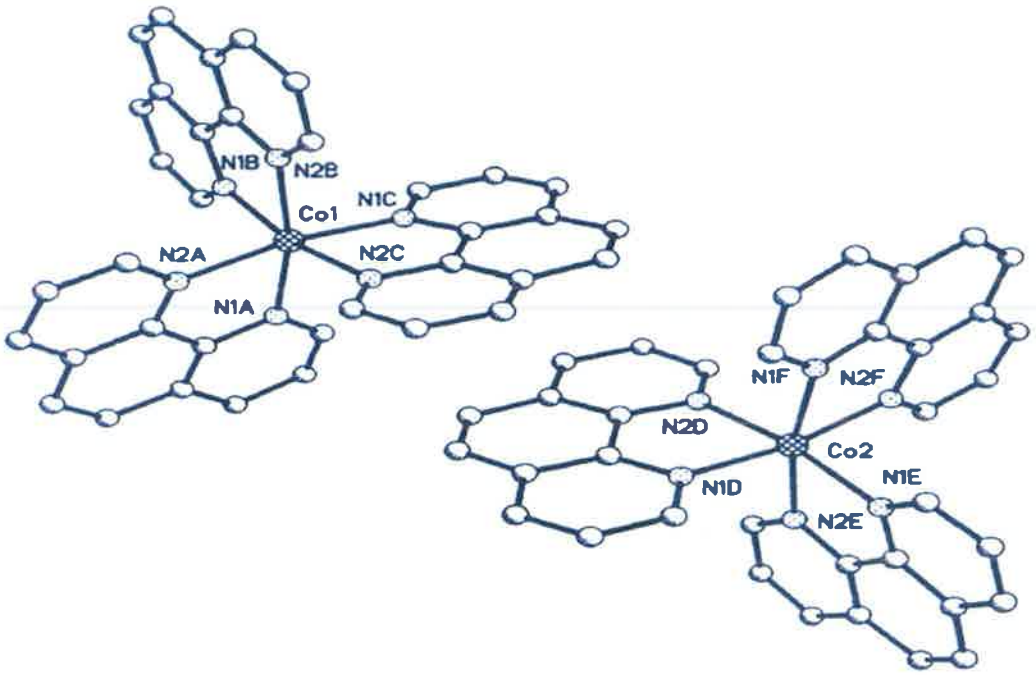

Figure 17: Structure of the $[Co(phen)_3]^{2+}$ moieties in $\{[Co(phen)_3](bdoa)\}_2.24H_2O$ **(2b)** (hydrogen atoms omitted)[16]

All complexes were tested for their ability to inhibit the growth of *Candida*.

Table 9: Anti-fungal activity of compounds tested at a concentration of 20 μg/ml[16]

Test Compound	% Cell Kill		
	Isolate 1	Isolate 2	Isolate 3
Control	0	0	0
$bdoaH_2$	9	0	0
phen	88	86	85
bipy	25	20	0
$[Co(bdoa)(H_2O)_3].H_2O$ **(1a)**	37	30	22
$[Co(phen)_3]bdoa.10H_2O$ **(2a)**	45	35	23
$[Mn(bdoa)(phen)_2].H_2O$ **(3)**	90	94	93
$[Cu_2(bdoa)(phen)_4]bdoa.13H_2O$ **(4)**	85	78	89
$[Cu_2(bdoa)(bipy)_4]bdoa.8.6H_2O$ **(5)**	4	13	3

As shown in Table 9, the Co^{2+}, Mn^{2+} and Cu^{2+} phen complexes $[Co(phen)_3]bdoa.10H_2O$ **(2a)**, $[Mn(bdoa)(phen)_2].H_2O$ **(3)** and $[Cu_2(bdoa)(phen)_4]bdoa.13H_2O$ **(4)** dramatically inhibited the growth of all three isolates, with the Mn^{2+} and Cu^{2+} species showing the greater activity[16].

As stated earlier, "metal-free" 1,10-phen showed very high anti-*Candida* activity but the activity of the Mn^{2+} phen complex $[Mn(bdoa)(phen)_2].H_2O$ **(3)** was greater. In contrast to the performance of the phen, bipy along with Cu^{2+} bipy complex $[Cu_2(bdoa)(bipy)_4]bdoa.8.6H_2O$ **(5)** is ineffective at preventing the growth of *Candida* cells[16].

Recently, as part of the studies of novel transition metal-based drugs [10] this group and its co-workers have generated a range of Ag^+ complexes incorporating chelating phenanthroline and related nitrogen donor ligands [2, 3, 4, 10, 17, 18, 19] (Figure 18). The aim

of this work was to examine the effect of combining the potent anti-fungal phenanthroline ligand with silver, a potent anti-microbial in its own right.

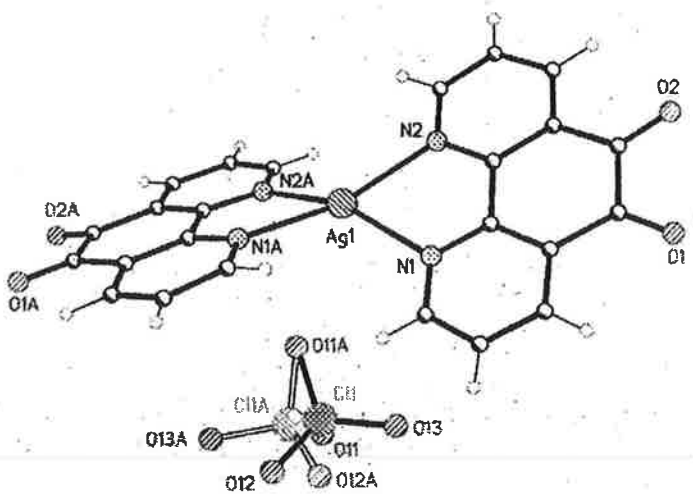

Figure 18: The X-Ray crystal structure of $[Ag(phendione)_2]ClO_4$[17]

The most potent silver complexes are those incorporating the strong chelators phen and phendione {Figure 1 (a)-(b)} [4,17].

$[Ag(phendione)_2]ClO_4$ (Figure 18) was found to exhibit anti-fungal activity sixty times greater than that of simple free Ag^+ ions and it is believed that the activity of these complexes is not just reliant on the release of simple Ag^+ ions but may involve a chelated form of the metal[17].

I.1.4 The mode of anti-fungal action of phenanthrolines and their metal complexes

In 2004, this group examined the mode of action of phen and a number of potent anti-*Candida* metal complexes of phen {M = Cu^{2+}, Mn^{2+} or Ag^{+}}[10]. They reported that phen and its metal complexes have minimum inhibitory concentrations (MIC's) in the range of 1.25-5 μg/ml and at a concentration of 10 μg/ml display some fungicidal activity[10].

Yeast cells exposed to these compounds showed a diminished ability to reduce 2,3,5-triphenyltetrazolium chloride (TTC), indicating a reduction in respiratory function. Treating exponential and stationary phase yeast cells with phen and the Cu^{2+} and Mn^{2+} complexes caused a dramatic increase in oxygen consumption. All of the drugs promoted reduction in levels of cytochrome b and c in the cells, whilst the Ag^{+} complexes also lowered the levels of cytochrome aa. Cells treated with phen and the Cu^{2+} and Ag^{+} species showed reduced level of ergosterol whilst the Mn^{2+} complex induced an increase in the sterol concentration. The general conclusion was that phen and its Cu^{2+}, Mn^{2+} and Ag^{+} complexes damage mitochondrial function and uncouple respiration. The fact that these drugs were not uniformly active suggests that their biological activity has a degree of metal-ion dependency.

The conclusion was that phen and the metal-phen complexes have the potential to induce apoptosis in fungal and mammalian cells. This group has concluded that select phen metal complexes represent a novel set of highly active anti-fungal agents whose mode of action is significantly different to that of state-of-the-art polyene and azole

prescription drugs. Compounds that kill fungal cells in a different biochemical way to these drugs may not have the same resistance and toxicity problems[11].

In conclusion, the phen molecule whether it be uncomplexed or chelated to a metal centre, exhibits potent anti-*Candida* activity. The work carried out so far by this group and its collaborators also suggest that the type of metal present can influence the anti-*Candida* responses of this class of complex with the well known anti-microbial silver ion being the most superior. Furthermore, when phen is derivatised to form phendione the anti-*Candida* capability of the resultant metal complexes increases greatly. Whereas phendione is superior to phen as a ligand for generating novel anti-microbial agents, the structurally related bipy is inactive as an anti-*Candida* agent either in the metal free state or when complexed to a metal centre. Significantly the phen and phendione ligands both exhibit very potent cytotoxicity and when complexed to metals this activity increases. This property may limit the use of this type of compound as anti-microbial agents.

I.2 1,10-PHENANTHROLINE (PHEN)

The metabolic processes of entire animals and mammalian or microbial cells in culture can become interfered with, by metal binding agents, known as chelators[20]. Phen {Figure 1(a)} is a heterocyclic ligand that belongs to the phenanthrene family and is best considered as an α-di-iminic ligand[17,21,22]. This well-known N-heterocyclic chelating agent is a tricyclic molecule in which two pyridine rings are fused to a central benzene ring[23]. It can also be described as a bidentate ligand as it functions through the nitrogen atoms in the 1 and 10 position with the formation of 5 membered rings.

Ramirez-Silva et al. [24] carried out a study on the effect of substituents over different positions of the 1,10-phenanthroline (phen) molecule (Figure 19).

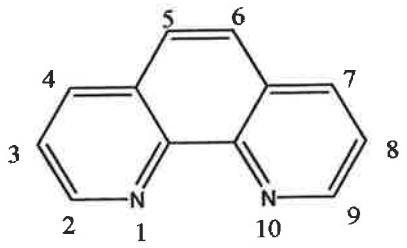

Figure 19: Structure and assignment of 1,10-phenanthroline

It was reported that the positions related to nucleophilic substitution were assigned to positions 2, 4, 7 and 9 on the phen molecule[24]. The 2 and 9 positions are nucleophilic due to the electron withdrawing effect the two nitrogens. Since both the 4 and 7 positions are adjacent to quaternary carbons experiencing strong electron withdrawing resulting neucleophilic substitution. Positions 3, 5, 6 and 8 are electrophilic due to their higher electron densities[24].

Phen can take action as either a chelator or as a ligand in chelate complexes. When phen acts as a chelator its toxicity is manifested by its capacity to combine with e.g. zinc, and by doing this the zinc-containing nucleotidyl transferases and DNA synthesis becomes inhibited[20]. Also, since phen is cis in structure, it has the ability to coordinate in such a way that the metal atom contained by the phen chelating ring is co-planar with the rest of the molecule[5]. Phen holds a rigid planar framework and when divalent metal ions such as Cu^{2+}, Co^{2+}, Fe^{2+}, Zn^{2+} and Ru^{2+} have been chelated with phen, cytotoxicity has been reported. The degradation of DNA is prompted by the cuprous chelate in a model cell-free system[20]. Metal complexes of phen have been reported with anti-cancer, anti-fungal, anti-bacterial, anti-neoplastic, anti-microbial and anti-viral properties[20,25,26,27].

I.2.1 Synthesis of 1,10-phenanthroline

It has been documented by Brandt et al.[5] that in the late 1800's Blau et al.[28,29,30] reported the first synthesis of 1,10-phenanthroline.

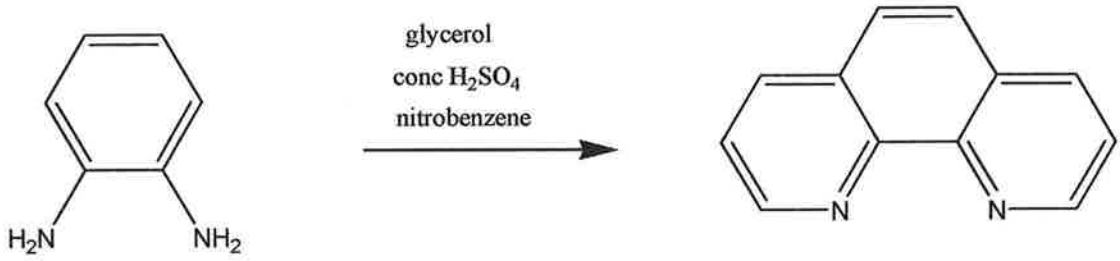

Scheme 1: Synthetic route to 1,10-phenanthroline (phen) [31]

Phen is synthesized via the Skraup synthesis by heating o-phenylenediamine with glycerol, nitrobenzene and concentrate sulphuric acid (Scheme 1).

Recently, Chelucci et al.[23] reported a protocol for the synthesis of substituted 1,10-phenanthrolines. This group began this process by carrying out the synthesis of phen from pyridine molecules (Scheme 2).

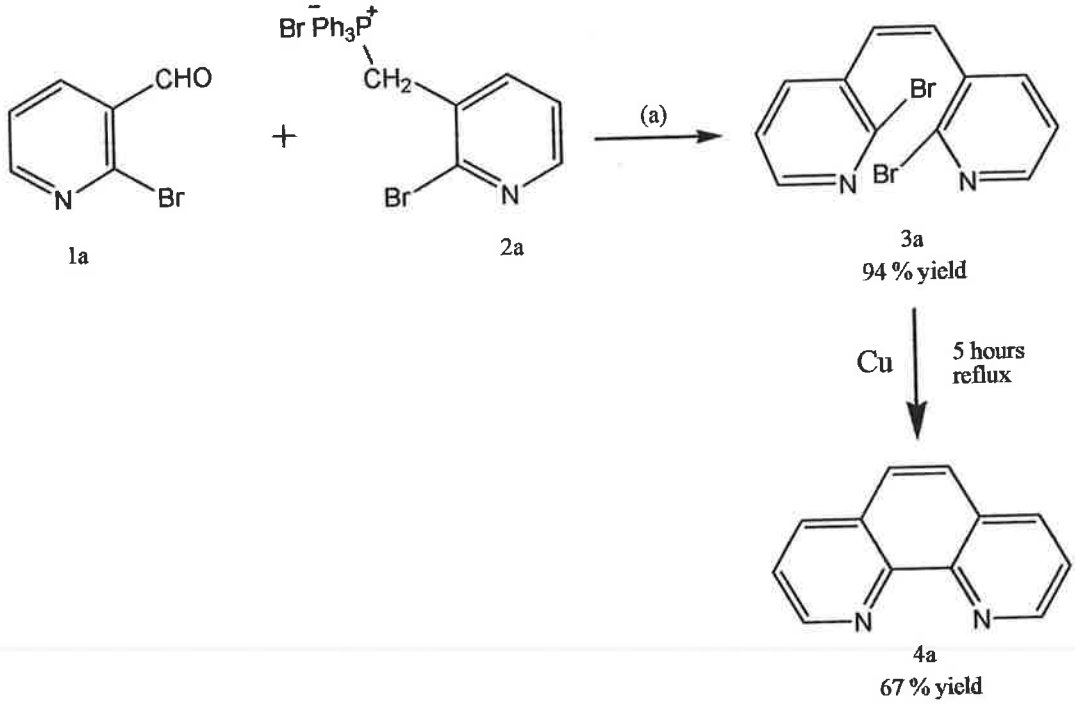

Scheme 2: Two step synthesis of phen, {(a): 2a (1.2 equivalence), $KOBu^t$ (2.2 equivalence), DMF, room temperature, 18 hours}[23]

The Wittig reaction was used which involves the reaction of 2-bromonicotinaldehye **(1a)** with the phosphonium salt **(2a)** of 2-bromo-3-bromomethylpyridine (1.2 equivalence of **2a**, 2.2 equivalence of $KOBu^t$, TMF, R.T., 18 hours) and achieving a 94 % yield of (z)-1,2-di(2-bromo-3-pyridinyl)ethane **(3a)**. By reacting **3a** (0.5 mmol) with copper powder (3.0 mmol) in DMF (2 ml) and refluxing the solution under argon for 5 hours, a 67 % yield of 1,10-phenanthroline was achieved[23].

I.2.1.1 Properties of phen

Phen can exist as either a monohydrate compound, m.p. 94 °C or as an anhydrous compound, m.p. 117 °C[31,32]. It is slightly soluble in water and fully soluble in ethanol, acetone, ether and benzene. In the structure of phen, the shortest bond lengths are the two N-C bonds at 1.36 Å, whilst the longest bonds are C-C bonds that join the pyridyl rings at 1.40 Å[33].

Phen and the similar bipy ligand (Figure 2) coordinate through their two nitrogen atoms with delocalized π orbitals providing suitable empty π* orbitals[34]. Phen and bipy bond to metals forming very stable five membered chelate rings. This is a key feature of such heterocyclic ring ligands, as their π electron deficiency creates excellent π-accepter ligands. As a result, phen and bipy have been used to assist in the stabilization of a variety of metal complexes in lower oxidation states[35].

Phen has a strong ligand field causing spin pairing and due to its stability, the phen complex $[Fe^{2+}(phen)_3]^{2+}$ can be used for the colorimetric determination of iron. Phen is employed as a redox indicator 'ferroin' in titrations and can also be used in determination of ruthenium, nickel, silver and other metals[32,36].

I.2.1.2 Isomers of phen

Phen can exist as different isomers depending on the position of the two nitrogens, such as 1,7-phenanthroline, 1,8-phenanthroline, 2,7-phenanthroline, 2,9-phenanthroline, 4,7-phenanthroline, 5,6-phenanthroline and 3,8-phenanthroline (Figure 20)[37]. The nitrogen atoms are best considered as α-di-imines, as indicated in section I.2[36].

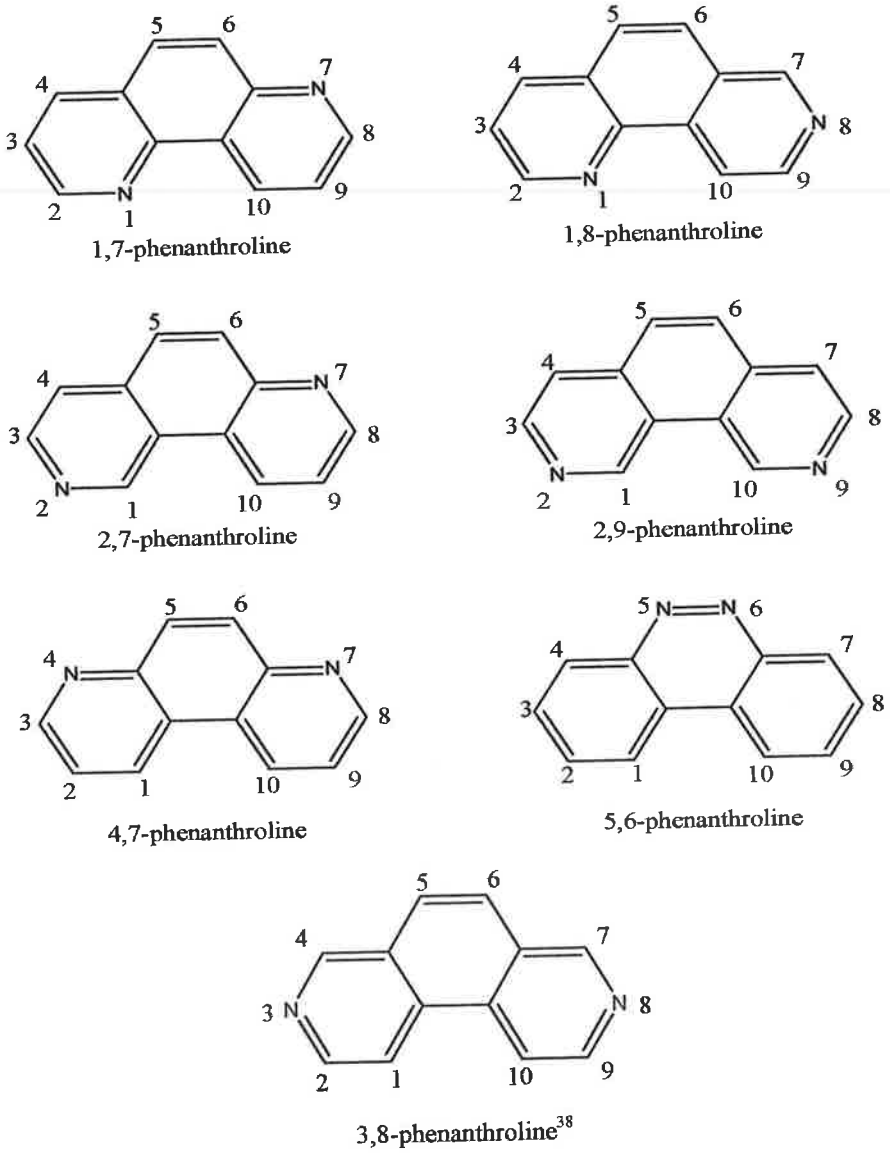

Figure 20: Structure of the Isomers of Phenanthroline

I.3 1,10-PHENANTHROLINE-5,6-DIONE (PHENDIONE)

Phendione is similar to phen in structure with the addition of two carboxyl groups attached at position 5 and position 6, as indicated in Figure 1(b). Phendione is a chelate ligand and possesses two coordination functionalities (the quinoid functionality which is redox reactive and di-iminic functionalities which is a Lewis base). Thus, it is possible for phendione to interact with other compounds or metal centres through the quinonoid or the di-imine functionality[33]. This o-quinoid moiety is considered to have many interesting biological properties[22].

I.3.1 Synthesis of phendione

Phendione has been known since 1947[39] and several synthetic procedures have been reported in the literature[33,39]. Four such methods have been reported by Paw et al.[39] in 1997, Calderazzo et al.[33] in 1999, Calucci et al.[40] in 2006 and Zhong et al.[26] in 2008. These four methods are modified versions of the procedure reported by Yamada and co-workers[41].

Paw et al.[39] reported a procedure that used an ice-cooled mixture of a 2:1 molar ratio of concentration H_2SO_4 and HNO_3, added to a 1:1.5 molar ratio of phen/KBr mixture at room temperature and refluxing for 3 hours. Zhong at al.[26] also used an ice cold mixture of concentration H_2SO_4 and HNO_3 but this time a 1:1 molar ratio was added to a 1:1.5 molar ratio of phen/KBr at room temperature. Refluxing time in this case was doubled to 6 hours, unlike Paw et al. Calderazzo et al.[33] added a 1:10 molar ratio of phen/KBr to

concentration H_2SO_4 pre-cooled to liquid nitrogen temperature. Once the mixture had reached room temperature, HNO_3 (room temperature) was added in a dropwise fashion. Reflux was carried out for 3 hours. The final procedure reported by Calucci et al.[40] adopted pre-cooling to all starting materials. A mixture of 1:1.5 molar ratio of phen/KBr was pre-cooled at -10 °C, while the acid mixture was cooled at -78 °C. The acid mixture was carefully added to the phen/KBr mixture over 30 minutes. Once the reaction mixture had warmed up to room temperature the solution was heated at 150 °C until the evolution of Br_2 had ceased which took between 5-7 hours.

Three of the four methods used sodium hydroxide to aid neutralisation, while Calderazzo et al.[33] used sodium carbonate. Paw et al.[39] and Zhong et al.[26] both used chloroform during the extraction process, while Calderazzo et al.[33] and Calucci et al.[40] used dichloromethane. Sodium sulphate was used as a drying agent in three of the four methods with the exception of Calderazzo et al.[33] using magnesium sulphate. All of the methods, except for Calucci et al. used ethanol in the purification process, Calucci et al.[40] used hot methanol.

I.3.2 Properties of phendione

Phendione exists in the form of a yellow compound, m.p. 258 °C and it is soluble in water, ethanol, methanol, acetone, dimethylsulphoxide and chloroform. It is a versatile ligand as it has the ability to form stable complexes with a wide variety of metal ions due to the presence of its two reactive sites, (the quinonoid and the di-imine functions) [33,40,42,43]. All of the atoms with the exception of the hydrogens are sp^2 hydridised and with the presence of the o-quinone moiety, phendione is electrochemically active. The two di-iminic nitrogen atoms permit the ligand to behave as a Lewis base. Resonance conjugation of the phendione ligand makes it possible to adjust the electron density in different parts of the molecule, particularly by the interaction of an external electrophile with the unshared pairs of electrons of the heteroatom[33,37,40,42,44,45].

Coordination of the phendione ligand with a metal can occur through the quinonoid functionality, the di-iminic functionality or both. When coordination occurs through the nitrogen atoms of the ligand with metals of a low oxidation state, the whole complex may be used as a 'quinone equivalent' ligand. Alternatively, when phendione is reacted with a Lewis acid, coordination occuring through the oxygens of the ligand, leaves way for the complex to be used as a 'phenanthroline equivalent' ligand[40,44].

The X-ray crystal structure of phendione (Figure 21) shows the C=O bonds at 1.210 Å to be the shortest, closely followed by the N-C bonds at 1.36 Å, while the C-C bonds joining the pyridyl rings are the longest at 1.49 Å[33]. Selected bond lengths and angles of phendione are listed in Table 10[33].

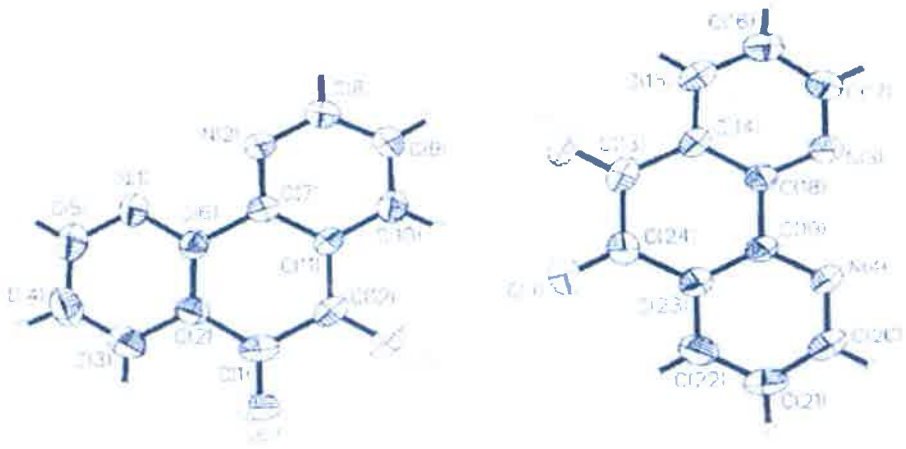

Figure 21: X-Ray crystal structure of two independent molecules of phendione, with the atom numbering scheme used[33]

Table 10: A selection of bond distances (Å) and angles (°) for phendione

Molecule 1		Molecue 2	
O(1)–C(1)	1.213(3)	O(3)–C(13)	1.207(3)
C(1)–C(2)	1.477(4)	C(13)–C(14)	1.477(3)
C(1)–C(12)	1.529(4)	C(13)–C(24)	1.539(4)
C(5)–N(1)	1.335(3)	C(17)–N(3)	1.336(3)
N(1)–C(6)	1.343(3)	N(3)–C(18)	1.338(3)
C(6)–C(7)	1.489(3)	C(18)–C(19)	1.494(3)
C(7)–N(2)	1.339(3)	C(19)–N(4)	1.343(3)
N(2)–C(8)	1.339(3)	N(4)–C(20)	1.337(3)
C(12)–O(2)	1.208(3)	C(24)–O(4)	1.209(3)
O(1)–C(1)–C(2)	123.1(3)	O(3)–C(13)–C(14)	123.0(3)
O(1)–C(1)–C(12)	118.8(2)	O(3)–C(13)–C(24)	119.1(2)
C(2)–C(1)–C(12)	118.1(2)	C(14)–C(13)–C(24)	117.9(2)
N(1)–C(5)–C(4)	125.0(3)	N(3)–C(17)–C(16)	125.2(3)
C(5)–N(1)–C(6)	116.7(2)	C(17)–N(3)–C(18)	116.7(2)
N(1)–C(6)–C(2)	122.2(2)	N(3)–C(18)–C(14)	122.4(2)
N(1)–C(6)–C(7)	116.6(2)	N(3)–C(18)–C(19)	117.0(2)
N(2)–C(7)–C(11)	122.0(2)	N(4)–C(19)–C(23)	122.1(2)
N(2)–C(7)–C(6)	117.4(2)	N(4)–C(19)–C(18)	117.3(2)
N(2)–C(8)–C(9)	124.7(3)	N(4)–C(20)–C(21)	124.3(3)
C(7)–N(2)–C(8)	117.0(2)	C(20)–N(4)–C(19)	117.3(2)
O(2)–C(12)–C(1)	119.5(2)	O(4)–C(24)–C(13)	118.9(2)
O(2)–C(12)–C(11)	122.3(2)	O(4)–C(24)–C(23)	123.2(3)
C(11)–C(12)–C(1)	118.2(2)	C(23)–C(24)–C(13)	117.9(2)

In the IR spectrum bands characteristic to phendione can be clearly seen at 1685 cm^{-1} {Appendix 1(1)} representing the stretching vibration of the carbonyl group. Also bands

characteristic of the phen moiety are present at 806 cm^{-1} and 735 cm^{-1}; which represent the C-N-C stretching frequency of the ligand. When ^1H NMR examination of phendione proceeds, three distinct signals result in double doublets which integrate for two hydrogens {Appendix 2(1)}.

I.3.3 Isomers of phendione

Phendione can exist as an isomer depending on the position of the two nitrogens; such as 4,7-phenanthroline-5,6-dione (Figure 21).

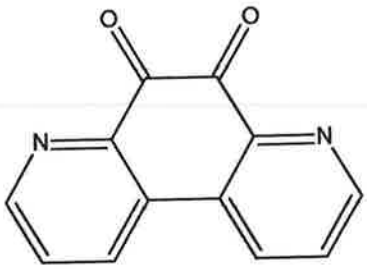

Figure 22: Structure of an Isomer of 1,10-Phenanthroline-5,6-dione (4,7-phenanthroline-5,6-dione)

Phanquinone (4,7-phenanthroline-5,6-dione) (Figure 22) has been used in the treatment of Alzheimer's disease and unlike other known treatments it has no adverse side effects[46]. Alzheimer's disease is a major cause of dementia in adults generally diagnosed in people over the age of sixty five. This degenerative brain disorder is recognized by symptoms such as loss of memory, confusion, mood swings and eventually death. Amyloid-beta (Aβ) is a peptide composed of 39-43 amino acids and it has been suggested that Aβ deposits are essentially the cause of Alzheimer's disease. It has been reported by Yankner et al.[47] that when Aβ is directly added to neuronal cell cultures *in-vitro*, Aβ is found to be toxic. The effect of phanquinone on Aβ(25-35)

dose-response in PC12 cells (Rats PC12 pheochromocytoma cells) were studied and shown to have a distinct effect on the redox activity of the cells. When the cells were exposed to 1 μM Aβ(25-35) cells, the redox activity was restored to normal indicating phanquinone has the ability to lessen the adverse effects of Aβ when administered to humans[46].

I.4 CHELATING 1,10-PHENANTHROLINE LIGANDS

As previously mentioned, it was reported in the late 1800's that Blau et al.[28,29,30] was the first to synthesise the aromatic nitrogen heterocyclic phen and related ligand bipy. Both chelating ligands have since been extensively used in the areas of analytical and coordination chemistry[38,48]. The physical and chemical properties of complexes containing these ligands can be significantly modified when substitution occurs on the pyridine rings. Much greater changes can happen when one or both of the pyridine rings are replaced by other nitrogen containing heterocyclics, resulting in changes in electronic properties, δ-donating ability of the nitrogen donor atom and π-acceptor and π-donor properties of the ligand[38,48]. Six-membered aromatic nitrogen heterocyclics have relatively low energy π* orbitals which act as excellent π-acceptors of metal d-orbital electron density in metal-ligand backbonding, while being poor π-donors. The reverse is true for five-membered aromatic nitrogen heterocyclics, having the ability to exist as anionic ligands by protonation of acidic N-H groups in the free ligand. These factors have important consequences when attempts are being made to allow metal-ligand interactions by the specific metal and ligands involved[38,48].

In 2008, Brahma et al.[25] synthesized and structurally characterised the mono phen complex bis(acetylacetonato-k^2O,O')(1,10-phenanthroline-k^2N,N')-zinc(II) and its structure is shown in Figure 23[25].

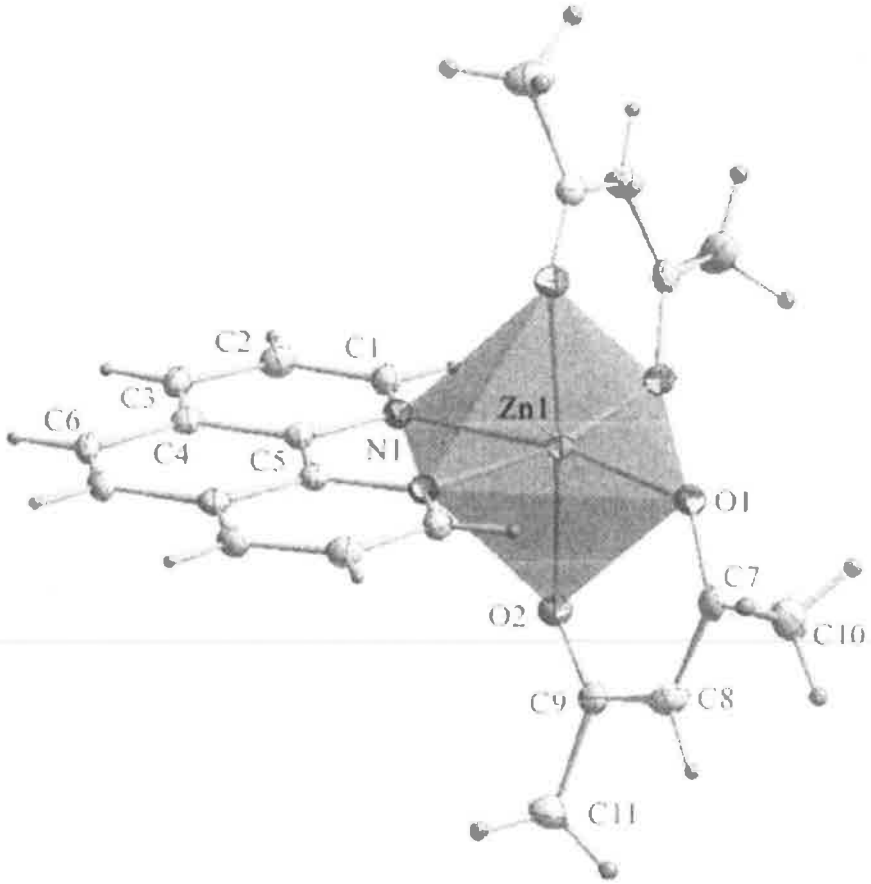

Figure 23: X-Ray crystal structure of mono-phen complex bis(acetylacetonato-k^2O,O')(1,10-phenanthroline-k^2N,N')-zinc(II)[25]

As shown in Figure 23, the six coordinated Zn^{2+} atom in the centre of symmetry has a distorted octahedral coordinated geometry. The two acetylacetonato ligands are coordinated to the Zn^{2+} via four O atoms and the mono phen ligand is also coordinated to the Zn^{2+} atom via two N atoms. From the data of the crystal structure, the Zn-O bonds were found to be trans to the N atoms (2.0441 Å) which are shorter than those trans to the O atoms (2.0853 Å). Intramolecular hydrogen bonding is ruled out in complex bis(acetylacetonato-k^2O,O')(1,10-phenanthroline-k^2N,N')-zinc(II) presumably due to the presence of the rigid phenanthroline framework and to a degree the

crystallographically imposed symmetry inhibiting the donor and acceptor groups coming closer and forming non-bonded interactions[25].

Recently, Thati et al.[49] have synthesized and structurally characterised the bis-phen complex [Ag(hnc)(phen)$_2$], (hnc = 4-oxy-3 nitro-coumarin). As shown in Figure 24, the Ag^+ atom at the centre of symmetry is coordinated by two bidentate phen ligands via four nitrogen atoms and the hnc ligand via two O atoms[49].

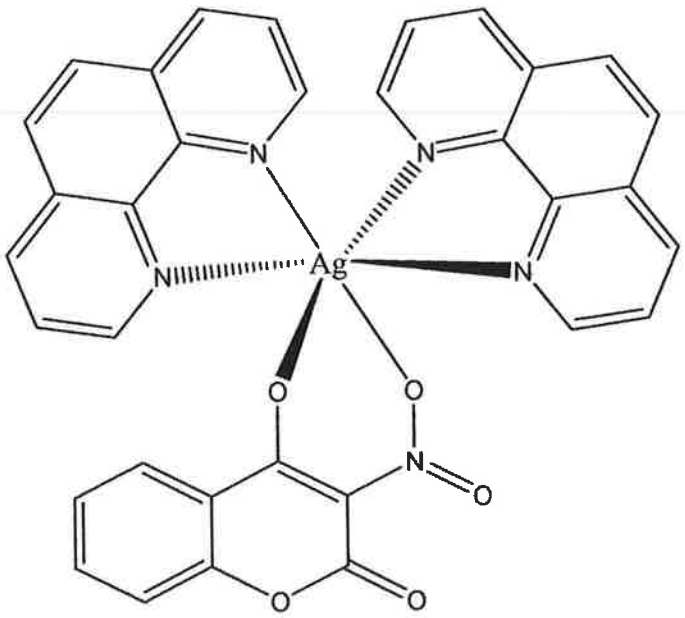

Figure 24: Structure of Bis-Phen complex [Ag(hnc)(phen)$_2$][49]

Investigation has found that complex $[Ag(hnc)(phen)_2]$ exhibits significant anti-cancer activity against human carcinoma cell lines compared to their free ligands. Four cell lines were used, two neoplastic renal (A-498) and hepatic (Hep G2) cells, and the other two were non-neoplastic renal (HK-2) and hepatic (Chang) cell lines. The non-neoplastic hepatic cell (Chang) appeared to be less sensitive to the effect of the complex, while based on the IC_{50} values, $[Ag(hnc)(phen)_2]$ was found to be almost four times more potent than cisplatin using Hep G2 cells. In addition, this bis phen silver complex was found to induce apoptic cell death yet did not intercalate with DNA[49].

Very recently, Sharma et al.[50] synthesized and structurally characterised a novel red-coloured single crystal structure of bis phen complex $[Co(phen)_2CO_3](3,5\text{-dinitrobenzoate}).5H_2O$ (Scheme 3), by reacting carbonatobis (1,10-phenanthroline) cobalt(III) chloride and the sodium salt of 3,5-dinitrobenzoic acid (dnb) in an aqueous medium in an effort to explore the potential of $[Co(phen)_2CO_3]^+$ as an anion receptor[50].

$$\mathbf{[Co(phen)_2CO_3]Cl + Na\ dnb \xrightarrow{H_2O} [Co(phen)_2CO_3](dnb).5H_2O + Na\ Cl}$$

Scheme 3: Synthetic route to $[Co(phen)_2CO_3](3,5\text{-dinitrobenzoate}).5H_2O$[50]

"Synthetic anion receptors should have the following characteristic features: (i) a positively charged component for effective electrostatic interactions, (ii) hydrogen bond donor groups and (iii) a suitable framework onto which these structural components can be assembled"[50]. Since the complex cation $[Co(phen)_2CO_3]^+$ has a positively charged unit for electrostatic interaction, hydrogen bond donor groups of 16 C-H, a hydrogen

bond acceptor operated by one oxygen atom of the carbonate group and a framework that is fairly stable, it can be said that this complex cation fulfills all the criteria of an anion receptor[50].

The complex cation $[Co(phen)_2CO_3]^+$ contains an octahedral geometry around the Co^{3+} metal centre which is bonded to four nitrogen atoms from two bidentate phenanthroline ligands and two oxygen atoms from the bidentate carbonate group[50].

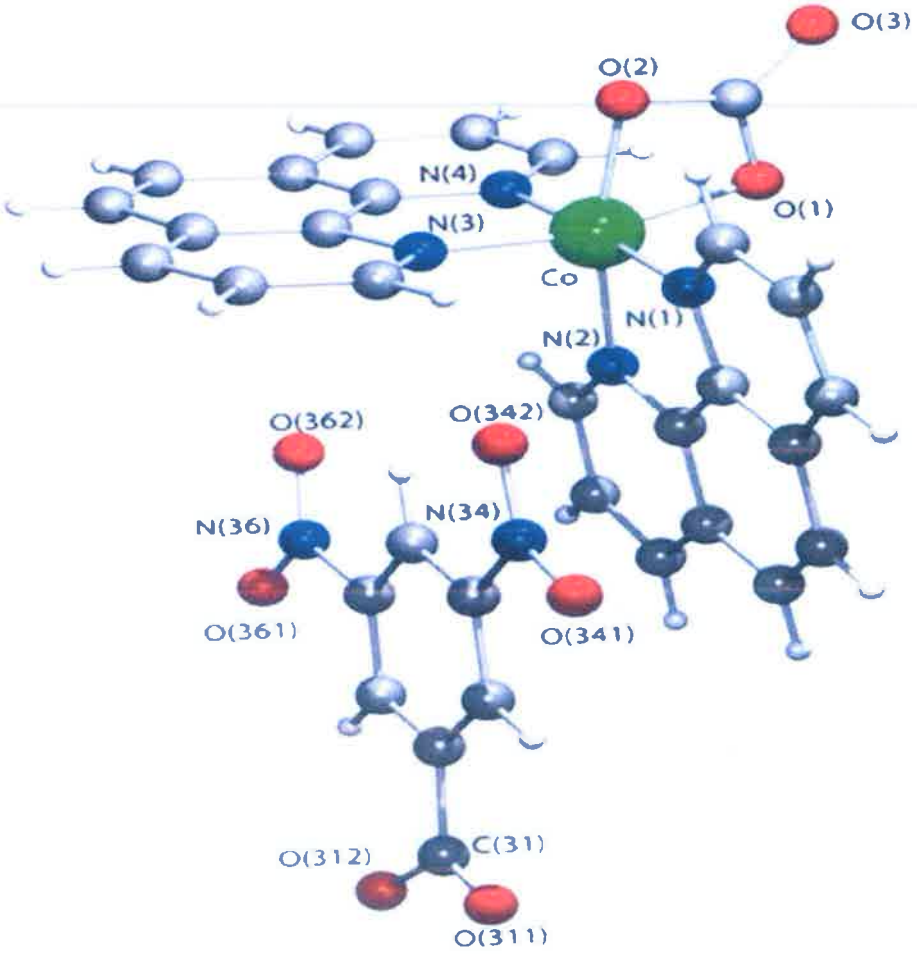

Figure 25: X-Ray crystal structure of the bis phen complex $[Co(phen)_2CO_3](dnb).5H_2O$[50]

The crystal structure of $[Co(phen)_2CO_3](dnb).5H_2O$ as shown in Figure 25, consists of one carbonato bis(1,10-phenanthroline)cobalt(III) cation, one 3,5-dinitrobenzoate anion and five lattice water molecules. Once the formation of a salt of definite composition was coupled with the solubility of product measurements, it can be concluded that the cation complex of $[Co(phen)_2CO_3](dnb).5H_2O$ is a promising anion receptor for 3,5-dinitrobenzoate anion[50].

Recently, tris 1,10-phenanthroline complexes $[Co(phen)_3](IO_4)_3.2H_2O$ **(1)** (Figure 26), $(IO_4)^-$ = periodate ion, $[Co(phen)_3]Cl[(CH_3)_3C_6H_2SO_3]_2.11H_2O$ **(2)** (Figure 27) and $[Co(phen)_3](dmp)_3.4H_2O$ **(3)** (Figure 28), have been synthesized and characterised by Sharma et al.[51, 52, 53].

Complexes 1-3, were prepared by mixing an aqueous solution of tris(phen)cobalt(II) chloride with sodium metaperiodate to give complex **(1)**, sodium mesitylonesulphonate to give complex **(2)** and sodium 2,3-dinitrophenolate in complex **(3)** all in a 1:3 molar ratio, as shown in Scheme 4 [51,52,53].

(1) $[Co(phen)_3]Cl_3 + 3NaIO_4 \longrightarrow [Co(phen)_3](IO_4)_3 + 3NaCl$

(2) $[Co(phen)_3]Cl_3 + 3Na[(CH_3)_3C_6H_2SO_3] \xrightarrow{H_2O} [Co(phen)_3][(CH_3)_3C_6H_2SO_3] + 3NaCl$

(3) $[Co(phen)_3]Cl_3 + 3Na[OC_6H_3(NO_2)_2] \xrightarrow{H_2O} [Co(phen)_3][OC_6H_3(NO_2)_2] + 3NaCl$

Scheme 4: Synthetic routes to complexes 1-3 [51,52,53]

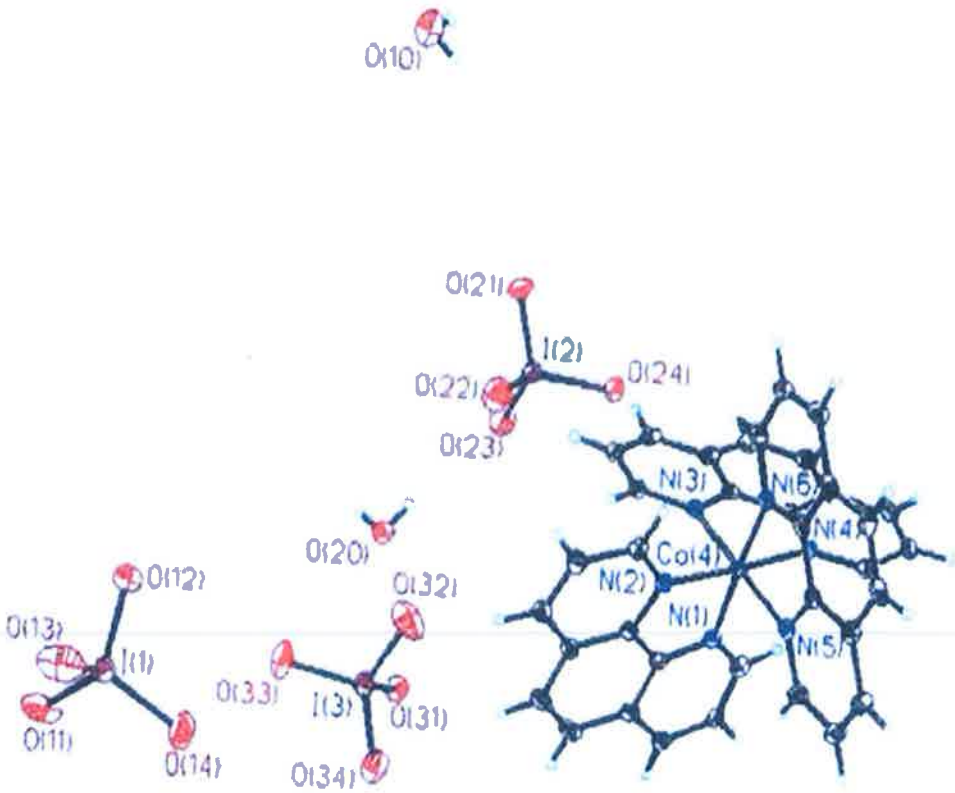

Figure 26: X-Ray crystal structure of $[Co(phen)_3](IO_4)_3.2H_2O$ **(1)**[51]

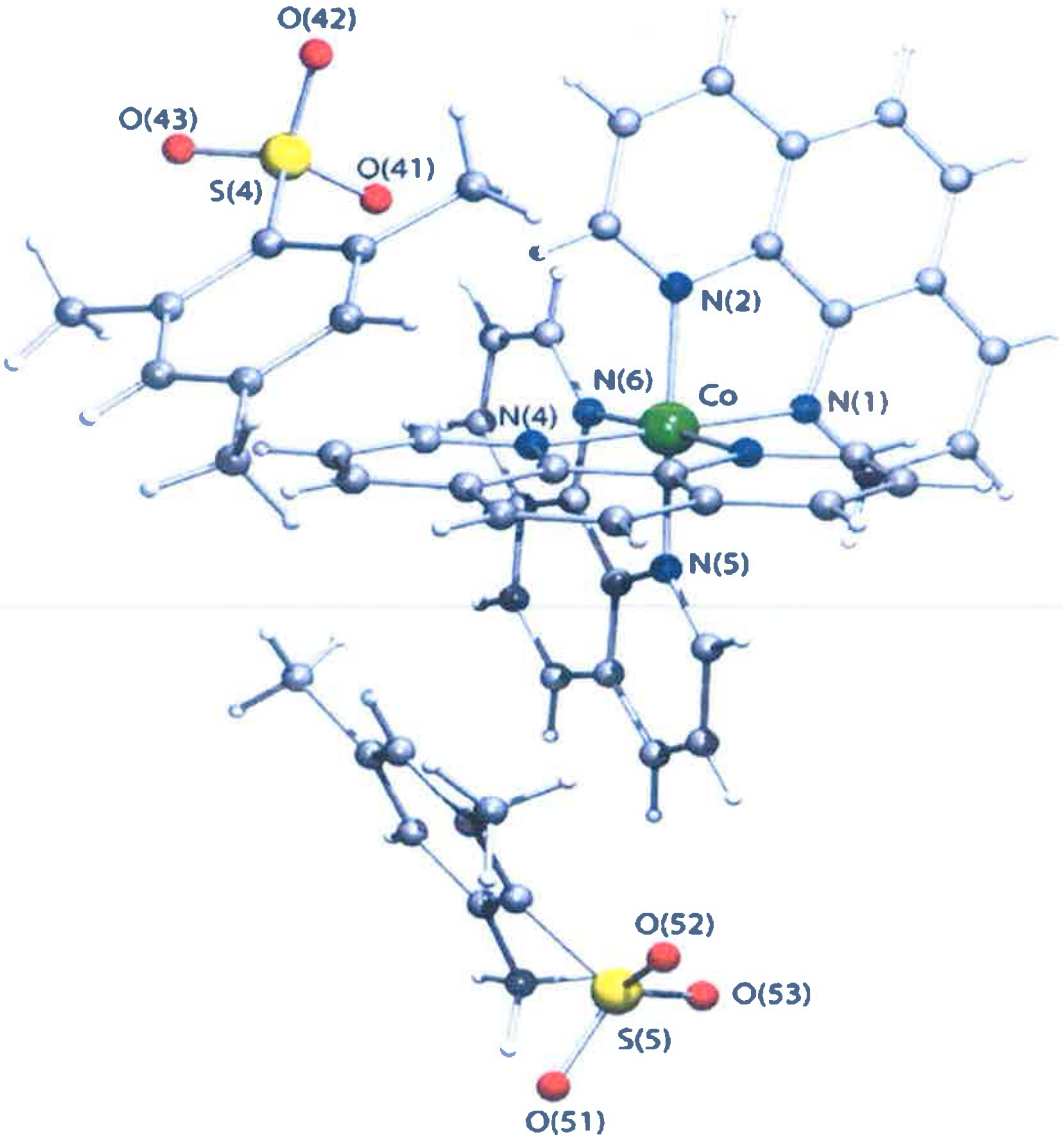

Figure 27: X-Ray crystal structure of $[Co(phen)_3]Cl[(CH_3)_3C_6H_2SO_3]_2.11H_2O$ **(2)**[52]

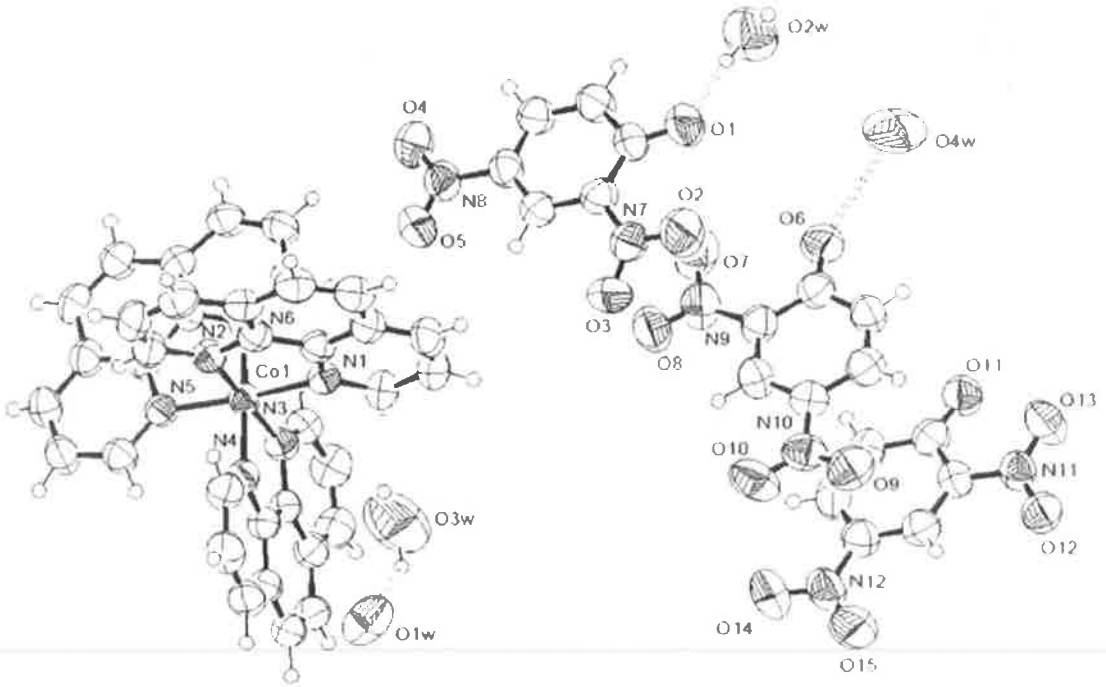

Figure 28: X-Ray crystal structure of $[Co(phen)_3](dnp)_3.4H_2O$ **(3)**[53]

The X-ray crystal structures of all three complexes are very similar as three bidentate 1,10-phenanthroline ligands are coordinated to cobalt(III) metal centres, present in all crystal structures with a single distorted octahedral geometry. In addition, the crystal structure of complex **(1)** shows three $[IO_4]^-$ anions and two water molecules , complex **(2)** possesses one chloride ion, two mesitylenesulphonate ions and eleven water molecules, whereas complex **(3)** consists of three dnp and four water molecules. In all three cases, the potential of the cationic metal complex $[Co(phen)_3]^{3+}$ as an ion receptor for metaperiodic anion in complex **(1)**, mesitylenesulphonate anion in complex **(2)** and 2,3-dinitrophenolate anion in complex **(3)**, has been explored. From experimental data, results revealed all three complexes were promising anion receptors in aqueous medium[51,52,53].

I.4.1 1,10-Phenanthroline-5,6-dione as chelating ligand

As earlier discussed, phendione is a chelating ligand which possesses two coordination functionalities, (the quinoid functionality which is redox reactive and the di-iminic functionality which is a Lewis base). Thus, since there are two sets of donor ligands, the oxygen and nitrogen atoms, it is possible for phendione to interact with other compounds through the quinonoid and/or the di-iminic functionality forming stable complexes with a wide range of transition metal ions[43, 54, 55].

In 1975, Balch et al.[33,56] synthesized mono-phendione complexes of platinum(0) or palladium(II) obtaining $[Pt(PPh_3)_2\text{-}(C_{12}H_6N_2O_2\text{-}O,O')]$ and $[PdCl_2(C_{12}H_6N_2O_2\text{-}N,N')]$, shown in Scheme 5 and Scheme 6. When transition metal complexes of phendione involve oxygen bonds, Lewis acids are used (Scheme 5)[43,44].

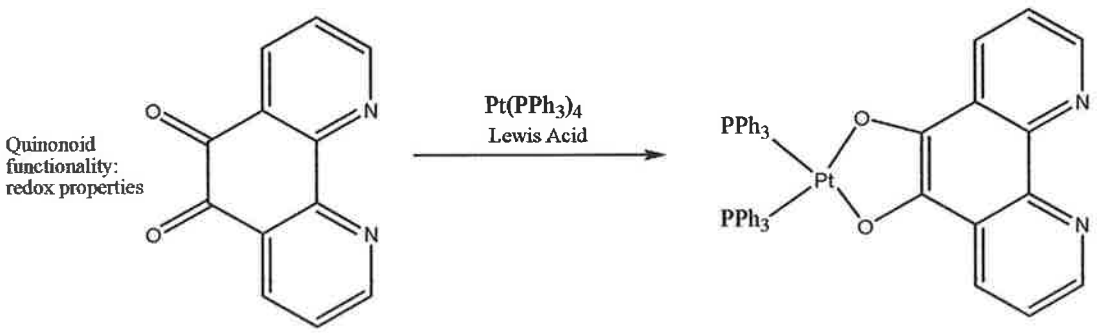

Scheme 5: The synthetic route to Bis(triphenylphosphine)1,10-phenanthroline-5,6-dione platinum $[Pt(PPh_3)_2\text{-}(C_{12}H_6N_2O_2\text{-}O,O')]$, an oxygen bound complex of phendione used as a phenanthroline equivalent ligand in reactions with Lewis acids[43, 44].

The red brown complex [$Pt(PPh_3)_2$-($C_{12}H_6N_2O_2$-*O,O'*)] (Scheme 5), was synthesized by oxidatively adding phendione to the low-valent complex platinum tetra(triphenylphosphine) [$Pt(PPh_3)_4$]. It was also reported by this group that when this complex was characterised by IR spectroscopy, the strong peak at approximately 1700 cm^{-1}, representative of the C=O stretching frequency of the phendione ligand was no longer present in the IR spectra, enhancing the evidence that the metal interaction was through the quinonoid functionality of the phendione ligand [56,57].

When transition metals coordinate through the two di-iminic nitrogen atoms of the phendione ligand, the entire complex may be used as 'quinone equivalent' in reactions containing metals in a low oxidation state (Scheme 6)[39,44].

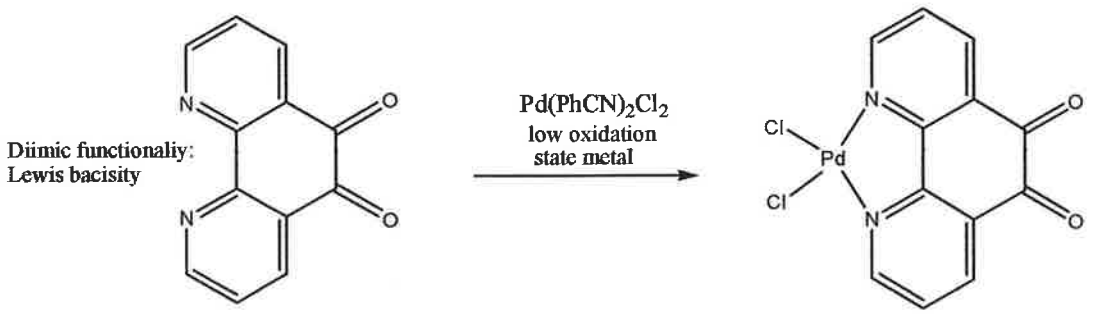

Scheme 6: The synthetic route to [$PdCl_2$($C_{12}H_6N_2O_2$-*N,N'*)], a nitrogen – bound complex of phendione containing low oxidation state metal[39,44]

In comparison, the yellow complex [$PdCl_2$($C_{12}H_6N_2O_2$-*N,N'*)] was synthesised when $Pd(PhCN)_2Cl_2$ was reacted with phendione. Due to the nucleophilic metal complex, $PdCl_2$ coordinated with the nitrogen donor site of phendione. Also when complex [$PdCl_2$($C_{12}H_6N_2O_2$-*N,N'*)] was characterised by IR spectroscopy, the carbonyl (C=O) stretching absorption band of the free ligand, phendione was shown to shift only very

slightly, indicating that the coordination of the metal to the phendione was through the two di-iminic nitrogen atoms and not the quinonoid functionality as previously shown[56, 57]. This demonstrated the versatility of the phendione ligand showing it can interact with the metal centres through the quinonoid and the di-iminic functionality.

Sometime later, Pierpoint[57] and co-workers and Paw et al.[39] confirmed that due to phendione having two different functionalities on the same molecule it was capable of acting as a bridging ligand as shown in Scheme 7.

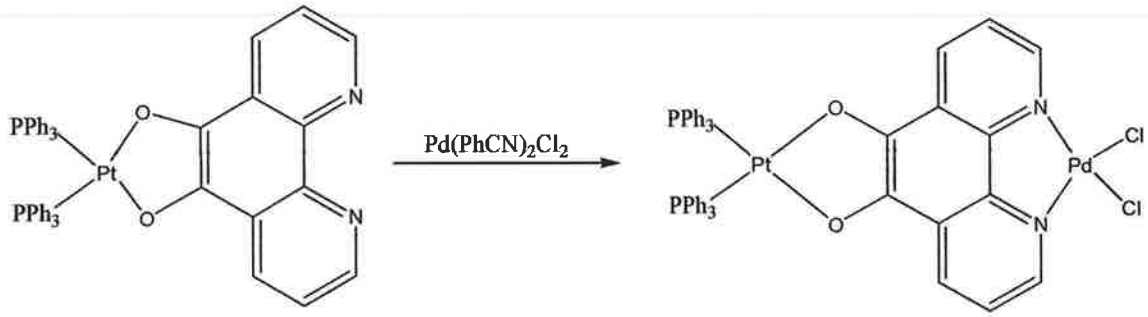

Scheme 7: The synthetic route of bridging ligand $[(PPh_3)_2Pt(O',O\text{-}C_{12}H_6N_2O_2\text{-}N,N')PdCl_2]$ [57]

The crystal structure of bridging complex $[(PPh_3)_2Pt(O',O\text{-}C_{12}H_6N_2O_2\text{-}N,N')PdCl_2]$ is shown in Figure 29.

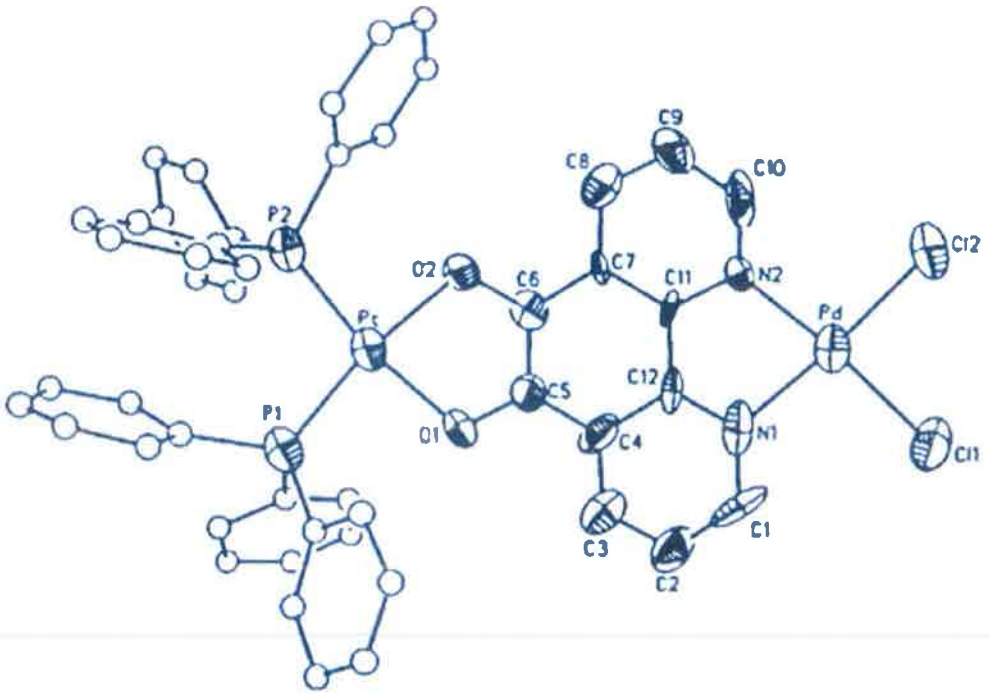

Figure 29: X-Ray crystal structure of $[(PPh_3)_2Pt(O',O\text{-}C_{12}H_6N_2O_2\text{-}N,N')PdCl_2]$[57]

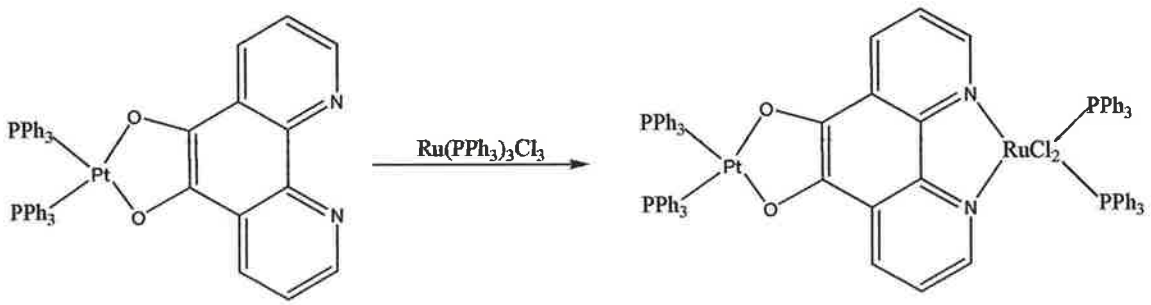

Scheme 8: The synthetic route to bridging ligand $[(PPh_3)_2Pt(O',O\text{-}C_{12}H_6N_2O_2\text{-}N,N')Ru(PPh_3)_2Cl_2$[57]

When complex [$Pt(PPh_3)_2$-($C_{12}H_6N_2O_2$-*O,O'*)], (Scheme 5), was reacted with $Ru(PPh_3)_3Cl_3$, the displacement of one PPh_3 ligand resulted, forming complex [$(PPh_3)_2Pt(O',O$- $C_{12}H_6N_2O_2$-*N,N'*)$Ru(PPh_3)_2Cl_2$ as shown in Scheme 8. The crystal structure of the bridged complex [$(PPh_3)_2Pt(O',O$- $C_{12}H_6N_2O_2$-*N,N'*)$Ru(PPh_3)_2Cl_2$ is shown in Figure 30[57].

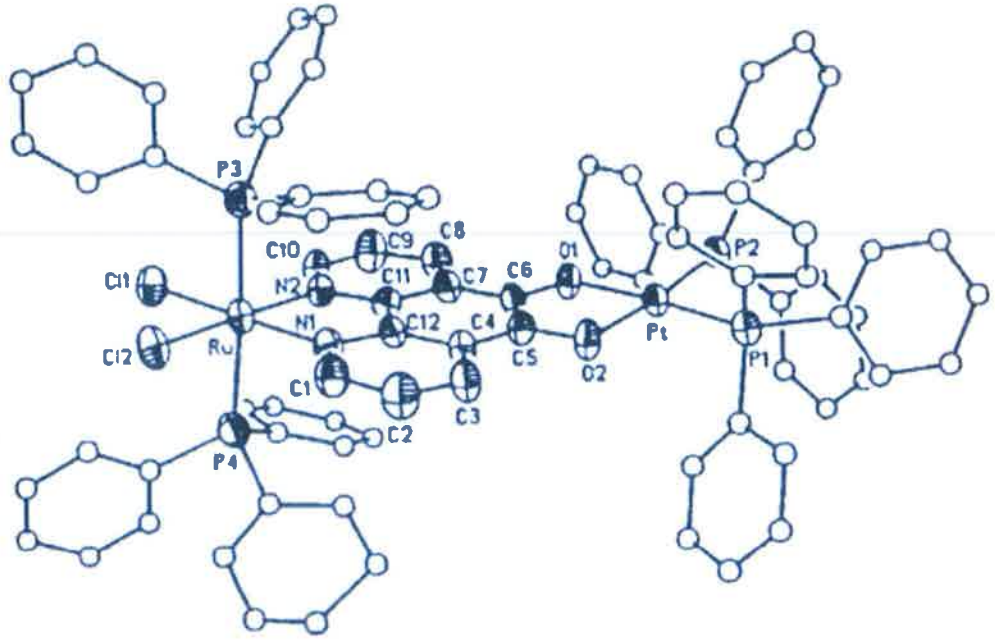

Figure 30: X-Ray crystal structure of [$(PPh_3)_2Pt(O',O$- $C_{12}H_6N_2O_2$-*N,N'*)$Ru(PPh_3)_2Cl_2$[57]

In 2007, Saravani et al.[43] reported the synthesis and characterisation of the mono-phendione complex [Cu(tpy)(phendione)]$(PF_6)_2.CH_3CN$, (tpy = 2,2';6',2"-terpyridine), (Figure 31)[43].

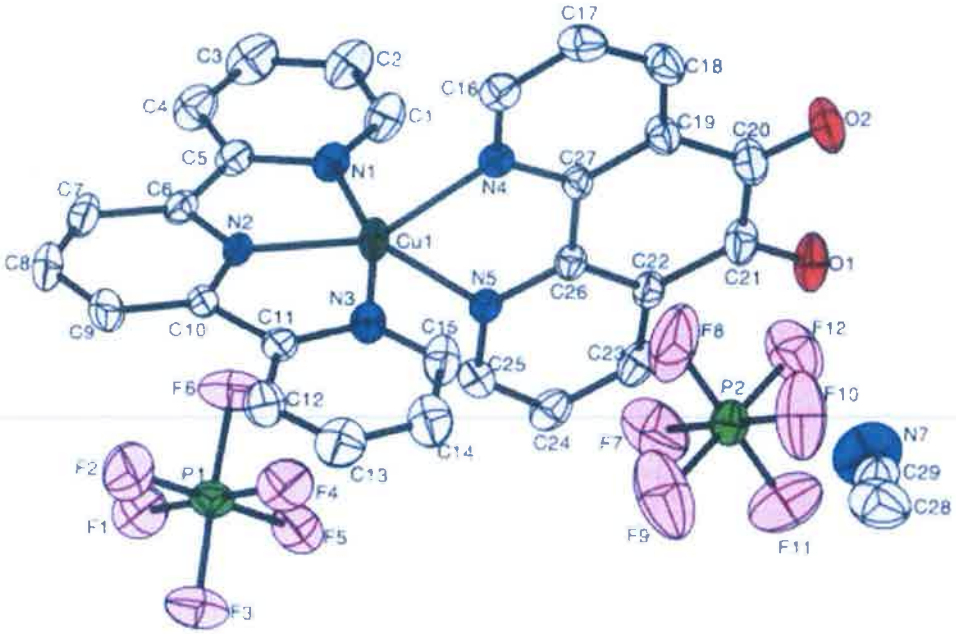

Figure 31: X-Ray crystal structure of mono-phendione complex [Cu(tpy)(phendione)]$(PF_6)_2.CH_3CN$[43]

The five coordinated Cu^{2+} complex [Cu(tpy)(phendione)]$(PF_6)_2.CH_3CN$ was synthesized (Figure 31) in good yield, forming green crystals. From the crystal structure, the Cu^{2+} complex has a coordinated geometry with a distorted trigonal bipyramid. The 2,2';6',2"-terpyridine ligand is coordinated to the Cu^{2+} via three N atoms and the mono-phendione ligand is also coordinated to the Cu^{2+} atom via two N atoms. Since PF_6 is experiencing steric hinderance in the unit cell, π-π interaction of the terpyridine ligand cannot occur[43].

As previously mentioned by this group[17], for its anti-fungal activity, the Ag^+ complex $[Ag(phendione)_2]ClO_2$ is an example of a bis-phendione complex as indicated in Figure 18. The Ag^+ atom which lies in a pseudo tetrahedral environment is bonded to four N atoms from two bidentate phendione ligands. The perchlorate ion is uncoordinated to the Ag^+ atom and distorted about the axis.

I.5 DERIVATIVES OF 1,10-PHENANTHROLINE AND 1,10-PHENANTHROLINE-5,6-DIONE (1)

1,10-Phenanthroline (phen) can essentially be substituted at all of the positions from position 2 to 9 {Figure 1(a)}. Some examples of mono-substituted phen derivatives are shown in Figures 32(a)-(h).

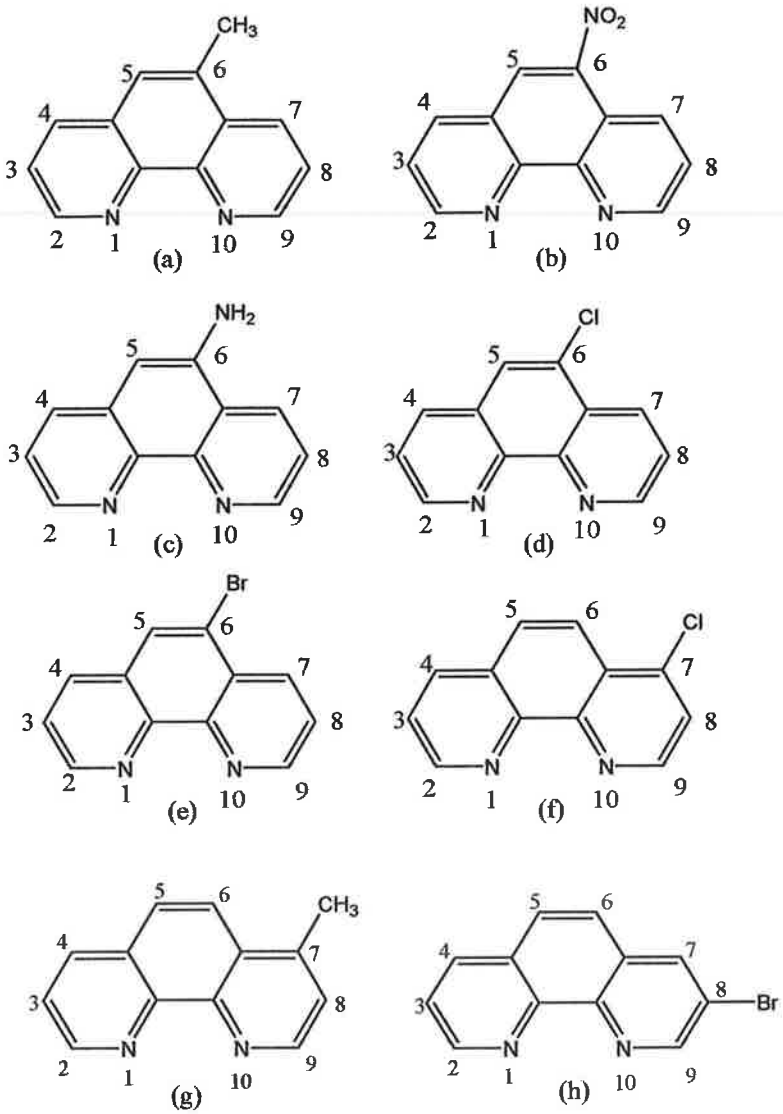

Figure 32: Examples of mono-substituted phen derivatives

5-Methyl-1,10-Phenanthroline (5MPhen) is similar in structure to the unsubstituted-phen ligand with the addition of a methyl group at position 5 as indicated in Figure 32(a). The synthesis and structural characterization of a novel Cu^{2+} derivative from phen and tda (thiodiacetate (2-) ion) was reported in 2005 by Alarcon-Payer et al.[58] As shown in Scheme 9, copper(II) carbonate hydroxide and thiodiacetic acid were reacted in water by heating and stirring under reduced pressure. Once a clear blue solution was obtained 5MPhen was added and stirred. The resulting blue solution was then filtered followed by evaporation, yielding blue crystals of complex $[Cu(tda)(5Mphen)].2H_2O$[58].

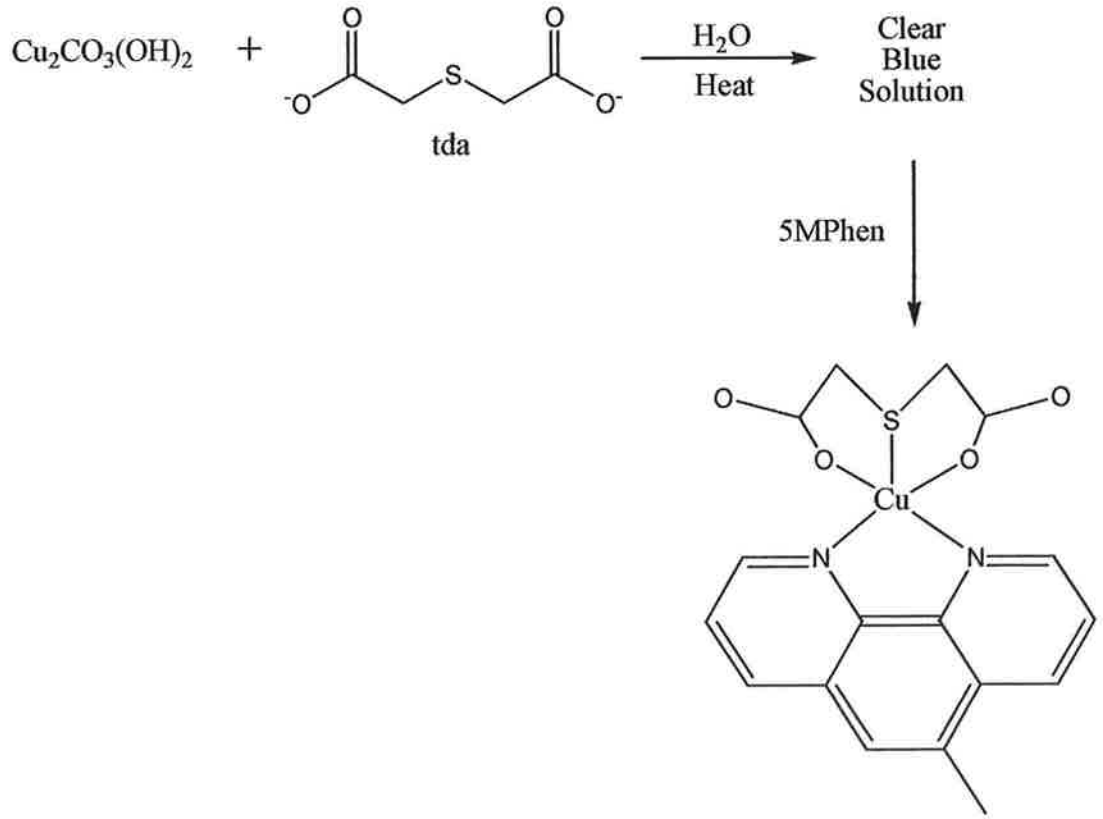

Scheme 9: Synthetic route to $[Cu(tda)(5Mphen)].2H_2O$[58]

The crystal structure of the asymmetric copper(II) complex [Cu(tda)(5Mphen)].$2H_2O$ as shown in Figure 33, consists of complex molecules and non-coordinated water molecules. The Cu(tda) is ligated by two nitrogen atoms from the chelating 5Mphen molecule. The copper(II) displays a distorted square pyramidal coordination of type 4 + 1, while the tda ligand exhibits only a fac-O_2 and S (apical) – tridentate conformation. The Cu-S (apical) has a bond length of 2.572 Å. Both chelating rings in the mean planes of complex [Cu(tda)(5Mphen)].$2H_2O$ share the Cu-S bond. This Cu-S bond defines a dihedral angle of 84.4 °. The Cu-S bond diverges from the perpendicular plane to the mean based plane at an angle of 19.3 °. Owing to the centroid-centroid distance and the slipping angles of appropriate rings exceed from 4.4 Å and 40 °, respectively, there are no π,π-stacking interactions between aromatic rings of adjacent 5Mphen ligands[58].

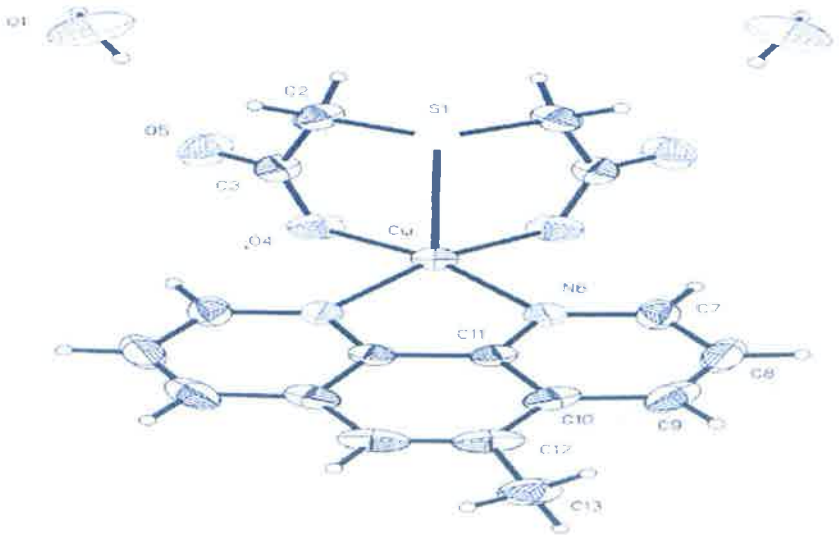

Figure 33: The X-Ray crystal structure of [Cu(tda)(5Mphen)].$2H_2O$[58]

5-Nitro-1,10-phenanthroline (5-NO_2-phen) is a ligand derived from 1,10-phenanthroline in which it has a nitro group attached to the phen molecule on position 5, {Figure 31(b)}. The molecular structure and binding of cobalt complex [Co(mnt)(5-NO_2-phen)], (mnt = maleonitriledithiolate) was recently reported by Liu et al.[59] In this case, the Co(mnt) is ligated by two nitrogen atoms from the chelating phen molecule as indicated in Figure 34[59].

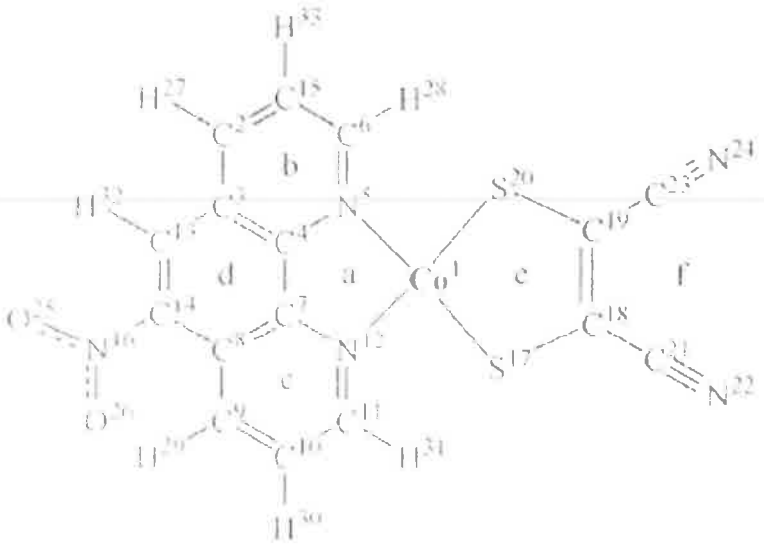

Figure 34: The molecular structure and binding of cobalt complex Co(mnt)(5-NO_2-phen)[59]

Complex Co(mnt)(5-NO_2-phen) contains bands in the visible region (400 nm–500 nm), which are not present in 5-NO_2-Phen. These bands are characteristic of inter-ligand π-π* charge transfer transitions (LL'CT) from dithiolate to di-imine ligands or metal to ligand charge transfer (MLCT) from the metal/dithiolate to the di-imine[59].

5-Amino-1,10-phenanthroline (5-NH_2-phen) as indicated in Figure 32(c), is a widely used chelating ligand in coordination chemistry. 5-NH_2-phen has been used in either the form of a ligand or in the form of a complex, in areas such as "molecular catalysis, solar energy conversion, colorimetric analysis, herbicides, molecular recognition, self-assembly, anti-neoplastic agents, nucleic acid probes and the development of luminescene base sensors for pH, anions and cations"[24].

Recently, the synthesis and characteristics of a novel palladium(II) 5-NH_2-phen complex, has been reported by Wesselinova et al.[60]. Reaction of Pd^{2+} with 5-NH_2-phen yielded orange brown crystals of Pd(5-NH_2-phen)$_2$(NO_3)$_2$, resulting in a strong action against the cancer myeloid s.c. tumor transplanted in hamsters. The anti-tumor activity of Pd(5-NH_2-phen)$_2$(NO_3)$_2$ was compared with the activity of palladium(II) 1,10-phenanthroline complex Pd(phen)$_2$(H_2O)(NO_3)$_2$ also synthesized by this group. (It has been stated by this group, "Unfortunately, detailed structure studies by X-ray analysis was not possible because of the difficulties in obtaining suitable single crystals."[60]) When the activity of both complexes were compared, the palladium(II) 1,10-phenanthroline complex did not show any anti-tumour activity, whereas the palladium(II) 5-NH_2-phen complex demonstrated a strong anti-tumour effect. As the amino group is an electron donor substituent, the electron density in the aromatic ring is increased and also since the cation Pd^{2+} contains 8d-electrons in the outer shell, the complexes formed with bidentate ligands are very stable. The presence of the amino group attached to the aromatic system of the 1,10-phenanthroline in complex [Pd(5-NH_2-phen)$_2$(NO_3)$_2$] is essential for the activity as the mean survival time of the

hamster suffering from the cancerous myeloid s.c. tumour is 1.65 times longer than the control[60].

5-Chloro-1,10-phenanthroline, 5-bromo-1,10-phenanthroline and 4-chloro-1,10-phenanthroline as indicated in Figures 31(d), (e) and (f) are examples of mono-substituted 1,10-phenanthroline derivatives with the addition of a halide ion on position 5 or position 4 of the chelating phenanthroline ligand. An example of a 1,10-phenanthroline ligand mono-substituted with a methyl group on the fourth position is 4-methyl-1,10-phenanthroline, as shown in Figure 32(g).

A 1,10-phenanthroline ligand with the addition of halide ions on position 3 is indicated in Scheme 10. Tor et al.[61] demonstrated that by reacting phen with bromine in bromobenzene, the synthesis of 3-bromo-1,10-phenanthroline {Figure 32(h)} could be successfully achieved, {Scheme 10(1)}[61].

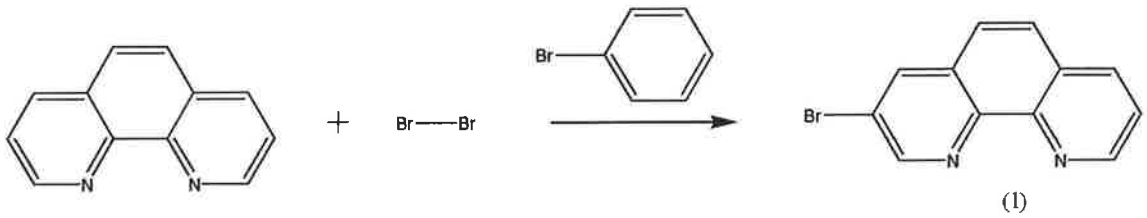

(1)

Scheme 10: Synthesis of 3-bromo-1,10-phenanthroline **(1)**[61]

The 4-position of the coordinated pyridine ring of 3-bromo-1,10-phenanthroline **(1)** is naturally electrophilic, which is not the case for the 3-position. From the synthesis of 3-bromo-1,10-phenanthroline **(1)** complex **2** was prepared[61], (Figure 35).

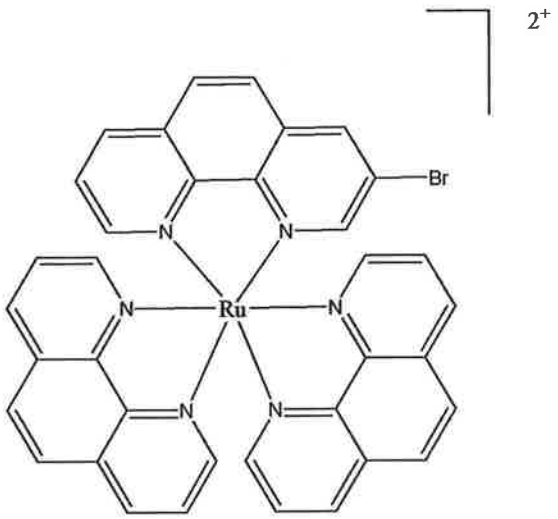

Figure 35: 1,10-phen derivative ruthenium complex **(2)**[61]

During the synthesis of ruthenium complex **2,** high efficiency was achieved by "(i) 'protection' of the phen nitrogens from coordinating the transition metal catalysts, and (ii) the electron deficiency of the Ru^{2+} coordinated 3-bromo-1,10-phenanthroline that facilitates the oxidative-addition of the catalytically-active Pd(0) species across the phen-Br bond"[61].

This group also discovered that when complex **2** was reacted with soft nucleophiles such as thiolates, the substitution reaction worked reasonably well, Scheme 11. The use of other nucleophiles such as hard nucleophiles (fluoride ions) may not work as well as soft nucleophiles or nucleophiles reacted under different conditions may not work at all[61].

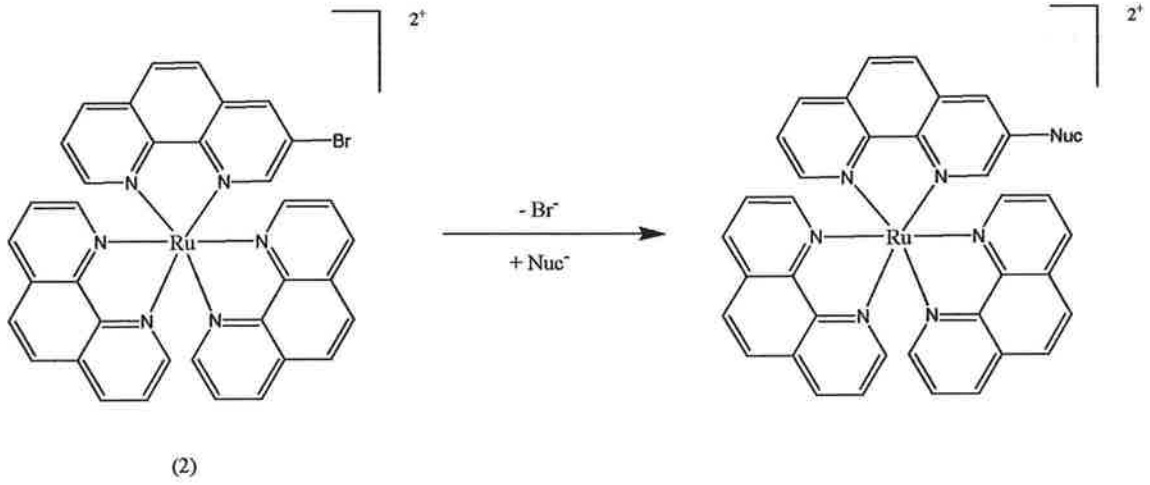

(2)

Scheme 11: Functionalised coordination compounds can be substituted with various nucleophiles (Nuc = RS, RO, Aro, Ar_2P, F)[61].

Metal-containing amino acid complexes were also reported by this group such as a ruthenium phen complex containing cysteine obtained by an aromatic nucleophilic substitution reaction[61], (Scheme 12).

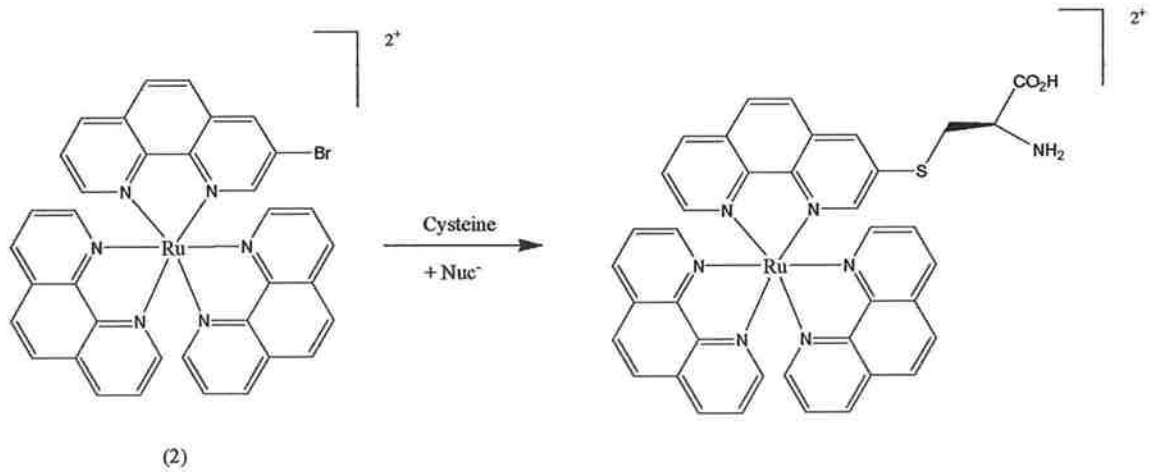

(2)

Scheme 12: A metal-containing amino acid aromatic nucleophilic substitution reaction with functionalized complex **2**[61]

Progressively more and more important roles have been described for the 1,10-phenanthroline ligands in different transition metal complexes which has stimulated the preparation of many phen derivatives such as 2,9-, 5,6-, 3,8- and 4,7-disubstitutes. Some examples of di-substituted phen and 1,10-phenanthroline-5,6-dione (phendione) derivatives are shown in 36(a)-(j).

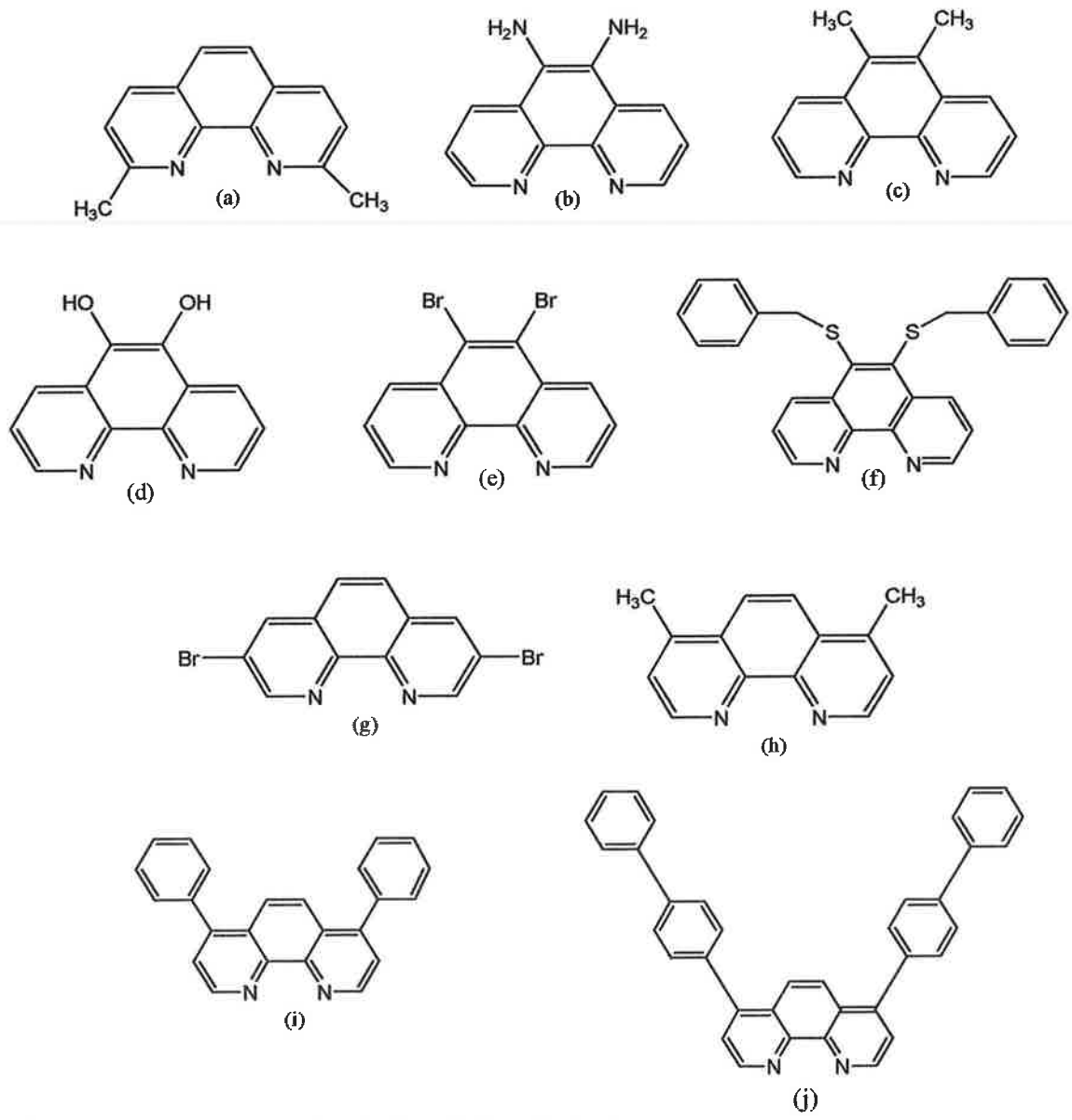

Figure 36: Examples of di-substituted phen derivatives

In achieving a method to develop the first synthesis of substituted 1,10-phenanthrolines from pyridines, Chelucci et al.[62] once again employed the Wittig reaction between 2-bromo-6-methylpyridine-3-carbaldehyde **(1b)** and phosphomiun salt **(2b)** (1.2 equivalant of **2b**, 2.2 equivalence of $KOBu^t$, TMF, room temperature, 18 hours), resulting in the formation of (z)-1,2-bis(2-bromo-6-methylpyridine-3-yl)ethane **(3b)** with an exceptional yield of 97 %. Furthermore, (z)-1,2-bis(2-bromo-6-methylpyridine-3-yl)ethane **(3b)** was submitted to intra-molecular Ullman coupling resulting in phen derivative 2,9-dimethyl-1,10-phenanthroline **(4b)**[62], (Scheme 13).

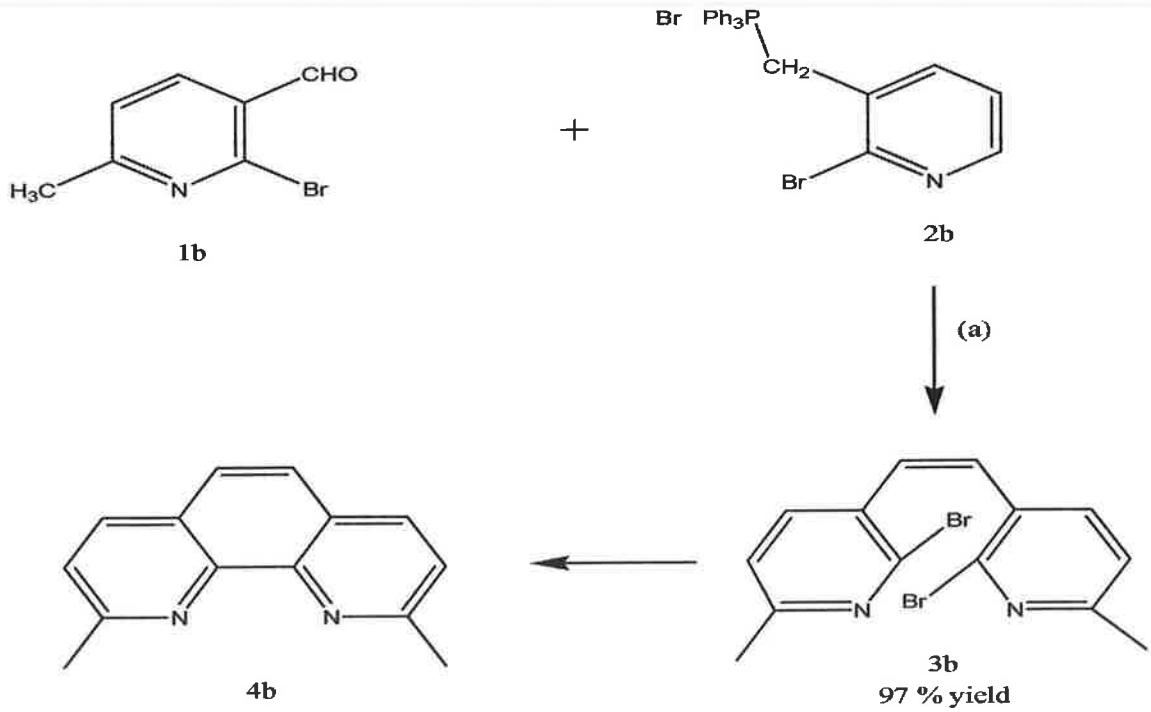

Scheme 13: Two step synthesis of 1,10-Phenanthroline derivative 2,9-dimethyl-1,10-phenanthroline **(4b)**, {**(a)** : 2b (1.2 equivalence), $KOBu^t$ (2.2 equivalence), TMF, room temperature, 18 hours}[62]

2,9-Dimethyl-1,10-phenanthroline (2,9-DMP) commonly known as neocuproine is similar to phen in structure with the addition of two methyl groups at position 2 and position 9 as indicated in Figure 36(a).

The 2 and 9 positioning of the methyl groups on the phen bestows upon this derivative specificity for the cuprous ions. It has been reported by Mohindru et al.[20] that 2,9-DMP is a potent copper-dependent cytotoxin which is biologically active only as the coordinated metal complex. When tested *in-vivo* against the L1210 leukemia-bearing mice the copper-2,9-DMP was only slightly effective and when testing took place on P388 leukemia-bearing mice their life span increased significantly[20].

The synthesis and structural characterization of three novel Cu^{+} and Cu^{2+} derivatives from phen and dmp (2,9-dimethyl-1,10-phenanthroline) has been recently reported by Latham et al.[63]. Spontaneous oxidation took place during the addition of phenylphosphate acid to $[Cu^{+}(phen)_2]Cl^{-}$ as Cu^{+} changes to an oxidation state of Cu^{2+} in the production of $[Cu^{2+}(phen)_2Cl][C_6H_5PO_2(OH)\cdot C_6H_5PO_2(OH)_2]$ **(1)**. Reaction of Cu^{+} chloride with dmp yielded red, needle–like crystals of complex $[Cu^{+}(dmp)_2]Cl.MeOH.5H_2O$ **(2)**. The oxidation state of Cu^{+} in this case remained. When Cu^{+} and phen forms a complex, the phenanthroline ligand tends to leave the Cu^{+} centre exposed to oxidation but when Cu^{+} and dmp forms complexes the Cu^{+} centre is more likely to be protected from oxidation than in the case of the phen copper complex. This could be due to the somewhat bulky 2- and 9- positions on the dmp containing complex or that the geometry of a Cu^{+} complex is more preferential than a Cu^{2+}complex[63].

Addition of phenylphosphonic acid to complex **2**, resulted in the formation of green needle-like crystals of $[Cu^{2+}(dmp).(H_2O)_2.(C_6H_5PO_2(OH))_2]$ **(3),** Scheme 14.

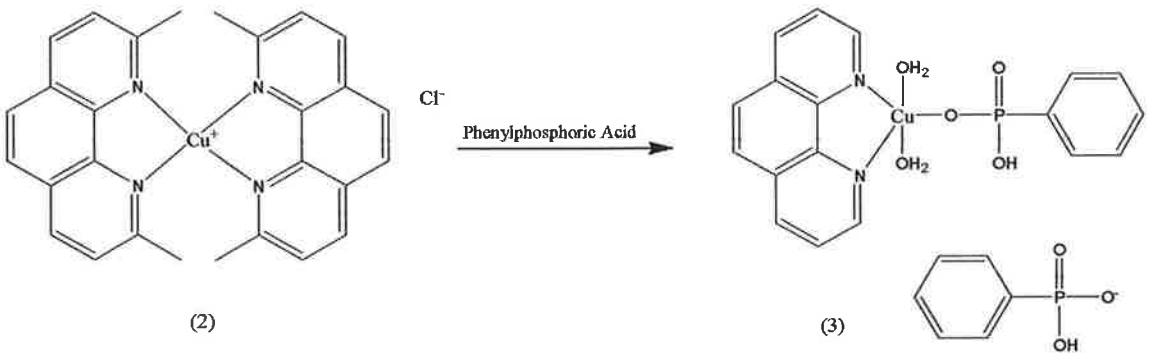

(2) (3)

Scheme 14: Synthesis of $[Cu^{2+}(dmp).(H_2O)_2.C_6H_5PO_2(OH)].[C_6H_5PO_2(OH)]$ **(3)**[63]

It is clear from Scheme 14 that unlike complex **2**, complex **3** does not contain any chloride. The single dmp ligand is now bonded to a 5-coordinated Cu^{2+} species. Prior to the addition of the acid, the Cu^{+} state in complex **2** was not maintained, resulting in the cleavage of the dmp ligand and the oxidation of the metal[64].

The analysis confirmed the Cu^{+} atom was ligated by four nitrogen atoms from the two chelating dmp molecules. The cationic $[Cu^{+}(dmp)_2]^{+}$ is counter balanced by a chloride anion with one methanol and five water molecules (Figure 37). Complex **2** can be said to have a 4-coordinated geometry which is characteristic of a Cu^{+} d^{10} complex. This is due to the fully filled d^{10} orbital shell partaking in metal-to-ligand charge–transfer and the excitation of electrons the Cu^{+} donated to the ligand (phen and phenanthroline derivatives)[63].

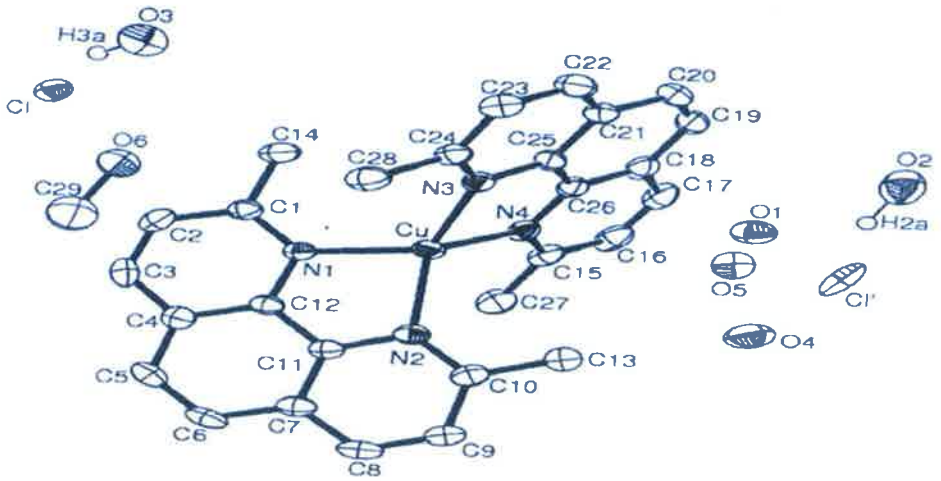

Figure 37: X-Ray crystal structure of $[Cu^{+}(dmp)_2]Cl.MeOH.5H_2O$ **(2)**[63]

X-Ray crystal analysis of complex **3** illustrated that Cu^{2+} atom was ligated by two nitrogen atoms from a single chelating dmp molecule, one phenyl phosphate ion and two water molecules (Figure 38). It can be clearly seen that complex **3** has a 5-coordinated geometry. It is characteristic of a complex with the oxidation state of Cu^{2+} d^9 to have either a 5- or 6- coordinated geometry[63].

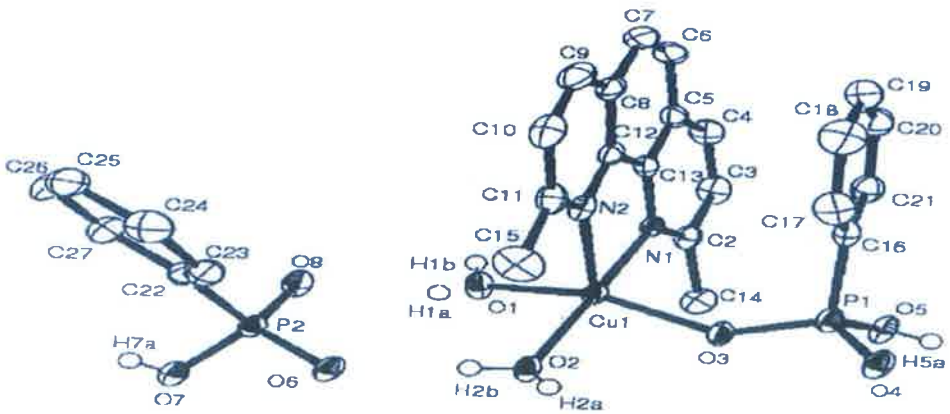

Figure 38: X-Ray crystal structure of

$[Cu(dmp).(H_2O)_2{\cdot}C_6H_5PO_2(OH)].[C_6H_5PO_2(OH)]$**(3)**[63]

1,10-Phenanthroline-5,6-diamine (phendiamine), {Figure 36(b)} contains important properties in respect to its abilities to directly bridge two metal centres through its four nitrogen atoms or alternatively be condensed with a range of ortho-quinones to form other derivatives[42] such as di-pyrido[3,2-f:2',3'-h]quinoxaline (dpy) {Figure 39(a)} and dipyrido[3,2-a:2',3'-c]phenazine (dppz) {Figure 39(b)}. Both dpy and dppz act as good bidentate ligands, binding well to DNA since their π accepting character and nitrogen sites enables them to intercalate with DNA[64].

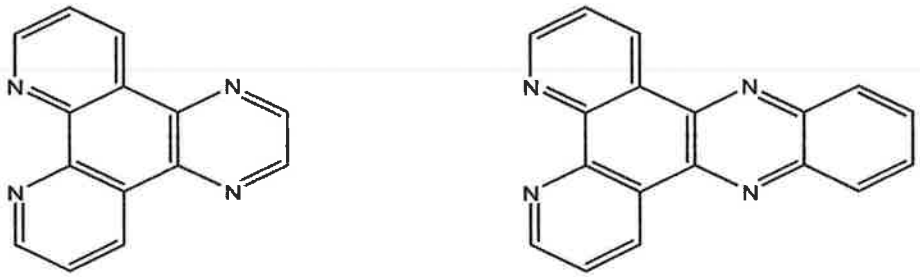

(a) (b)

Figure 39: Structure of **(a)** di-pyrido[3,2-f:2',3'-h]quinoxaline (dpy) and **(b)** dipyrido[3,2-a:2',3'-c]phenazine (dppz)[64]

Recently, Miranda et al.[64] reported the synthesis of a new polycyclic conjugate derivative of phendione, known as dipyrido[3,2-f:2',3'-h]quinoxaline[2,3-b]quinoxaline ring (dpq-QX), (Figure 40).

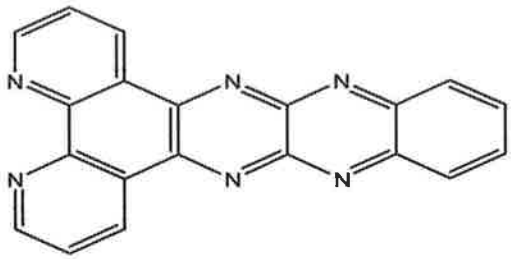

Figure 40: Structure of dpq-QX[64]

This ligand is the first of its kind to contain both the tetraazonaphthacene and the bipyridine moieties in the same molecule. The structure of heterocyclic dpq-QX contains six condensation rings and six nitrogen atoms. Among the six nitrogen atoms, two of them are di-iminic nitrogen atoms of the phendione ligand and the other four are positioned on the tetraaza region of the ligand[64].

After other groups had reported the synthesis of phendiamine but failed to produce yields of any great proportions, Bodige et al.[65] reported a two step synthesis of phendiamine from phendione with a significantly high yield of 83 %, approximately triple the yield in comparison of those previously obtained, (Scheme 15)[65].

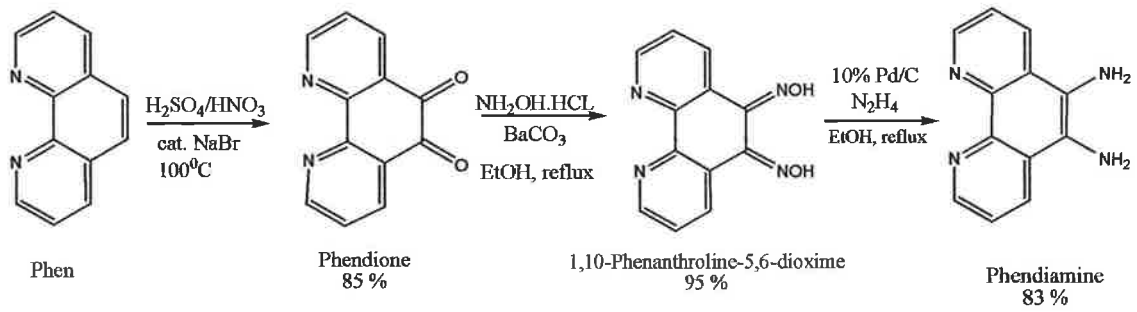

Scheme 15: Reaction scheme for the synthesis of 1,10-phenanthroline-5,6-diamine[65]

In 2006, a series of Ru^{2+} complexes of 5,6-dimethyl-1,10-phenanthroline (5,6-dmp), {Figure 36(c)}, were synthesized and characterised by Maheswari et al[66]. When tris(5,6-dmp) complex $[Ru(5,6\text{-dmp})_3]^{2+}$ was investigated, it was found to bind to DNA and when DNA binding was compared to that of the phen analogue $[Ru(phen)_3]^{2+}$, $[Ru(5,6\text{-dmp})_3]^{2+}$ was found to bind more strongly to DNA[66].

Another example of Ru^{2+} complexes of 5,6-dmp being the stronger binder to DNA than its phen analogue was when the bis(5,6-dmp) complex $[Ru(5,6\text{-dmp})_2(dppz)]^{2+}$ was reported to bind to calf thymus DNA more strongly than $[Ru(phen)_2(dppz)]^{2+}$ [66]. It was also reported by this group that complexes of 5,6-dmp bind to DNA through the co-ligand face while the 5,6-dmp ligands are concerned with hydrophobic interaction with the DNA exterior. When the number of 5,6-dmp ligands in each of the Ru^{2+} complexes were compared, the DNA binding constants varied in the order of tris(5,6-dmp)Ru(II) being the strongest followed by bis(5,6-dmp)Ru(II) and then mono(5,6-dmp)Ru(II) being the least strong of the three types of complexes. This is due to the shape and hydrophobicity of the complex. For this reason it can be said that the shape and hydrophobicity of the complex preside over the DNA binding affinity of complexes[66].

1,10-Phenanthroline-5,6-diol (H_2pdol) is similar to phendione in structure in which the C=O groups of the phendione positioned on the 5 and 6 position are replaced by the C-OH groups as indicated in Figure 36(d). In 2004, Larsson et al.[67] prepared and structurally characterised the complex $[Co(H_2pdol)_2(pdon)]^{3+}$, (pdon = phendione) (Figure 41) by X-ray crystallography. From the crystal structure the Co is octahedraly coordinated to two H_2pdol and one pdon ligand[67].

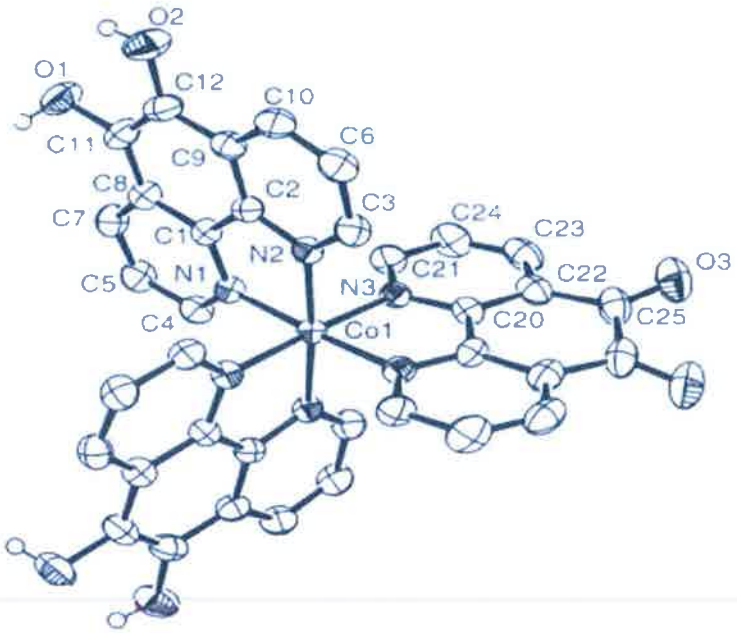

Figure 41: X-Ray crystal structure of $[Co(H_2pdol)_2(pdon)]^{3+}$ [67]

Rabaca et al.[68] have recently investigated 1,10-Phenanthroline-5,6-diol in the synthesis of 5,6-bistosyl-1,10-phenanthroline. To a suspension of 1,10-phenanthroline-5,6-diol in dry pyridine was added p-toluene sulphonyl chloride and reacted to synthesise 5,6-bistosyl-1,10-phenanthroline, as shown in Scheme 16 [68].

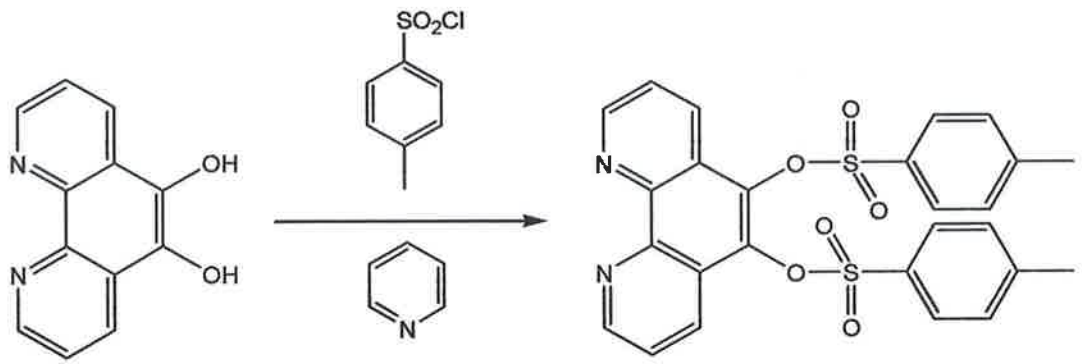

Scheme 16: Synthesis of 5,6-bistosyl-1,10-phenanthroline[68]

Rabaca et al.[68] have also investigated the synthesis and characterization of 5,6-dibenzyltiol-1,10-phenanthroline from starting material 5,6-dibromo-1,10-phenanthroline, {Figure 36(e)}.

5,6-bistosyl-1,10-phenanthroline (Scheme 16) and 5,6-dibenzyltiol-1,10-phenanthroline {Figure 36(f)} ligands are very interesting and attractive dithio-diazo ligands as they possess two different coordination functionalities (the di-imine functionality and the dithiolate functionality). The ability of these ligands to connect to different coordination species may be helped by their extensive electronic delocalization[68].

The compounds 5,6-bistosyl-1,10-phenanthroline and 5,6-dibenzyltiol-1,10-phenanthroline have been characterised by simple crystal X-ray diffraction. The crystal structure of 5,6-bistosyl-1,10-phenanthroline (Figure 42), consists of the two oxygen atoms attached to the 5,6-substituted positions of the 1,10-phenanthroline core molecule, which are almost planar. The two tosyl groups are positioned in opposite directions with respect to the 1,10-phenanthroline core plane[68].

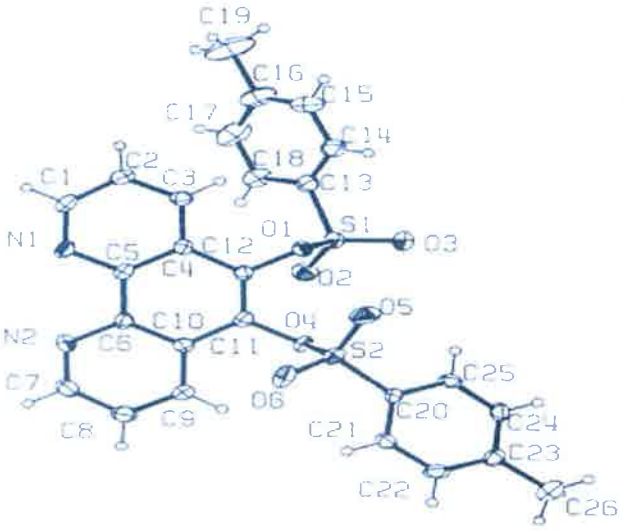

Figure 42: X-Ray crystal structure of 5,6-bistosyl-1,10-phenanthroline[68]

The crystal structure of 5,6-dibenzyltiol-1,10-phenanthroline (Figure 43), consists of two sulphur atoms attached to the 5,6-substituted positions of the 1,10-phenanthroline core molecule, which is almost planar. The two benzyl groups are attached to the two sulphur atoms[68].

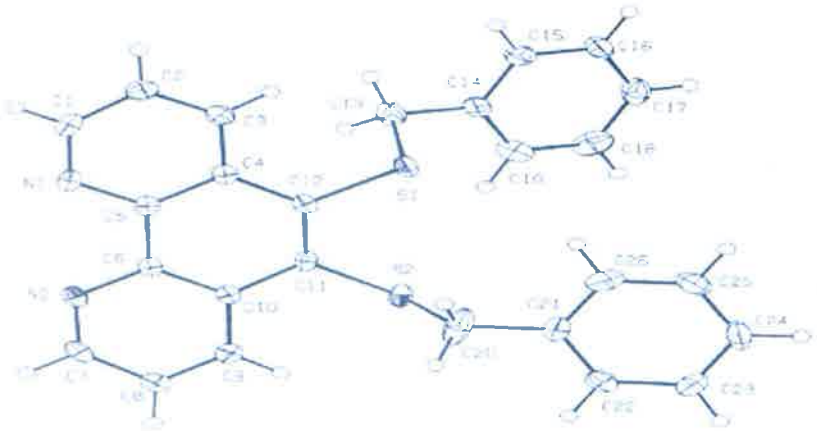

Figure 43: X-Ray crystal structure of 5,6-dibenzyltiol-1,10-phenanthroline[68]

To date, not many structural investigations have been performed on halide substituted phen complexes. As shown in Figure 36(g), 3,8-dibromo-1,10-phenanthroline is an example of a di-halide substituted 1,10-phenanthroline complex. Recently, Wang et al.[69] synthesized and structurally characterised two novel cadmium(II) complexes of $[Cd(3,8\text{-dibromo-}1,10\text{-phen-}_K{}^2N,N')\text{-}(_L\text{-tar})]_n$ **(1)** and $[Cd(3,8\text{-dibromo-}1,10\text{-phen-}_K{}^2N,N')_2(NO_3\text{-}_K{}^2O,O')_2)](CH_3CN)$ **(2)**[69].

The crystal structure of complex **1**, (Figure 44) in each independent crystal unit, is composed of one Cd^{2+} ion, two half $_L$-tar ($_L$-tartaric acid) dications and one chelating 3,8-dibromo-phen ligand. The central Cd^{2+} ion is coordinated to seven different atoms, two nitrogen atoms from the chelating 3,8-dibromo-phen ligand, three oxygen atoms from two μ-carboxylic ends of two $_L$-tar dications and two oxygen atoms from the third chelating carboxylic end of the $_L$-tar ligand, forming a distorted pentagonal bipyramid geometry[69].

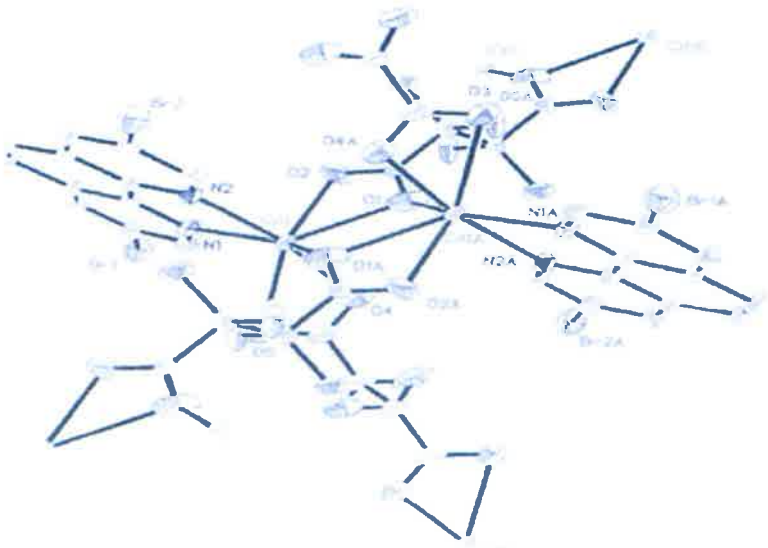

Figure 44: X-Ray crystal structure of $[Cd(3,8\text{-dibromo-}1,10\text{-phen-}_K{}^2N,N')\text{-}(_L\text{-tar})]_n$ **(1)**[69]

The crystal structure of complex **2**, (Figure 45) contains one Cd^{2+} ion, two bidentate 3,8-dibromo-1,10-phenanthroline molecules and two bidentate NO_3^- anions. A single solvent molecule of CH_3CN is also present, (not shown in Figure 45). The central Cd^{2+} ion is coordinated to eight different atoms, four are chelated from the Cd^{2+} to the four nitrogen atoms of the two phen ligands and the other four are four oxygen atoms of the two NO_3^- anions[69].

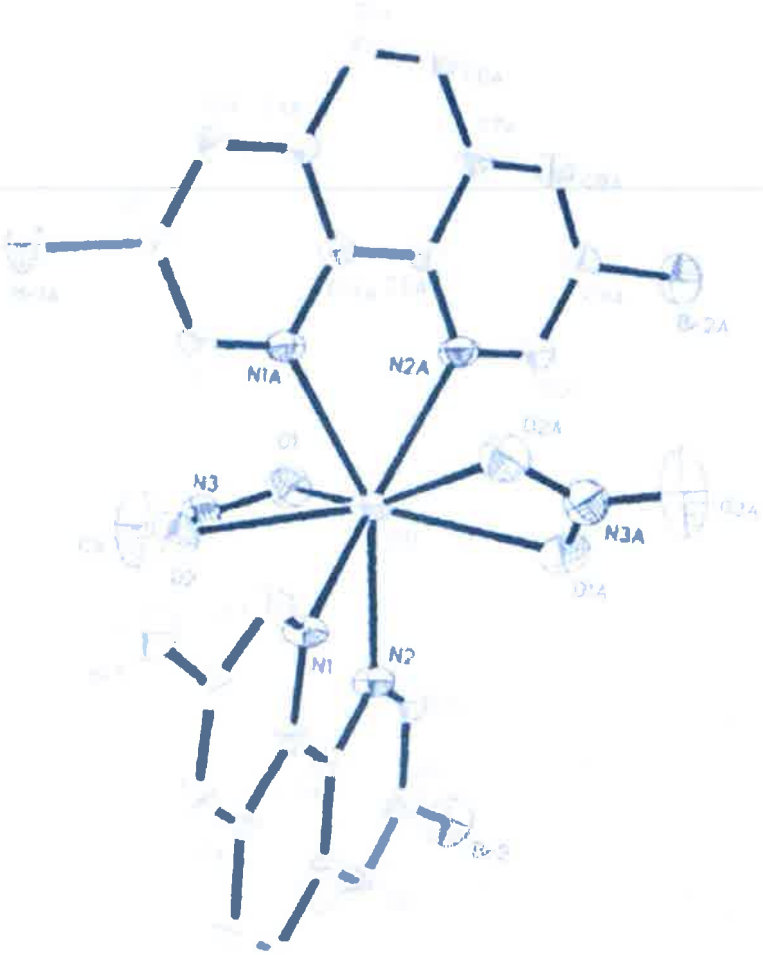

Figure 45: X-Ray crystal structure of

$[Cd(3,8\text{-dibromo-}1,10\text{-phen-}\kappa^2N,N')_2(NO_3\text{-}\kappa^2O,O')_2)](CH_3CN)$ **(2)**[69]

Up to now, there are not too many investigations on anti-cancer activity of metal derivatives of 4,7-dimethyl-1,10-phenanthroline, {Figure 36(h)}. Recently, Shahabadi et al.[70] synthesized the complex [$PtCl_2$(4,7-Me_2Phen)], (Figure 46), where 4,7-Me_2Phen corresponds to 4,7-Dimethyl-1,10-phenanthroline. Once characterised, this platinum(II) complex was reported to have a strong intercalating relationship with calf thymus DNA[70].

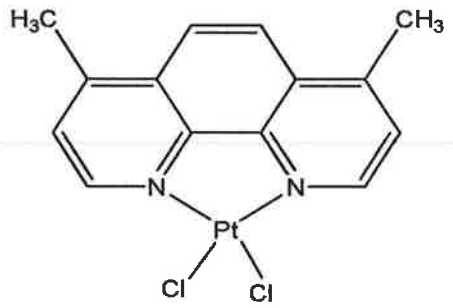

Figure 46: Structure of [$PtCl_2$(4,7-Me_2Phen)][70]

When ligand 4,7-diphenyl-1,10-phenanthroline (Ph_2phen), {Figure 36(i)}, was used in a Ru^{2+} metal complex, it was found to interact with DNA. It was reported by Mongelli et al.[71] that complex [Ru(Ph_2phen)$_3$]$^{2+}$ had the ability to groove bind with double stranded DNA. When compared with its phen analogue, the binding with the major groove of DNA was weaker while its bipy analogue could only achieve electrostatic binding to DNA[71].

4,7-Bis(biphenyl)-1,10-phenanthroline, {Figure 36(j)}, is similar in structure to 4,7-diphenyl-1,10-phenanthroline shown in {Figure 36(i)}, with the addition of two phenyl

I.6 METAL COMPLEXES AS ANTI-CANCER AGENTS

I.6.1 Introduction

Many agents used as anti-cancer, anti-viral and anti-septic drugs become active while binding to DNA and these drugs bind by hydrogen bonds, hydrophobic interaction and through electrostatic forces[73,74].

There are three main modes which allow drugs to bind to DNA; intercalation, groove binding and electrostatic binding[73,74]. Intercalation is the most favourable mode of binding for metal complexes to DNA. This is due to the involvement of π-stacking intercalation of a ligand between base pairs of DNA. For π-stacking intercalation to be achieved, the intercalating ligand must be "a flat, extended aromatic system, which is annulated with heterocyclic rings, e.g. pyridine and pyrazine"[75]. Metal complexes of phen and modified phen ligands are being recognised as novel diagnostic and therapeutic agents that can cleave and recognise DNA[44]. This class of complex generally interacts with DNA by intercalation.

One of the best known transition metal complexes used today as an anti-cancer agent is the platinum complex, cisplatin [cis-diaminedichloroplatinum(II)]. The cytotoxicity of cisplatin occurs due to its ability to bind to DNA and the chloride ions of the cisplatin complex become displaced by hydroxyl groups. The major adduct formed by covalent cross-linking results in the inhibition of DNA replication and transcription[76,77]. Since its discovery several synthesized derivatives have exhibited similar and, in some cases, improved activity in the treatment of a variety of solid tumors, especially testicular

cancer. Cisplatin is used in combination with other drugs and brain, ovarian, bladder and breast cancer can be successfully treated[78]. Alternative transition metal complexes are being researched at present which are as effective yet do not cause the potent side effects associated with cisplatin (nausea, vomiting and severe nephrotoxicity)[22,79].

I.6.2 Metal phenanthroline anti-cancer agents

Phen and its derivative phendione disturb the functioning of a wide range of biological systems in both the metal free-state and coordinated to transition metals. They are not readily expelled from cells and unlike cisplatin, phen and phendione complexes are non-mutagenic[80] . When metal-free N-N'- chelating bases are found to be bioactive it is usually assumed that the sequestering of trace metals *in situ* is involved and that the resulting metal complexes are the active species[22,81]. This group and its co-workers have shown that these donor ligands in their metal-free state or in a range of their Cu^{2+}, Mn^{2+} and Ag^{+} carboxylate complexes are considerably more active anti-cancer agents than the well known cisplatin against selective cancer cell lines[80].

In 1996, it was reported by Tsang et al.[77] that $[Cu(phen)_2]^{2+}$ when incubated in a human hepatic cell line (Hep-G2), internucleosomal DNA fragemtation resulted which is a characteristic of apoptosis[22,49,77]. It was then reported by Zhou et al.[82] in 2002, that $[Cu(phen)_2]^{2+}$ caused G_1-specific apoptosis in a liver carcinoma cell line (Bel-7402). Furthermore, this Cu-bis phen complex was shown to up-regulate the DNA-binding activity of p53, a molecule known to be pivotal in the regulation of cell progression, cell survival, and apoptosis[22,49,77,83]. In 2006, Yokoyama et al.[84] reported that ruthenium

phendione complexes can chemically modify proteins such as cytochrome c. This is due to the ability of phendione to coordinate directly with different metal centres via its o-quinoid moiety. As a result, reactivity is increased giving reason to suggest that these metal complexes may act as chemical modifiers[84].

Palaniandavar et al.[85] reported in 2006, the DNA binding properties of two Cu^{2+} complexes derived from iminodiacetic acid and incorporating the phen ligand. The complex Cu(imda)(phen)(H_2O) **(1)** (imda = iminodiacetic acid) bonded to DNA through partial intercalation, while complex Cu(imda)(5,6-dmp) **(2)** (5,6-dmp = 5,6-dimethyl-1,10-phenanthroline) was involved in groove binding of DNA. In the presence of ascorbic acid both complexes showed cleavage of pBR322 supercoiled DNA and when light or a reducing agent was restricted these complexes showed hydrolytic DNA cleavage activity[86]. Then in 2008, Chanderasekhar et al.[87] reported the DNA cleavage ability of complex $[Cu(\mu\text{-}OH)(\mu_3\text{-}C_6H_{11}PO_3)_2(phen)_4(H_2O)_2](NO_3)_3$ resulting in only partial conversion of the supercoiled pBR322 DNA of only 40 %[87].

In 2006, this research group reported the chemotherapeutic potential for phen, phendione and a series of its coordinated analogues, where malonic acid acts as a coordinated counter ion[4], as shown in Table 11. Also shown in the same table are the chemotherapeutic potentials of Cu^{2+} and Ag^{+} perchlorate complexes of phendione[22]. These results are shown in conjunction with the activity of cisplatin and simple metal salts.

Table 11: The chemotherapeutic potential for phen, phendione and their metal complexes along with the metal salts[4,22]

Complex	**Hep-G_2 IC_{50} (μM) ± SEM**	**A-498 IC_{50} (μM) ± SEM**
Cisplatin	15.0 ± 2.6	14.0 ± 2.3
$Cu(ClO_4)_2.6H_2O$	>1000	> 1000
$Mn(ClO_4)_{2\cdot6}H_2O$	626.7 ± 27.29	880.0 ± 20.0
$AgClO_4$	7.6 ± 0.7	44.4 ± 2.3
phen	4.1 ± 0.54	5.8 ± 0.31
phendione	4.2 ± 0.36	1.4 ± 1.34
phen malonate complexes		
$[Cu(phen)_2(mal)].2H_2O$	0.8 ± 0.02	3.8 ± 0.41
$[Mn(phen)_2(mal)].2H_2O$	0.8 ± 0.07	4.2 ± 0.57
$[Ag_2(phen)_2(mal)].2H_2O$	4.7 ± 0.26	4.0 ± 0.32
phendione complexes		
$[Cu(phendione)_3](ClO_4).4H_2O$	0.88 ± 0.06	0.78 ± 0.09
$[Ag(phendione)_2](ClO_4)$	1.4 ± 0.47	0.86 ± 0.87

Uncoordinated phen, is found to be active against Hep-G_2 (IC_{50} = 4.1 μM) and A-498 (IC_{50} = 5.8 μM) cell lines and once coordinated together with malonic acid displayed enhanced chemotherapeutic potential with IC_{50}'s ranging between 0.8–4.7 μM for the liver derived carcinoma cell line (Hep-G_2) and between 3.8–4.0 μM for the kidney derived cells (A-498)[4,22].

Further studies were carried out on the phen-malonate complexes in order to elucidate the reduction in cancer cell viability. The effect these compounds had on DNA synthesis was also examined. Phen along with all its coordinated malonate analogues were found to prevent DNA synthesis but were not found to intercalate. Additionally a standard Ames test proved that each of the complexes were non-mutagenic. Importantly this

group of complexes showed IC_{50} cytotoxicity values of between 3 and 18 times greater than those obtained for cisplatin. It was therefore concluded that phen and these malonate metal complexes offer a possible alternative to cisplatin in the successful treatment and management of cancer[4,22].

Phendione was also found to be active with a similar cytotoxicity IC_{50} value to phen against Hep-G_2 (4.2 ± 0.36) carcinoma and a significantly improved value compared with phen against A-498 (1.4 ± 1.34) carcinoma. Coordination of phendione to Cu^{2+} and Ag^{+} yields an improvement in cytotoxicity against both cell lines with Cu^{2+} being slightly more potent than its Ag^{+} analogue (Hep-G2 IC_{50} = 0.88 ± 0.06, A-498 IC_{50} = 0.78 ± 0.09). Although the Cu^{2+} and Mn^{2+} phen malonates exhibit almost identical IC_{50} values against Hep-G_2 as the $[Cu(phendione)_3](ClO_4).4H_2O$ complex, there is improvement in activity in both of the phendione Ag^{+} and Cu^{2+} complexes compared to the phen malonate complexes against the A-498 kidney derived cell line, with the phendione complexes being approximately 5 times more active. The mechanism of action for these exciting and novel anti-cancer agents has yet to be determined but it has been demonstrated that, unlike doxorubicin, they do not intercalate DNA[4].

The cytotoxicity of phen, phendione and selected metal complexes containing these ligands was studied recently by this group[4,22]. It can be concluded that the selected studies showed that phen, phendione and their metal complexes inhibit DNA synthesis which did not appear to be mediated through intercalation[4,22]. Ames testing highlighted that the ligands and their complexes, and their phase I metabolites were non-mutagenic, unlike cisplatin. Taken together, these results suggest that phen, phendione and their

metal complexes may have a therapeutic role to play in the successful treatment and management of cancer.

R. RATIONALE

Complexes incorporating 1,10-phenanthroline and 1,10-phenanthroline-5,6-dione studied so far by this group have established very good anti-*candida* activity. However the toxicity of 1,10-phenanthroline and its metal complexes has been a limiting factor.

The present study seeks firstly to generate new derivatives of 1,10-phenanthroline retaining the chelating capabilities of phen but trying to reduce the toxicity effects by adding structural diversity to its backbone. A further objective of this study is to compare the activity of some metal complexes of these new compounds with that of existing metal complexes.

DISCUSSION

D.1 SYNTHESIS AND CHARACTERISATION OF 1,10-PHENANTHROLINE- 5,6-DIONE (phendione)

D.1.1 Rationale for the three synthetic methods of phendione

1,10-phenanthroline-5,6-dione (phendione) is a very expensive compound and therefore it was decided to investigate the literature methods for its synthesis. Three methods were examined and modified in an effort to develop an optimal synthetic route to phendione (see methods a-c in section E.2.2 of the experimental section)[33,39,88]. Method (a)[39] (Scheme 17) was found to give consistent yields of phendione {Figure 1(b), I.1.2} and was found to be a more reliable route to the product. It should be noted that the differences between the three methods are subtle but it was found that this reaction was extremely sensitive and the subtle differences associated with method (a) were critical in terms of its advantages over methods (b) and (c).

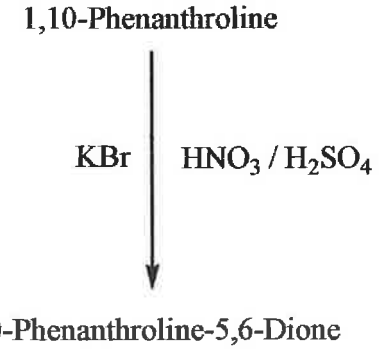

Scheme 17: Formation of phendione **(1)**

The three different methods {(a)–(c)} were successful, giving average yields of (a) 62 %, (b) 11 % and (c) 38 %, respectively.

Method (a) was modified repeatedly in an effort to maximize the yield as well as the time spent developing the synthesis. Initially, phen and KBr were added together at room temperature and stirred over an ice bath. A mixture of concentration H_2SO_4 and concentration HNO_3 (room temperature) were then added. This process was very exothermic and it was assumed that a higher yield would be achieved if this heat was eliminated from the process. To minimize this excessive heat, both acids were chilled separately overnight in a fridge (4 °C), mixed together and further chilled in an ice bath. Both powders were cooled separately in a freezer (-20 °C) for 30 minutes. Yields improved but the method was modified further to optimize the yield. The phen and KBr were cooled separately overnight in a fridge, mixed together in a chilled conical flask and further chilled in an ice bath. All of the glassware was chilled before the experiment commenced.

During the first attempt to neutralize the reaction mixture of method (a) sodium hydroxide was used (3M NaOH) resulting in good yields. In an effort to optimize the yield of phendione, 3M NaOH was replaced by sodium bicarbonate ($NaHCO_3$). $NaHCO_3$ was added very slowly over the course of 8 days. During this time the pH was closely monitored with the aid of universal litmus paper. Many problems occurred using this method of neutralization as the pH was very slow to change as $NaHCO_3$ did not dissolve easily. After 8 days the solution was a deep orange colour and finally neutralized. Any remaining insoluble material in this extract was removed by filtration and the aqueous solution was extracted three times with chloroform. Once this process

was achieved the solution was placed in a fridge at 4 °C overnight. During this time long transparent crystals formed in the bottom of the beaker and when dried and analysed, IR identified them to be sodium bicarbonate crystals. This method of neutralization was painstakingly long and due to the time factor and low yield obtained, this method was abandoned. The neutralization process for method (a) was adopted using chilled 3M NaOH by slow addition of approximately 400 mls over a period of an hour, optimizing the time, materials used and most importantly the yield.

There were subtle differences in method (a) in comparison to method (b) as starting materials and acids used were the same but of different molar ratios. In method (a) a 1:1.5 molar ratio of phen and KBr was used whereas in method (b) a molar ratio of 1:10.4 for these reactants was employed. In the case of method (c), a 1:1.14 molar ratio was used. All three methods used the same 2:1 molar ratio of concentration H_2SO_4 and HNO_3. There is a major difference between the ways these three methods utilize the acids, as the acids in method (a) were chilled continuously before being incorporated into the experiment, whereas method (c) involved starting materials at room temperature as concentration H_2SO_4 was transferred into a round bottomed flask (250 ml), equipped with a reflux condenser, and phen was dissolved in it in small portions. Then sodium bromide was added which was followed by an addition of concentration HNO_3. The reaction mixture was heated to boiling and refluxed for 1 hour. Method (b) also has a 2:1 molar ratio of H_2SO_4 and HNO_3 but in this case the phen, KBr and concentration H_2SO_4 were chilled independently before being added together for 30 minutes at -20 °C. Concentration HNO_3 was then added dropwise to this solution and the resulting mixture was refluxed for 3 hours.

Sodium carbonate powder (Na_2CO_3) was used during the neutralization stage in large quantities. After many attempts, poor yields were obtained, and method (b) was abandoned.

Method (c) was very similar to method (a) with subtle differences, such as a reflux time of 1 hour compared with 3 hours in method (a) and method (b). This method yielded on average 38 % of product which is nearly half the average yield of method (a) (62 %). In conclusion, method (a) was adopted for the synthesis of phendione.

Phendione was obtained as a yellow powder and was characterised by comparison with a commercially available sample. Based on microanalysis the product compared very well with the commercial compound:

% Commercial sample of phendione: C, 68.28; H, 2.90; N, 13.18

% Found for the synthesized phendione: C, 68.57; H, 2.88; N, 13.33

In the IR spectrum of phendione, a band at 1685 cm^{-1} {Appendix 1(1)} is due to the stretching frequency of the C=O band on the ligand. Bonds which are characteristic of the phen moiety are present at 806 cm^{-1} and 735 cm^{-1}. These bands represent the C-N-C stretching frequency of the ligand.

The ^{1}H NMR spectrum of phendione contains three distinct signals, which are double doublets and integrate of two hydrogens, (Figure 48 and Figure 49).

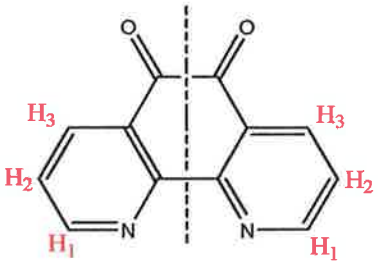

Figure 48: Structure and assignment of 1,10-phenanthroline-5,6-dione

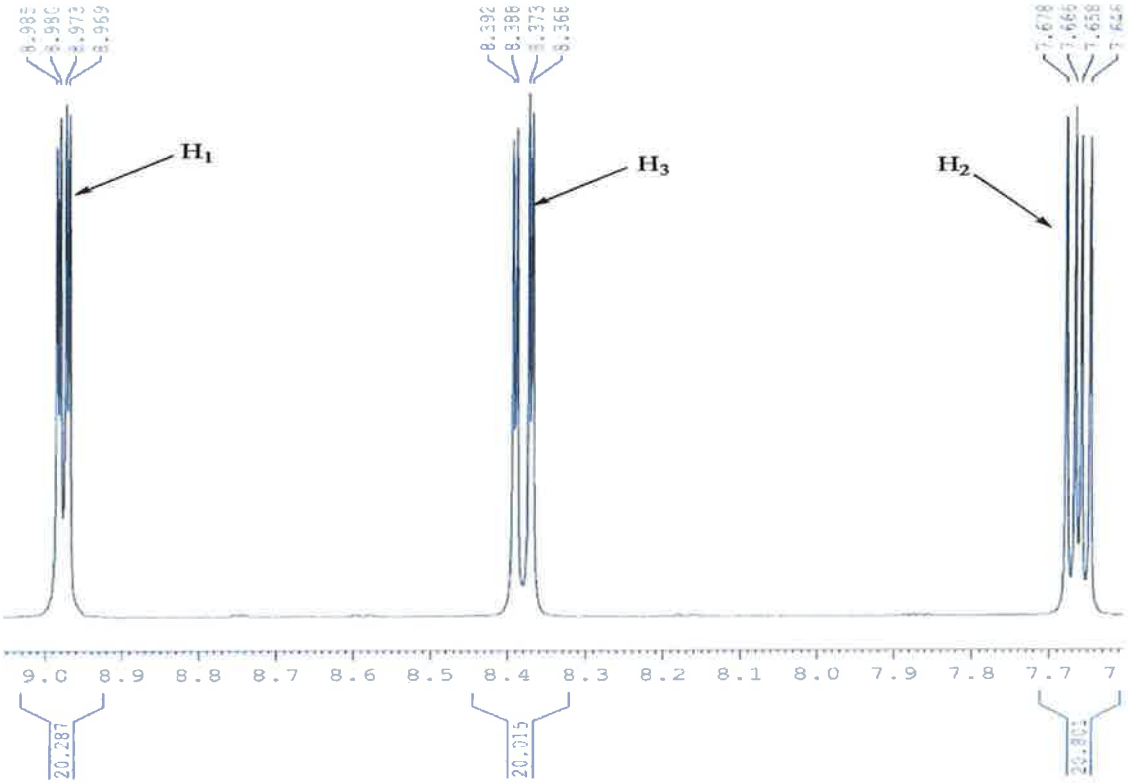

Figure 49: ^{1}H NMR spectrum of 1,10-phenanthroline-5,6-dione

Protons H_1 and H_3 are each coupled to H_2 (Figure 49), via a vicinal coupling with coupling constants ($J_{1\text{-}2} = 4.8$ Hz and $J_{2\text{-}3} = 8.0$ Hz). H_1 and H_3 also couple to each other via a 'W'- coupling ($J_{1\text{-}3} = 1.6$ Hz), (Figure 48). Analysis from ^{13}C NMR {Appendix 3(1)} confirms the assignment of the proton, made from the ^{1}H-NMR spectrum, {Appendix 2(1)}.

D.2 1,10-PHENANTHROLINE AND 1,10-PHENANTHROLINE-5,6-DIONE DERIVATIVES OF SIMPLE METAL SALTS

Previous studies in this and collaborating laboratories showed that 1,10-phenanthroline (phen) and 1,10-phenanthroline-5,6-dione (phendione) are themselves excellent anti-*Candida* agents[2,3,4,17]. Coordination of phen or phendione to a metal centre resulted in a significant increase in their anti-microbial activity and also a significant increase in their chemotherapeutic potential was observed[4,17,13,21]. It was also demonstrated that the nature of the metal and counter ion in the complex could influence anti-microbial potency. The counterion used in these studies were usually organic anions such as aromatic and aliphatic carboxylates and dicarboxylates[3,4,6,7].

During the present study phen and phendione were reacted with nitrate, chloride and sulphate salts of copper(II), cobalt(II), zinc(II) and manganese(II). The copper(II) acetate derivative of phen and phendione were also generated. The anti-*Candida* activity of these compounds was also studied.

D.2.1 Nitrate derivatives

The nitrate salts of copper(II), cobalt(II), zinc(II) and manganese(II) were reacted with phen and phendione, respectively to yield the nitrate complexes **2–9** in accordance with Scheme 18.

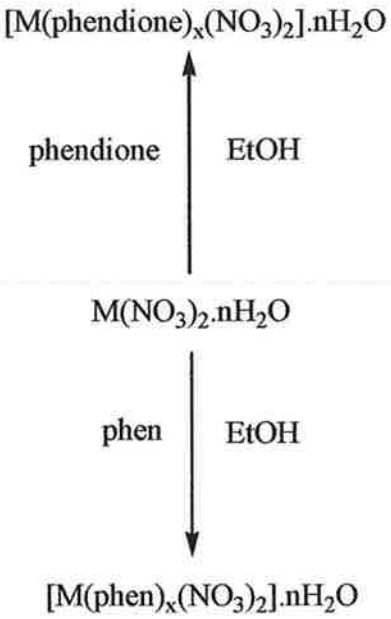

Scheme 18

where M = Cu^{2+}, Co^{2+}, Zn^{2+}, Mn^{2+}

x = 2, 3

n = 1, 2, 2.5, 3, 4, 6

The complexes were obtained as green **{2, 6}**, orange **{3}**, white **{4}** and yellow **{5, 7, 8, 9}** powders and were formulated as shown below.

(2) **$[Cu(phen)_2NO_3]NO_3.2H_2O$**

% Calc: C, 49.36; H, 3.45; N, 14.39

% Found: C, 48.86; H, 3.33; N, 14.10

(3) **$[Co(phen)_2NO_3]NO_3.2H_2O$**

% Calc: C, 49.75; H, 3.48; N, 14.51

% Found: C, 50.05; H, 3.18; N, 14.59

(4) **$[Zn(phen)_2NO_3]NO_3.2H_2O$**

% Calc: C, 49.20; H, 3.44; N, 14.35

% Found: C, 48.63; H, 3.24; N, 14.25

(5) **$[Mn(phen)_3NO_3]NO_3.2H_2O$**

% Calc: C, 57.22; H, 3.74; N, 14.83

% Found: C, 57.23; H, 3.43; N, 14.32

(6) **$[Cu(phendione)_2NO_3]NO_3.2H_2O$**

% Calc: C, 44.76; H, 2.50; N, 13.05.

% Found: C, 45.46; H, 1.89; N, 12.27.

(7) **$[Co(phendione)_2NO_3]NO_3.H_2O$**

% Calc: C, 46.39; H, 2.27; N, 13.53

% Found: C, 46.20; H, 2.03; N, 13.08

(8) **$[Zn(phendione)_2(NO_3)_2].3H_2O$**

% Calc: C, 43.42; H, 2.73; N, 12.66

% Found: C, 43.90; H, 1.91; N, 12.46

(9) **$[Mn(phendione)_2(NO_3)_2].H_2O$**

% Calc: C, 46.69; H, 2.29; N, 13.61

% Found: C, 46.03; H, 1.99; N, 13.15

The IR spectra of complexes **2, 3, 4** and **5** are very similar in appearance {Appendix 1(2)-(5), Table 12}. Bands which are characteristic of the presence of the chelating phen are present in all spectra at approximately 846 cm^{-1} and 725 cm^{-1}. New bands appear in the spectra of **2, 3, 4** and **5** which are indicative of the presence of coordinated (in the range 1298-1330 cm^{-1}) and uncoordinated (in the range 1360-1385 cm^{-1}) nitrate groups. Aromatic C-H stretching vibrations appear in all four spectra in the region of 3050 cm^{-1}.

The IR spectra of complexes **6, 7, 8** and **9** are very similar in appearance {Appendix 1 (6)-(9), Table 12}. The strong peak present in all four spectra at approximately 1700 cm^{-1} is a stretching frequency of the C=O band, characteristic of the phendione ligand. Another characteristic of the phendione ligand present in all spectra are bands at approximately 830 cm^{-1} and 735 cm^{-1}. Aromatic C-H stretches appear in all four spectra in the region of 3080 cm^{-1} and 3090 cm^{-1}. New bands appear in the spectra of **6** and **7** which are indicative of the presence of coordinated (in the range 1298-1330 cm^{-1}) and uncoordinated (in the range 1360-1385 cm^{-1}) nitrate groups. The spectra of complexes **8**

and **9** only possess bands due to the presence of coordinated nitrates (1300 cm^{-1} and 1301 cm^{-1} respectively).

Table 12: Characteristic Infrared bands of complexes **2–9**

Band Assignment cm^{-1}	**phen**	**phendione**	**2**	**3**	**4**	**5**	**6**	**7**	**8**	**9**
C-N-C stretching frequency	853, 738	806, 735	846, 720	846, 725	847, 725	839, 727	828, 729	833, 734	833, 734	823, 735
C=O	-	1685	-	-	-	-	1701	1700	1699	1698
Aromatic C-H	3379-3054	3434-3066	3052	3050	3057	3050	3082	3091	3090	3088
NO_3^- (coord)	-	-	1298	1312	1302	1328	1299	1302	1300	1301
NO_3^- (uncoord)	-	-	1363	1384	1384	1383	1384	1384	-	-

The room temperature magnetic moments of powdered samples of complexes **2-9** are shown in Table 13. The μ_{eff} value for complex **2** (1.96 B.M.) and complex **6** (1.77 B.M) are in the range excepted (μ_{eff} = 1.8-2.1 B.M.) for copper(II) complexes where there is no significant exchange interactions between adjacent metal centres[89]. The magnetic moment of the cobalt(II) complexes **3** (4.79 B.M.) also lies within the expected range of high spin cobalt(II) complexes (μ_{eff} = 4.3-5.2 B.M.). The magnetic moment of cobalt(II) complex **7** (6.12 B.M.) however is above the expected value. Complexes **5** (6.01 B.M) and **9** (5.99 B.M.) were found to have a μ_{eff} value that were in the expected range (μ_{eff} = 5.7-6.0 B.M.) for a manganese(II) high spin complex in which no interactions between the metal centres occurs[36].

Table 13: Magnetic Susceptibility for complexes **2-9**

Complexes	μ_{eff} (B.M.) {R.T.}
$[Cu(phen)_2NO_3]NO_3.2H_2O$ **(2)**	1.96
$[Co(phen)_2NO_3]NO_3.2H_2O$ **(3)**	4.79
$[Zn(phen)_2NO_3]NO_3.2H_2O$ **(4)**	-
$[Mn(phen)_3NO_3]NO_3.2H_2O$ **(5)**	6.01
$[Cu(phendione)_2NO_3]NO_3.2H_2O$ **(6)**	1.77
$[Co(phendione)_2NO_3]NO_3.H_2O$ **(7)**	6.12
$[Zn(phendione)_2(NO_3)_2].3H_2O$ **(8)**	-
$[Mn(phendione)_2(NO_3)_2].H_2O$ **(9)**	5.99

D.2.2 Chloride derivatives

The chloride salts of copper(II), cobalt(II), zinc(II) and manganese(II) were reacted with phen and phendione, respectively to yield complexes **10–17** in accordance with Scheme 19.

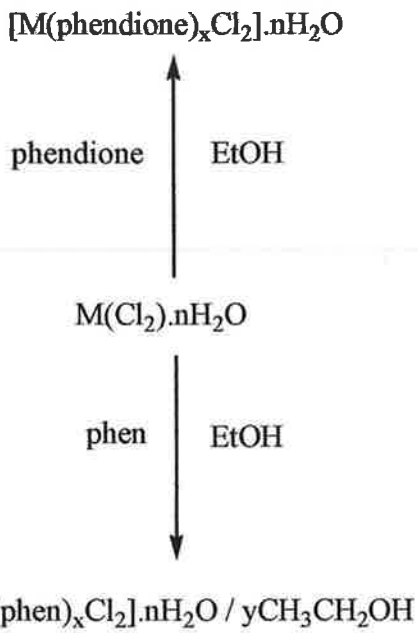

Scheme 19

where $M = Cu^{2+}, Co^{2+}, Zn^{2+}, Mn^{2+}$

$x = 2$

$n = 1, 2, 3, 4, 6$

$y = 1$

The complexes were obtained as blue **{10}**, dark red **{11}**, white **{12}**, yellow **{13** and **16}**, green **{14}** and orange **{15, 17}** powders and were formulated as shown below.

(10) $[Cu(phen)_2]Cl_2.6H_2O$

% Calc: C, 47.81; H, 4.68; N, 9.29

% Found: C, 48.83; H, 2.98; N, 9.32

(11) $[Co(phen)_2]Cl_2.3H_2O$

% Calc: C, 52.96; H, 4.07; N, 10.29

% Found: C, 52.88; H, 3.74; N, 10.44

(12) $[Zn(phen)_2]Cl_2.H_2O$

% Calc: C, 56.00; H, 3.52; N, 10.88

% Found: C, 56.30; H, 3.44; N, 10.93

(13) $[Mn(phen)_2]Cl_2.CH_3CH_2OH$

% Calc: C, 58.66; H, 4.17; N, 10.52

% Found: C, 59.02; H, 3.15; N, 11.46

(14) $[Cu(phendione)_2Cl_2].2H_2O$

% Calc: C, 48.79; H, 2.73; N, 9.48.

% Found: C, 49.57; H, 2.43; N, 9.29.

(15) $[Co(phendione)_2Cl_2].H_2O$

% Calc: C, 50.73; H, 2.48; N, 9.86

% Found: C, 50.21; H, 2.40; N, 9.21

(16) $[Zn(phendione)_2Cl_2].3H_2O$

% Calc: C, 47.20; H, 2.97; N, 9.17

% Found: C, 46.29; H, 2.07; N, 8.27

(17) $[Mn(phendione)_2Cl_2].2H_2O$

% Calc: C, 49.51; H, 2.77; N, 9.62

% Found: C, 49.79; H, 2.34; N, 9.11

The IR spectra of complexes **10, 11, 12** and **13** are very similar reflecting their structural similarities, {Appendix 1(10)-(13), Table 14}. The spectra contain absorption bands which are characteristic of the presence of phen [853 cm^{-1} and 722 cm^{-1} **(10)**, 849 cm^{-1} and 726 cm^{-1} **(11)**, 846 cm^{-1} and 728 cm^{-1} **(12)** and 845 cm^{-1} and 729 cm^{-1} **(13)**]. Aromatic C-H stretches are present in all four spectra in the region of 3050-3045 cm^{-1}.

The IR spectra of complexes **14, 15, 16** and **17** are very similar, {Appendix 1(14)-(15), Table 14}. A characteristic of the phendione ligand is the carbonyl (C=O) stretching absorption band at [1697 cm^{-1} **(14),** 1694 cm^{-1} **(15),** 1694 cm^{-1} **(16)** and 1694 cm^{-1} **(17)**]. Another characteristic of the phendione ligand present in all four spectra are bands at approximately 830 cm^{-1} and 735 cm^{-1}. Aromatic C-H stretches appear in all spectra in the region of 3070 cm^{-1} and 3000 cm^{-1}. The presence of a new band assigned to M-Cl vibrations at approximately 547 cm^{-1} in the spectra of **14, 15, 16** and **17** which is not present in the spectrum of phendione, may indicate that at least one chloride anion is bound to the central metal.

Table 14: Characteristic Infrared bands of complexes **10–17**

Band assignment cm^{-1}	**phen**	**Phendione**	**10**	**11**	**12**	**13**	**14**	**15**	**16**	**17**
C-N-C stretching frequency	853, 738	806, 735	853, 722	849, 726	846, 728	845, 729	839, 733	839, 730	842, 737	841, 737
C=O	-	1685	-	-	-	-	1697	1694	1694	1694
Aromatic C-H	3379-3054	3434 – 3066	3051	3046	3046	3046	3069	3069-3007	3069-3013	3068-3012
M-Cl stretch	-	-	-	-	-	-	548	547	547	546

The room temperature magnetic moments of powdered samples of complexes **10-17** are shown in Table 15. The μ_{eff} value for copper(II) complexes **10** and **14** are in the expected range (μ_{eff} = 1.8-2.1 B.M.) where there is no significant exchange interactions between adjacent metal centres[36]. The room temperature magnetic moment of complex **11** (4.38 B.M.) falls within the range expected for cobalt(II) complexes (4.3-5.2 B.M.). The magnetic moment for the high spin cobalt(II) complex **15** (6.21 B.M.) is above the expected value. The value for complex **13** (6.07 B.M.) falls within the expected value for a high spin manganese(II) complex, whereas the value of complex **17** (8.16 B.M.) is significantly higher than expected (μ_{eff} = 5.7-6.0 B.M.).

Table 15: Magnetic Susceptibility for complexes **10-17**

Complex	μ_{eff} (B.M.) {R.T.}
$[Cu(phen)_2]Cl_2.6H_2O$ **(10)**	1.72
$[Co(phen)_2]Cl_2.3H_2O$ **(11)**	4.38
$[Zn(phen)_2]Cl_2.H_2O$ **(12)**	-
$[Mn(phen)_2]Cl_2.CH_3CH_2OH$ **(13)**	6.07
$[Cu(phendione)_2Cl_2].2H_2O$ **(14)**	2.09
$[Co(phendione)_2Cl_2].H_2O$ **(15)**	6.21
$[Zn(phendione)_2Cl_2].3H_2O$ **(16)**	-
$[Mn(phendione)_2Cl_2].2H_2O$ **(17)**	8.16

D.2.3 Sulphate derivatives

The sulphate salts of copper(II), cobalt(II), zinc(II) and manganese(II) were reacted with phen and phendione, respectively to yield the complexes **18-25** in accordance with Scheme 20.

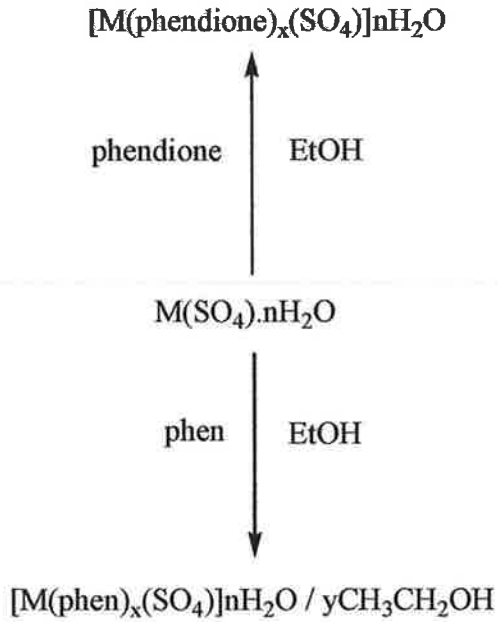

Scheme 20

where M = Cu^{2+}, Co^{2+}, Zn^{2+}, Mn^{2+}

x = 1, 2

n = 1, 2, 3, 4, 6, 7

y = 1

The complexes were obtained as blue **{18}**, pink **{19}**, white **{20}**, yellow **{21}**, green **{22}**, orange **{23}** and mustard coloured **(24** and **25)** powders and were formulated as shown below.

(18) $[Cu(phen)_2SO_4].3H_2O$

% Calc: C, 50.21; H, 3.86; N, 9.76

% Found: C, 50.00; H, 3.41; N, 9.13

(19) $[Co(phen)_2SO_4].6H_2O$

% Calc: C, 46.23; H, 4.53; N; 8.99

% Found: C, 46.94; H, 3.22; N, 9.04

(20) $[Zn(phen)SO_4].2H_2O$

% Calc: C, 38.16; H, 3.20; N, 7.42

% Found: C, 37.78; H, 3.21; N, 7.09

(21) $[Mn(phen)SO_4].7H_2O$

% Calc: C, 31.52; H, 4.85; N, 6.13

% Found: C, 31.49; H, 2.62; N, 5.92

(22) $[Cu(phendione)SO_4].4H_2O$

% Calc: C, 32.62; H, 3.19; N, 6.34

% Found: C, 32.18; H, 2.35; N, 6.08

(23) $[Co(phendione)_2SO_4].7H_2O$

% Calc: C, 41.09; H, 3.74; N, 7.99

% Found: C, 41.66; H, 2.64; N, 7.82

(24) [Zn(phendione)SO_4].H_2O

% Calc: C, 37.00; H, 2.07; N, 7.19

% Found: C, 38.76; H, 2.56; N, 7.11

(25) [Mn(phendione)$_2SO_4$].CH_3CH_2OH

% Calc: C, 50.58; H, 2.94; N, 9.07

% Found: C, 51.09; H, 2.35; N, 9.74

The IR spectra of complexes **18, 19, 20** and **21** are very similar reflecting possible structural similarities, {Appendix 1(18)-(21), Table 16}. The spectra contain absorption bands which are characteristic of the presence of phen [852 cm^{-1} and 723 cm^{-1} **(18)**, 843 cm^{-1} and 725 cm^{-1} **(19)**, 865 cm^{-1} and 725 cm^{-1} **(20)** and 821 cm^{-1} and 729 cm^{-1}**(21)**]. As well as the bands that have been assigned to the phen ligand the spectra of all four complexes also contain bands that are characteristic of sulphate {1121 cm^{-1} **(18),** 1116 cm^{-1} **(19)**, 1118 cm^{-1} **(20)** and 1107 cm^{-1} **(21)**} anions. The presence of the sulphate anion is further evidenced by the appearance of a new characteristic band at approximately 600 cm^{-1} in all four spectra.

The IR spectra of complexes **22, 23, 24** and **25** are very similar, {Appendix 1(22)-(25), Table 16}. The spectra contain absorption bands which are characteristic of the presence of phendione [819 cm^{-1} and 726 cm^{-1} **(22)**, 820 cm^{-1} and 732 cm^{-1} **(23)** 821 cm^{-1} and 733 cm^{-1} **(24)** and 817 cm^{-1} and 733 cm^{-1} **(25)**]. The strong carbonyl stretching absorption band at [1700 cm^{-1} **(22),** 1696 cm^{-1}, **(23)** 1696 cm^{-1} **(24)** and 1685 **(25)**] characteristic of phendione ligand are also present in the spectra of these complexes. As

well as the bands that have been assigned to the phendione ligand the spectra of all four complexes also contain bands that are characteristic of sulphate {1096 cm^{-1} **(22)**, 1117 cm^{-1} **(23)**, 1116 cm^{-1} **(24)** and 1121 **(25)**} anions. The presence of the sulphate anion is further evidence by the appearance of a new characteristic band at approximately 600 cm^{-1} in all four spectra.

Table 16: Characteristic Infrared bands of complexes **18–25**

Band assignment cm^{-1}	**phen**	**phendione**	**18**	**19**	**20**	**21**	**22**	**23**	**24**	**25**
C-N-C stretching frequency	853, 738	806, 735	852, 723	843, 725	865, 725	821, 729	819, 726	820, 732	821, 733	817, 733
C=O	-	1685	-	-	-	-	1700	1696	1696	1685
Aromatic C-H	3379-3054	3434-3066	3054	3054	3059	3065	3081	3085	3085	3060
SO_4^{2-}	-	-	1121, 618	1116, 620	1118, 613	1107, 605	1096 611	1117, 619	1116, 604	1121, 613

The room temperature magnetic moments of powdered samples of complexes **18-25** are shown in Table 17. The μ_{eff} value for complex **18** (1.99 B.M.) and complex **22** (1.88 B.M.) fall in the expected region for a mono-nuclear copper species[36]. The magnetic moments for both cobalt(II) complexes **19** (4.43 B.M.) and **23** (4.4 B.M) fall within expected for high spin values (μ_{eff} = 4.3-5.2). The values for manganese complex **21** (5.61 B.M.) and **25** (5.77 B.M.) are normal for mononuclear Mn(II) high spin complexes.

Table 17: Magnetic Susceptibility for complexes **18-25**

Complex	μ_{eff} **(B.M.) {R.T.}**
$[Cu(phen)_2SO_4].3H_2O$ **(18)**	1.99
$[Co(phen)_2SO_4].6H_2O$ **(19)**	4.43
$[Zn(phen)SO_4].2H_2O$ **(20)**	-
$[Mn(phen)SO_4].7H_2O$ **(21)**	5.61
$[Cu(phendione)SO_4].4H_2O$ **(22)**	1.88
$[Co(phendione)_2SO_4].7H_2O$ **(23)**	4.4
$[Zn(phendione)SO_4].H_2O$ **(24)**	-
$[Mn(phendione)_2SO_4].CH_3CH_2OH$ **(25)**	5.77

D.2.4 Copper(II) acetate derivatives

Copper(II) acetate was reacted with phen and phendione, respectively, to yield the acetate complexes **26–27** in accordance with Scheme 21.

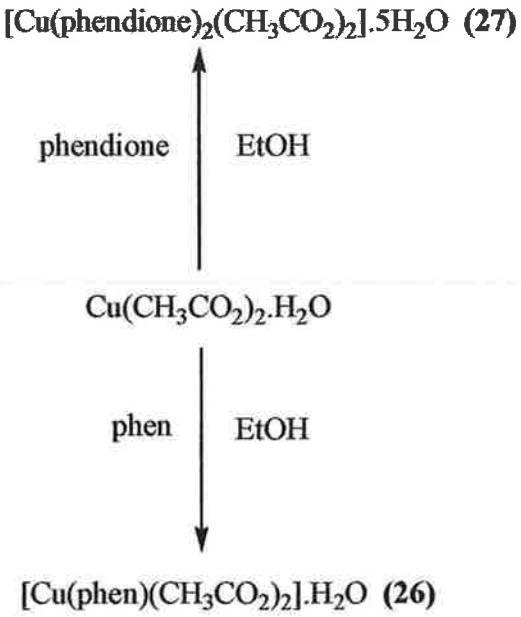

Scheme 21

The complexes were obtained as blue {**26**} and dark blue {**27**} powders and were formulated as shown below.

(26) $[Cu(phen)(CH_3CO_2)_2].H_2O$

% Calc: C, 50.59; H, 4.25; N, 7.38

% Found: C, 51.05; H, 4.16; N, 7.96

(27) $[Cu(phendione)_2(CH_3CO_2)_2].5H_2O$

% Calc: C, 48.59; H, 4.08; N, 8.10

% Found: C, 48.03; H, 2.28; N, 8.91

The IR spectrum of **26** contains distinctive vOCOasym and vOCOsym bands at 1572 cm^{-1} and 1426 cm^{-1} {Appendix 1(26)}. Bands which are characteristic of the presence of the phen ligand are present at 851 cm^{-1} and 723 cm^{-1}. The IR spectrum of **27** contains distinctive vOCOasym and vOCOsym bands at 1576 cm^{-1} and 1369 cm^{-1}, {Appendix 1(27)}. A characteristic of the phendione ligand is the carbonyl (C=O) stretching absorption band at 1703 cm^{-1} and bands which are present at 796 cm^{-1} and 732 cm^{-1} are also characteristic of the presence of the phendione ligand. Aromatic C-H stretches appear in both spectra at 3052 cm^{-1} and 3057 cm^{-1}, respectively.

The room temperature magnetic moments of powdered samples of complexes **(26)** (2.08 B.M.) and **(27)** (2.03 B.M), fall in the region expected for copper(II) complexes where there is no significant exchange interaction between adjacent metal centres[36].

D.2.4.1 ANTI-*CANDIDA* ACTIVITY OF THE PHEN AND PHENDIONE METAL SALTS

The metal complexes **2–27** were screened for their ability to inhibit the growth of an isolate of *Candida albicans* at concentrations of 50 μg/ml, 20 μg/ml, 10 μg/ml and 5 μg/ml.

The anti-fungal activity of the metal free ligands phen and phendione shows significant activity at the lowest tested concentration of 5 μg/ml which is comparable to that of prescription drug Amphothericin B (Table 18). The growth curves for phen, phendione and Amphothericin B are shown in Figures 50, 51 and 52. It can be clearly seen that both phen and phendione are more active than the prescription drug Amphotherican B at the lower concentration of 5 μg/ml.

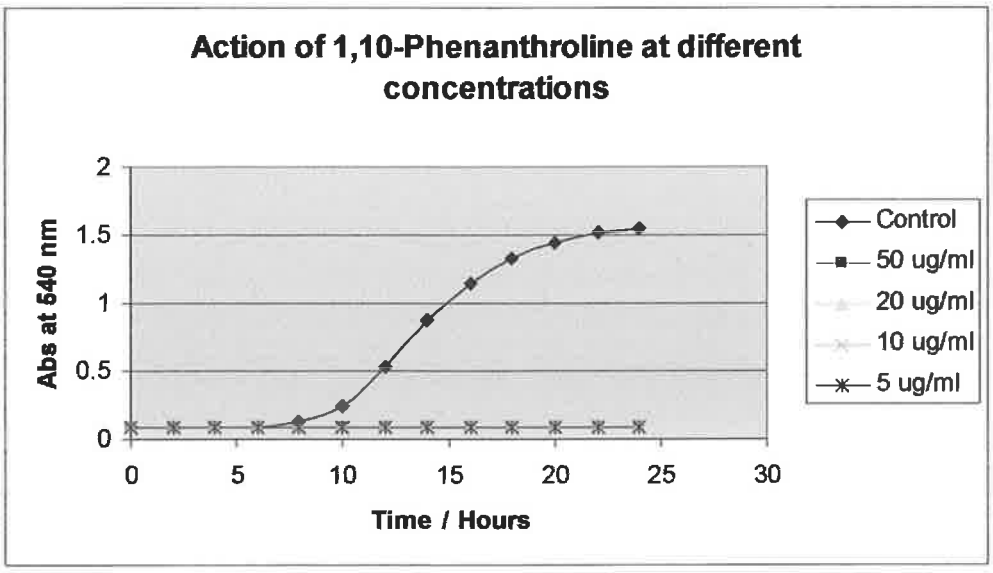

Figure 50: Kinetic growth curve of control cells and cells treated with 1,10-phenanthroline

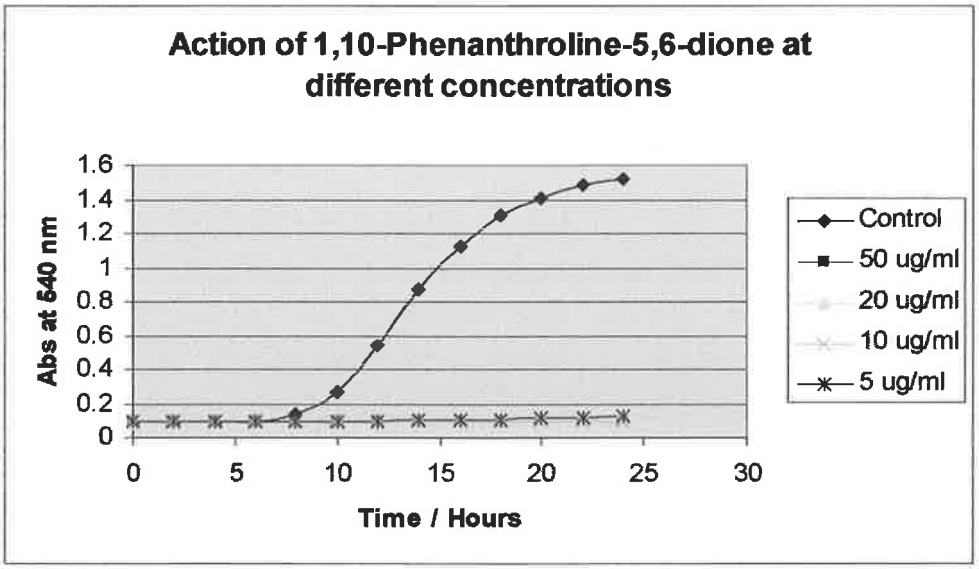

Figure 51: Kinetic growth curve of control cells and cells treated with 1,10-phenanthroline-5,6-dione **(1)**

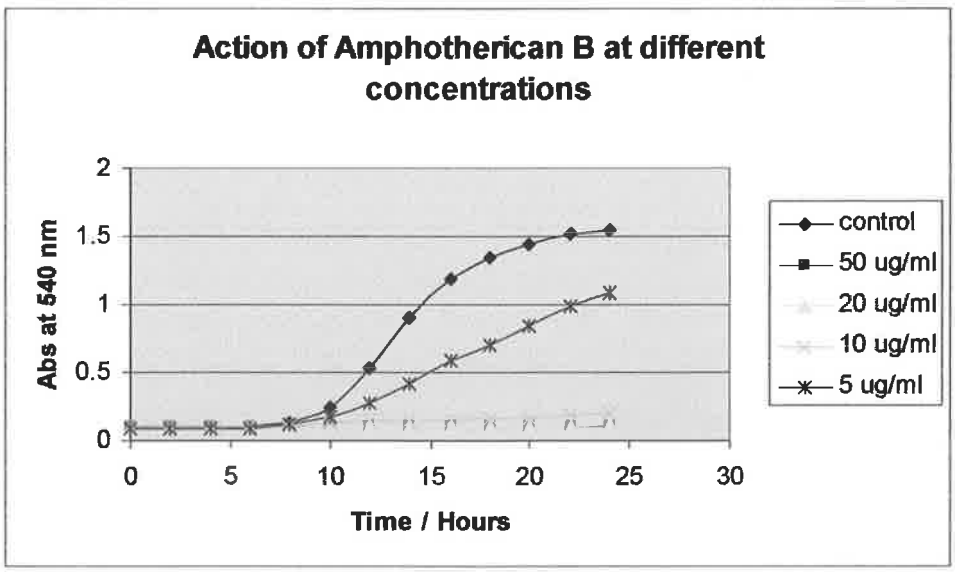

Figure 52: Kinetic growth curve of control cells and cells treated with Amphothericin B

The anti-*Candida* activity of the simple metal salts and their phen and phendione derivatives are shown in Table 18 (nitrates), Table 19 (chlorides), Table 20 (sulphates) and Table 21 (acetates).

Table 18: Anti-*Candida* activity of Amphothericin B, phenanthroline ligands, copper salts and copper complexes **2, 10,18, 26, 6, 14, 22** and **27**

Test Compound	**% Cell Growth (at concentrations of 50 - 5 μg/ml)**				**IC_{50} value μg/ml**	**IC_{50} value μM**
	50	**20**	**10**	**5**		
Control	100	100	100	100		
Amphothericin B	6.9±9.6	7.01±9.6	13.12±33	70.5±56	10	1.08×10^{-5}
Phen	5.2±15	5.6±3.2	5.7±3.5	5.9±3	5	2.77×10^{-5}
Phendione	5.6±12	5.62±10	5.55±6.1	8.3±42	5	2.37×10^{-5}
Commercial $Cu(NO_3)_2$	34±64	67±21	85±34	102±12	50	2.66×10^{-4}
Commercial $CuCl_2$	13±9.2	30±6.6	57±21	70±21	50	3.71×10^{-4}
Commercial $CuSO_4$	25±30	39±79	81±27	99±49	50	3.13×10^{-4}
Commercial $Cu(CH_3CO_2)_2$	9.3±9.8	10.6±7.8	42±36	82±31	20	1.10×10^{-4}
$[Cu(phen)_2NO_3]NO_3.2H_2O$ **(2)**	91.5±16	103±20	107±17	-	50	8.56×10^{-5}
$[Cu(phen)_2]Cl_2.6H_2O$ **(10)**	56±33	75±13	79±4.7	82±20	50	8.29×10^{-5}
$[Cu(phen)_2SO_4].3H_2O$ **(18)**	90±3.3	98.7±56	100±2.2	105±18	50	8.70×10^{-5}
$[Cu(phen)(CH_3CO_2)_2].H_2O$ **(26)**	66±150	69±242	87±363	87±412	50	1.31×10^{-4}
$[Cu(phendione)_2NO_3]NO_3.2H_2O$ **(6)**	9.8±1.7	9.5±0	13.4±8	89±37	10	1.55×10^{-5}
$[Cu(phendione)_2Cl_2].2H_2O$ **(14)**	9.7±5.3	10.3±9	108±8.3	116±11	20	3.38×10^{-5}
$[Cu(phendione)SO_4].4H_2O$ **(22)**	10±2.3	24±29	86.9±44	98±32	50	1.13×10^{-4}
$[Cu(phendione)_2(CH_3CO_2)_2].5H_2O$ **(27)**	66±5.3	70±53	83±14	89±53	50	7.22×10^{-5}

Note: - indicates no activity or 100% cell growth

Table 19: Anti-*Candida* activity of cobalt salts and cobalt complexes

Test Compound	**% Cell Growth (at concentrations of 50 - 5 μg/ml)**				**IC_{50} value μg/ml**	**IC_{50} value μM**
	50	**20**	**10**	**5**		
Control	100	100	100	100		
Commercial $Co(NO_3)_2$	17.8±12	19.9±2	28±2	57±8	50	2.73×10^{-4}
Commercial $CoCl_2$	20±2	49±6	22±14	34±18	50	3.85×10^{-4}
Commercial $CoSO_4$	19.9±30	23±36	22.9±41	46±11	50	3.22×10^{-4}
$[Co(phen)_2NO_3]\ NO_3.2H_2O$ **(3)**	83±7	105±29	112±43	113±112	50	8.62×10^{-5}
$[Co(phen)_2Cl_2].3H_2O$ **(11)**	45±22	82±49	82±36	93±8	50	9.18×10^{-5}
$[Co(phen)_2SO_4].6H_2O$ **(19)**	61±68	85±8.7	96±60	112±78	50	8.01×10^{-5}
$[Co(phendione)_2NO_3]NO_3.H_2O$ **(7)**	9.8±4	9.5±1.6	13.2±13	108±52	10	1.60×10^{-5}
$[Co(phendione)_2Cl_2].H_2O$ **(15)**	10.3±5.6	11±3.9	77±46	112±46	20	3.51×10^{-5}
$[Co(phendione)_2SO_4].7H_2O$ **(23)**	6±3.8	6±2.3	6±2.3	12.3±2.1	5	7.12×10^{-6}

Table 20: Anti-*Candida* activity of zinc salts and zinc complexes

Test Compound	% Cell Growth (at concentrations of 50 - 5 μg/ml)				IC_{50} value μg/ml	IC_{50} valueμM
	50	**20**	**10**	**5**		
Control	100	100	100	100		
Commercial $Zn(NO_3)_2$	100±44	100±5.5	97±33	97±16	50	2.63×10^{-4}
Commercial $ZnCl_2$	105±15	102±68	103±72	104±10	50	3.66×10^{-4}
Commercial $ZnSO_4$	98±61	99.5±15	96±1.1	96±13	50	3.09×10^{-4}
$[Zn(phen)_2NO_3]NO_3.2H_2O$ **(4)**	20±13	121±1.6	122±174	130±60	50	8.54×10^{-5}
$[Zn(phen)_2]Cl_2.H_2O$ **(12)**	17±3.2	80±70	120±93	127±4.9	50	9.71×10^{-5}
$[Zn(phen)SO_4].2H_2O$ **(20)**	113±21	124±116	126±62	128±52	50	1.32×10^{-4}
$[Zn(phendione)_2(NO_3)_2].3H_2O$ **(8)**	10.4±4	12.2±5.9	75±52	115±16	20	3.01×10^{-5}
$[Zn(phendione)_2Cl_2].3H_2O$ **(16)**	10.4±10	11±6.9	29±54	112±74	20	3.27×10^{-5}
$[Zn(phendione)SO_4].H_2O$ **(24)**	10.5±21	86.5±18	-	115±26	50	1.28×10^{-4}

Note: - indicates no activity or 100% cell growth

Table 21: Anti-*Candida* activity of manganese salts and manganese complexes

Test Compound	% Cell Growth (at concentrations of 50 - 5 μg/ml)				IC_{50} value μg/ml	IC_{50} value μM
	50	20	10	5		
Control	100	100	100	100		
Commercial $Mn(NO_3)_2$	95±10	93±2	94±18	103±2	50	2.79×10^{-4}
Commercial $MnCl_2$	99±8.5	95±22	106±16	107±51	50	3.97×10^{-4}
Commercial $MnSO_4$	104±42	94±25	104±25	105±5.4	50	3.31×10^{-4}
$[Mn(phen)_3NO_3]NO_3.2H_2O$ **(5)**	6.4±6.5	6.6±7.6	6.6±15	6.8±8	5	6.61×10^{-6}
$[Mn(phen)_2]Cl_2.CH_3CH_2OH$ **(13)**	9.8±3.8	9.3±1.8	9.5±0.5	101±30	10	1.87×10^{-5}
$[Mn(phen)SO_4].7H_2O$ **(21)**	9.7±2.6	9.5±3.4	12±39	104±81	10	2.18×10^{-5}
$[Mn(phendione)_2(NO_3)_2].H_2O$ **(9)**	9.9±4.8	9.6±1.8	9.8±9.4	12.9±1.3	5	8.09×10^{-6}
$[Mn(phendione)_2Cl_2].2H_2O$ **(17)**	9.5±2.3	9.3±1.5	9.5±1.1	101±16	10	1.71×10^{-5}
$[Mn(phendione)_2SO_4].CH_3CH_2OH$ **(25)**	10.3±1.8	9.6±1.4	9.8±0.5	12.9±0.5	5	8.09×10^{-6}

The copper(II) and cobalt(II) salts are themselves reasonably active towards the *Candida albicans* (Tables 18-21) at the higher concentration of 20 μg/ml and 50 μg/ml. Upon coordination of the phen to the metal centres in these salts the activity is reduced significantly. In contrast the phendione derivatives of the copper(II) and cobalt(II) salts are very active at 50 μg/ml and 20 μg/ml . Complexes **6** and **7** exhibit excellent activity at 10 μg/ml and $[Co(phendione)_2SO_4].7H_2O$ **(23)** is the most active of the cobalt(II) complexes exhibiting excellent activity at 5 μg/ml . The growth curve for **23** is shown in Figure 53.

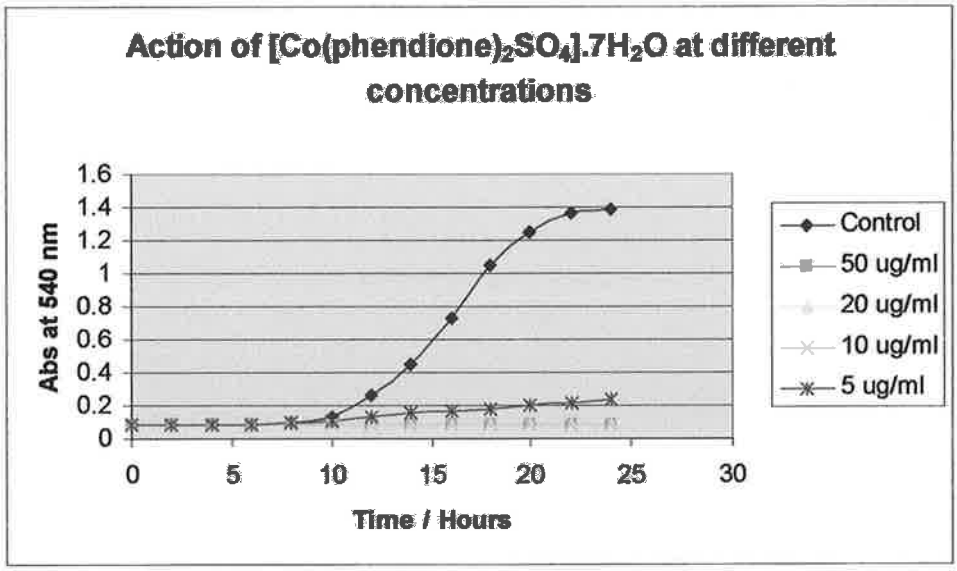

Figure 53: Kinetic growth curve of control cells and cells treated with complex **23**

The simple zinc(II) and manganese(II) salts all exhibit very poor anti-*Candida* properties over the concentration range studied (Tables 18-21). The phen derivatives **4, 5, 12, 13, 20** and **21** display a range of activities. The zinc(II) nitrate derivative **4** only exhibits activity at 50 μg/ml whereas the manganese(II) nitrate derivative **5** is an excellent anti-*Candida* agent, (Figure 54 and 55).

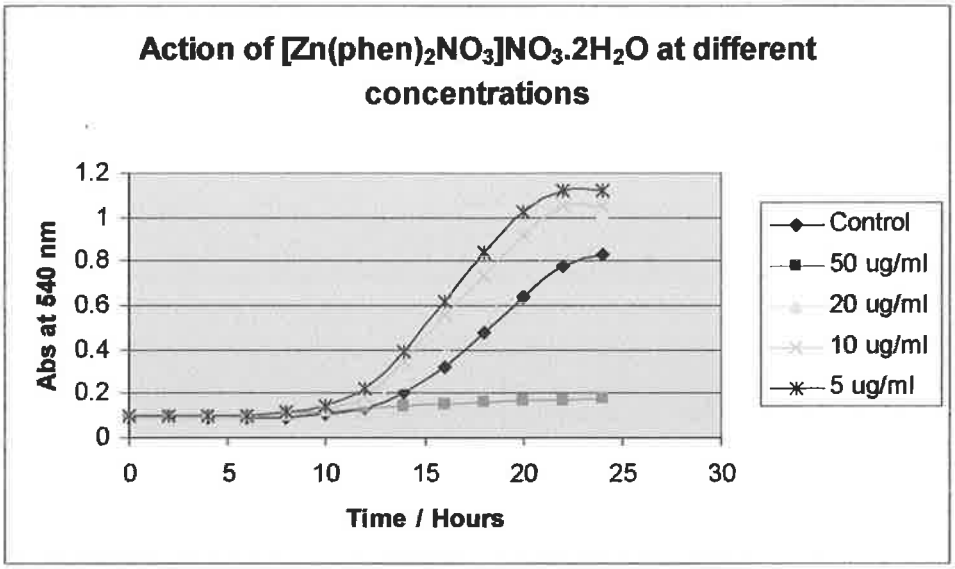

Figure 54: Kinetic growth curve of control cells and cells treated with complex **4**

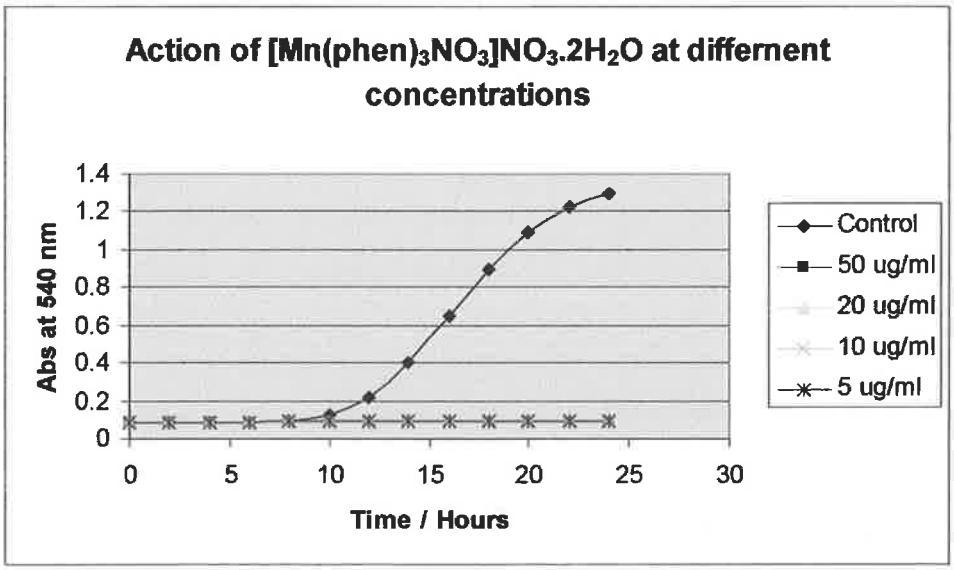

Figure 55: Kinetic growth curve of control cells and cells treated with complex **5**

The trend is the same for the chloride (**12** and **13**) and sulphate (**20** and **21**) phen derivatives whereby the manganese complexes **13** and **21** are superior anti-fungals to the zinc complexes **12** and **20** (Figures 56, 57, 58 and 59).

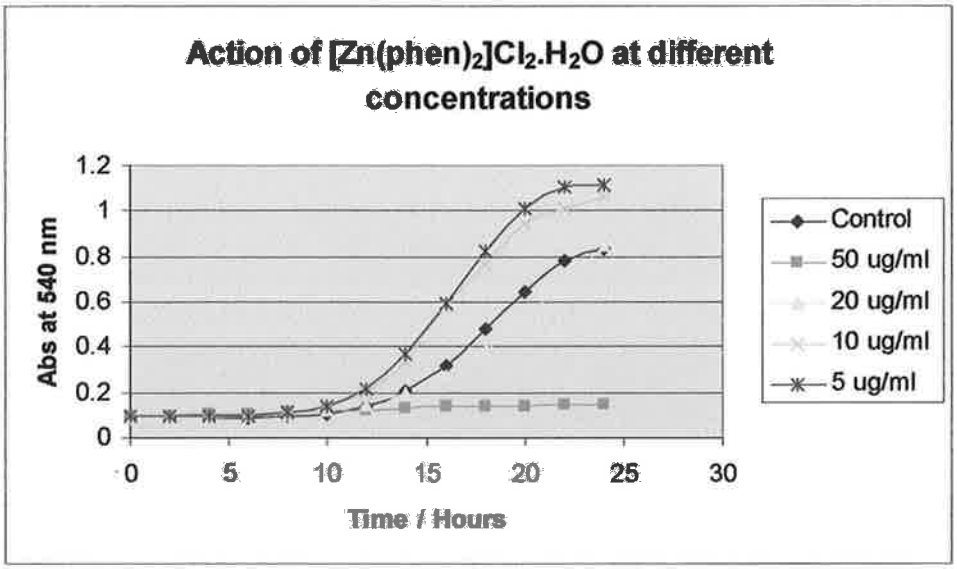

Figure 56: Kinetic growth curve of control cells and cells treated with complex **12**

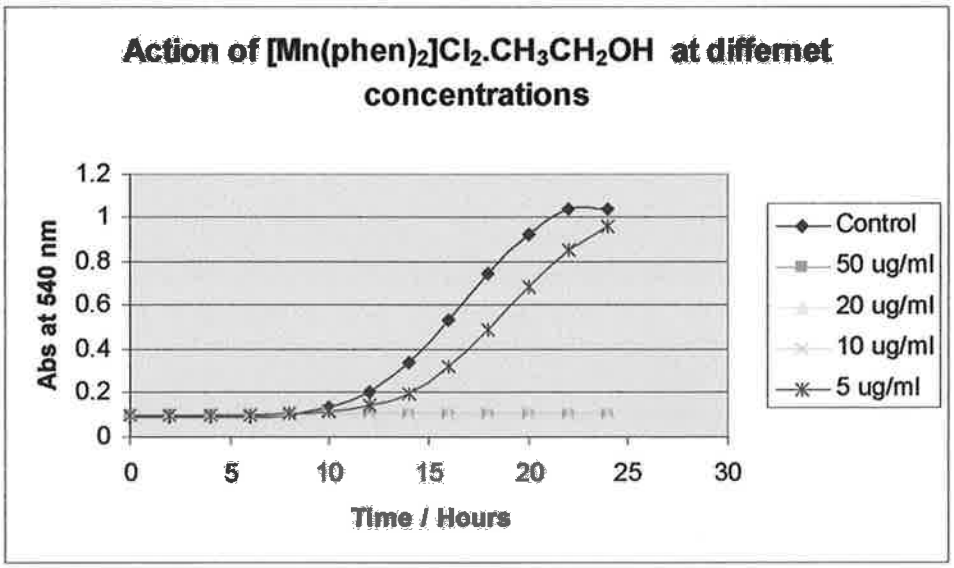

Figure 57: Kinetic growth curve of control cells and cells treated with complex **13**

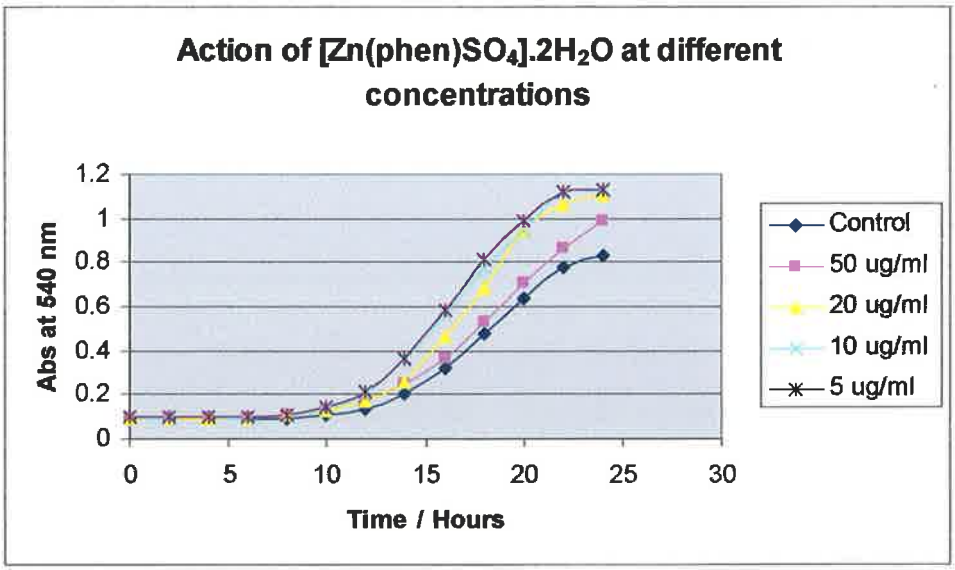

Figure 58: Kinetic growth curve of control cells and cells treated with complex **20**

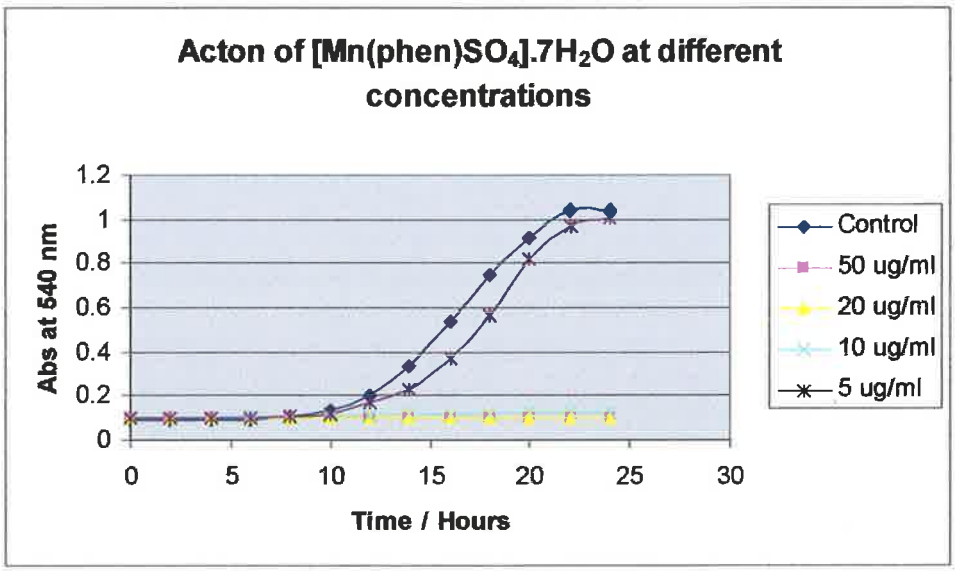

Figure 59: Kinetic growth curve of control cells and cells treated with complex **21**

When the zinc(II) and manganese(II) salts are reacted with phendione the activity of the salts is again increased significantly. As was seen for the phen derivatives the manganese complexes **(9, 17** and **25)** are superior anti-fungals compared to the zinc

complexes **(8, 16** and **24)** with complexes **9** and **25** displaying excellent anti-*Candida* activity at 5 μg/ml, (Figures 60 and 61).

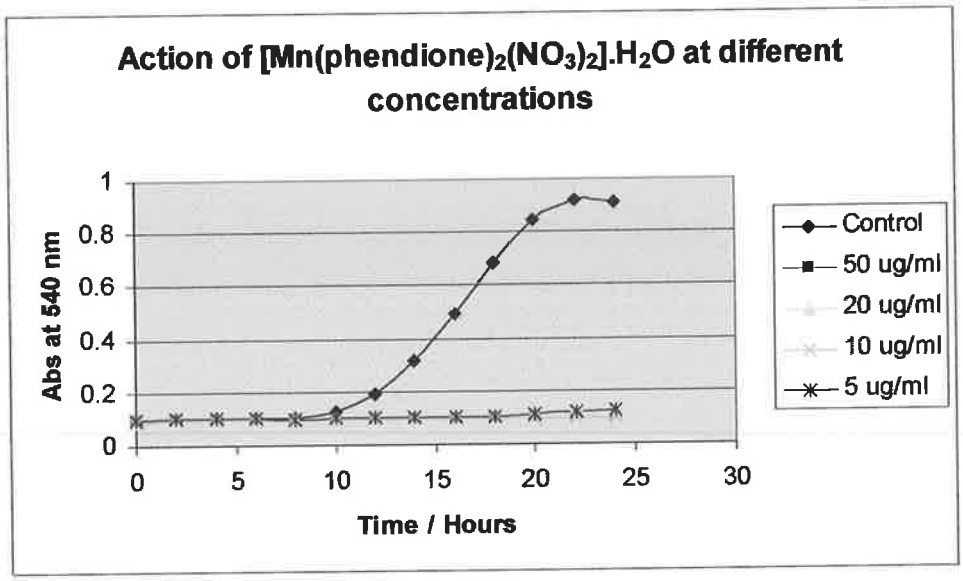

Figure 60: Kinetic growth curve of control cells and cells treated with complex **9**

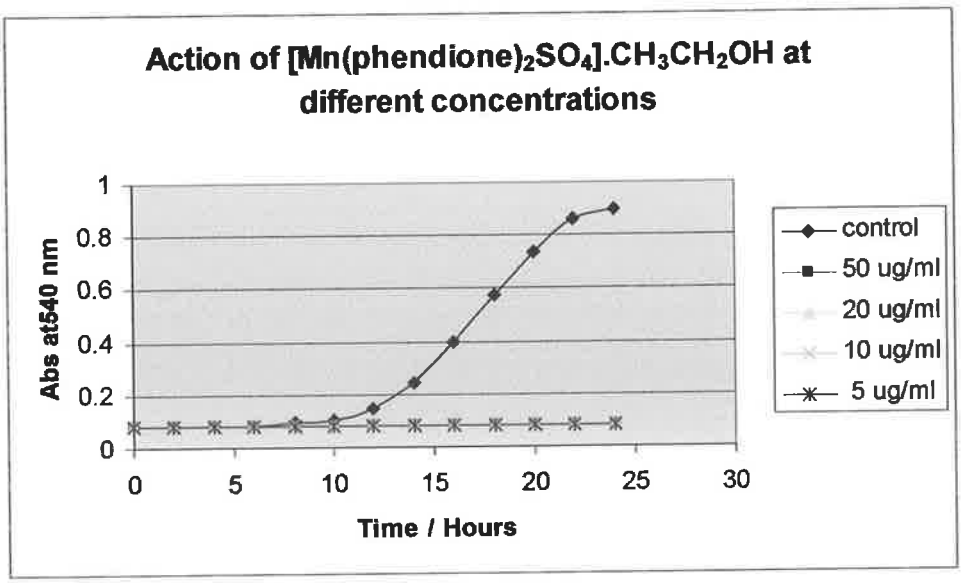

Figure 61: Kinetic growth curve of control cells and cells treated with complex **25**

Although a number of the phen and phendione derivatives display excellent anti-*Candida* activity it must be noted that none of them are as active as the free ligands themselves. Furthermore, complexing phen and phendione to metal centres in these metal salts has yielded a series of compounds which exhibit a range of fungitoxic abilities suggesting that the type of metal and counterion present influence the biological activity of the phen and phendione molecules.

D.3 ORGANIC DERIVATIVES OF 1,10-PHENANTHROLINE-5,6-DIONE

D.3.1 Synthesis of 1,3-bis([1,10]phenanthroline-[5,6-d]-imidazol-2-yl)benzene ($mbpibH_2.6H_2O$) (28)

The synthetic route to 1,3-bis([1,10]phenanthroline-[5,6-d]-imidazol-2-yl)benzene ($mbpibH_2.6H_2O$) **(28)** is shown in Scheme 22. The structure of **28** is shown in Figure 62.

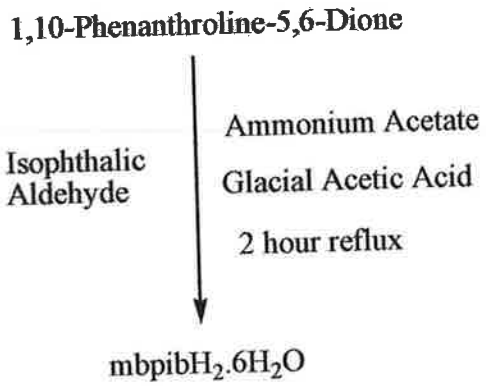

Scheme 22: Formation of $mbpibH_2.6H_2O$ **(28)**

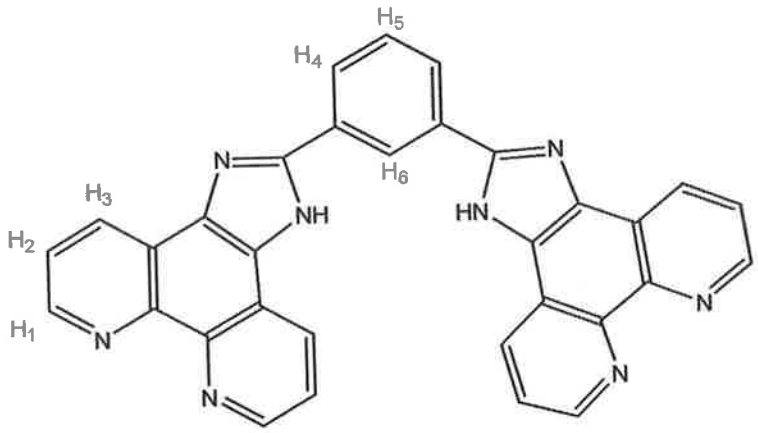

Figure 62: Structure and assignment of $mbpibH_2.6H_2O$ **(28)**

This compound formed as a yellow powder and formulated as shown below.

(28) $mbpibH_2.6H_2O$

% Calc: C, 61.73; H, 4.86; N, 18.00

% Found: C, 61.15; H, 3.45; N, 17.47

The IR spectrum of **28** {Appendix 1(28)} contains characteristic peaks as shown in Table 22.

Table 22: Characteristic IR-spectral bands of compound **(28)**

Band Assignment	**cm^{-1}**
NH stretching vibrations	3424
NH (m) bending	1624
Aromatic C-H stretching	3065
C-N-C stretching frequency	805, 738

The ^1H NMR spectrum of **28** in DMSO solvent is shown in Figure 63. The ^1H NMR spectrum indicates that each half of the ligand is equivalent due to the presence of internal symmetry. The proton signals at (ppm) 9.18, 7.86, 9.05, 8.49, 7.81 and 9.53 are assigned to H_1, H_2, H_3, H_4, H_5 and H_6. It has been reported that the proton on the nitrogen atom of the imidazole resonates at 14.05 ppm as a broad singlet[90], but it is unobserved in this experimental spectrum. It is assumed that the absence of this peak is due to quick exchange between the two nitrogens of the imidazole ring {Appendix 2(28)}.

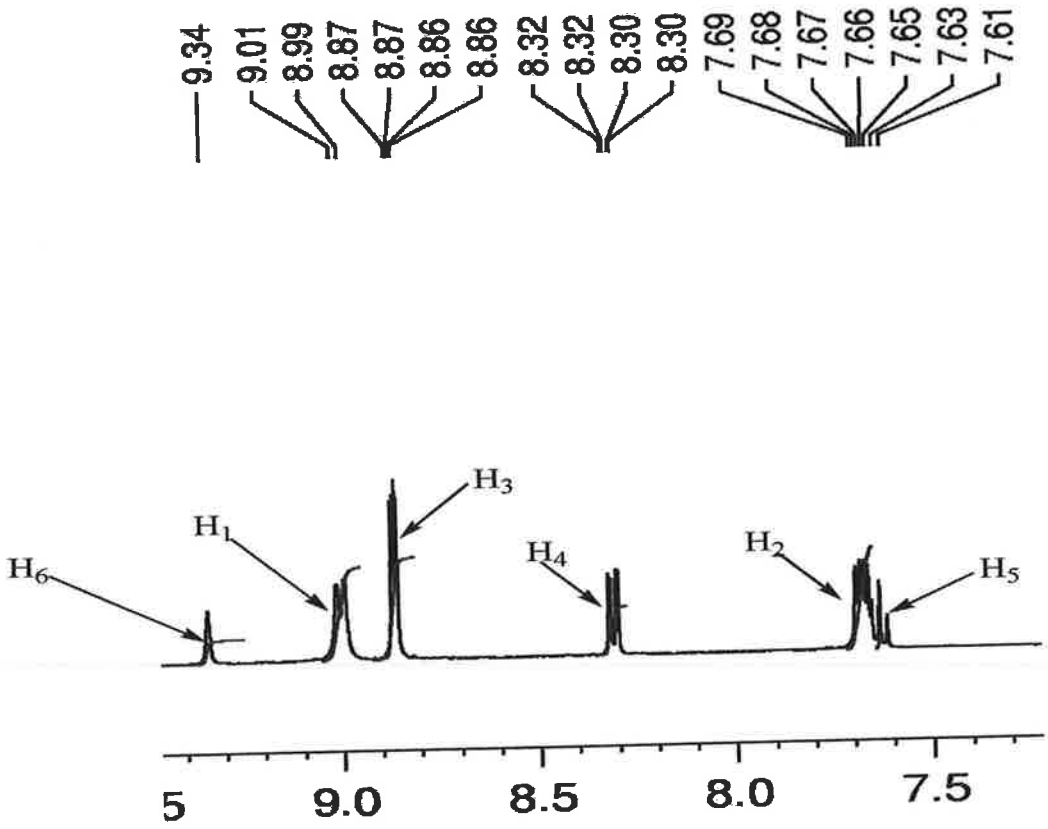

Figure 63: ^{1}H NMR spectrum of mbpibH_2.6H_2O **(28)**

D.3.2 Synthesis of 2-(3-formylphenyl)imidazo[4,5-f]-[1,10]phenanthroline (mfmp.$4H_2O$) (29)

The synthetic route to 2-(3-formylphenyl)imidazo[4,5-f]-[1,10]phenanthroline (mfmp.$4H_2O$) **(29)** is shown in Scheme 23. The structure of **29** is shown in Figure 64.

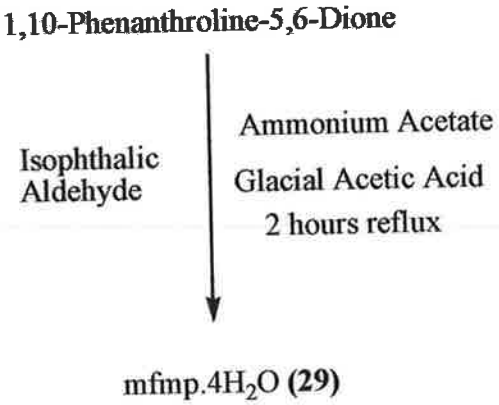

Scheme 23: Formation of mfmp.$4H_2O$ **(29)**

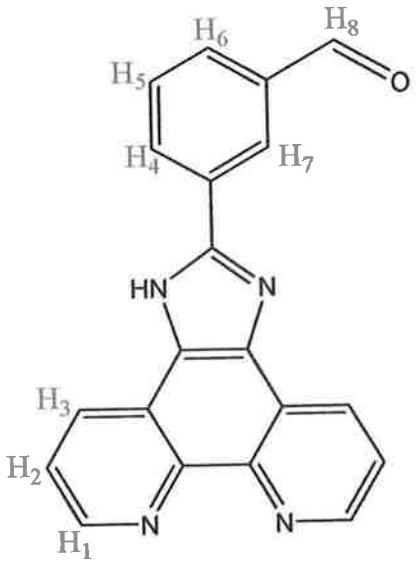

Figure 64: The structure and assignment of mfmp.$4H_2O$ **(29)**

(29) mfmp.4H_2O

% Calc: C, 60.60; H, 5.09; N, 14.13

% Found: C, 61.94; H, 4.01; N, 15.49

The IR spectrum of mfmp.4H_2O **(29)** {Appendix 1(29)} contained characteristic peaks as shown in Table 23.

Table 23: Characteristic IR-spectral bands of mfmp.4H_2O **(29)**

Band Assignment	**cm $^{-1}$**
NH stretching vibrations	3424
NH (m) bending	1558
C=O	1698
C-N-C stretching frequency	802, 738

The ^{1}H NMR spectrum of **29** in DMSO solvent is shown in Figure 65. The proton signals at (ppm) 9.04, 7.85, 8.95, 8.62, 7.87, 8.07, 8.81 and 10.17 are assigned to H_1, H_2, H_3, H_4, H_5, H_6, H_7 and H_8. As previously stated, it has been reported that the proton on the nitrogen atom of the imidazole resonates at 13.94 ppm as a singlet[90], but it is unobserved in this experimental spectrum. It is assumed that the absence of this peak is due to quick exchange between the two nitrogens of the imidazole ring {Appendix 2(29)}.

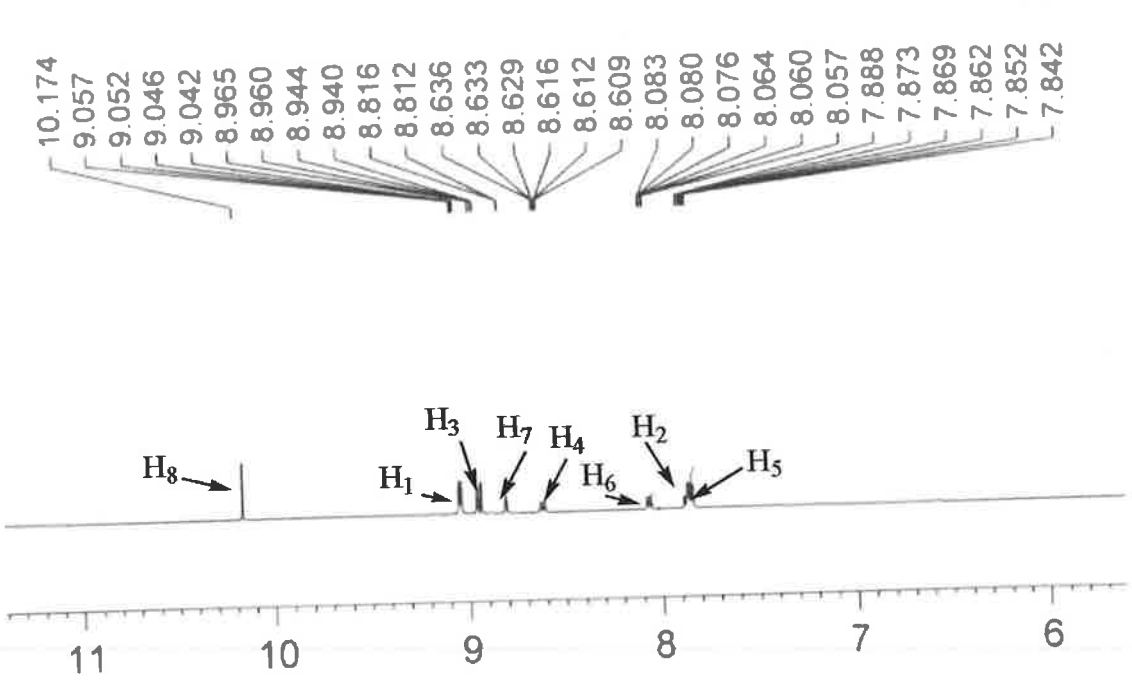

Figure 65: ^{1}H NMR spectrum of mfmp.4H_2O **(29)**

Analysis from ^{13}C-NMR {Appendix 3(29)} confirms the assignment of the protons.

D.3.3 Attempted synthesis of 2-(2-pyridinecarbox)imidazo[4,5-f] [1,10]phenanthroline (PCIP) (30)

The attempted synthetic route to 2-(2-pyridinecarbox)imidazo[4,5-f][1,10]phenanthroline (PCIP) **(30)** is shown in Scheme 24. The structure of **30** is shown in Figure 66.

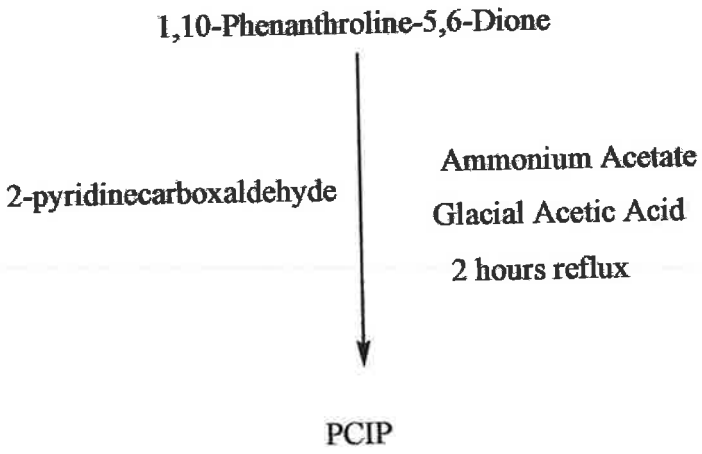

Scheme 24: Attempted formation of PCIP **(30)**

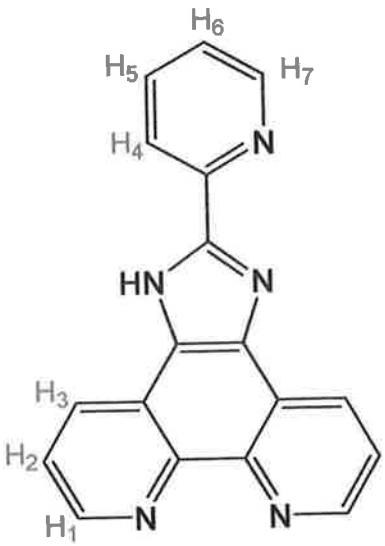

Figure 66: Assignment of proposed structure of PCIP **(30)**

The IR spectrum of the product from this reaction {Appendix 1(30)} contains characteristic peaks as shown in Table 24.

Table 24: Characteristic IR-spectral bands for the product from the attempted synthesis of PCIP **(30)**

Band Assignment	**cm $^{-1}$**
NH stretching vibrations	3423
NH (m) bending	1751
Aromatic C-H stretching	3112–3046
C-N-C stretching frequency	768, 736

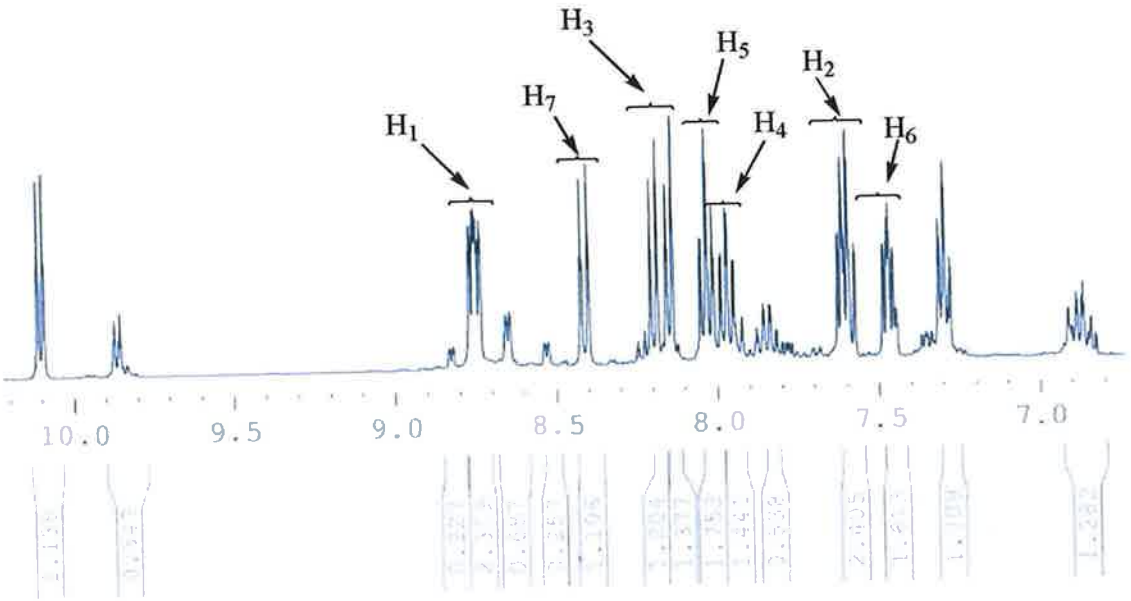

Figure 67: ^{1}H NMR spectrum of PCIP **(30)**

From the IR and ^{1}H NMR spectra, {Appendix 1(30) and Appendix 2(30)} there is some evidence that compound **30** was formed. In the ^{1}H NMR, the proton signals at (ppm) 8.73, 7.58, 8.15, 7.96, 8.02, 7.45 and 8.39 are assigned to H_1, H_2, H_3, H_4, H_5, H_6 and H_7. However, it can be clearly seen that there were unexpected peaks suggesting that there were impurities remaining after attempted purification, (Figure 67). This is also evident from the C^{13} spectra, as 22 carbon peaks were present when there should have only been 12 carbon peaks, {Appendix 3(30)}.

D.3.4 Synthesis of 4-(2,3-Dihydro-1H-1,3,7,8-tetraazacyclopenta-[I]-phenanthrene-2-yl)-benzonitrile (DPBN.$3H_2O$) (31)

The synthetic route to DPBN.$3H_2O$ **(31)** is shown in Scheme 25. The structure of **31** is shown in Figure 68.

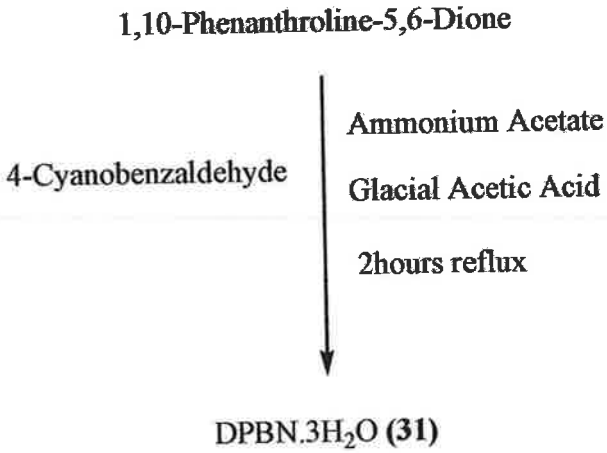

Scheme 25: Formation of DPBN.$3H_2O$ **(31)**

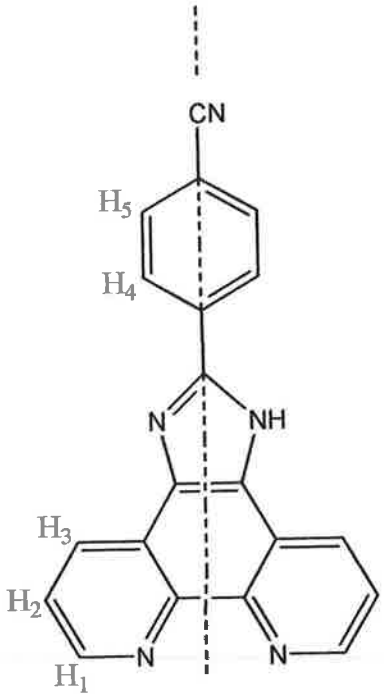

Figure 68: The structure and assignment of DPBN.3H_2O **(31)**

This ligand was obtained as a yellow powder and was formulated as shown below.

(31) DPBN.3H_2O

% Calc: C, 63.99; H, 4.56; N, 18.66

% Found: C, 63.49; H, 3.73; N, 17.74

The IR-spectrum of DPBN.3H_2O **(31)** {Appendix 1(31)} contains characteristic peaks as shown in Table 25.

Table 25: Characteristic IR-spectral peaks of DPBN.$3H_2O$ **(31)**

Band Assignment	cm^{-1}
NH stretching vibrations	3417
NH (m) bending	1610
CN	2225
C-N-C stretching frequency	802, 738

The ^1H NMR spectrum of **31** has five signals representing its ten hydrogens due to an axis of symmetry {Figure 69, Appendix 2(31)}.

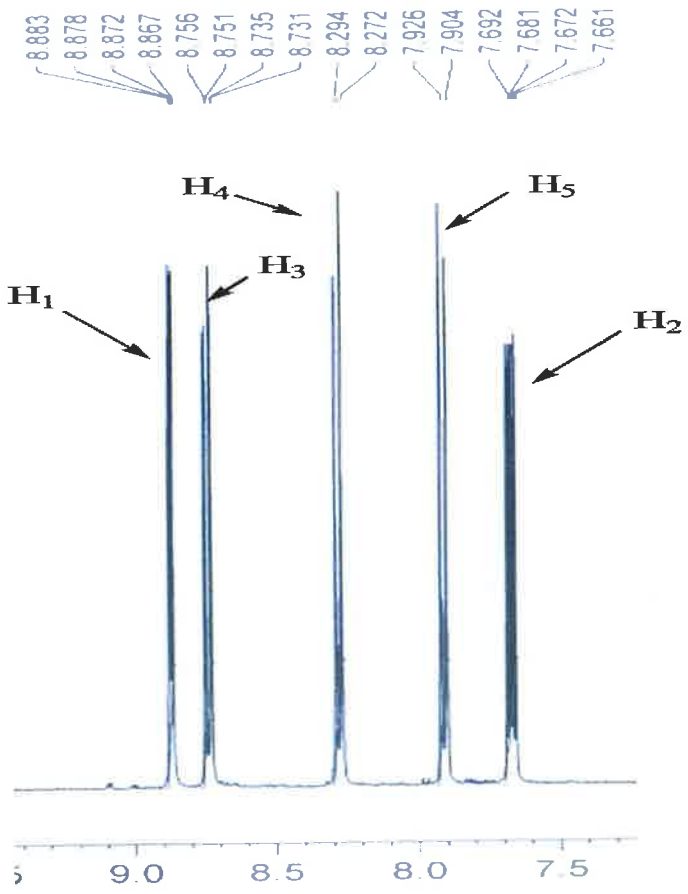

Figure 69: ^1H NMR spectrum of DPBN.$3H_2O$ **(31)**

The protons from the benzene ring H_4 and H_5 are coupled to each other via a vicinal coupling resulting in doublets. The coupling constant (J in Hz) for protons H_4 and H_5 is 8.8 Hz. The resonance of the proton on the nitrogen atom of the imidazole is not observed in this spectrum. Therefore it is assumed that the absence of this peak is due to a rapid exchange between the two nitrogens of the imidazole ring {Appendix 2(31)}.

D.3.4.1 ANTI-FUNGAL ACTIVITY OF $mbpibH_2.6H_2O$ (28), $mfmp.4H_2O$ (29), PCIP (30) and $DPBN.3H_2O$ (31) AGAINST *CANDIDA ALBICANS*

Compounds **28–31** were screened for their ability to inhibit the growth of an isolate of *Candida albicans* at concentrations of 50 μg/ml, 20 μg/ml, 10 μg/ml and 5 μg/ml.

The anti-fungal activity of compounds **28-31** was compared to the activity of phendione **(1)** and prescription drug Amphothericin B (Table 26). Compounds **28-31** were shown to be relatively inactive against *Candida albicans*. This is in contrast to the potent activity displayed by phendione **(1)**. The growth curves for compounds **28-31** are shown in Figures 70, 71, 72 and 73.

Table 26: Anti-*Candida* activity of Amphothericin B and compounds **(1), (28)-(31)**

Test Compound	**% Cell Growth (at concentrations of 50 - 5 μg/ml)**				**IC_{50} value μg/ml**	**IC_{50} value μM**
	50	**20**	**10**	**5**		
Control	100	100	100	100		
Amphothericin B	6.9±9.6	7.01±9.6	13.12±33	70.5±56	10	1.08×10^{-5}
Phendione **(1)**	5.6±12	5.62±10	5.55±6.1	8.3±42	5	2.37×10^{-5}
$mbpibH_26H_2O$ **(28)**	66±167	83±111	91±149	94±100	50	8.03×10^{-5}
$mfmp.4H_2O$ **(29)**	63±13	66±348	74±81	82±161	50	1.26×10^{-4}
PCIP **(30)**	74±30	94±237	96±374	96±237	50	1.68×10^{-4}
$DPBN.3H_2O$ **(31)**	76±39	82±122	86±166	89±124	50	1.33×10^{-4}

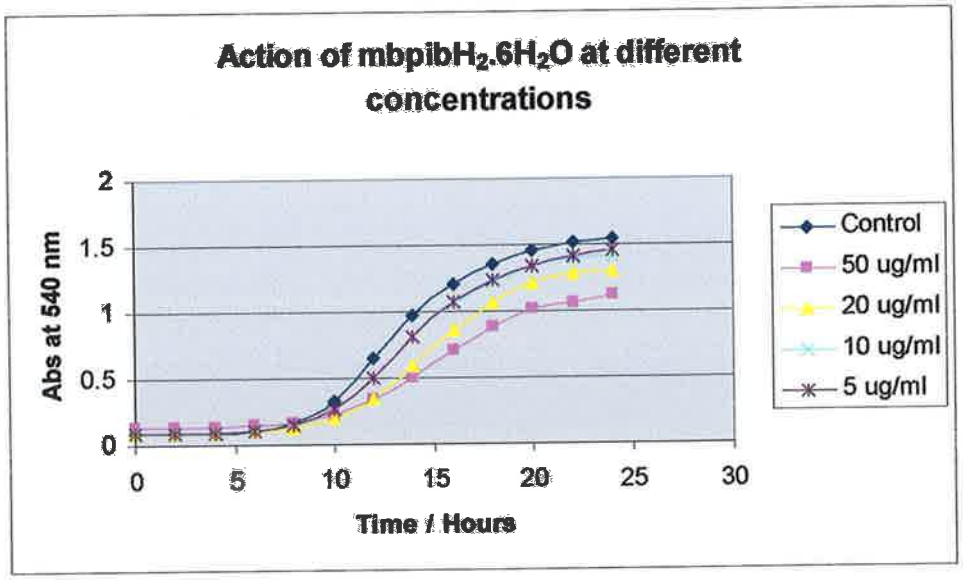

Figure 70: Kinetic growth curve of control cells and cells treated with complex **28**

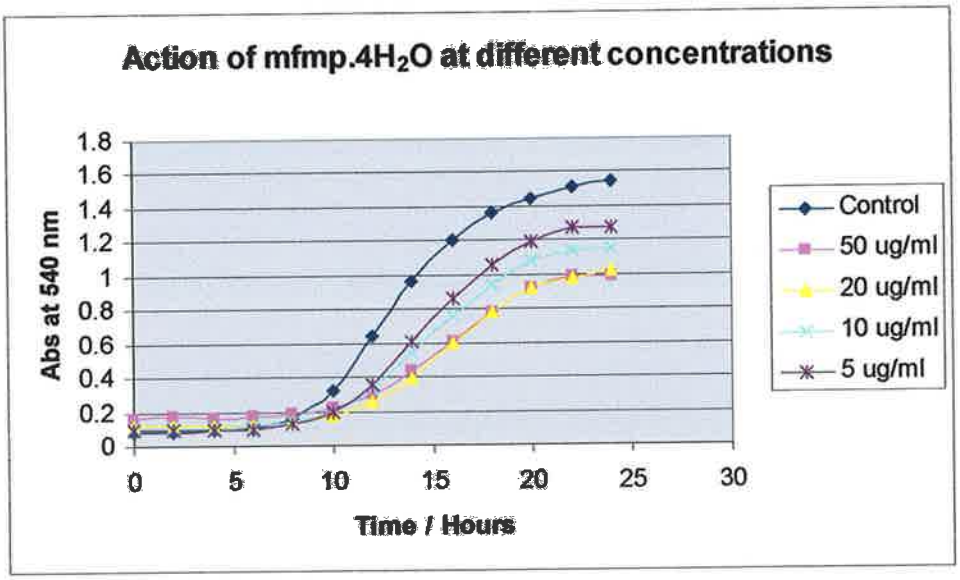

Figure 71: Kinetic growth curve of control cells and cells treated with complex **29**

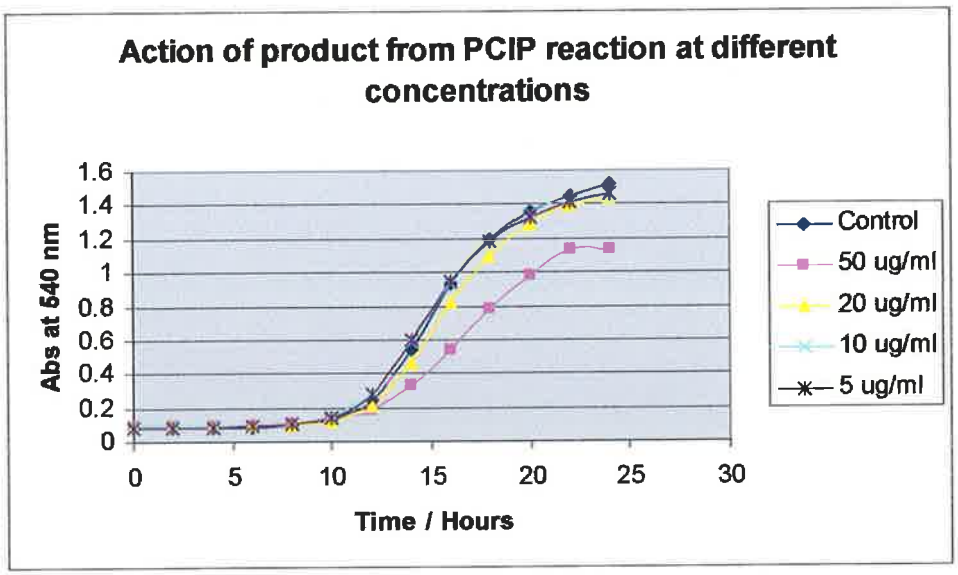

Figure 72: Kinetic growth curve of control cells and cells treated with complex **30**

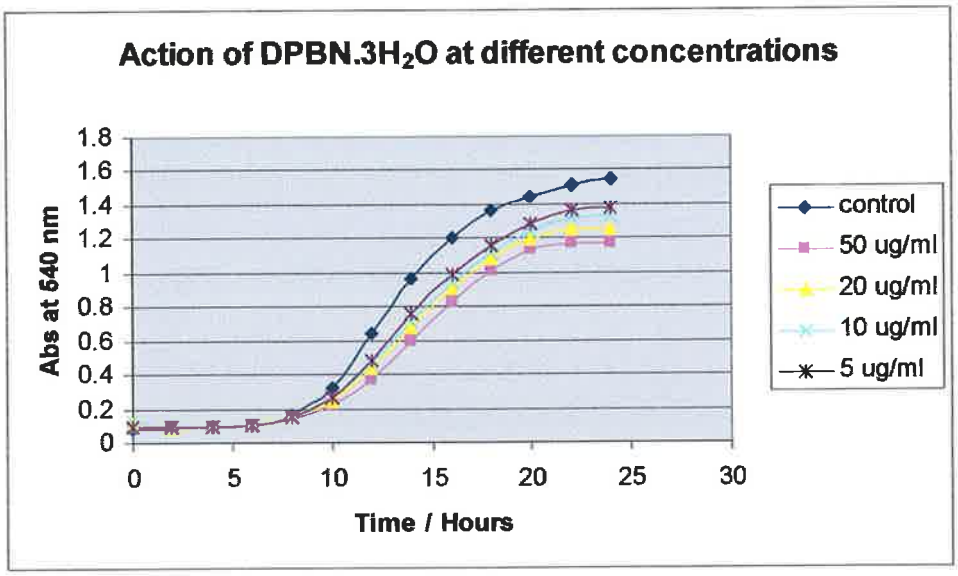

Figure 73: Kinetic growth curve of control cells and cells treated with complex **31**

D.4 SYNTHESIS OF TRANSITION METAL COMPLEXES OF $mbpibH_2.6H_2O$ (28)

Three manganese(II) metal salt (nitrate, chloride and acetate) complexes incorporating the chelating $mbpibH_2.6H_2O$ **(28)** ligand were synthesized and tested for their anti-*Candida* activity.

The manganese(II) metal salts of nitrate, chloride and acetate were reacted with complex **28**, to yield the novel complexes **32–34** respectively in accordance with Scheme 26.

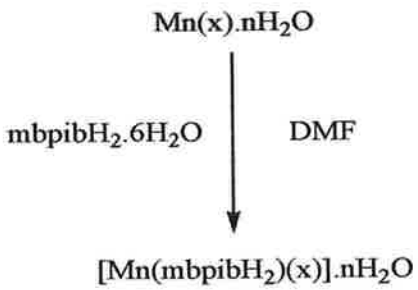

Scheme 26

where x = NO_3^-, Cl^-, CH_3COO^-

n = 3, 4 or 9

All three complexes were obtained as yellow powders and were formulated as shown below.

(32) $[Mn(mbpibH_2)](NO_3)_2.3H_2O$

% Calc: C, 51.41; H, 3.24; N, 18.74

% Found: C, 51.63; H, 3.34; N, 16.80

(33) $[Mn(mbpibH_2)]Cl_2.4H_2O$

% Calc: C, 53.95; H, 3.68; N, 15.73

% Found: C, 54.23; H, 3.37; N, 15.95

(34) $[Mn(mbpibH_2)(CH_3CO_2)_2].9H_2O$

% Calc: C, 50.89; H, 4.98; N, 13.19

% Found: C, 50.04; H, 3.39; N, 13.51

The IR spectra of complexes **32-34** {Appendix 1(32–34)} contain characteristic peaks as shown in Table 27.

Table 27: Characteristic IR-spectral bands of complexes **32–34**

Band assignment cm^{-1}	**$mbpibH_2.6H_2O$**	**32**	**33**	**34**
NH stretching vibrations	3424	3403	3421	3419
NH (m) bending	1624	1655	1657	1660
C-N-C stretching frequency	805, 738	813, 735	812, 736	813, 736
NO_3^- (uncoord)	-	1383	-	-
NO_3^- (coord)	-	-	-	-
vOCO asym	-	-	-	1562
vOCO sym	-	-	-	1407

The room temperature magnetic moments of powdered samples of complexes **32** (5.81 B.M), **33** (5.91 B.M) and **34** (5.89 B.M) were found to have a μ_{eff} value that was in the expected range (μ_{eff} = 5.7-6.0 B.M.) for high spin manganese(II) complexes in which no interactions between the metal centre occurs.

Attempts to react **28** with cobalt(II) nitrate yielded an orange solution which upon standing deposited a small number of pink crystals. No other product was isolated from this reaction despite several attempts being made. The pink crystals were suitable for X-ray analyses and the structure of the complex which formulates as $[Co(phendione)(H_2O)_4](NO_3)_2.H_2O$ **(35)** is shown in Figure 74 and selected bond lengths are listed in Tables 28 and 29.

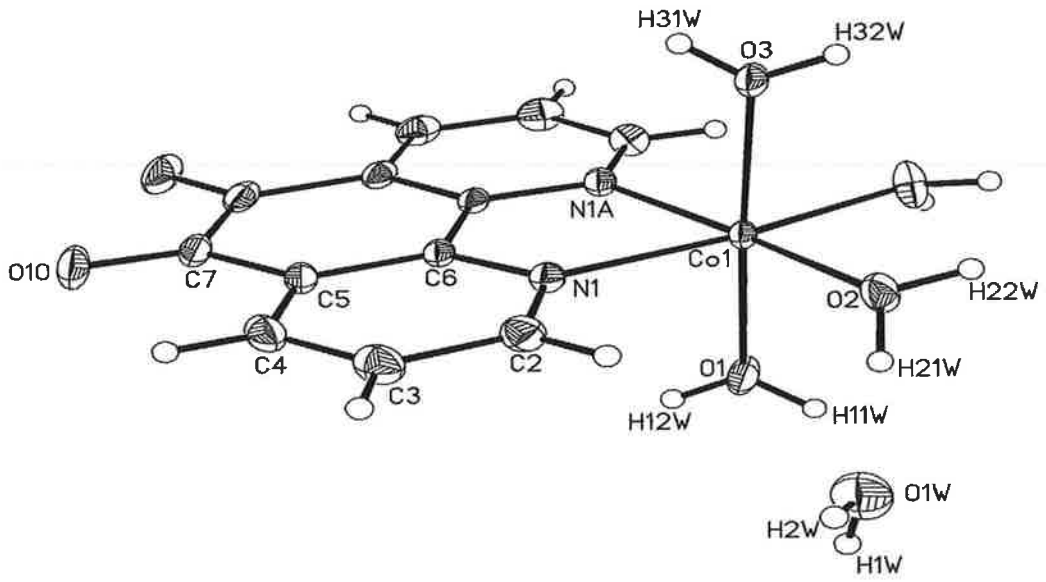

Figure 74: The X-ray crystal structure of $[Co(phendione)(H_2O)_4](NO_3)_2.H_2O$ **(35)**

Table 28: Selected bond lengths [Å], angles [°] and torsion angles [°] around the cobalt centres in $[Co(phendione)(H_2O)_4](NO_3)_2.H_2O$ **(35)**

Complex (35)	
Bond lengths Å	
Co(1)-O(1)	2.0371(17)
Co(1)-O(2)	2.0802(12)
Co(1)-O(2)#1	2.0802(12)
Co(1)-O(3)	2.0918(16)
Co(1)-N(1)#1	2.1258(12)
Co(1)-N(1)	2.1258(12)
Bond angles °	
O(1)-Co(1)-O(2)	92.07(5)
O(1)-Co(1)-O(2)#1	92.07(5)
O(2)-Co(1)-O(2)#1	88.53(7)
O(1)-Co(1)-O(3)	177.51(7)
O(2)-Co(1)-O(3)	86.15(5)
O(2)#1-Co(1)-O(3)	86.15(5)
O(1)-Co(1)-N(1)#1	89.88(5)
O(2)-Co(1)-N(1)#1	174.06(5)
O(2)#1-Co(1)-N(1)#1	97.01(5)
O(3)-Co(1)-N(1)#1	92.07(5)
O(1)-Co(1)-N(1)	89.88(5)
O(2)-Co(1)-N(1)	97.00(5)
O(2)#1-Co(1)-N(1)	174.06(5)
O(3)-Co(1)-N(1)	92.07(5)

N(1)#1-Co(1)-N(1)	77.38(7)
C(2)-N(1)-Co(1)	126.30(10)
C(6)-N(1)-Co(1)	115.11(10)
Co(1)-O(1)-H(11W)	121(3)
Co(1)-O(1)-H(12W)	120(3)
Co(1)-O(2)-H(21W)	124.5(18)
Co(1)-O(2)-H(22W)	116.6(18)
Co(1)-O(3)-H(31W)	120(2)
Co(1)-O(3)-H(32W)	117(2)
Torsion angles °	
O(1)-Co(1)-N(1)-C(2)	89.44(13)
O(2)-Co(1)-N(1)-C(2)	-2.63(13)
O(2)#1-Co(1)-N(1)-C(2)	-161.4(4)
O(3)-Co(1)-N(1)-C(2)	-89.00(13)
N(1)#1-Co(1)-N(1)-C(2)	179.34(10)
O(1)-Co(1)-N(1)-C(6)	-87.60(10)
O(2)-Co(1)-N(1)-C(6)	-179.67(10)
O(2)#1-Co(1)-N(1)-C(6)	21.6(5)
O(3)-Co(1)-N(1)-C(6)	93.96(10)
N(1)#1-Co(1)-N(1)-C(6)	2.30(11)
Co(1)-N(1)-C(2)-C(3)	-178.49(12)
Co(1)-N(1)-C(6)-C(5)	178.29(10)
Co(1)-N(1)-C(6)-C(6)#1	-2.00(10)

Table 29: Hydrogen bonds for $[Co(phendione)(H_2O)_4](NO_3)_2.H_2O$ [Å and °]

D-H...A	d(D-H)	d(H...A)	d(D...A)	<(DHA)
O(1)-H(11W)...O(4)#2	0.84(3)	1.90(3)	2.741(2)	179(4)
O(1)-H(11W)...Cl(1)#2	0.84(3)	2.86(3)	3.6293(18)	152(3)
O(1)-H(12W)...O(7)#1	0.84(3)	1.92(3)	2.708(3)	158(2)
O(1)-H(12W)...O(7)	0.84(3)	1.92(3)	2.708(3)	158(2)
O(1)-H(12W)...Cl(1)	0.84(3)	3.06(3)	3.8870(18)	169(3)
O(2)-H(21W)...O(1W)	0.85(2)	1.85(2)	2.672(3)	162(3)
O(2)-H(21W)...O(1WA)	0.85(2)	1.89(2)	2.736(4)	178(3)
O(2)-H(22W)...O(4)#3	0.87(2)	1.91(2)	2.7320(18)	158(3)
O(2)-H(22W)...Cl(1)#3	0.87(2)	2.86(2)	3.5917(13)	143(2)
O(3)-H(32W)...O(5)#3	0.87(3)	1.80(3)	2.672(2)	178(3)
O(3)-H(32W)...Cl(1)#3	0.87(3)	2.89(3)	3.6974(17)	155(3)
O(3)-H(31W)...O(10)#4	0.81(3)	2.33(2)	3.020(2)	143.6(8)
O(3)-H(31W)...O(10)#5	0.81(3)	2.33(2)	3.020(2)	143.6(8)
O(1WA)-H(1W)...O(1WA)#6	0.37(3)	1.87(3)	2.236(7)	167(6)
O(1WA)-H(1W)...O(1W)#6	0.37(3)	2.37(3)	2.721(5)	158(6)
O(1W)-H(2W)...O(6)#7	0.82(2)	1.51(3)	2.170(4)	135(3)
O(1W)-H(2W)...O(7)#7	0.82(2)	1.97(3)	2.778(4)	167(3)
O(1W)-H(2W)...Cl(1)#8	0.82(2)	2.73(3)	3.515(3)	160(3)
O(1W)-H(2W)...O(4)#8	0.82(2)	2.94(3)	3.595(3)	138(3)

Symmetry transformations used to generate equivalent atoms:

#1 x,-y,z #2 -x+1,-y,-z+1 #3 x+1,y,z #4 -x+1,-y,-z

#5 -x+1,y,-z #6 -x+3/2,-y+1/2,-z+1 #7 x+1/2,-y+1/2,z

#8 x+1/2,y+1/2,z

In $[Co(phendione)(H_2O)_4](NO_3)_2.H_2O$ **(35)** there is only one phendione ligand chelating the metal centre with 4 coordinated water molecules completing an octahedral geometry. The two nitrate anions are essentially unbound and exist in the lattice as counter ions for the $[Co(phendione)(H_2O)_4]^{2+}$ ions. The formation of **35** is unexpected. However given the small amount of crystals obtained it is likely that it results from the presence of phendione as an impurity in $mbpibH_2.6H_2O$ **(28)** ligand. However attempts to generate this mono-phendione derivative of cobalt(II) nitrate using pure phendione and $Co(NO_3)_2$ were not successful with the known di-phendione cobalt(II) nitrate derivative being indicated. To the best of our knowledge $[Co(phendione)(H_2O)_4](NO_3)_2.H_2O$ **(35)** is a novel complex.

The IR spectrum of complex **35** is shown in Appendix 1(35). The strong peak present at 1694 cm^{-1} is a stretching frequency of the C=O band, characteristic of the phendione ligand. Another characteristic of the phendione ligand is bands at 820 cm^{-1} and 734 cm^{-1}. A band appears in the spectra at 1307 cm^{-1} which is indicative of the presence of a coordinated nitrate group.

D.4.1 ANTI-FUNGAL ACTIVITY OF mbpibH_2.6H_2O (28) COMPLEXES AGAINST *CANDIDA ALBICANS*

Complexes **32–34** were screened for their ability to inhibit the growth of an isolate of *Candida albicans* at concentrations of 50 μg/ml, 20 μg/ml, 10 μg/ml and 5 μg/ml.

The anti-fungal activity of the metal free ligand **28** was found to be very low at the highest tested concentration of 50 μg/ml, showing no comparability to that of prescription drug Amphothericin B. The growth curves for **28** and prescription drug Amphothericin B are shown in Figures 70 and 52.

The anti-fungal activity of complexes **32-34** was compared to the activity of mbpibH_2.6H_2O **(28)** and prescription drug Amphothericin B (Table 30). Complexes **32-34** were shown to be moderately active against *Candida albicans*, in contrast to the activity displayed by **28**, (Table 30). The growth curves for complexes **32-34** are shown in Figures 75, 76 and 77.

Table 30: Anti-*Candida* activity of Amphothericin B, $mbpibH_2.6H_2O$ **(28)** and complexes **32-34**

Test Compound	% Cell Growth (at concentrations of 50 - 5 µg/ml)				IC_{50} value µg/ml	IC_{50} value µM
	50	20	10	5		
Control	100	100	100	100		
Amphothericin B	6.9±9.6	7.01±9.6	13.12±33	70.5±56	10	1.08×10^{-5}
$mbpibH_2.6H_2O$ **(28)**	66±167	83±111	91±149	94±100	50	8.03×10^{-5}
$[Mn(mbpibH_2)](NO_3)_2.3H_2O$ **(32)**	45±30	61±104	65±164	71±49	50	6.68×10^{-5}
$[Mn(mbpibH_2)]Cl_2.4H_2O$ **(33)**	48±144	49±185	54±127	55±118	50	7.01×10^{-5}
$[Mn(mbpibH_2)(CH_3CO_2)_2].9H_2O$ **(34)**	47±102	54±98	55±198	60±50	50	5.88×10^{-5}

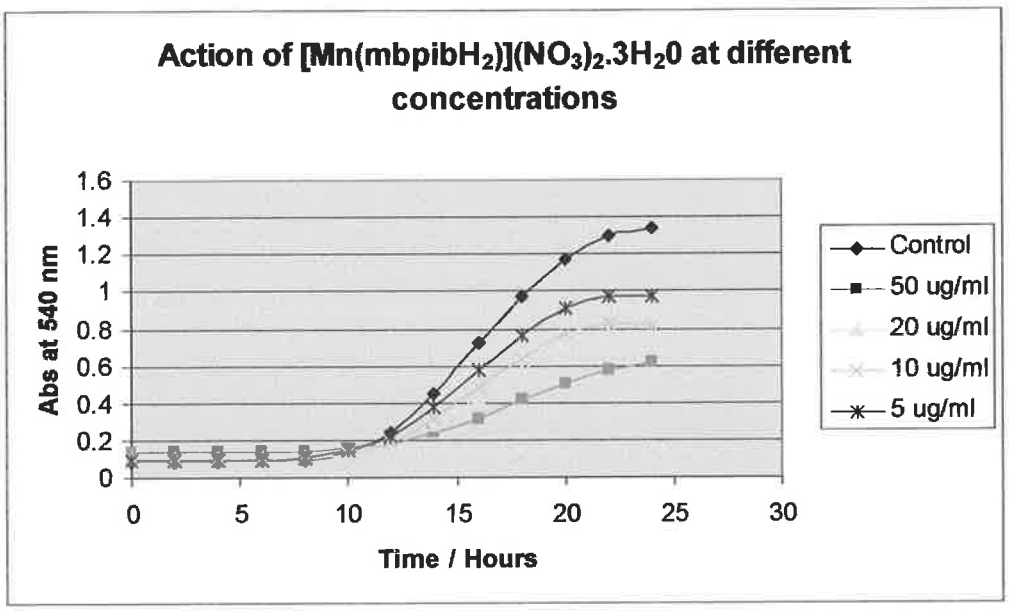

Figure 75: Kinetic growth curve of control cells and cells treated with complex **32**

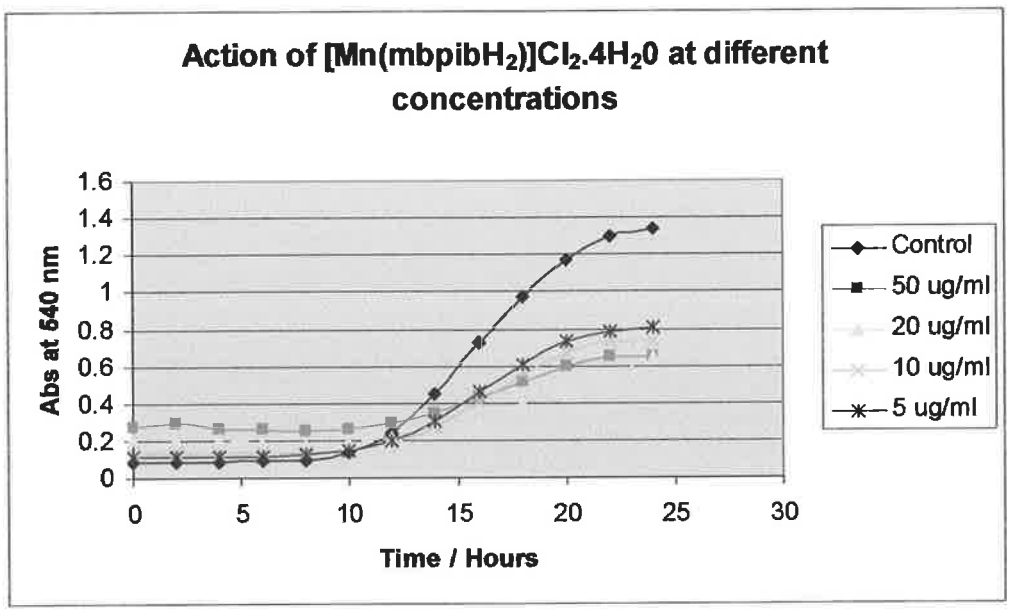

Figure 76: Kinetic growth curve of control cells and cells treated with complex **33**

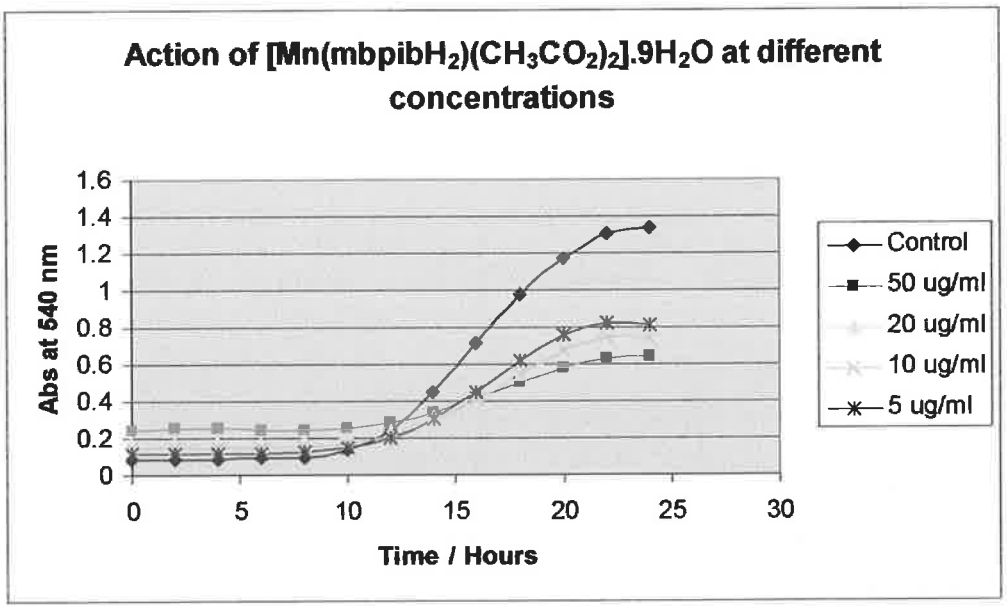

Figure 77: Kinetic growth curve of control cells and cells treated with complex **34**

D.5 SYNTHESIS OF TRANSITION METAL COMPLEX OF DPBN.$3H_2O$ (31)

Copper(II) nitrate was reacted with DPBN.$3H_2O$ **(31)**, to yield the novel nitrate complex **36**, in accordance with Scheme 27.

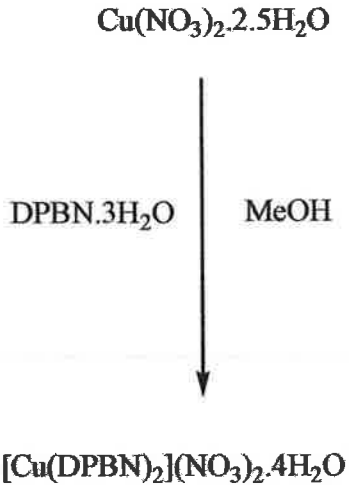

Scheme 27

Complex **36** was obtained as an aqua blue powder and was formulated as shown below.

(36) [Cu(DPBN)$_2$](NO$_3$)$_2$.4H$_2$O

% Calc: C, 53.25; H, 3.35; N, 18.63

% Found: C, 53.55; H, 2.61; N, 18.44

The IR spectrum of complex **36** {Appendix 1(36)} contains characteristic peaks as shown in Table 31.

Table 31: Characteristic IR-spectral bands of complex **36**

Band assignment cm^{-1}	**DPBN. $3H_2O$**	**36**
NH stretching vibrations	3417	3427
NH (m) bending	1610	1608
CN	2225	2227
C-N-C stretching frequency	802, 738	812, 726
NO_3^- (uncoord)	-	1384

The room temperature magnetic moment of the powdered complex **36** (1.91 B.M.) is in the range excepted (μ_{eff} = 1.8-2.1 B.M.) for a copper(II) complex where there is no significant exchange interactions between adjacent metal centres[36].

D.5.1 ANTI-FUNGAL ACTIVITY OF $[Cu(DPBN)_2(NO_3)_2].4H_2O$ (36) AGAINST *CANDIDA ALBICANS*

Complex **36** was examined for its ability to inhibit the growth of an isolate of *Candida albicans* at concentrations of 50 μg/ml, 20 μg/ml, 10 μg/ml and 5 μg/ml, (Table 32).

The anti-fungal activity of complex **36** was compared to the activity of $DPBN.3H_2O$ **(31)** and prescription drug Amphothericin B (Table 32). **36** displays moderate to good activity (Figure 78) when compared with that of the free $DPBN.3H_2O$ ligand. However it should be noted that copper(II) nitrate shows some activity against the pathogen (Table 18) but it is not as active as **36**.

Table 32: Anti-Candida activity of Amphothericin B, $DPBN.3H_2O$ **(31)** and complex **36**

Test Compound	**% Cell Growth (at concentrations of 50 - 5 μg/ml)**				**IC_{50} value μg/ml**	**IC_{50} value μM**
	50	**20**	**10**	**5**		
Control	100	100	100	100		
Amphothericin B	6.9±9.6	7.01±9.6	13.12±33	70.5±56	10	1.08×10^{-5}
$DPBN.3H_2O$ **(31)**	76±39	82±122	86±166	89±124	50	1.33×10^{-4}
$[Cu(DPBN)_2](NO_3)_2.4H_2O$ **(36)**	31±91	33±184	44±54	46±454	50	5.54×10^{-5}

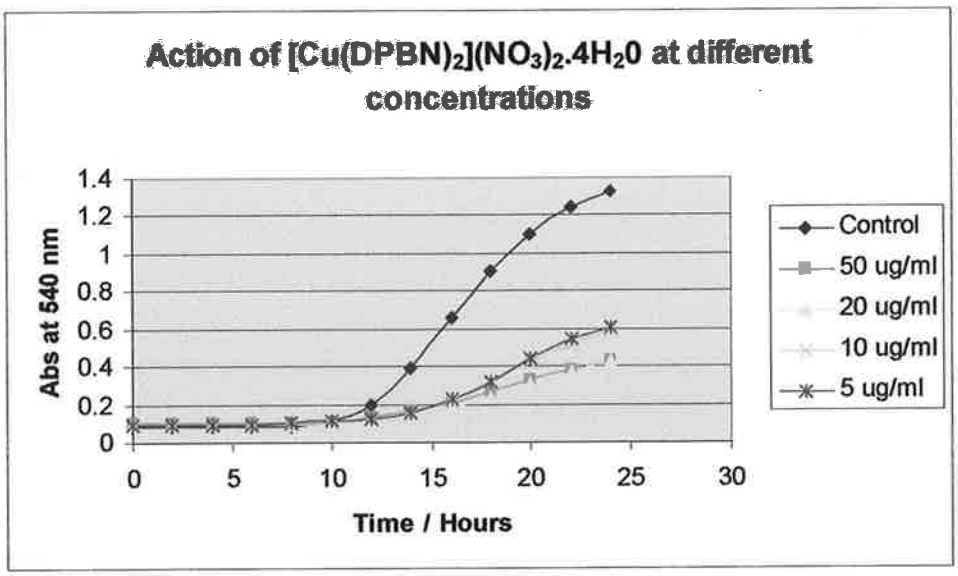

Figure 78: Kinetic growth curve of control cells and cells treated with complex **36**

D.6 REACTION OF PHENDIONE WITH AMINO ACID ESTERS

In another attempt to modify the backbone of the phenanthroline ligand it was decided to attempt reacting a series of amino acids with phendione. The first reaction involves the methyl ester of L-tyrosine as this was available in the laboratory. L-Tyrosine methyl ester reacted very smoothly with phendione in refluxing methanol to yield PhenTyrOMe.CH_3OH **(37)** as shown in Scheme 28. The product was isolated in moderate yield.

Attempts to react the ethyl ester of L-tyrosine with phendione yielded exactly the same product as from the methyl ester reaction in similar yields. It is believed that the methanol reacted with the L-tyrosine ethyl ester converting it to the methyl ester (as shown in Scheme 29) and that the resulting product was produced through the reaction of the methyl ester with the phendione.

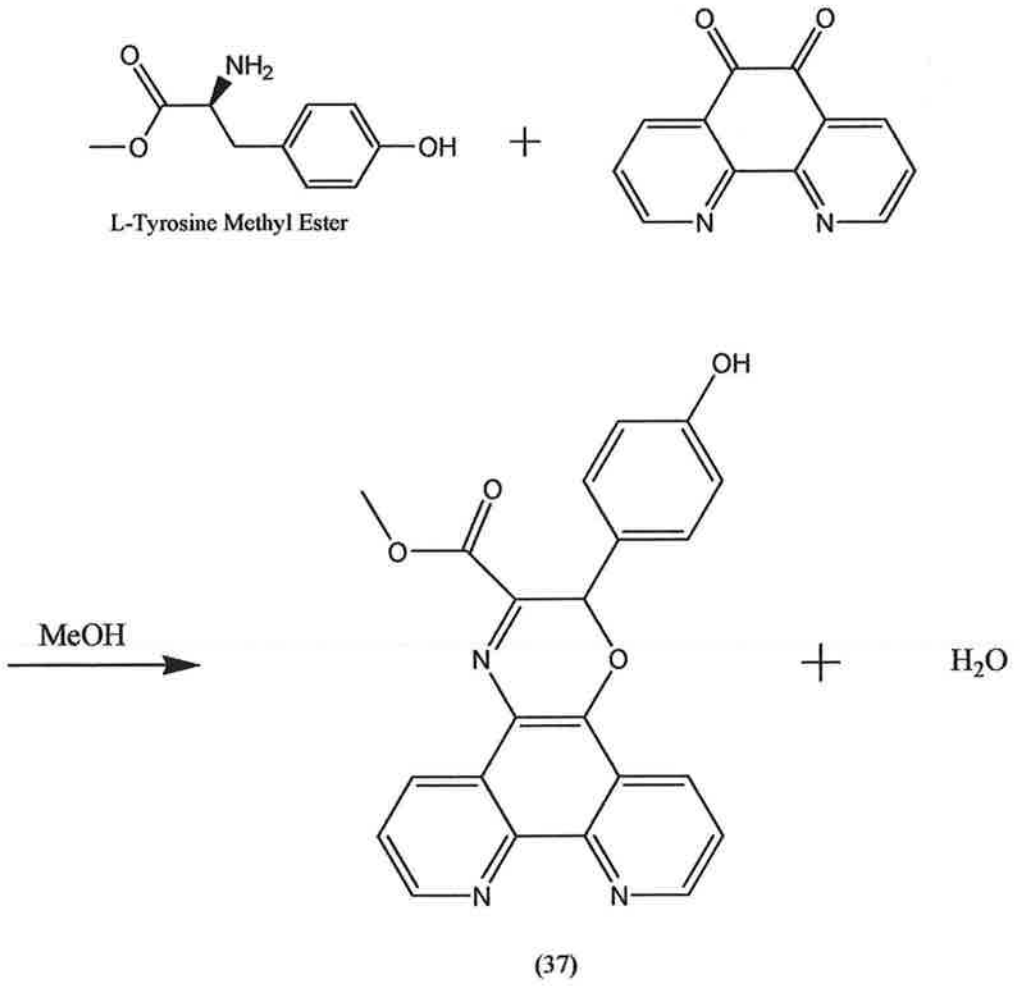

(37)

Scheme 28: Synthetic route to PhenTyrOMe.CH_3OH **(37)**

Compound 37 formed as orange crystals and formulated as follows:

(37) PhenTyrOMe.CH_3OH

% Calc: C, 66.18; H, 4.59; N, 10.07.

% Found: C, 67.00; H, 4.36; N, 10.24

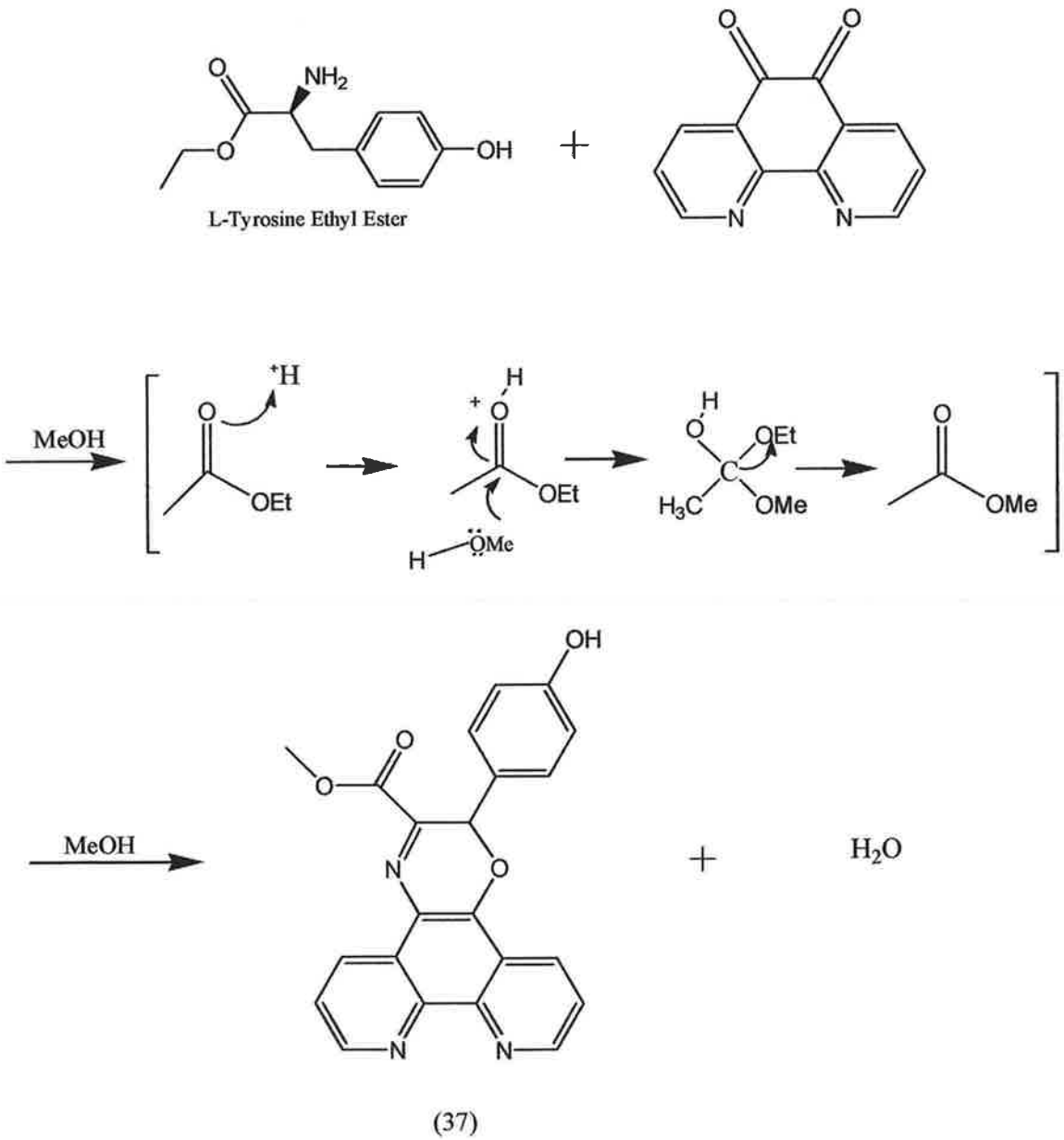

(37)

Scheme 29: Synthetic route to PhenTyrOMe.CH_3OH **(37)**

The crystals of **37** were suitable for X-ray crystallographic analysis and the structure of PhenTyrOMe.CH_3OH **(37)** is shown in Figures 79, 80 and 81. Selected bond lengths and angles are listed in Table 33 and 34.

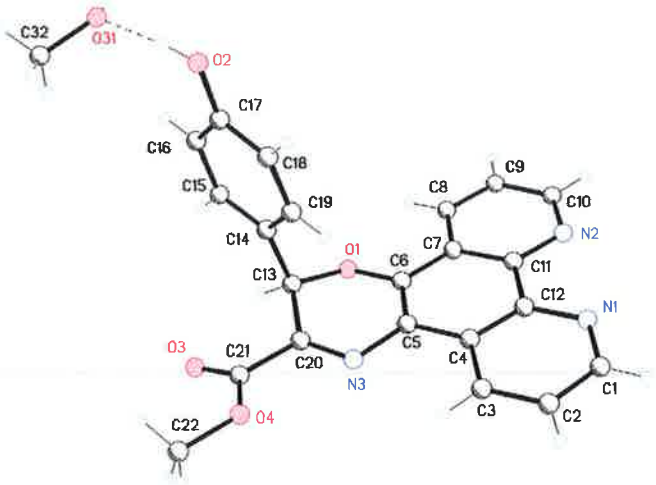

Figure 79: X-Ray crystal structure of PhenTyrOMe.CH_3OH **(37)**

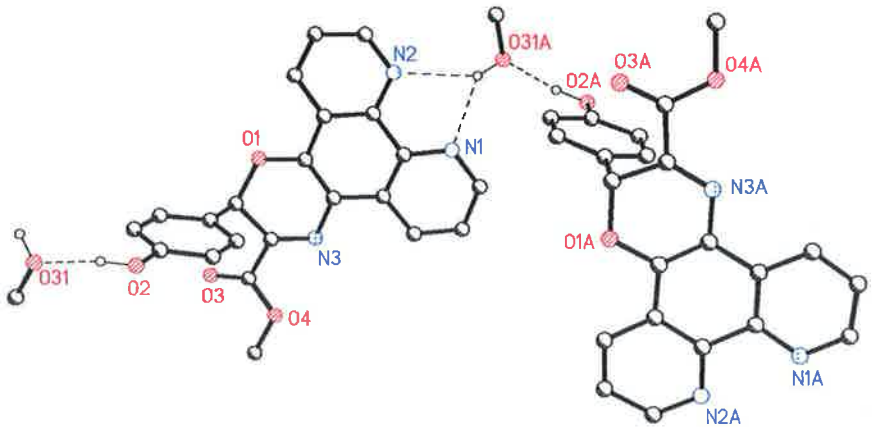

Figure 80: The hydrogen bonding in crystal of PhenTyrOMe.CH_3OH **(37)**

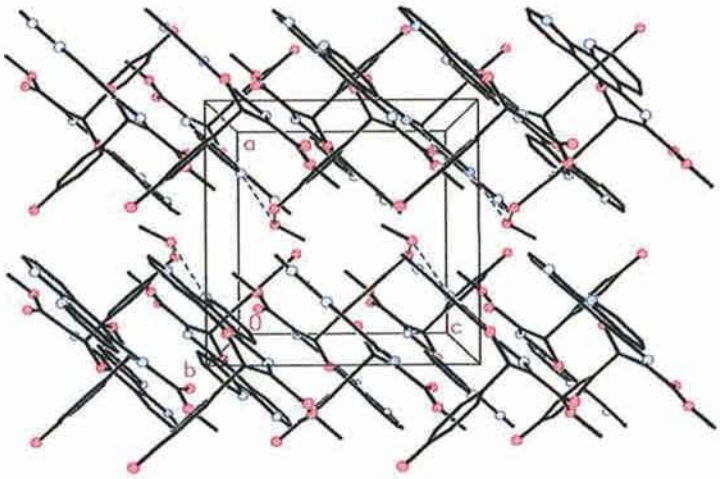

Figure 81: The packing diagram for PhenTyrOMe.CH_3OH **(37)** showing the Π-Π stacking

Table 33: Bond lengths for PhenTyrOMe.CH_3OH **(37)**

N(1)-C(1)	1.3262(18)	C(11)- C(12)	1.4542(18)
N(1)- C(12)	1.3539(16)	O(1)- C(13)	1.4552(15)
C(1)- C(2)	1.399(2)	C(13)- C(14)	1.5053(18)
C(2)- C(3)	1.3730(18)	C(13)- C(20)	1.5089(17)
C(3)- C(4)	1.4072(17)	C(14)- C(15)	1.3893(17)
C(4)- C(12)	1.4096(17)	C(14)- C(19)	1.3945(17)
C(4)- C(5)	1.4405(17)	C(15)- C(16)	1.3856(19)
C(5)- C(6)	1.3647(17)	C(16)- C(17)	1.3942(19)
C(5)- N(3)	1.4101(16)	C(17)- O (2)	1.3534(16)
C(6)- O(1)	1.3580(15)	C(17)- C(18)	1.3933(18)
C(6)- C(7)	1.4318(18)	C(18)- C(19)	1.3778(19)
C(7)- C(8)	1.4087(17)	C(20)- N(3)	1.2817(16)
C(7)- C(11)	1.4098(18)	C(20)- C(21)	1.4989(18)
C(8)- C(9)	1.367(2)	C(21)- O(3)	1.2006(16)
C(9)- C(10)	1.395(2)	C(21)- O(4)	1.3284(16)
C(10)- N(2)	1.3254(18)	O(4)- C(22)	1.4509(17)
N(2)- C(11)	1.3556(17)	O(31)- C(32)	1.418(2)

Table 34: Bond angles for PhenTyrOMe.CH_3OH **(37)**

C(1)-N(1)-C(12)	117.63(12)	N(1)-C(12)-C(11)	117.49(11)
N(1)-C(1)-C(2)	123.52(12)	C(8)-C(7)-C(11)	118.42(12)
C(3)-C(2)-C(1)	119.10(12)	C(9)-C(8)-C(7)	119.00(13)
C(2)-C(3)-C(4)	119.14(12)	C(8)-C(9)-C(10)	118.43(13)
C(3)-C(4)-C(12)	117.49(11)	N(2)-C(10)-C(9)	124.68(13)
C(3)-C(4)-C(5)	122.52(11)	C(10)-N(2)-C(11)	117.34(12)
C(12)-C(4)-C(5)	119.96(11)	N(2)-C(11)-C(7)	122.12(12)
C(6)-C(5)-N(3)	121.25(11)	N(2)-C(11)-C(12)	118.25(12)
C(6)-C(5)-C(4)	119.89(11)	C(7)-C(11)-C(12)	119.64(11)
N(3)-C(5)-C(4)	118.72(10)	N(1)-C(12)-C(4)	123.11(12)
O(1)-C(6)-C(5)	122.26(11)	N(1)-C(12)-C(11)	117.49(11)
O(1)-C(6)-C(7)	115.60(11)	C(4)-C(12)-C(11)	119.37(11)
C(8)-C(7)-C(6)	122.50(12)	C(6)-O(1)-C(13)	116.42(9)
C(11)-C(7)-C(6)	119.08(11)	O(1)-C(13)-C(14)	111.69(10)
O(1)-C(13)-C(20)	110.37(10)	C(19)-C(18)-C(17)	120.46(12)
C(14)-C(13)-C(20)	110.76(10)	C(18)-C(19)-C(14)	120.99(12)
C(15)-C(14)-C(19)	118.19(12)	N(3)-C(20)-C(21)	121.25(11)
C(15)-C(14)-C(13)	120.97(11)	N(3)-C(20)-C(13)	125.31(11)
C(19)-C(14)-C(13)	120.84(11)	C(21)-C(20)-C(13)	113.39(10)
C(16)-C(15)-C(14)	121.39(12)	O(3)-C(21)-O(4)	124.95(13)
C(15)-C(16)-C(17)	119.79(12)	O(3)-C(21)-C(20)	121.84(12)
O(2)-C(17)-C(18)	117.90(12)	O(4)-C(21)-C(20)	113.19(11)
O(2)-C(17)-C(16)	122.97(12)	C(21)-O(4)-C(22)	114.72(12)
C(18)-C(17)-C(16)	119.12(12)	C(20)-N(3)-C(5)	116.22(11)

The IR spectrum of **37** was compared to that of L-tyrosine methyl ester and several differences were observed (Table 35). The broad OH bands of the free amino acid from between 3568 cm^{-1} and 2236 cm^{-1} and the N-H stretching vibrations at 3355 cm^{-1} and 3297 cm^{-1} were replaced by the O-H stretch at 3614-2848 cm^{-1}, aromatic C-H stretch at

3069–3011 cm^{-1} and aliphatic C-H stretch at 2812 cm^{-1}. Bands which are characteristic of the presence of the phen moiety are present in the spectrum at 809 cm^{-1} and 740 cm^{-1}, (these bands represent the C-N-C stretching mode). The v symmetric (OCO) band for the amino acid ester shifted from 1178 cm^{-1} to 1717 cm^{-1} for compound **37**. In the spectrum of the amino acid ester a sharp peak at 1744 cm^{-1} was assigned to the v asymmetric (OCO) stretching frequency. A strong peak present in the phendione at 1685 cm^{-1} represents the C=O stretching band. In the spectrum of **37** the band due to C=O is found at 1741 cm^{-1}, {Appendix 1(37)}.

Table 35: Characteristic Infrared bands of PhenTyrOMe.CH_3OH **(37)** and its free amino acid

Band Assignment	**L- Tyrosine Methyl Ester (cm^{-1})**	**PhenTyrOMe.CH_3OH (37) (cm^{-1})**
NH stretch	3355, 3297	-
OH stretch	3568 - 2236	3614 - 2848
Aromatic C-H	3042 - 3005	3069 - 3011
C=O	1744	1741
vOCO sym	1178	1172
C-N-C stretching frequency	-	809, 740

The ^1H NMR spectrum of **37** contains nine distinct signals representing eleven hydrogens due to the axis of symmetry on the phenol group as shown in ^1H NMR spectrum {Figure 82, Appendix 2(37)}. The protons from the aromatic phenol ring H_7 and H_8 are coupled to each other via a vicinal coupling resulting in doublets. The proton signals at (ppm) 9.14, 7.61, 9.00, 8.60, 7.68, 9.06, 7.22, 6.72 and 6.56 are assigned to H_1, H_2, H_3, H_4, H_5, H_6, H_7, H_8 and H_9 (Figure 83).

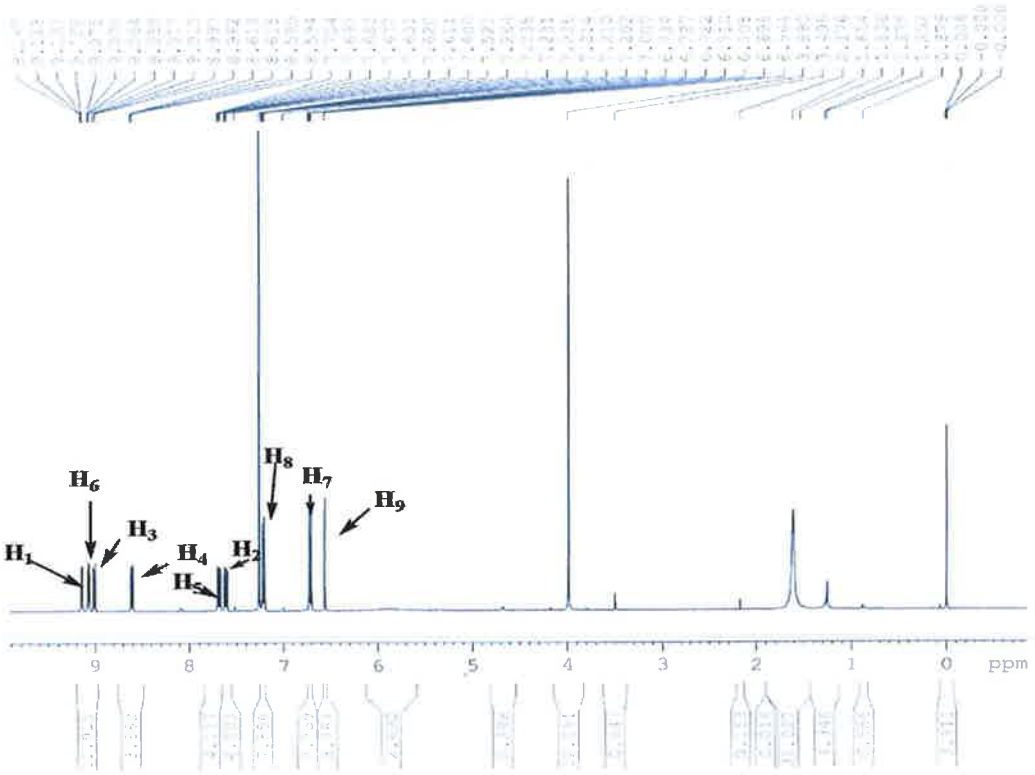

Figure 82: ^{1}H NMR spectrum of PhenTyrOMe.CH_3OH **(37)**

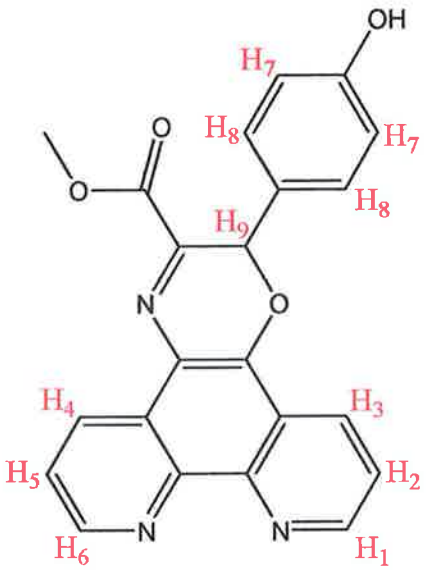

Figure 83: Assignment of PhenTyrOMe.CH_3OH **(37)**

Attempts to react the methyl and ethyl ester of the amino acids L-cysteine, L-phenylalanine and L-threonine with phendione were unsuccessful. The products from the reaction of the methyl and ethyl esters of L-cysteine are thought to have yielded 1,10-phenanthroline-5,6-dicarboxylic acid (identified by spectral data). The product of reaction of the methyl and ethyl esters of l-phenylalanine resulted in unreacted product and the reaction of L-threonine methyl ester resulted in only the recovery of unreacted phendione.

Attempts to react the seven simple amino acids L-valine, L-tyrosine, L-threonine, L-serine, L-cysteine, L-glutamine and L-asparagine with phendione were essentially unsuccessful (Scheme 30).

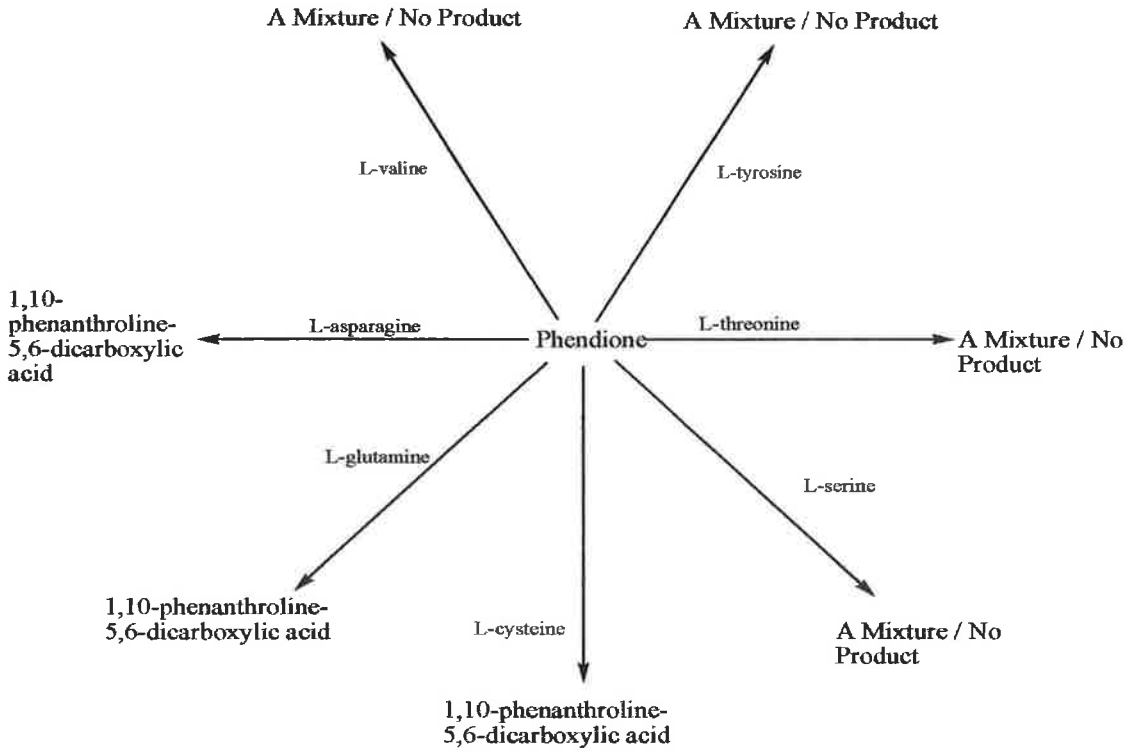

Scheme 30: Synthetic route to compounds

As shown in Scheme 30, attempts to react L-valine, L-tyrosine, L-threonine and L-serine yielded only mixtures from which no pure products were obtained. The products which were isolated from the reaction of L-cysteine, L-glutamine and L-asparagine are thought to be 1,10-phenanthroline-5,6-dicarboxylic acid (Figure 84) (identified by spectral data).

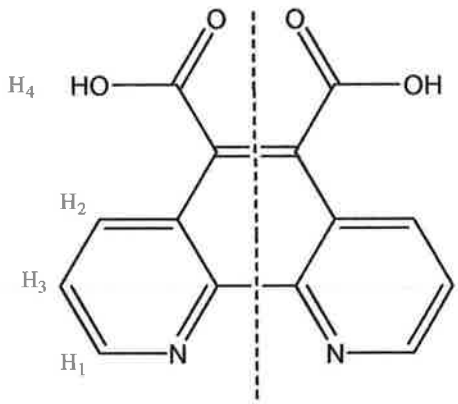

Figure 84: The structure and assignment of 1,10-phenanthroline-5,6-dicarboxylic acid

In the IR spectrum of 1,10-phenanthroline-5,6-dicarboxylic acid, (Figure 85) a band at 1710 cm^{-1} is due to the stretching frequency of the C=O bands on the ligand. Bands which are characteristic of the phen moiety are present at 825 cm^{-1} and 725 cm^{-1}, which represent the C-N-C stretching frequency bands on the ligand.

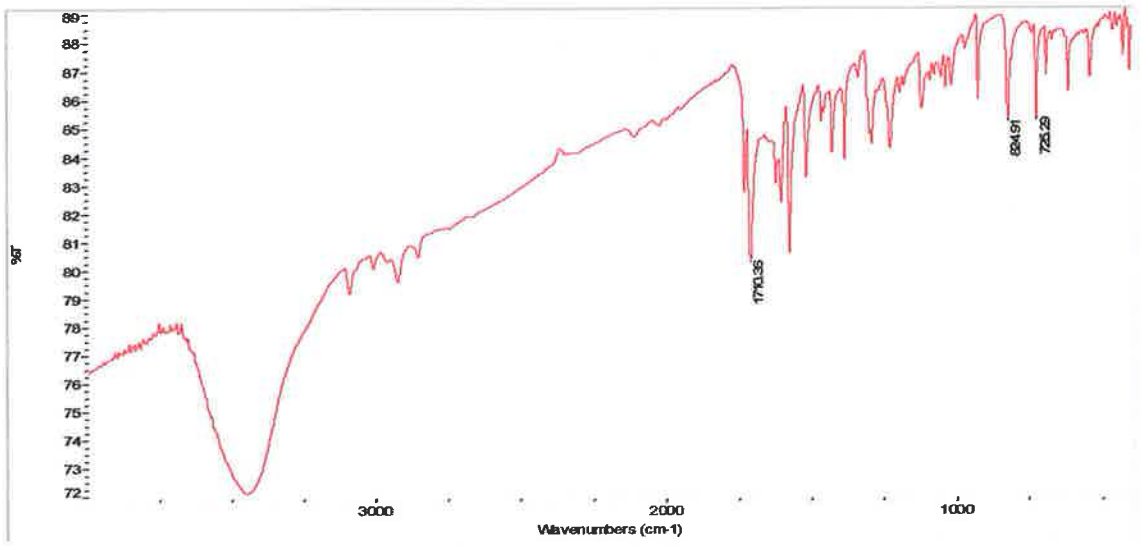

Figure 85: IR spectrum of 1,10-phenanthroline-5,6-dicarboxylic acid

The ^{1}H NMR spectrum of what is suggested to be 1,10-phenanthroline-5,6-dicarboxylic acid contains four distinct signals. All four signals integrate for two hydrogens and have an axis of symmetry (shown as dashed lines in Figure 84).

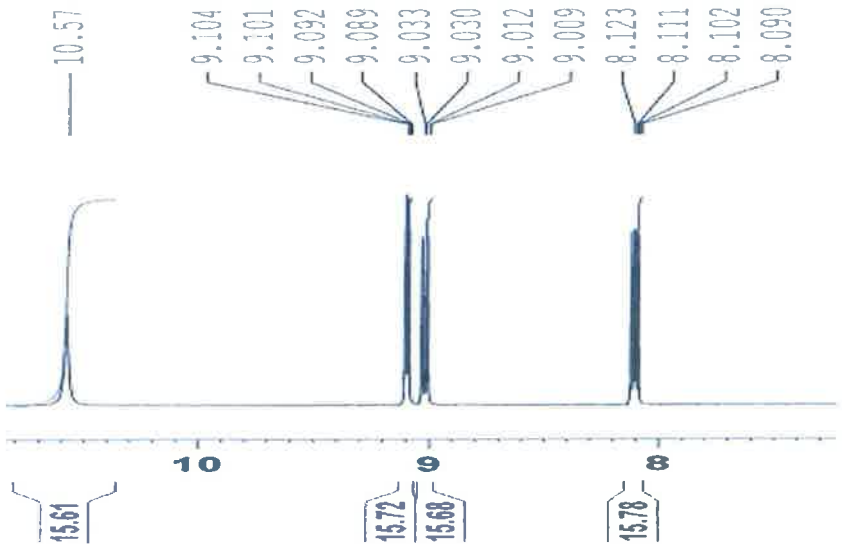

Figure 86: ^{1}H NMR spectrum of 1,10-phenanthroline-5,6-dicarboxylic acid

The proton signals at approximately (ppm) 9.09, 9.02, 8.11 and 10.57 in the spectrum are assigned to H_1, H_2, H_3 and H_4, (Figure 86). The down field signal at approximately 10.57 ppm integrated for two hydrogens, suggesting there are two carboxyl groups attached to the -5 and -6 position carbon on the phendione ligand, (Figure 84).

D.6.1 ANTI-FUNGAL ACTIVITY OF PhenTyrOMe.CH_3OH (37) AGAINST *CANDIDA ALBICANS*

The ethanol soluble compound **37** was tested for its ability to inhibit the growth of the pathogen *Candida albicans* at concentrations of 50 μg/ml, 20 μg/ml, 10 μg/ml and 5 μg/ml. Its activity was compared to that of the free amino acid L-tyrosine methyl ester and the phendione.

The phendione shows significant activity at the lowest tested concentration of 5 μg/ml.

Table 36: Percentage cell growth of *C. albicans* for compounds **(37)**

Test Compound	**% Cell Growth (at concentrations of 50 - 5 μg/ml)**				**IC_{50} value μg/ml**	**IC_{50} value μM**
	50	**20**	**10**	**5**		
Control	100	100	100	100		
Amphothericin B	6.9±9.6	7.01±9.6	13.12±33	70.5±56	10	1.08×10^{-5}
Phendione	5.6±12	5.62±10	5.55±6.1	8.3±42	5	2.37×10^{-5}
PhenTyrOMe.CH_3OH **(37)**	5.5±4.8	5.48±1.8	5.8±9.4	5.6±1.3	5	1.04×10^{-5}
L-Tyrosine Methyl Ester	99.6±62	100.8±19	94.4±24	97.2±28	50	2.56×10^{-4}

As shown in Table 36, free amino acid L-tyrosine methyl ester was found to be essentially inactive against the pathogen. Compound **37** exhibited exceptional anti-*Candida* activity, showing significant fungitoxicity with only 5.6 % cell growth at 5 ug/ml. The growth curve of compound **37** is shown below in Figure 86.

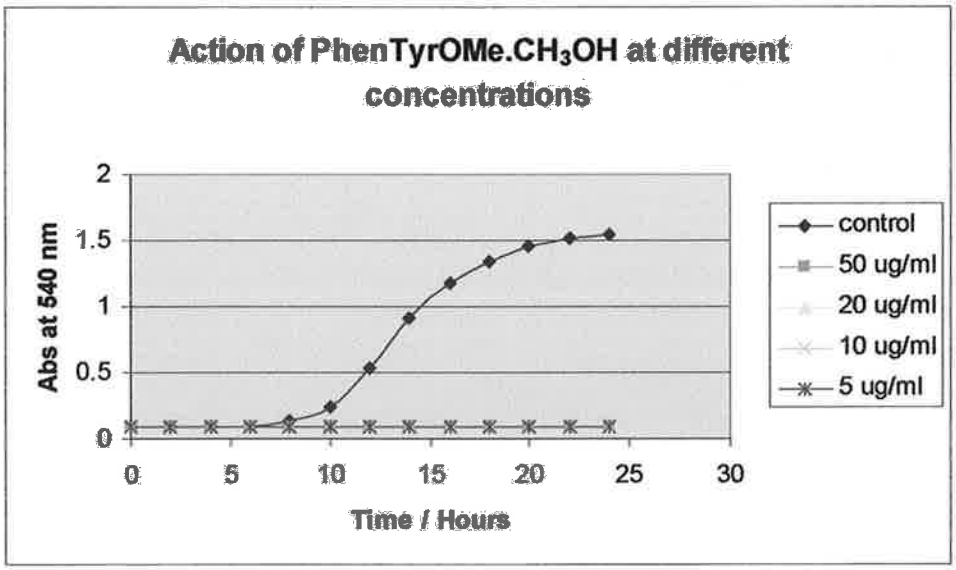

Figure 87: Kinetic growth curve of control cells and cells treated with compound **37**

EXPERIMENTAL

E.1 INSTRUMENTATION

E.1.1 General Experimental Details

All chemicals were purchased from commercial sources and were used without further purification.

Risk assessments were carried out for all chemicals used in these experiments.

E.1.2 Microanalysis

Elemental analyses were carried out by Mr. Adam Coburn at the Microanalytical Laboratory, University College Dublin, Ireland.

E.1.3 X-Ray Crystallography

X-Ray crystallography was carried out by Prof. Vicky McKee, Chemistry Department, Loughborough University, Loughborough, Leics, LE11 3TU, UK.

E.1.4 Melting Point

Melting points were measured using the Stuart Melting Point apparatus.

E.1.5 IR and NMR Spectra

IR spectra were recorded in the range 4000-400 cm^{-1} using a Nicolet FT-IR 5DXB infrared spectrometer and peaks are reported in wavenumbers (cm^{-1}). Solid samples were prepared and run in a KBr matrix.

^{1}H, ^{13}C and DEPTQ NMR were recorded on Bruker ACE 250 FT, Varian Gemini 300 and Bruker Advance 400 FT instruments. ^{13}C spectra were ^{1}H-decoupled. Spectral data is presented in the form: chemical shift in ppm and for ^{1}H NMR spectra: (number of nuclei, appearance of signal, coupling constant, assignment).

The symbols used in the descriptions of NMR spectra are:

δ = chemical shift in ppm

J = coupling constant in Hz

s = singlet

d = doublet

dd = doublet of doublets

dt = doublet of triplets

td = triplet of doublets

q = quartet

m = multiplet

An arbitrary numbering system was employed to aid assignment.

E.1.6 Magnetic Moment

Room temperature magnetic susceptibly measurements were carried out using a Johnson Matthey Magnetic Susceptibility Balance. $Hg[(Co(SCN)_4]$ was used as a reference standard.

E.1.7 Microbiology

Measurement of drug minimum inhibitory concentrations (MIC) against *Candida albicans* was carried out using an Anthos bt 3 plate reader.

SECTION 1

ORGANIC SYNTHESIS

E.2 SYNTHESIS OF 1,10-PHENANTHROLINE-5,6-DIONE (1)

E.2.1 Analytical details of a commercial sample of 1,10-phenanthroline-5,6-dione (1)

Analysis: (%) C, 68.28; H, 2.90; N, 13.18

Literature m.p.: 258 °C

IR (KBr): 3060, 1702, 1685, 1570, 1560, 1413, 1314, 1292, 1204, 1114, 1082, 1038, 1009, 924, 806, 738, 667, 613 cm^{-1}

^{1}H NMR (d_6 – DMSO, δ/ppm): 8.97 (2H, dd, J_{1-2} = 4.8 Hz, J_{1-3} = 1.6 Hz, H-1), 8.38 (2H, dd, J_{3-1} = 1.6 Hz, J_{3-2} = 8.0 Hz, H-3), 7.66 (2H, dd, J_{2-1} = 4.8 Hz, J_{2-3} = 8.0 Hz, H-2)

Product Colour: yellow powder

E.2.2 The synthesis of 1,10-phenanthroline-5,6-dione (1)

Method (a)[39]: Concentration H_2SO_4 (40 ml) and concentration HNO_3 (20 ml) were separately chilled overnight in a 4 °C fridge, mixed together and further chilled in an ice bath. 1,10-Phenanthroline (4 g, 22 mmol) and potassium bromide (4 g, 33.6 mmol) were also separately chilled overnight in a 4 °C fridge, mixed together in a chilled conical flask and further chilled in an ice bath. To a chilled mixture of 1,10-phenanthroline (4 g, 22 mmol) and potassium bromide (4 g, 33.6 mmol) was added, very slowly, an ice cold solution of concentration H_2SO_4 (40 ml) and concentration HNO_3 (20 ml). The resulting solution was refluxed for 3 hours. To this solution ice cold water (500 ml) was added, the resulting solution was neutralized with 3M NaOH, extracted with chloroform, dried over $MgSO_4$ and the solvent removed using a rotatory evaporator. The resulting powder was purified by recrystallisation in EtOH.

Average yield: 2.87 g, (62.05 %)

m.p.: 259-260 °C

% Commercial Sample: C, 68.28; H, 2.90; N, 13.18

% Found: C, 68.57; H, 2.88; N, 13.33

IR (KBr): 3057, 1702, 1685, 1576, 1560, 1458, 1413, 1314, 1292, 1204, 1183, 1114, 1082, 1060, 1009, 924, 806, 738, 667, 613 cm^{-1}

^{1}H NMR (d_6 – DMSO, δ/ppm): 8.97 (2H, dd, J_{1-2} = 4.8 Hz, J_{1-3} = 1.6 Hz, H-1), 8.38 (2H, dd, J_{3-1} = 1.6 Hz, J_{3-2} = 8.0 Hz, H-3), 7.66 (2H, dd, J_{2-1} = 4.8 Hz, J_{2-3} = 8.0 Hz, H-2)

^{13}C NMR (d_6 – DMSO, δ/ppm): 154.2 (1), 125.1 (2), 35.6 (3), 129.0 (4), 152.2 (5), 177.6 (6)

Product Colour: yellow powder

Solubility: H_2O, EtOH, MeOH, acetone, DMSO, chloroform

Method (b)[33]: 1,10-phenanthroline (0.91 g, 5 mmol), KBr (6.21 g, 52 mmol) and concentration H_2SO_4 (20.5 ml) were chilled independently before being added together for 30 mins at -20 °C. Concentration HNO_3 (11.25 ml) was added dropwise to this solution and the resulting mixture was refluxed for 3 hours. To this solution deionised water (250 ml) was added. The resulting solution was neutralized with Na_2CO_3, extracted using CH_2Cl_2, dried over $MgSO_4$ and the solvent removed using a rotary evaporator. The resulting product was purified by recrystallisation from EtOH.

Yield: 0.5 g, (10.7 %)

IR (KBr): 3125, 1701, 1685, 1575, 1560, 1443, 1412, 1390, 1291, 1203, 1098, 997, 901, 806, 740 cm^{-1}

Product Colour: yellow powder

Solubility: H_2O, EtOH, MeOH, acetone, DMSO, chloroform

Method (c)[88]: Concentration H_2SO_4 (30 ml) was transferred into a round bottomed flask (250 ml), equipped with a reflux condenser, and 1,10-phenanthroline (5 g, 27.7 mmol) was dissolved in it in small portions. Then sodium bromide (2.5 g, 24.3 mmol) was added which was followed by an addition of concentration HNO_3 (15 ml). The reaction mixture was heated to boiling and refluxed for 1 hour. Heating was then reduced and the reflux condenser removed to allow the developing bromide vapours to escape by gentle boiling (15 mins).

While the mixture was cooling down to room temperature, a sodium hydroxide solution (3 M) was prepared. The cool reaction mixture was poured onto crushed ice (400 g) and then carefully neutralized with the solution of sodium hydroxide (approx. 350 ml). The solution was then allowed to stand overnight in the fridge.

After decanting and storing the supernatant liquid in a beaker (500 ml), the remaining insoluble material in this extract was removed by filtration and finally the aqueous extractions were combined and extracted three times with dichloromethane (each 200 ml, anhydrous 99.8%). The two phases were then separated and the organic phase was washed with water (50 ml) and then dried over anhydrous sodium sulphate (approx. 3 g).

After removing the solvent under vacuum on a rotary evaporator the remaining crude product was recrystallised from a mixture of toluene (90 ml) and methanol (16 ml) to yield the yellow-orange, amorphous solid 1,10-phenanthroline-5,6-dione which was filtered on a Buchnar funnel.

Yield: 1.94 g, (38.1 %)

% Commercial Sample: C, 68.28; H, 2.90; N, 13.18

% Found: C, 68.07; H, 2.87; N, 13.18

IR (KBr): 3060, 1702, 1685, 1579, 1560, 1458, 1413, 1315, 1292, 1204, 1114, 1057, 1003, 924, 806, 738, 663, 613 cm^{-1}

^{1}H NMR (d_6 – DMSO, δ/ppm): 8.98 (2H, dd, J_{1-2} = 4.8 Hz, J_{1-3} = 2.0 Hz, H-1), 8.38 (2H, dd, J_{3-1} = 2.0 Hz, J_{3-2} = 8.0 Hz, H-3), 7.66 (2H, dd, J_{2-1} = 4.8 Hz, J_{2-3} = 8.0 Hz, H-2)

Product Colour: Yellow powder

Solubility: H_2O, EtOH, MeOH, acetone, DMSO, chloroform

E.3 SYNTHESIS OF TRANSITION METAL COMPLEXES OF 1,10-PHENANTHROLINE

To a suspension of 1,10-phenanthroline (phen) (0.3 g, 1.66 mmol) in ethanol (30 ml) was added to the relevant metal salt (0.83 mmol) and the resulting suspension refluxed for 1.5 hours. On cooling to room temperature the product was filtered off, washed with ethanol, and then air-dried.

E.3.1 Synthesis of metal nitrate – phen derivatives

E.3.1.1 $[Cu(phen)_2NO_3]NO_3.2H_2O$ (2)

Yield: 0.386 g, (80 %)

% Calc: C, 49.36; H, 3.45; N, 14.39

% Found: C, 48.86; H, 3.33; N, 14.10

IR (KBr): 3423, 3052, 2917, 1626, 1599, 1580, 1518, 1429, 1416, 1363, 1298, 1223, 1148, 1034, 846, 784, 720, 651 cm^{-1}

Solubility: H_2O, MeOH, warm acetone, DMF, DMSO

Colour: bright green powder

μ_{eff}: 1.96 B.M.

E.3.1.2 $[Co(phen)_2NO_3]NO_3.2H_2O$ (3)

Yield: 0.342 g, (71 %)

% Calc: C, 49.75; H, 3.48; N, 14.51

% Found: C, 50.05; H, 3.18; N, 14.59

IR (KBr): 3423, 3050, 2925, 1619, 1579, 1519, 1426, 1384, 1312, 1223, 1141, 1102, 1029, 846, 725, 643 cm^{-1}

Solubility: H_2O, EtOH, MeOH, DMF, DMSO

Colour: orange powder

μ_{eff}: 4.79 B.M.

E.3.1.3 $[Zn(phen)_2NO_3]NO_3.2H_2O$ (4)

Yield: 0.347 g, (72 %)

% Calc: C, 49.20; H, 3.44; N, 14.35

% Found: C, 48.63; H, 3.24; N, 14.25

IR (KBr): 3423, 3057, 2923, 1624, 1581, 1519, 1495, 1427, 1384, 1302, 1222, 1141, 1102, 1035, 847, 725, 642 cm^{-1}

Solubility: H_2O, DMF, DMSO

Colour: white powder

E.3.1.4 $[Mn(phen)_3NO_3]NO_3.2H_2O$ (5)

Yield: 0.42 g, (67.7 %)

% Calc: C, 57.22; H, 3.74; N, 14.83

% Found: C, 57.23; H, 3.43; N, 14.32

IR (KBr): 3527, 3050, 2925, 1621, 1590, 1515, 1428, 1383, 1328, 1222, 1137, 1099, 863, 771, 727, 639 cm^{-1}

Solubility: hot EtOH, hot MeOH, DMF, DMSO

Colour: yellow powder

μ_{eff}: 6.01 B.M.

E.3.2 Synthesis of metal chloride – phen derivatives

E.3.2.1 $[Cu(phen)_2]Cl_2.6H_2O$ (10)

Yield: 0.39 g, (78 %)

% Calc: C, 47.81; H, 4.68; N, 9.29

% Found: C, 48.83; H, 2.98; N, 9.32

IR (KBr): 3388, 3051, 1625, 1585, 1516, 1426, 1339, 1226, 1142, 1103, 853, 722, 647, 621 cm^{-1}

Solubility: water, hot EtOH, MeOH, hot DMSO

Colour: blue powder

μ_{eff}: 1.72 B.M.

E.3.2.2 $[Co(phen)_2]Cl_2.3H_2O$ (11)

Yield: 0.17 g, (38 %)

% Calc: C, 52.96; H, 4.07; N, 10.29

% Found: C, 52.88; H, 3.74; N, 10.44

IR (KBr): 3423, 3046, 2929, 1623, 1584, 1512, 1493, 1423, 1341, 1222, 1141, 1103, 849, 726, 639 cm^{-1}

Solubility: H_2O, EtOH, MeOH, DMF, DMSO

Colour: dark red powder

μ_{eff}: 4.38 B.M.

E.3.2.3 $[Zn(phen)_2]Cl_2.H_2O$ (12)

Yield: 0.271 g, (64 %)

% Calc: C, 56.00; H, 3.52; N, 10.88

% Found: C, 56.30; H, 3.44; N, 10.93

IR (KBr): 3440, 3046, 2993, 2922, 2852, 1621, 1587, 1515, 1492, 1428, 1415, 1345, 1223, 1143, 1092, 846, 780, 728, 638 cm^{-1}

Solubility: H_2O, EtOH, DMF, DMSO

Colour: colourless powder

E.3.2.4 $[Mn(phen)_2]Cl_2.CH_3CH_2OH$ (13)

Yield: 0.321 g, (87.5 %)

% Calc: C, 58.66; H, 4.17; N, 10.52

% Found: C, 59.02; H, 3.15; N, 11.46

IR (KBr): 3440, 3046, 2991, 1621, 1590, 1576, 1515, 1492, 1426, 1344, 1217, 1142, 1091, 843, 777, 729, 636 cm^{-1}

Solubility: H_2O, EtOH, MeOH, DMF, DMSO

Colour: lemon yellow powder

μ_{eff}: 6.07 B.M.

E.3.3 Synthesis metal sulphate – phen derivatives

E.3.3.1 $[Cu(phen)_2SO_4].3H_2O$ (18)

Yield: 0.462 g, (97 %)

% Calc: C, 50.21; H, 3.86; N, 9.76

% Found: C, 50.00; H, 3.41; N, 9.13

IR (KBr): 3422, 3051, 2953, 2922, 1625, 1579, 1517, 1427, 1337, 1228, 1121, 1040, 951, 866, 853, 786, 723, 618 cm^{-1}

Solubility: H_2O, EtOH, MeOH, acetone, DMF, DMSO

Colour: light blue powder

μ_{eff}: 1.99 B.M.

E.3.3.2 $[Co(phen)_2SO_4].6H_2O$ (19)

Yield: 0.351 g, (66 %)

% Calc: C, 46.23; H, 4.53; N, 8.99

% Found: C, 46.94; H, 3.22; N, 9.04

IR (KBr): 3423, 3057, 2917, 1624, 1586, 1516, 1425, 1116, 1049, 865, 847, 725, 642 cm^{-1}

Solubility: H_2O, EtOH, MeOH

Colour: pink powder

μ_{eff}: 4.43 B.M.

E.3.3.3 $[Zn(phen)SO_4].2H_2O$ (20)

Yield: 0.412 g, (132 %)

% Calc: C, 38.16; H, 3.20; N, 7.42

% Found: C, 37.78; H, 3.21; N, 7.09

IR (KBr): 3416, 3059, 2922, 2852, 1624, 1579, 1517, 1426, 1174, 1118, 1051, 1021, 868, 848, 722, 619 cm^{-1}.

Solubility: H_2O, MeOH

Colour: colourless powder

E.3.3.4 [Mn(phen)SO_4].7H_2O (21)

Yield: 0.29 g, (78 %)

% Calc: C, 31.52; H, 4.85; N, 6.13

% Found: C, 31.49; H, 2.62; N, 5.92

IR (KBr): 3407, 3060, 1625, 1518, 1428, 1107, 1017, 821, 729, 659, 623, 605, 510 cm^{-1}

Solubility: H_2O

Colour: yellow powder

μ_{eff}: 5.61 B.M.

E.3.4 Synthesis of copper(II) acetate – phen derivatives

E.3.4.1 [Cu(phen)$(CH_3CO_2)_2$].H_2O (26)

Yield: 0.56 g, (180 %)

% Calc: C, 50.59; H, 4.25; N, 7.38

% Found: C, 51.05; H, 4.16; N, 7.96

IR (KBr): 3415, 3067, 1585, 1518, 1429, 1392, 1336, 1223, 1144, 1107, 1019, 851, 722, 676, 644 cm^{-1}

Solubility: H_2O, EtOH, MeOH

Colour: blue powder

μ_{eff}: 2.08 B.M.

E.4 SYNTHSIS OF TRANSITION METAL COMPLEXES OF 1,10- PHENANTHROLINE-5,6-DIONE

A suspension of 1,10-phenanthroline-5,6-dione (phendione) (0.3 g, 1.43 mmol) in ethanol (30 ml) was added to the relevant metal salt (0.715 mmol) and the resulting suspension refluxed for 2.5 hours. On cooling to room temperature the product was filtered off, washed with ethanol, and then air-dried.

E.4.1 Synthesis of metal nitrate – phendione derivatives

E.4.1.1 $[Cu(phendione)_2NO_3]NO_3.2H_2O$ (6)

Yield: 0.259 g, (58 %)

% Calc: C, 44.76; H, 2.50; N, 13.05

% Found: C, 45.46; H, 1.89; N, 12.27

IR (KBr): 3432, 3082, 1701, 1577, 1456, 1429, 1384, 1299, 1202, 1128, 1071, 1024, 937, 828, 729 cm^{-1}

Solubility: H_2O, DMSO

Colour: green powder

μ_{eff}: 1.77 B.M.

E.4.1.2 $[Co(phendione)_2NO_3]NO_3.H_2O$ (7)

Yield: 0.21 g, (48 %)

% Calc: C, 46.39; H, 2.27; N, 13.53

% Found: C, 46.20; H, 2.03; N, 13.08

IR (KBr): 3433, 3091, 2921, 1700, 1577, 1479, 1425, 1384, 1302, 1208, 1126, 1071, 1023, 936, 833, 734, 709 cm^{-1}

Solubility: H_2O, MeOH, DMSO

Colour: mustard powder

μ_{eff}: 6.12 B.M.

E.4.1.3 $[Zn(phendione)_2(NO_3)_2].3H_2O$ (8)

Yield: 0.27 g, (57 %)

% Calc: C, 43.42; H, 2.73; N, 12.66

% Found: C, 43.90; H, 1.91; N, 12.46

IR (KBr): 3426, 3090, 2917, 1699, 1578, 1479, 1425, 1300, 1207, 1190, 1125, 1071, 1024, 935, 833, 734, 696, cm^{-1}

Solubility: H_2O, MeOH, DMSO

Colour: mustard powder

E.4.1.4 $[Mn(phendione)_2(NO_3)_2].H_2O$ (9)

Yield: 0.17 g, (38.6 %)

% Calc: C, 46.69; H, 2.29; N, 13.61

% Found: C, 46.03; H, 1.99; N, 13.15

IR (KBr): 3427, 3089, 2917, 1698, 1576, 1476, 1424, 1384, 1301, 1208, 1190, 1123, 1071, 1024, 934, 823, 735, 694 cm^{-1}

Solubility: H_2O, MeOH, DMSO

Colour: yellow powder

μ_{eff}: 5.99 B.M.

E.4.2 Synthesis of metal chloride – phendione derivatives

E.4.2.1 $[Cu(phendione)_2Cl_2].2H_2O$ (14)

Yield: 0.1 g, (24 %)

% Calc: C, 48.79; H, 2.73; N, 9.48

% Found: C, 49.57; H, 2.43; N, 9.29

IR (KBr): 3433, 3069, 2999, 1697, 1575, 1484, 1427, 1304, 1256, 1210, 1137, 1071, 1023, 935, 839, 739 cm^{-1}

Solubility: H_2O, MeOH, DMSO

Colour: lime green powder

μ_{eff}: 2.09 B.M.

E.4.2.2 $[Co(phendione)_2Cl_2].H_2O$ (15)

Yield: 0.135 g, (33 %)

% Calc: C, 50.73; H, 2.48; N, 9.86

% Found: C, 50.21; H, 2.40; N, 9.21

IR (KBr): 3433, 3069, 3012, 2922, 2852, 1694, 1575, 1425, 1307, 1257, 1210, 1133, 1071, 1021, 934, 842 cm^{-1}

Solubility: H_2O, EtOH, MeOH, DMSO

Colour: bright orange powder

μ_{eff}: 6.21 B.M.

E.4.2.3 $[Zn(phendione)_2Cl_2].3H_2O$ (16)

Yield: 0.2 g, (46 %)

% Calc: C, 47.20; H, 2.97; N, 9.17

% Found: C, 46.29; H, 2.07; N, 8.27

IR (KBr): 3433, 3069, 3013, 1694, 1575, 1472, 1426, 1308, 1258, 1210, 1133, 1072, 1021, 933, 842, 737, 685 cm^{-1}

Solubility: H_2O, DMSO

Colour: yellow powder

E.4.2.4 [Mn(phendione)$_2$Cl$_2$].2H$_2$O (17)

Yield: 0.18 g, (44 %)

% Calc: C, 49.51; H, 2.77; N, 9.62

% Found: C, 49.79; H, 2.34; N, 9.11

IR (KBr): 3427, 3068, 3012, 1694, 1575, 1471, 1425, 1306, 1256, 1210, 1130, 1072, 1021, 932, 841, 737, 695 cm^{-1}

Solubility: H$_2$O, MeOH, DMSO

Colour: orange powder

μ_{eff}: 8.16 B.M.

E.4.3 Synthesis of metal sulphate – phendione derivatives

E.4.3.1 [Cu(phendione)SO$_4$].4H$_2$O (22)

Yield: 0.32 g, (103 %)

% Calc: C, 32.62; H, 3.19; N, 6.34

% Found: C, 32.18; H, 2.35; N, 6.08

IR (KBr): 3604, 3059, 1697, 1577, 1479, 1431, 1387, 1301, 1029, 823, 730, 611 cm^{-1}

Solubility: H$_2$O, DMSO

Colour: light green powder

μ_{eff}: 1.88 B.M.

E.4.3.2 [Co(phendione)$_2$SO$_4$].7H$_2$O (23)

Yield: 0.26 g, (52 %)

% Calc: C, 41.09; H, 3.74; N, 7.99

% Found: C, 41.66; H, 2.64; N, 7.82

IR (KBr): 3419, 3085, 1697, 1575, 1479, 1458, 1426, 1310, 1293, 1261, 1207, 1165, 1115, 1096, 1010, 935, 882, 733, 718, 611 cm^{-1}

Solubility: H_2O, DMSO

Colour: dark orange powder

μ_{eff}: 4.4 B.M.

E.4.3.3 [Zn(phendione)SO$_4$].H$_2$O (24)

Yield: 0.3 g, (108 %)

% Calc: C, 37.00; H, 2.07; N, 7.19

% Found: C, 38.76; H, 2.56; N, 7.11

IR (KBr): 3426, 3089, 1696, 1576, 1477, 1429, 1384, 1303, 1211, 1116, 1069, 986, 934, 821, 733, 698, 604 cm^{-1}

Solubility: H_2O, Acetone, DMSO

Colour: mustard powder

E.4.3.4 [Mn(phendione)$_2$SO$_4$].CH$_3$CH$_2$OH (25)

Yield: 0.19 g, (43 %)

% Calc: C, 50.58; H, 2.94; N, 9.07

% Found: C, 51.09; H, 2.35; N, 9.74

IR (KBr): 3422, 3060, 2922, 1685, 1572, 1458, 1424, 1293, 1183, 1121, 1061, 1013, 925, 817, 733, 653, 613 cm^{-1}

Solubility: insoluble

Colour: mustard orange powder

μ_{eff}: 5.77 B.M.

E.4.4 Synthesis of copper(II) acetate – phendione derivatives

E.4.4.1 [Cu(phendione)$_2$(CH$_3$CO$_2$)$_2$].5H$_2$O (27)

Yield: 0.27 g, (55 %)

% Calc: C, 49.89; H, 3.89; N, 8.31

% Found: C, 48.03; H, 2.28; N, 8.91

IR (KBr): 3434, 3057, 2921, 2851, 1703, 1576, 1477, 1458, 1429, 1414, 1369, 1333, 1292, 1201, 1114, 1062, 1034, 796, 732, 711 cm^{-1}

Solubility: insoluble

Colour: dark blue powder

μ_{eff}: 2.03 B.M.

E.5 ATTEMPTED SYNTHESIS OF ORGANIC DERIVATIVES OF 1,10-PHENANTHROLINE-5,6-DIONE

E.5.1 Synthesis of 1,3-bis([1,10] phenanthroline-[5,6-d]-imidazol-2-yl) benzene (mbpibH_2.6H_2O) (28)[90]

A mixture of phendione (0.63 g, 3 mmol), ammonium acetate (4.62 g, 60 mmol), isophthalic aldehyde (0.201 g, 1.5 mmol) and glacial acetic acid (50 ml) was refluxed for 2 hours and then cooled to room temperature. The precipitate was collected and washed with small amounts of ice cold water. The cloudy orange crude product was recrystallised from DMF.

Experimental Yield: 0.77g, (83 %)

m.p.: > 300 °C

% Calc: C, 61.73; H, 4.86; N, 18.00

% Found: C, 61.15; H, 3.45; N, 17.47

IR (KBr): 3424, 3062, 1624, 1561, 1507, 1449, 1399, 1352, 1191, 1073, 1031, 990, 805, 738, 706, 671, 618 cm^{-1}

^{1}H NMR (d_6 – DMSO, δ/ppm): 9.53 (1H, s, H-6), 9.18 (4H, d, J_{1-2} = 8.0 Hz, H-1), 9.05 (4H, dd, J_{3-2} = 4.4 Hz, H-3), 8.49 (2H, dd, J_{4-5} = 8.0 Hz, H-4), 7.86 (4H, m, J_{2-3} = 4.4 Hz, H-2), 7.81 (1H, d, J_{5-4} = 8Hz, H-5)

Solubility: hot DMF

Product Colour: yellow powder

E.5.2 Synthesis of 2-(3-formylphenyl)imidazo[4,5-f] [1,10]phenanthroline (mfmp.4H_2O) (29) [90]

A mixture of isophthalic aldehyde (0.201 g, 1.5 mmol), phendione (0.315 g, 1.5 mmol), ammonium acetate (2.31 g, 30 mmol) and glacial acetic acid (30 ml) were refluxed for 2 hours. On cooling to room temperature the product was diluted with water (60 ml). Dropwise addition of concentrated aqueous ammonia resulted in a yellow precipitate, which was collected and washed with water. The yellow crude product was recrystallised from ethanol.

Yield: 0.487 g, (83 %)

m.p.: > 300 °C

% Calc: C, 60.60; H, 5.09; N, 14.13

% Found: C, 61.95; H, 4.01; N, 15.44

IR (KBr): 3432, 2922, 1698, 1606, 1558, 1507, 1400, 1351, 1198, 1070, 1032, 806, 738, 675 cm^{-1}

^1H NMR (d_6 – DMSO, δ/ppm): 10.17 (1H, s, H-8), 9.04 (2H, dd, J_{1-2} = 4.0 Hz, J_{1-3} = 2.0 Hz, H-1), 8.95 (2H, dd, J_{3-2} = 8.0 Hz, J_{3-1} = 2.0 Hz, H-3), 8.81 (1H, s, J = 1.6 Hz, H-7), 8.62 (1H, d, J_{4-5} = 6.4 Hz, J_{4-6} = 1.6 Hz, H-4), 8.07 (1H, d, J_{6-5} = 6.4 Hz, J_{6-4} = 1.6 Hz, H-6), 7.87 (1H, t, J_{5-4} = 6.4 Hz, H-5), 7.85 (2H, t, J_{2-1} = 4 Hz, J_{2-3} = 8.0 Hz, H-2)

^{13}C NMR (d_6 – DMSO, δ/ppm): 147.7 (1), 123.2 (2) 143.5 (3), 127.2 (4), 150.4 (5), 123.2 (6), 150.1 (7), 131.0 (8), 136.5 (9), 129.7 (10), 129.9 (11), 143.5 (12), 130.7 (13), 173.1 (14)

Colour: yellow powder; **Solubility:** hot EtOH, hot MeOH, DMSO

E.5.3 Attempted synthesis of 2-(2-pyridinecarbox)imidazo[4,5f][1,10] phenanthroline (PCIP) (30)

A mixture of 2-pyridinecarboxaldehyde (0.328 ml, 3.5 mmol), phendione (0.21 g, 3mmol), ammonium acetate (4.62 g, 60 mmol) and glacial acetic acid (20 ml) was refluxed for 1.5 hours, cooled to room temperature and further chilled. The cooled solution was filtered off, diluted with water and neutralized with concentrated aqueous ammonia. The precipitate was collected and purified in small portions in boiling EtOH by recrystallisation.

Yield: 0.95 g, (95 %)

m.p.: 78-95 °C

IR (KBr): 3423, 3112, 2924, 1751, 1635, 1616, 1586, 1562, 1523, 1496, 1470, 1430, 1408, 1334, 1280, 1233, 1183, 1151, 1109, 1091, 1044, 1016, 901, 768, 747, 736, 698, 678, 658 cm^{-1}

^{1}H NMR (d_6 – DMSO, δ/ppm): 8.73 (2H, m, J_{1-2} = 2.8 Hz, J_{1-3} = 1.2 Hz, H-1), 8.39 (1H, dt, J_{7-6} = 1.2 Hz, H-7), 8.15 (2H, m, J_{3-2} = 1.2 Hz, H-3), 8.02 (1H, td, J_{5-4} = 7.6 Hz, J_{5-6} = 1.6 Hz, H-5), 7.96 (1H, td, J_{4-5} = 7.6 Hz, H-4), 7.58 (2H, dd, J_{2-1} = 2.8 Hz, J_{2-3} = 1.2 Hz, H-2), 7.45 (1H, dd, J_{6-7} = 1.2 Hz, H-6), 6.85 (1H), 7.27 (1H, m), 10.08 (1H, dt)

^{13}C NMR (d_6 – DMSO, δ/ppm): 149.1 (1), 122.2 (2), 136.4 (3), 128.3 (4), 149.4 (5), 127.2 (6), 150.2 (7), 155.9 (8), 125.4 (9), 137.4 (10), 119.1 (11), 148.5 (12), 186.53, 137.0, 136.7, 135.2, 131.9, 128.2, 124.8, 123.3, 121.7, 116.3

Solubility: partially soluble in hot H_2O, hot EtOH, MeOH, hot acetone, DMSO, partially soluble in chloroform

Product Colour: dark green powder

E.5.4 Synthesis of 4-(2,3-Dihydro-1H-1,3,7,8-tetraazacyclopenta-[l]-phenanthrene-2-yl)-benzonitrile (DPBN.3H_2O) (31)[88]

Phendione (0.315 g, 1.5 mmol), 4-cyanobenzaldehyde (0.201 g, 1.5 mmol), ammonium acetate (2.31 g, 30 mmol) and glacial acetic acid (30 ml) were transferred into a round bottomed flask (100 ml), equipped with a reflux condenser, and refluxed for 2 hours. After reflux, the mixture was cooled to room temperature, water (approx. 60 ml) was added and then concentration aqueous ammonia (10 ml) was added dropwise which led to the precipitation of yellow crude product which was filtered on a Buchner funnel and washed with water (approx. 20 ml). A H^1 NMR spectrum of the crude product in DMSO-d_6 was recorded and showed that no further purification step were required.

Yield: 0.4386 g, (78 %)

m.p.: > 300 °C; decomposition at 270 °C

% Calc: C, 63.99; H, 4.56; N, 18.66

% Found: C, 63.49; H, 3.73; N, 17.74

IR (KBr): 3417, 2225, 1610, 1552, 1479, 1453, 1398, 1318, 1279, 1182, 1115, 1070, 949, 844, 802, 738, 690, 649, 553 cm^{-1}

^{1}H NMR (d_6 – DMSO, δ/ppm): 9.04 (2H, dd, $J_{1\text{-}2}$ = 4.4 Hz, $J_{1\text{-}3}$ = 2.0 Hz, H-1), 8.91 (2H, dd, $J_{3\text{-}1}$ = 2.0 Hz, $J_{3\text{-}2}$ = 8.0 Hz, H-3), 8.45 (2H, dd,

$J_{4\text{-}5}$ = 8.8 Hz, H-4), 8.08 (2H, dd, $J_{5\text{-}4}$ = 8.8 Hz, H-5), 7.84 (2H, dd, $J_{2\text{-}1}$ = 4.4 Hz, H-2)

Product Colour: yellow powder

Solubility: DMSO

E.6 SYNTHESIS OF TRANSITION METAL COMPLEXES OF $mbpibH_2.6H_2O$ (28)

E.6.1 $[Mn(mbpibH_2)](NO_3)_2.3H_2O$ (32)

To a suspension of $mbpibH_2.6H_2O$ **(28)** (0.2 g, 0.38 mmol) in DMF (30 ml) was added manganese(II) nitrate (0.07 g, 0.38 mmol) and the resulting suspension refluxed for 3 hours. On cooling to room temperature the yellow powder was filtered off, and then air-dried.

Yield: 0.075 g, (26.5 %)

% Calc: C, 51.41; H, 3.24; N, 18.74

% Found: C, 51.63; H, 3.34; N, 16.80

IR (KBr): 3403, 3190, 1655, 1548, 1512, 1447, 1383, 1194, 1079, 1044, 992, 813, 735, 696 cm^{-1}

Solubility: insoluble

Colour: yellow powder

μ_{eff}: 5.81 B.M.

E.6.2 $[Mn(mbpibH_2)]Cl_2.4H_2O$ (33)

To a suspension of $mbpibH_2.6H_2O$ **(28)** (0.13 g, 0.25 mmol) in DMF (30 ml) was added manganese(II) chloride (0.025g, 0.125 mmol) and the resulting suspension refluxed for 2 hours. On cooling to room temperature the yellow powder was filtered off, and then air-dried.

Yield: 0.09 g, (101 %)

% Calc: C, 53.95; H, 3.68; N, 15.73

% Found: C, 54.23; H, 3.37; N, 15.95

IR (KBr): 3421, 3183, 1657, 1547, 1511, 1450, 1398, 1189, 1079, 991, 812, 736, 696 cm^{-1}

Solubility: hot EtOH

Colour: yellow powder

μ_{eff}: 5.91 B.M.

E.6.3 [Mn(mbpibH$_2$)(CH$_3$CO$_2$)$_2$].9H$_2$O (34)

To a suspension of mbpibH$_2$.6H$_2$O **(28)** (0.13 g, 0.25 mmol) in DMF (30 ml) was added manganese(II) acetate (0.03g, 0.125 mmol) and the resulting suspension refluxed for 3 hours. On cooling to room temperature the yellow powder was filtered off, and then air-dried.

Yield: 0.08 g, (38 %)

% Calc: C, 50.89; H, 4.98; N, 13.19

% Found: C, 50.04; H, 3.39; N, 13.51

IR (KBr): 3403, 1655, 1548, 1383, 1190, 1078, 813, 736, 703, 648 cm^{1}

Solubility: insoluble

Colour: yellow powder

μ_{eff}: 5.89 B.M.

E.6.4 Synthesis of $[Co(phendione)(H_2O)_4](NO_3)_2.H_2O$ (35)

To a suspension of $mbpibH_2.6H_2O$ **(28)** (0.083 g, 0.16 mmol) in DMF (30 ml) was added cobalt(II) nitrate (0.249 g, 0.79 mmol) and the resulting suspension refluxed for 3 hours. On cooling to room temperature the orange solution was left to stand and over a period of three months small pink crystals formed.

IR (KBr): 3527, 3365, 1694, 1650, 1577, 1476, 1428, 1307, 1255, 1202, 1141, 1086, 974, 936, 820, 734, 701, 620 cm^{-1}

% Found: C, 24.77; H, 4.52; N, 5.70

Colour: pink crystals

E.7 SYNTHESIS OF TRANSITION METAL COMPLEX OF DPBN.4H_2O (31)

E.7.1 Synthesis of DPBN.3H_2O (31) with metal nitrate

E.7.1.1 [$Cu(DPBN)_2$](NO_3)$_2$.4H_2O (36)

DPBN.3H_2O **(31)** (0.0838g, 0.26 mmol) and MeOH (10 ml) were transferred to a conical flask (100 ml) and heated until dissolved (approx. 15 mins). Copper(II) nitrate (0.03 g, 0.13 mmol) was added and the flask was equipped with a reflux condenser and refluxed for 3 hours. After cooling the reaction mixture to room temperature, the product was filtered on a Buchner funnel, and then air-dried.

Yield: 0.09 g, (77 %)

% Calc: C, 53.25; H, 3.35; N, 18.63

% Found: C, 53.55; H, 2.61; N, 18.44

IR (KBr): 3427, 2227, 1608, 1479, 1456, 1384, 1351, 1077, 1043, 857, 812, 726, 671, 644, 552 cm^{-1}

Solubility: DMF, DMSO

Product Colour: aqua blue powder

μ_{eff}: 1.91 B.M

SECTION 2

E.8 REACTION OF PHENDIONE WITH AMINO ACID ESTERS

E.8.1 Synthesis of PhenTyrOMe.CH_3OH (37)

To a solution of phendione (0.25 g, 1.19 mmol) in methanol (50 ml) was added L-tyrosine methyl ester (1.19 mmol). The resulting orange-yellow solution was stirred and refluxed for 7 hours and then allowed to stand for 7 days. The resulting yellow crystals were filtered off, and then air-dried.

Yield: 0.21 g, (42.8 %)

m.p.: 110–113 °C; decomposition at 70 °C

% Calc: C, 66.18; H, 4.59; N, 10.07

% Found: C, 67.00; H, 4.36; N, 10.24

IR (KBr): 3432, 3069, 2954, 2812,1741, 1717, 1607, 1588, 1516, 1502, 1432, 1379, 1345, 1315, 1286, 1257, 1245, 1220, 1172, 1130, 1094, 1020, 972, 842, 809, 740, 678, 631, 551 cm^{-1}

^1H NMR ($CDCl_3$, δ/ppm): 9.14 (1H, dd, J_{1-2} = 4.4 Hz, J_{1-3} = 2.0 Hz, H-1), 9.06 (1H, dd, J_{6-5} = 4.4 Hz, J_{6-4} = 2.0 Hz, H-6), 9.00 (1H, dd, J_{3-2} = 8.4 Hz, J_{3-1}= 2.0 Hz, H-3), 8.60 (1H, dd, J_{4-5} = 8.4 Hz, J_{4-6} = 2.0 Hz, H-4), 7.68 (1H, dd, J_{5-4} = 8.4 Hz, J_{5-6} = 4.4 Hz, H-5), 7.61 (1H, dd, J_{2-1} = 4.4 Hz, J_{2-3} = 8.4 Hz, H-2), 7.22 (2H, Ar-H(Ph), J_{8-7} = 6.8 Hz, J_{7-8} = 2.0 Hz, H-8), 6.72 (2H, Ar-H(Ph), J_{7-8} = 6.8 Hz, J_{8-7} = 2.0 Hz, H-7)

Solubility: H_2O, EtOH, MeOH, DMSO; **Colour:** yellow crystal

E.8.2 Reaction of phendione with L-tyrosine ethyl ester

To a solution of phendione (0.25 g, 1.19 mmol) in methanol (50 ml) was added L-tyrosine ethyl ester (0.25 g, 1.19 mmol). The resulting orange-yellow solution was stirred and refluxed for 2.5 hours, then allowed to cool and left stand overnight. The resulting yellow solid which deposited was filtered off, and then air-dried. This product was the same as above for the reaction with the methyl ester.

Yield: 0.23 g, (50 %)

% Calc: C, 68.57; H, 3.92; N, 10.90

% Found: C, 68.42; H, 4.31; N, 10.36

IR (KBr): 3425, 3069, 2924, 2844, 1741, 1711, 1608, 1578, 1515, 1433, 1380, 1322, 1283, 1262, 1236, 1171, 1127, 1094, 1053, 1015, 974, 920, 841, 808, 740, 671, 631, 555 cm^{-1}

^{1}H NMR (d_6 – DMSO, δ/ppm): 9.11 (1H, dd, J_{1-2} = 4.4 Hz, J_{1-3} = 2.0 Hz, H-1), 9.06 (1H, dd, J_{6-5} = 4.4 Hz, J_{6-4} = 2.0 Hz, H-6), 8.87 (1H, dd, J_{3-2} = 8.4 Hz, J_{3-1}= 2.0 Hz, H-3), 8.60 (1H, dd, J_{4-5} = 8.4 Hz, J_{4-6} = 2.0 Hz, H-4), 7.84 (1H, dd, J_{5-4} = 8.4 Hz, J_{5-6} = 4.4 Hz, H-5), 7.79 (1H, dd, J_{2-1} = 4.4 Hz, J_{2-3} = 8.4 Hz, H-2), 7.18 (2H, Ar-H(Ph), J_{8-7} = 6.8 Hz, J_{7-8} = 2.0 Hz, H-8), 6.64 (2H, Ar-H(Ph), J_{7-8} = 6.8 Hz, J_{8-7} = 2.0 Hz, H-7)

Solubility: H_2O, EtOH, MeOH, DMSO

Colour: yellow crystal

E.8.3 Reaction of phendione with L-threonine methyl ester

To a solution of phendione (0.25 g, 1.19 mmol) in methanol (50 ml) was added L-threonine methyl ester (0.2 g, 1.19 mmol). The resulting orange solution was stirred and refluxed for 2.5 hours and then allowed stand to cool. The resulting orange / red solid which deposited was filtered off, and then air-dried.

IR (KBr): 3442, 2923, 1735, 1617, 1570, 1493, 1421, 1344, 1313, 1117, 1060, 1019, 798, 731, 691, 630 cm^{-1}

^{1}H NMR (d_6 – DMSO, δ/ppm): 8.98 (2H, dd, J_{1-2} = 4.6 Hz, J_{1-3} = 1.8 Hz, H-1), 8.38 (2H, dd, J_{3-1} = 1.8 Hz, J_{3-2} = 7.8 Hz, H-3), 7.66 (2H, dd, J_{2-1} = 4.6 Hz, J_{2-3} = 7.8 Hz, H-2)

Solubility: DMF, DMSO

Colour: orange / red powder

E.8.4 Reaction of phendione with L-cysteine methyl ester

To a solution of phendione (0.25 g, 1.19 mmol) in methanol (50 ml) was added L-cysteine methyl ester (0.2 g, 1.19 mmol). The resulting orange / red solution was stirred and refluxed for 5.5 hours and then let stir overnight. The resulting orange / red solid which deposited was filtered off, and then air-dried.

IR (KBr): 3417, 3060, 2922, 1600, 1540, 1468, 1500, 1412, 1368, 1324, 1235, 1164, 1123, 1051, 1025, 965, 900, 804, 716, 671 cm^{-1}

^{1}H NMR (d_6 – DMSO, δ/ppm): 9.12 (2H, dd, J_{1-2} = 4.8Hz, J_{1-3} = 1.6 Hz, H-1), 9.03 (2H, dd, J_{3-1} = 1.6 Hz, J_{3-2} = 8.4 Hz, H-3), 8.14 (2H, dd, J_{2-1} = 4.8 Hz, J_{2-3} = 8.4 Hz, H-2), 10.36 (2H, s, H-4)

Solubility: DMF, DMSO

Colour: orange / red powder

E.8.5 Reaction of phendione with L-cysteine ethyl ester

To a solution of phendione (0.25 g, 1.19 mmol) in methanol (50 ml) was added L-cysteine ethyl ester (0.22 g, 1.19 mmol). The resulting orange / red solution was stirred and refluxed for 5.5 hours and then let stir overnight. The resulting orange / red solid which deposited was filtered off, and then air-dried.

IR (KBr): 3424, 3062, 2923, 1740, 1612, 1541, 1457, 1407, 1365, 1260, 1234, 1171, 1128, 1021, 959, 835, 807, 718, 670, 601 cm^{-1}

^{1}H NMR (d_6 – DMSO, δ/ppm): 9.11 (2H, dd, J_{1-2} = 4.8 Hz, J_{1-3} = 1.2 Hz, H-1), 9.02 (2H, dd, J_{3-1} = 1.2 Hz, J_{3-2} = 8.4 Hz, H-3), 8.13 (2H, dd, J_{2-1} = 4.8 Hz, J_{2-3} = 8.4 Hz, H-2), 10.38 (2H, s, H-4)

Solubility: DMF, DMSO

Colour: orange / red powder

E.8.6 Reaction of phendione with L-phenylalanine methyl ester

To a solution of phendione (0.25 g, 1.19 mmol) in methanol (50 ml) was added L-phenylalanine methyl ester (0.25 g, 1.19 mmol). The resulting orange / red solution was stirred and refluxed for 4.5 hours and then let stir overnight. The resulting orange / red solid which deposited was filtered off, and then air-dried.

IR(KBr): 3423, 2924, 2364, 1616, 1570, 1496, 1421, 1407, 1344, 1314, 1117, 1060, 1018, 798, 731, 691 cm^{-1}

^{1}H NMR (d_6 – DMSO, δ/ppm): 8.97 (2H, dd, J_{1-2} = 4.8 Hz, J_{1-3} = 1.6 Hz, H-1), 8.37 (2H, dd, J_{3-1} = 1.6 Hz, J_{3-2} = 8 Hz, H-3), 7.66 (2 H, dd, J_{2-1} = 4.8 Hz, J_{2-3} = 8.0 Hz, H-2), 10.19 (1H, s, H-4)

Solubility: DMF, DMSO

Colour: orange / red powder

E.8.7 Reaction of phendione with L-phenylalanine ethyl ester

To a solution of phendione (0.25 g, 1.19 mmol) in methanol (50 ml) was added L-phenylalanine ethyl ester (0.27 g, 1.19 mmol). The resulting orange / red solution was stirred and refluxed for 4.5 hours and then let stir overnight. The resulting orange / red solid which deposited was filtered off, and then air-dried.

IR (KBr): 3432, 2923, 1616, 1421, 1315, 1118, 1061, 1019, 798, 731, 692 cm^{-1}

^{1}H NMR (d_6 – DMSO, δ/ppm): 8.97 (2H, dd, J_{1-2} = 4.6 Hz, J_{1-3} = 1.8 Hz, H-1), 8.37 (2H, dd, J_{3-1} = 1.8 Hz, J_{3-2} = 7.6 Hz, H-3), 7.66 (2H, dd, J_{2-1} = 4.6 Hz, J_{2-3} = 7.6 Hz, H-2), 10.19 (1H, s, H-4)

Solubility: DMF, DMSO

Colour: orange / red powder

SECTION 3

E.9 REACTIONS OF PHENDIONE WITH AMINO ACIDS

To a suspension of amino acid (1.19 mmol) in MeOH (50 ml) was added approx. 10 drops of concentration HCl and the mixture was refluxed for 1 hour. Phendione (0.25 g, 1.19 mmol) was added and the resulting suspension refluxed for 3 hours. On cooling to room temperature, the mixture was filtered. The filtrate was rotary evaporated to approx. 5 ml and set aside. The reactions gave mixtures from which either impure products or 1,10-phenanthroline-5,6-dicarboxylic acid were isolated as follows:

E.9.1 Reaction of phendione with L-valine

Yield: 0.3 g

% Found: C, 65.27; H, 2.95; N, 11.71

IR (KBr): 3451, 3089, 3006, 2923, 1730, 1710, 1627, 1598, 1575, 1517, 1458, 1426, 1367, 1299, 1227, 1175, 1121, 1072, 1056, 1037, 1021, 972, 925, 835, 724, 691, 617, 541 cm^{-1}

^{1}H NMR (d_6 – DMSO, δ/ppm): 10.68 (2H, s), 9.11 (2H, dd), 9.06 (2H, dd), 9.00 (2H, dd), 8.46 (2H, dd), 8.13 (2H, dd), 7.74 (2H, dd)

Solubility: hot H_2O, hot EtOH, MeOH, hot DMSO

Colour: yellow powder

E.9.2 Reaction of phendione with L-tyrosine

Yield: 0.11 g

% Found: C, 48.17; H, 4.18; N, 8.62

IR (KBr): 3451, 3089, 3007, 1730, 1709, 1622, 1601, 1575, 1518, 1457, 1426, 1290, 1290, 1227, 1121, 1020, 925, 825, 725, 691, 618, 541 cm^{-1}

^{1}H NMR (d_6 – DMSO, δ/ppm): 10.66 (2H, s), 9.10 (2H, dd), 9.04 (2H, dd), 8.99 (2H, dd), 8.45 (2H, dd), 8.12 (2H, dd), 7.62 (2H, dd)

Solubility: hot EtOH, MeOH, hot DMSO

Colour: orange powder

E.9.3 Reaction of phendione with L-threonine

Yield: 0.15 g

% Found: C, 58.06; H, 4.87; N, 11.29

IR (KBr): 3411, 3089, 3006, 2109, 2023, 1730, 1710, 1622, 1601, 1575, 1518, 1458, 1426, 1337, 1290, 1227, 1121, 1014, 925, 825, 725, 691 cm^{-1}

^{1}H NMR (d_6 – DMSO, δ/ppm): 10.65 (2H, s), 9.10 (2H, dd), 9.04 (2H, dd), 8.99 (2H, dd), 8.45 (2H, dd), 8.12 (2H, dd), 7.73 (2H, dd)

Solubility: hot EtOH, MeOH, DMSO

Colour: orange powder

E.9.4 Reaction of phendione with L-serine

Yield: 0.29 g

% Found: C, 55.10; H, 2.88; N, 10.44

IR (KBr): 3444, 3088, 3007, 2923, 2108, 2022, 1730, 1710, 1644, 1602, 1575, 1517, 1426, 1289, 1226, 1193, 1120, 1037, 925, 825, 725, 691, 617 cm^{-1}

^{1}H NMR (d_6 – DMSO, δ/ppm): 10.51 (1H, s), 8.83 (1H, dd), 8.77 (1H, d), 8.75 (1H, d), 8.25 (1H, dd), 8.19 (2H, s), 7.85 (1H, dd), 7.53 (1H, dd)

Solubility: hot EtOH, MeOH, DMSO

Colour: orange powder

E.9.5 Reaction of phendione with L-cysteine

Yield: 0.24 g

% Found: C, 52.62; H, 3.27; N, 10.02

IR (KBr): 3432, 3089, 1729, 1624, 1595, 1577, 1535, 1508, 1498, 1458, 1404, 1339, 1317, 1298, 1226, 1193, 1122, 1051, 1020, 925, 806, 720 cm^{-1}

^{1}H NMR (d_6 – DMSO, δ/ppm): 9.09 (2H, dd, J_{1-2} = 4.8 Hz, J_{1-3} = 1.6 Hz, H-1), 9.01 (2H, 2 d, J_{3-1} = 1.6 Hz, J_{3-2} = 8.4 Hz, H-3), 8.11 (2H, dd, J_{2-1} = 4.8 Hz, J_{2-3} = 8.4 Hz, H-2), 10.59 (2H, OH, H-4)

Solubility: hot EtOH, MeOH, DMSO

Colour: yellow powder

E.9.6 Reaction of phendione with L-glutamine

Yield: 0.03 g

% Found: C, 52.28; H, 3.92; N, 10.06

IR (KBr): 3427, 3085, 2923, 2851, 1729, 1627, 1596, 1540, 1498, 1465, 1415, 1321, 12861, 1234, 1123, 1089, 1020, 810, 718 cm^{-1}

^{1}H NMR (d_6 – DMSO, δ/ppm): 9.09 (2H, dd, J_{1-2} = 4.8 Hz, J_{1-3} = 1.2 Hz, H-1), 9.02 (2H, dd, J_{3-1} = 1.2 Hz, J_{3-2} = 8.4 Hz, H-3), 8.11 (2H, dd, J_{2-1} = 4.8 Hz, J_{2-3} = 8.4 Hz, H-2), 10.57 (2H, OH, H-4)

Solubility: MeOH, DMSO

Colour: bright orange powder

E.9.7 Reaction of phendione with L-asparagine

Yield: 0.15 g

% Found: C, 50.00; H, 4.94; N, 13.72

IR(KBr): 3444, 3089, 2923, 1730, 1710, 1621, 1603, 1575, 1518, 1426, 1384, 1284, 1227, 1120, 1038, 925, 824, 725, 692, 618, 540 cm^{-1}

^{1}H NMR (d_6 – DMSO, δ/ppm): 9.10 (2H, dd, J_{1-2} = 1.6 Hz, J_{1-3} = 4.8Hz, H-1), 9.01 (2H, dd, J_{2-1} = 1.6 Hz, J_{2-3} = 8.4 Hz, H-2), 8.11 (2H, dd, J_{3-1} = 4.8 Hz, J_{3-2} = 8.4 Hz, H-3), 10.42 (2H, s, H-4)

Solubility: partially soluble in H_2O, partially soluble in hot MeOH, DMSO;

Colour: green brown powder

E.10 ANTI-MICROBIAL SUSCEPTIBILITY TESTING

E.10.1 Biological preparations

Fungal isolates: Isolates of *C. albicans* were obtained from Oxiod (ATCC 10231). Isolates were stored on Sabouraud dextrose agar (SDA) plates at 4 °C and were subcultured monthly from the initial received.

Sterilisation was achieved by autoclaving at 121 °C and 100 kPa for 15 minutes.

Cell density was measured using M°Farland standards.

Sabouraud dextrose agar (SDA) was obtained from Difco (0109-17-1) and made up according to the manufacturers instructions.

Minimal media: 2 % glucose, 0.17 % yeast nitrogen base without amino acids and 0.5 % ammonium sulfate were dissolved in a Duran bottle with distilled water. The resulting solution was autoclaved and stored at 4 °C.

E.10.2 Preparation of complex solutions for anti-microbial susceptibility testing

Tested complexes (0.1 g) were ground to a fine powder and dissolved/suspended in 5 ml of pure DMSO. This solution was then added to 95 ml of water to yield a stock solution

at a concentration of 1000 μg/ml. Dilutions of the stock solution were prepared; 50 μg/ml, 20 μg/ml, 10 μg/ml and 5 μg/ml.

E.10.3 Anti-microbial susceptibility testing method

Prior to testing yeast cells were grown for 24 hours on SDA at 37 °C. Cell suspensions were prepared in sterile PBS (5 ml) to a density of 0.5 M°Farland standard, yielding a final inoculum concentration of $3.5 \times 10^4 - 5.0 \times 10^5$ cells cm^{-3}. The prepared cell suspension (90 μl) was dispensed into microtitre plates and to this was added the test complex solution (10 μl) to yield working test complexes at concentrations of 50 μg/ml, 20 μg/ml, 10 μg/ml and 5 μg/ml. Plates were then incubated for 24 hours at 37 °C with continuous shaking. Each complex was assessed in triplicate and three independent experiments were performed.

CONCLUSION

The purpose of this study was to generate a series of complexes/compounds for application as potential anti-microbial agents.

1,10-phenanthroline-5,6-dione (phendione) **(1)** was generated by the oxidization of 1,10-phenanthroline (phen) using concentration sulfuric acid, concentration nitric acid and potassium bromide in a condensation reaction.

The chelating ligands phen and phendione reacted smoothly with metal nitrate salts to yield nitrate complexes $[Cu(phen)_2NO_3]NO_3.2H_2O$ **(2)**, $[Co(phen)_2NO_3]\ NO_3.2H_2O$ **(3)**, $[Zn(phen)_2NO_3]NO_3.2H_2O$ **(4)**, $[Mn(phen)_3NO_3]NO_3.2H_2O$ **(5)**, $[Cu(phendione)_2NO_3]NO_3.2H_2O$ **(6)**, $[Co(phendione)_2NO_3]NO_3.H_2O$ **(7)**, $[Zn(phendione)_2(NO_3)_2].3H_2O$ **(8)** and $[Mn(phendione)_2(NO_3)_2].H_2O$ **(9)**.

Complexes $[Cu(phen)_2]Cl_2.6H_2O$ **(10)**, $[Co(phen)_2]Cl_2.3H_2O$ **(11)**, $[Zn(phen)_2]Cl_2.H_2O$ **(12)**, $[Mn(phen)_2]Cl_2.CH_3CH_2OH$ **(13)**, $[Cu(phendione)_2Cl_2].2H_2O$ **(14)**, $[Co(phendione)_2Cl_2].H_2O$ **(15)**, $[Zn(phendione)_2Cl_2].3H_2O$ **(16)** and $[Mn(phendione)_2Cl_2].2H_2O$ **(17)** resulted from the reaction of either phen or phendione with metal chloride salts.

Simple metal sulphate salts reacted with chelating ligands phen or phendione to produce complexes $[Cu(phen)_2SO_4].3H_2O$ **(18)**, $[Co(phen)_2SO_4].6H_2O$ **(19)**, $[Zn(phen)SO_4].2H_2O$

(20), $[Mn(phen)SO_4].7H_2O$ **(21)**, $[Cu(phendione)SO_4].4H_2O$ **(22)**, $[Co(phendione)_2SO_4].7H_2O$ **(23)**, $[Zn(phendione)SO_4].H_2O$ **(24)** and $[Mn(phendione)_2SO_4].CH_3CH_2OH$ **(25)**.

Complexes $[Cu(phen)(CH_3CO_2)_2].H_2O$ **(26)** and $[Cu(phendione)_2(CH_3CO_2)_2].5H_2O$ **(27)** resulted from the reaction of phen or phendione with copper(II) acetate.

Complexes **2–27** were screened for their ability to inhibit the growth of an isolate of *Candida albicans* at concentrations of 50 $\mu g/cm^3$, 20 $\mu g/cm^3$, 10 $\mu g/cm^3$ and 5$\mu g/cm^3$. The anti-fungal activity of the metal free ligands phen and phendione show significant activity at the lowest tested concentration of 5 $\mu g/cm^3$ which is comparable to that of prescription drug Amphothericin B.

Complexes **5**, **9**, **23** and **25** are potent *in-vitro* anti-*Candida* agents which display activity superior to the state-of-the-art organic drug Amphothericin B at the low concentration of 5 $\mu g/cm^3$. Complexes **6**, **7**, **13**, **17** and **21** were found to exhibit excellent activity at 10 $\mu g/cm^3$ comparable to Amphothericin B, whereas complexes **4**, **8**, **12**, **14**, **15**, **16**, **22** and **24** exhibit reasonable activity at the higher concentration of 20 $\mu g/cm^3$ and 50 $\mu g/cm^3$.

Isophthalic aldehyde was reacted with phendione in a 2:1 and a 1:1 molar ratio to yield compounds $mbpibH_2.6H_2O$ **(28)** and $mfmp.4H_2O$ **(29)**. Attempts to react 2-pyridinecarboxaldehyde with phendione was not fully successful as impurities

remained after attempted purification of PCIP **(30)**. Phendione reacted with 4-cyanobenxaldehyde to generate compound DPBN.$3H_2O$ **(31)**.

Compounds **28–31** were screened for their ability to inhibit the growth of an isolate of *Candida albicans* at concentrations of 50 $\mu g/cm^3$, 20 $\mu g/cm^3$, 10 $\mu g/cm^3$ and 5$\mu g/cm^3$. Compounds **28-31** were shown to be relatively inactive against *Candida albicans*. This is in contrast to the potent activity displayed by phendione **(1)**.

Reaction of three manganese(II) metal salts (nitrate, chloride and acetate) with the chelating mbpibH_2.$6H_2O$ ligand yielded complexes [Mn(mbpibH_2)]$(NO_3)_2$.$3H_2O$ **(32)** [Mn(mbpibH_2)]Cl_2.$4H_2O$ **(33)** and [Mn(mbpibH_2)$(CH_3CO_2)_2$].$9H_2O$ **(34)**. Complexes **32-34** were shown to be moderately active against *Candida albicans*, in contrast to the activity displayed by mbpibH_2.$6H_2O$ **(28).**

Attempts to react mbpibH_2.$6H_2O$ with cobalt(II) nitrate yielded an orange solution which upon standing deposited a small number of pink crystals. Complex [Co(phendione)$(H_2O)_4$]$(NO_3)_2$.H_2O **(35)** was characterised by X-ray crystallography.

Reaction of copper(II) nitrate with chelating ligand DPBN **(31)** generated complex [Cu$(DPBN)_2$]$(NO_3)_2$.$4H_2O$ **(36)**. **36** displays moderate activity when compared with that of the free DPBN ligand.

L-Tyrosine methyl ester reacted with phendione to yield PhenTyrOMe.CH_3OH **(37)** and was characterised by X-ray crystallography. Compound **37** exhibited exceptional anti-

Candida activity, showing significant fungitoxicity with only 5.6 % cell growth at 5 ug/ml. Attempts to react methyl and ethyl ester of the amino acids and seven simple amino acids with phendione proved to be essentially unsuccessful.

[1] F. C. Odds, A. Brown and N. Gow, *Trends in Microbiology*, 2003, **11**, 272-279

[2] B. Coyle, P. Kinsella, M. McCann, M. Devereux, R. O'Connor, M. Clynes and K. Kavanagh, *Toxicology in Vitro*, 2004, **18**, 63-70

[3] A. Eshwika, B. Coyle, M. Devereux, M. McCann and K. Kavanagh, *Biometals*, 2004, **17**, 415-422

[4] C. Deegan, M. McCann, M. Devereux, B. Coyle and D. Egan, *Cancer Letters*, 2007, **247**, 224-233

[5] W. W. Brandt, F. P. Dwyer and E. C. Gyarfas, *Chemical Rev*iews, 1954, **54**, 959-1017

[6] M. McCann, M. Geraghty, M. Devereux, D. O'Shea, J. Mason, L. O'Sullivan, *Metal Based Drug*, 2000, **7**, 4.

[7] M. Geraghty, J. F. Cronin, M. Devereux and M. McCann, *BioMetals*, 2000, **13**, 1-8

[8] M. Geraghty, V. Sheridan, M. McCann, M. Devereux, V. McKee, *Polyhedron*, 1999, **18**, 2931-2939

[9] N. Margiotta, A. Bergamo, G. Sava, G. Padovano, E. de Clercq, G. Natile, *Journal of Inorganic Biochemistry*, 2004, **98**, 1385-1390

[10] M. Devereux, M. McCann, D. O'Shea, R. Kelly, D. Egan, C. Deegan, K. Kavanagh, , V. McKee, G. Finn, *Journal of Inorganic Biochemistry*, 2004, **98**, 1023-1031

[11] M. Devereux, M. McCann, V. Leon, R. Kelly, D. O'Shea and V. McKee, *Polyhedron*, 2003, **22**, 3187-3194

[12] M. Geraghty, M. McCann, M. Devereux and V. McKee, *Inorganica Chimica Acta*, 1999, **293**, 160-166

[13] M. Devereux, M. McCann, V. Leon, M. Geraghty, V. McKee and J. Wikaira, *Polyhedron*, 2000, **19**, 1205-1211

[14] B. S. Creaven, D. A. Egan, D. Karcz, K. Kavanagh, M. McCann, M. Mahon, A. Noble, B. Thati and M. Walsh, *Journal of Inorganic Biochemistry*, 2007, **101**, 1108-1119

[15] M. Devereux, M. McCann, V. Leon, M. Geraghty, V. McKee and J. Wikaira, *Metal Based Drugs*, 2000, **7**, 275-288

[16] M. Geraghty, M. McCann, M. Devereux, F. Cronin, M. Curran and V. McKee, *Metal Based Drugs*, 1999, **6**, 41-48

[17] M. McCann, B. Coyle, S. McKay, P. McCormack, K. Kavanagh, M. Devereux, V. McKee, P. Kinsela, R. O Connor and M. Clynes, *Biometals*, 2004, **17**, 635-654

[18] S. Abuskhuna, J. Briody, M. McCann, M. Devereux, K. Kavanagh, J. Fontecha and V. McKee, *Polyhedron*, 2004, **23**, 1249-1255

[19] B. Coyle, K. Kavanagh, M. McCann, M. Devereux and M. Geraghty, *Biometals*, 2003, **16**, 321-329

[20] A. Mohindru, J. M. Fisher and M. Rabinovitz, *Biochemical Pharmacology*, 1983, **32**, 3627-3632

[21] C. Deegan, M. McCann, M. Devereux, B. Coyle and D. A. Egan, *Cancer Letters*, 2007, **247**, 224-233

[22] C. Deegan, B. Coyle, M. McCann, M. Devereux and D. A. Egan, *Chemico-Biological Interactions*, 2006, **164**, 115-125

[23] G. Chelucci, D. Addis, S. Baldino, *Tetrahedron Letters*, 2007, **48**, 3359-3362

[24] M. T. Ramirez-Silva, M. Gomex-Hernandez, M. De L. Pacheco-Hernandez, A. Rojas-Hernandez, L. Galicia, *Spectrochimica Acta Part A*, 2004, **60**, 781-789

[25] S. Brahma, H. P. Sachin, S. A. Shivashankar, T. Narasimhamurthy and R. S. Rathore, *Acta crystallographica Section C, Crystal structure communications*, 2008, **64**, m140-m143

[26] C. Zhong, H. Huang, A. He and H. Zhang, *Dyes and Pigments*, 2008, **77**, 578-583

[27] H. Hadadzadeh, G. Mansouri, H. R. Khavasi, R. D. Hoffmann, U. C. Podewald and R. Pottgen, *Analytical Science*, 2007, **23**, 101-102

[28] F. Blau, *Berichte.*, 1888, **21**, 1077

[29] F. Blau, *Monatshefte für Chemie.*, 1898, **19**, 647

[30] F. Blau, *Berichte der Deutschen Chemischen Gesellschaft.*, 1888, **27**, 1077

[31] D. W. A Sharp, Dictonary of Chemistry 2nd edn., Great Britian by Penguin books Ltd (1990)

[32] Merck & Co., Inc, 13th edn., Whitehouse Station, NJ, USA (2001)

[33] F. Calderazzo, F. Marchetti, G. Pampaloni, V. Passarelli, *Dalton Trans*itions, 1999, 4389-4396

[34] R. Janes, E. Moore., *Metal-Ligand bonding*, 2004, The Open University

[35] M. Ghosh, P. Biswas, U. Florke, *Polyhedron*, 2007, **26**, 3750-3762

[36] F.A Cotton and G. Wilkinson, *Advanced Inorganic Chemistry*, 5th edn., J. Wiley & Sons, New York (1988)

[37] W. Z. Antkowiak, A. Sobczak, *Tetrahedron*, 2001, **57**, 2799-2805

[38] P. J. Steel, *Coordination Chemistry Reviews*, 1990, **106**, 227-265

[39] W. Paw and R. Eisenberg, *Inorganic Chemistry*, 1997, **36**, 2287-2293

[40] L. Calucci, G. Pampaloni, C. Pinzino, A. Prescimone, *Inorganica Chimica Acta*, 2006, **359**, 3911-3920

[41] M. Yamada, Y. Tanaka, Y. Yashimoto, S. Kuroda, I. Shimao, *Bulletin of the Chemistry Society of Japan*, 1992, **65**, 1006

[42] H. Hadadzadeh, M.M Olmstead, A. R. Rezvani, N. Safari, H. Saravani, *Inorganica Chimica Acta*, 2006, **359**, 2154 - 2158

[43] H. Saravani, A. R. Rezvani, M. Ghobad, A. R. Salehi Rad, H. R. Khavasi, H. Hadadzadeh, *Inorganica Chimica Acta*, 2007, **360**, 2829-2834

[44] F. Calderazzo, G. Pampaloni, V. Passarelli, *Inorganica Chimica Acta*, 2002, **330**, 136-142

[45] G.-X. Liu, R.-Y. Huang, H. Xu, X.-J. Kong, L.-F. Huang, K. Zhu, X.- M. Ren, *Polyhedron*, 2008, **27**, 2327-2336

[46] M. Xilinas, P. N. Gerolymatos, K. Attika, United States Patent, Application No.: US 6,670,369 B1 (2003)

[47] B. A. Yankner, Duffy L K, Kirschner DA, Science, 1990, 250, (4978): 279-282

[48] E. C. Constable, *Coordination Chemistry Reviews*, 1989, **93**, 205-223

[49] B. Thati, A. Noble, B. S. Creaven, M. Walsh, M. McCann, M. Devereux, K. Kavanagh and D. A. Egan, *European Journal of Pharmacology*, 2009, **602,** 203-214

[50] R. P. Sharma, A. Singh, P. Brandao, V. Felix and P. Venugopalan, *Journal of Molecular Structure,* 2009, **921,** 227-232

[51] R. P. Sharma, A. Singh, P. Brandao, V. Felix and P. Venugopalan, *Journal of Molecular Structure,* 2008, **888**, 291-299

[52] R. P. Sharma, A. Singh, P. Brandao, V. Felix and P. Venugopalan, *Journal of Molecular Structure,* 2009, **918**, 1-9

[53] R. P. Sharma, A. Singh, V. Felix and P. Venugopalan, *Journal of Molecular Structure,* 2009, **918,** 123-128

[54] S. Gao, X. Li, C. Yang, T. Li and R. Cao. *Journal of Solid State Chemistry,* 2006, **179**, 1407-1414

[55] G. Mansouri, A. R. Rezvani, H. Hadadzadeh, H. R. Khavasi and H. Saravani, *Journal of Organometallic Chemistry,* 2007, **692**, 3810-3816

[56] A. Y. Girgis, Y. S. Sohn and A. L. Balch, *Inorganic Chemistry*, 1975, **114,** 2327-2331

[57] G. A. Fox, S. Bhattacharya and C. G. Pierpont, *Inorganic Chemistry,* 1991, **30**, 2895-2899

[58] C. A.larcon-Payer, T. Pivetta, D. Choquesillo-Larate, J. M. Gonzalez-Perez, G. Crisponi, A. Catineiras and J. Niclos-Gutierrez, *Inorganic Chimica Acta*, 2005, **358**, 1918-1926

[59] Y. Liu, Z. Peng, D. Li and Y. Zhou, *Spectrochimica Acta Part A*, 2008, **69**, 471-477

[60] D. Wesselinova, M. Neykov, N. Kaloyanov, R. Toshkova and G. Dimitrov, European Journal of Medicinal Chemistry, 2009, **44**, 2720-2723

[61] Y. Tor, *Comptos Rendus Chimie*, 2003, **6**, 755-766

[62] G. Chelucci, D. Addis and S. Baldino, *Tetrahedron Letters*, 2007, **48**, 3359-3362

[63] K. Latham, K. F. White, K. B. Szpakolski, C. J. Rix and J. M. White, *Inorganic Chimica Acta*, 2009, **362**, 1872-1886

[64] F. da S. Miranda, A. M. Signori, J. Vicente, B. de Sourza, J. P. Priebe, B. Szpoganicz, N. S. Goncalves and A. Neves, *Tetrahedron*, 2008, **64**, 5410-5415

[65] S. Bodige and F. M. MacDonnell, *Tetrahedron Letters*, 1997, **38**, 8159-8160

[66] P. U. Maheswari, V. Rajendiran, M. Palaniandavar and R. Thomas, G. *Inorganic Chimica Acta*, 2006, **359**, 4601-4612

[67] K. Larsson and L. Ohrstrom, *Inorganic Chimica Acta*, 2004, **357**, 657-664

[68] S. Rabaca, M. C. Duarte, I. C. Santos, L. C. J. Pereire, M. Fourmigue, R. T. Henriques, M. Almeida, *Polyhedron*, 2008, **27**, 1999-2006

[69] L. Wang, W. You and W. Huang, *Journal of Molecular Structure*, 2009, **920,** 270-276

[70] N. Shahabadi, S. Kashanian and M. Purfoulad, *Spectrochimica Acta Part A: Molecular and Biomolecular Spectroscopy*, 2009, **72**, 757-761

[71] M. T. Mongelli, J. Heinecke, S. Mayfield, B. Okyere, B. S.J. Winkel and K. J. Brewer, *Journal of Inorganic Biochemistry*, 2006, **100**, 1983-1987

[72] W. D. Mc. Fadyen, L. P. G. Wakelin, I. A. G. Roos, V. A. Leopold, *Journal of Medicinal Chemistry*, 1984, **28,** 1113-1116

[73] J. Liu, W. Zheng, S. Shi, C. Tan, J. Chen, K. Zheng and L. Ji, *Journal of Inorganic Biochemistry, 2008,* **102**, 192-202

[74] S. Md, S.R. Chowdhury and K. K. Mukherjea, *International Journal of Biological Macromolecules*, 2007, **41**, 579-583

[75] B. Jing, M. Zhang and T. Shen, *Spectrochimica Acta Part A*, 2004, **60**, 2635-2641

[76] C. Xin Zhang and S. J. Lippard, *Current Opinion in Chemical Biology*, 2003, **7**, 481-489

[77] B. Thati, A. Noble, B. S. Creaven, M. Walsh, K. Kavanagh and D. A. Egan, *European Journal of Pharmacology*, 2007, **569**, 16-28

[78] C. Marzano, A. Trevisan, L. Giovagnini and D. Fregonal, *Toxicology In Vitro*, 2002, **16**, 413-419

[79] S. Ghosh, A.C. Barve, A. A. Kumbhar, A. S. Kumbhar, V. G. Puranik, P. A. Datar, U. B. Sonawane and R. R. Joshi, *Journal of Inorganic Biochemistry*, 2006, **100**, 331-343

[80] M. Devereux, D. O' Shea, A. Kellett, M. McCann, M. Walsh, D. Egan, C. Deegan, K. Kędziora, G. Rosair and H. Müller-Bunz, *Journal of Inorganic Biochemistry*, 2007, **101**, 881-892

[81] D. O' Shea, *Ph.D. Thesis*, Dublin Institute of Technology, Dublin, Ireland, 2004.

[82] H. Zhou, Y. Lui, C. Zhen, J. Gong, Y. Liang, C. Wang, C. Zou, *Thermochimica Acta.*, 2002, **397**, 87-95

[83] B. Thati, A. Noble, B. S. Creaven, M. Walsh, K. Kavanagh and D. A. Egan, *Chemico-Biological Interactions*, 2007, **168**, 143-158

[84] K. Yokoyama, T. Asakura, N. Nakamura and H. Ohno, *Inorganic Chemistry Communications*, 2006, **9**, 281-283

[85] B. Selvakumar, V. Rajendiran, P. U. Masheswari, H. Stoeckli-Evans and M. Palaniandavar, *Journal of Inorganic Biochemistry*, 2006, **100**, 316-330

[86] F. Li, W. Chen, C. Tang and S. Zhang, *Talanta*, 2008, **77**, 1-8

[87] V. Chandrasekhar, R. Azhzkzr, T. Senapati, P. Thilagar, S. Ghosh, S. Verma, R. Boomishankar, A. Steiner and P. Kogerler, *Dalton Transition*, 2008, 1150-1160

[88] Lukas Stulik, BSc (Ordinary) Physical and Life Sciences, Chemistry Option, DIT, 3rd Year Project "Spectrocopic Investigation of Drug-DNA Interactions"

[89] F. A. Cotton and G. Wilkinson, Advanced Inorganic Chemistry, 6th Edition, J. Wiley & Sons, New York (1999)

[90] Hui Chao, Bao-Hui Ye, Hong Li, Run-Hua Li, Jian-Ying Zhou and Liang-Nian Ji, *Polyhedron*, 2000, **19,** 1975-1983

APPENDICES

APPENDIX 1 – IR Spectra

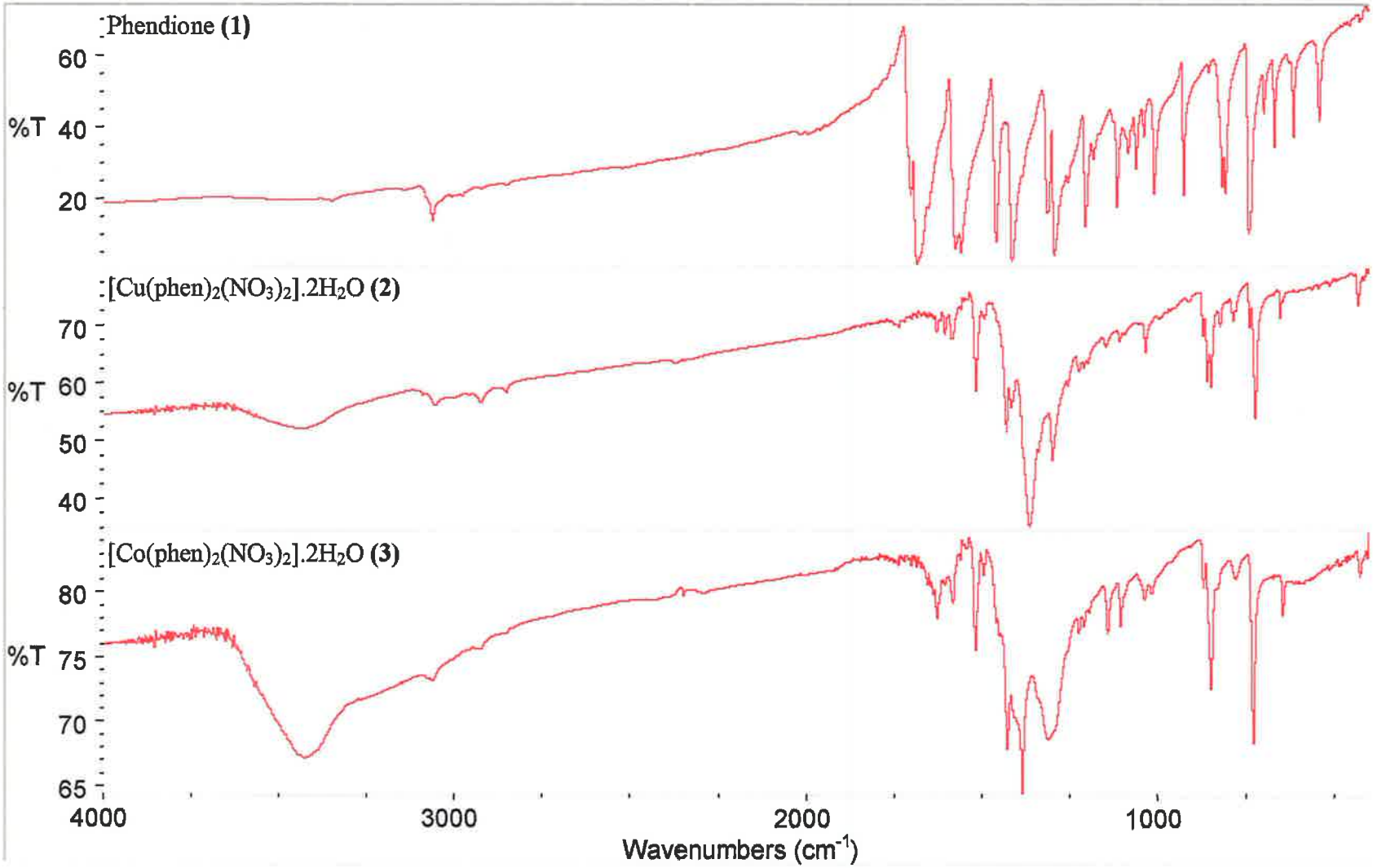
Phendione (1)
%T
60
40
20
[Cu(phen)2(NO3)2].2H2O (2)
%T
70
60
50
40
[Co(phen)2(NO3)2].2H2O (3)
%T
80
75
70
65
4000
3000
2000
1000
Wavenumbers (cm-1)

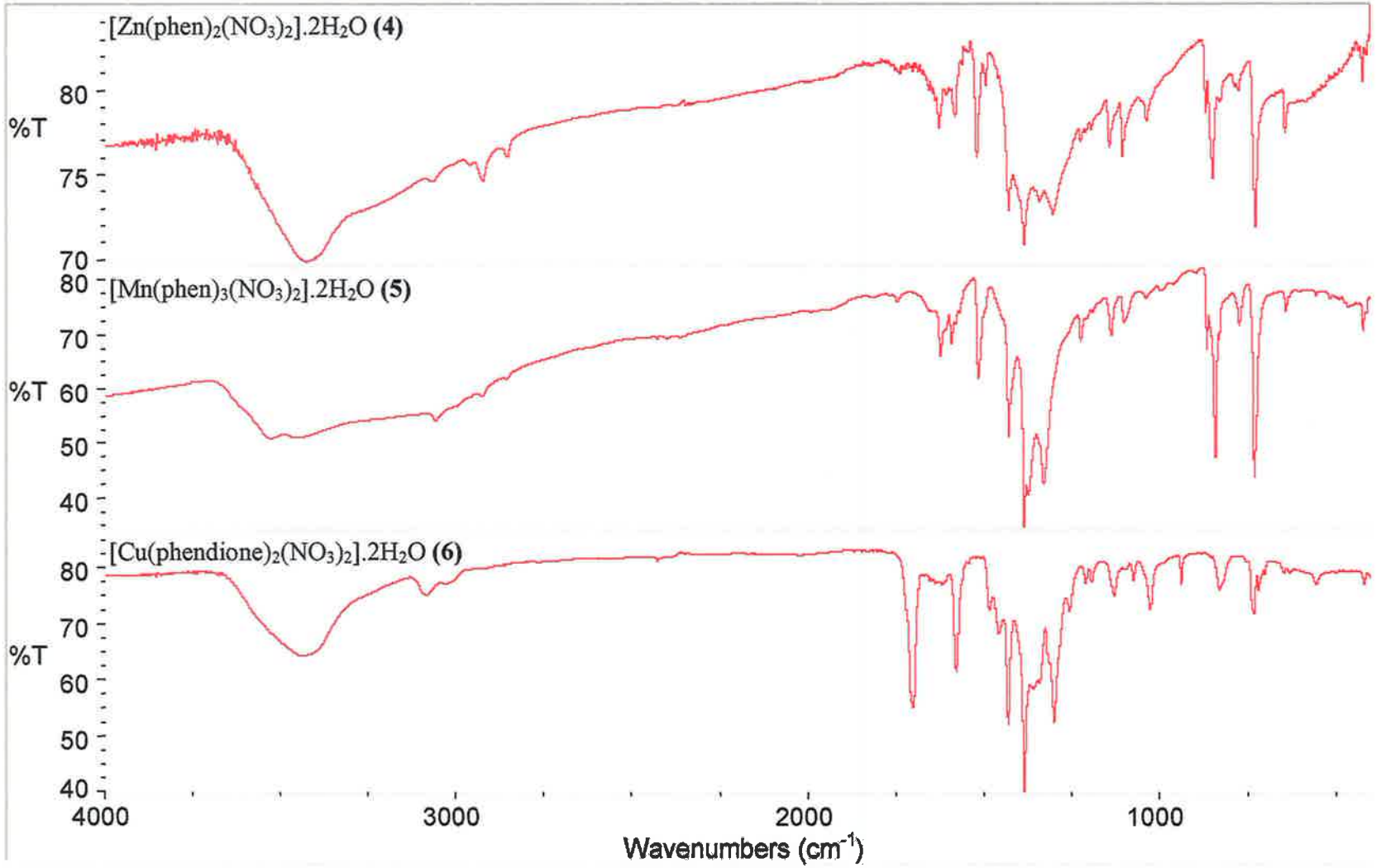
[Zn(phen)2(NO3)2].2H2O (4)
%T
80
75
70
[Mn(phen)3(NO3)2].2H2O (5)
%T
80
70
60
50
40
[Cu(phendione)2(NO3)2].2H2O (6)
%T
80
70
60
50
40
4000
3000
2000
1000
Wavenumbers (cm-1)

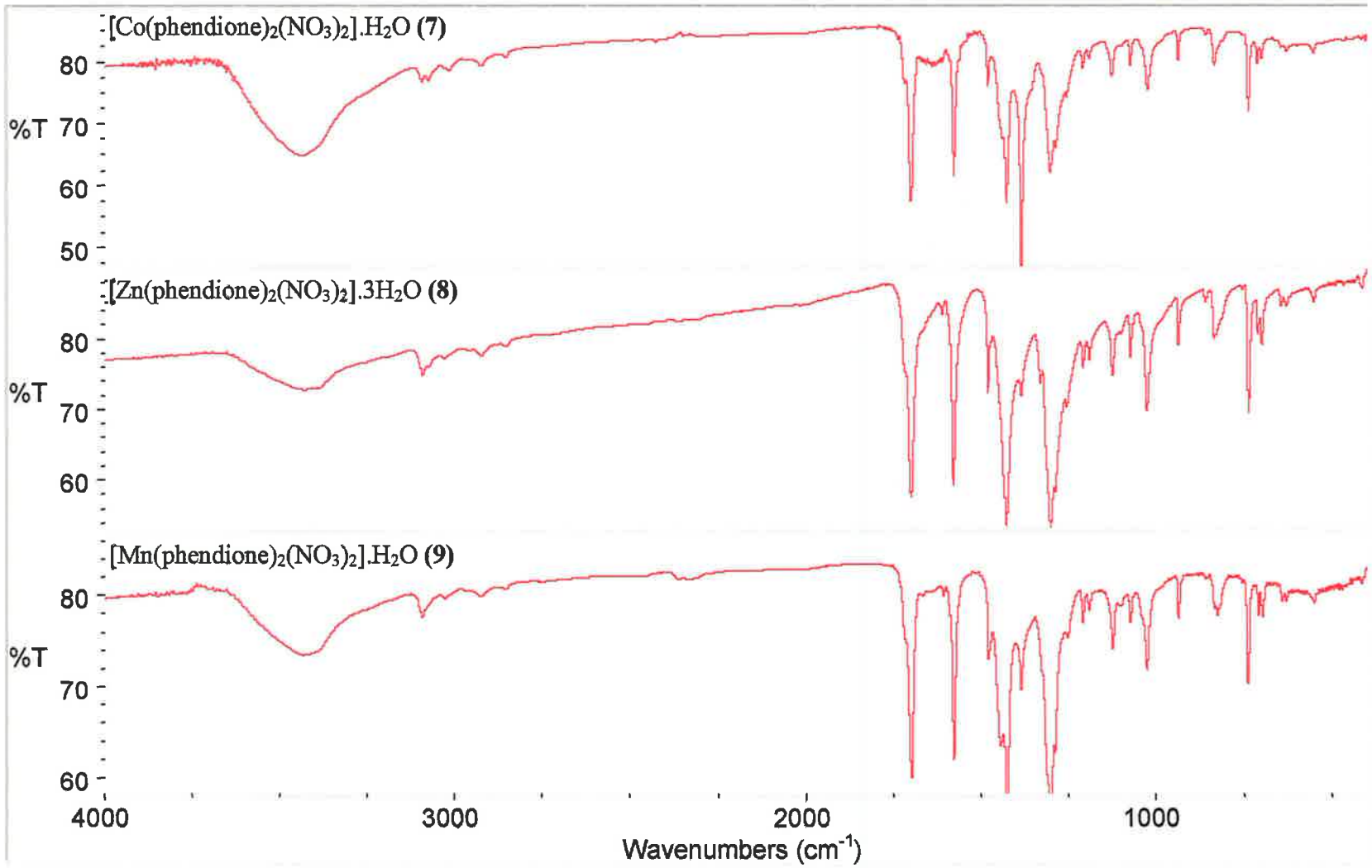
[Co(phendione)2(NO3)2].H2O (7)
80
%T 70
60
50
[Zn(phendione)2(NO3)2].3H2O (8)
80
%T
70
60
[Mn(phendione)2(NO3)2].H2O (9)
80
%T
70
60
4000
3000
2000
1000
Wavenumbers (cm-1)

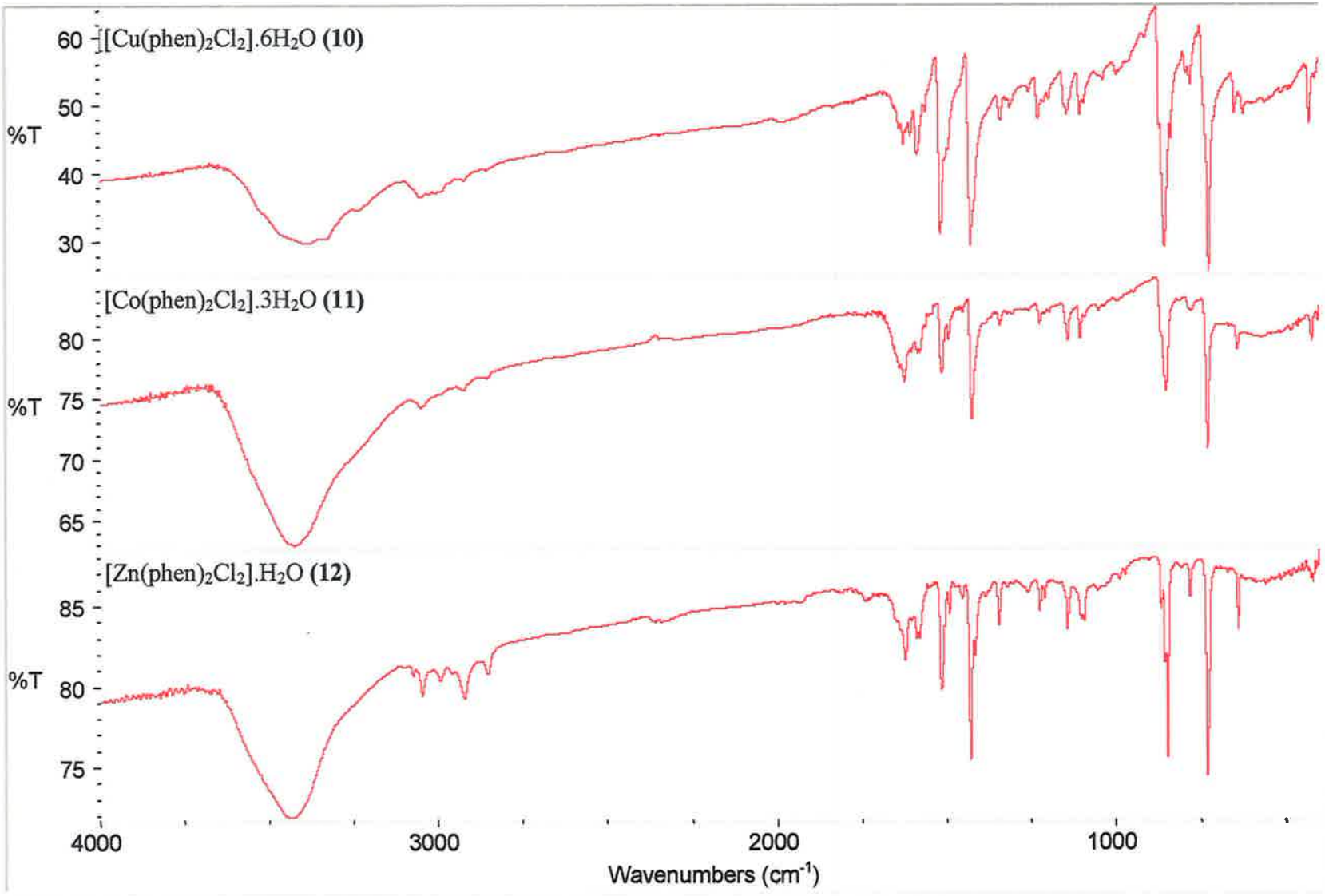
[Cu(phen)2Cl2].6H2O (10)
%T
60
50
40
30
[Co(phen)2Cl2].3H2O (11)
%T
80
75
70
65
[Zn(phen)2Cl2].H2O (12)
%T
85
80
75
4000
3000
2000
1000
Wavenumbers (cm-1)

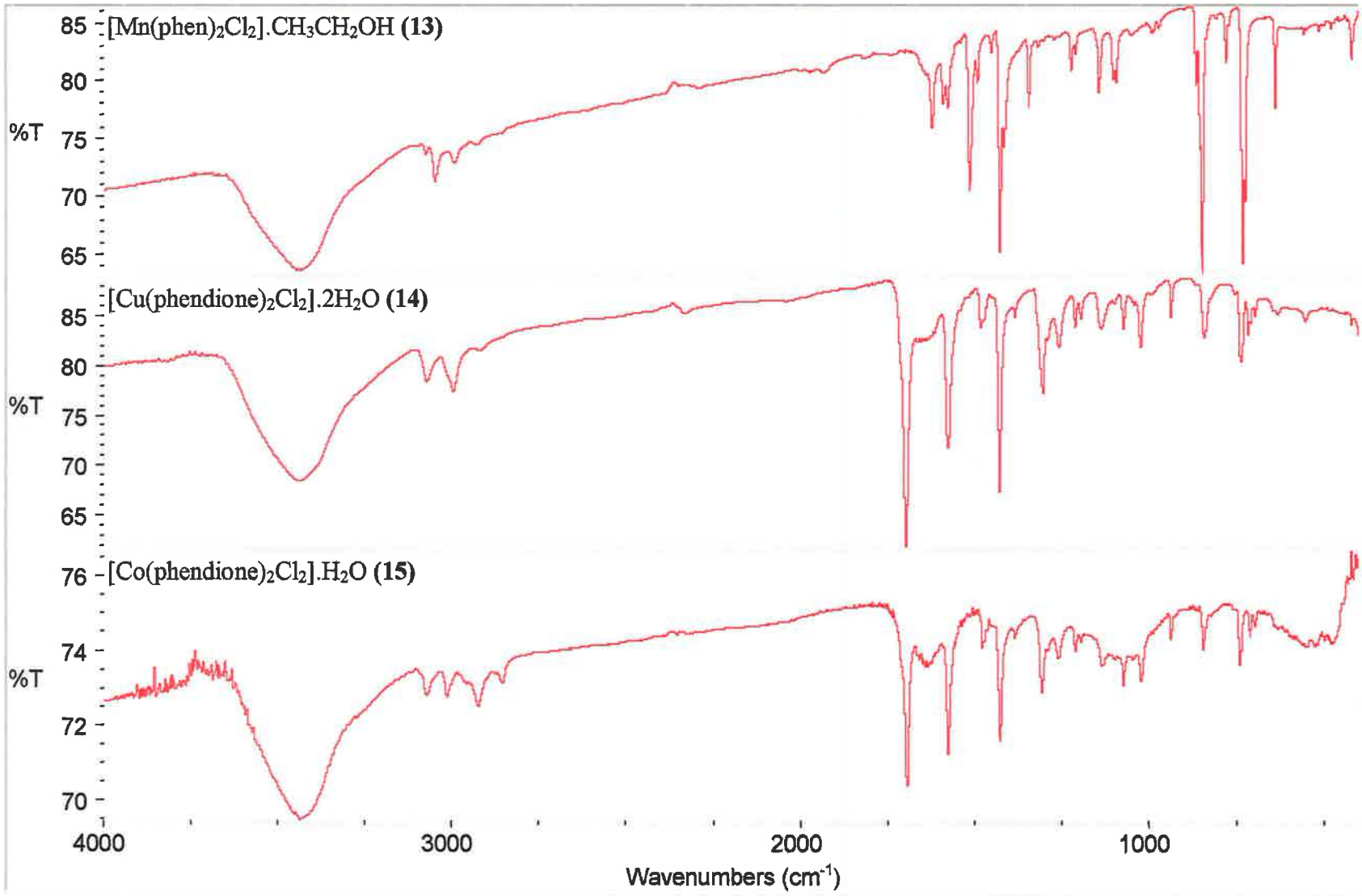
[Mn(phen)2Cl2].CH3CH2OH (13)
%T
85
80
75
70
65
[Cu(phendione)2Cl2].2H2O (14)
%T
85
80
75
70
65
[Co(phendione)2Cl2].H2O (15)
%T
76
74
72
70
4000
3000
2000
1000
Wavenumbers (cm-1)

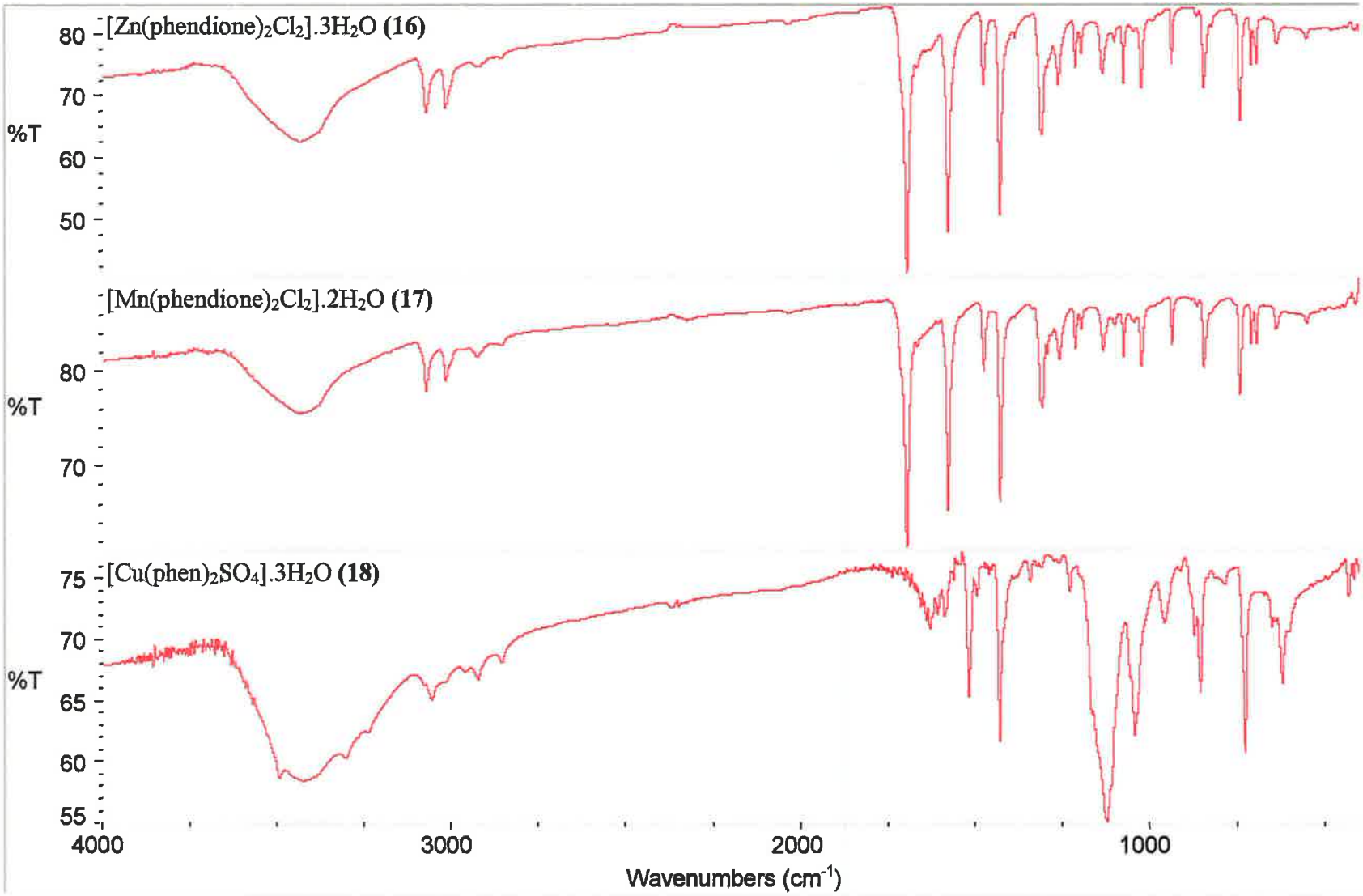
[Zn(phendione)2Cl2].3H2O (16)
[Mn(phendione)2Cl2].2H2O (17)
[Cu(phen)2SO4].3H2O (18)
%T
80
70
60
50
80
70
75
70
65
60
55
4000
3000
2000
1000
Wavenumbers (cm-1)

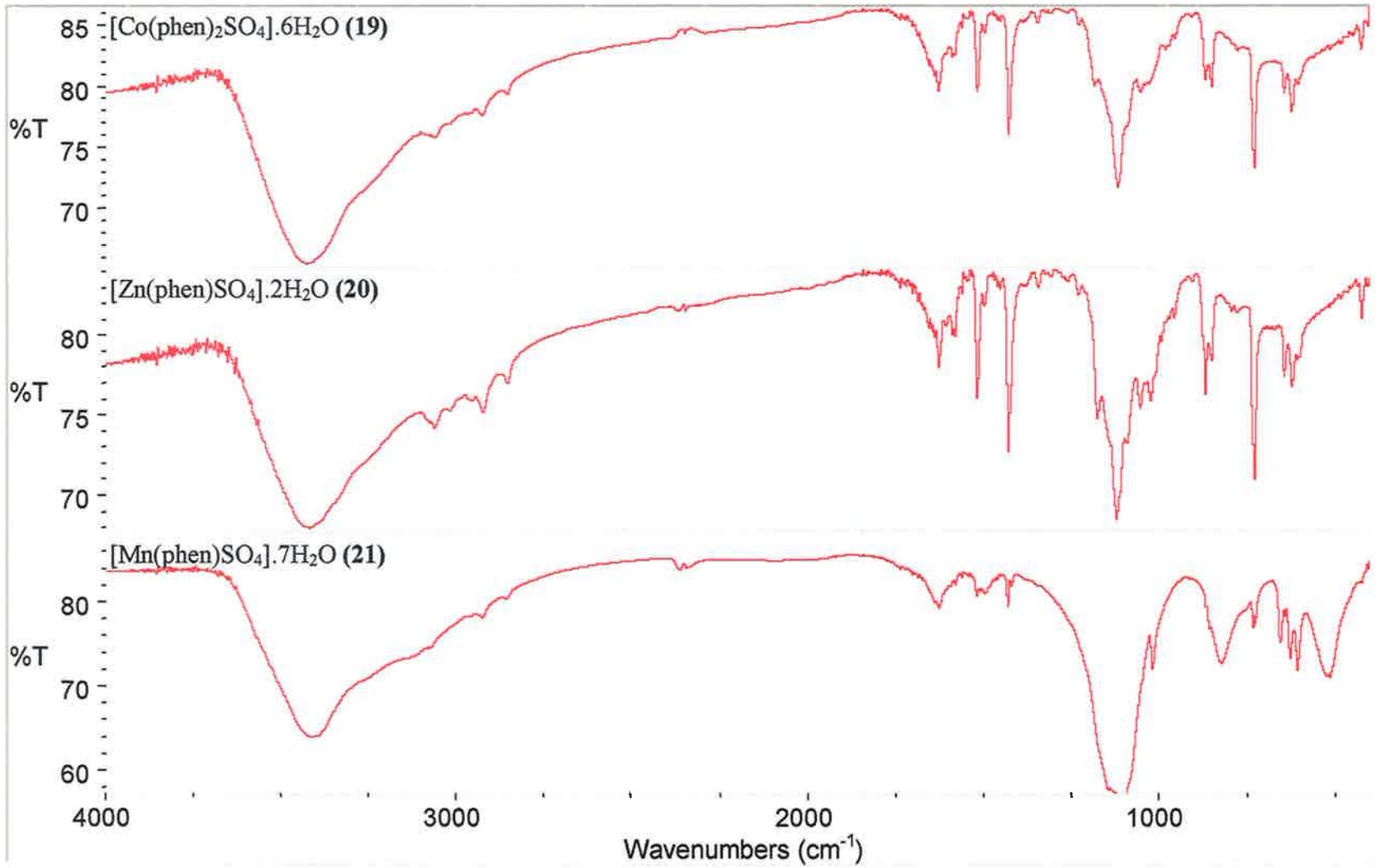
[Co(phen)2SO4].6H2O (19)
%T
85
80
75
70
[Zn(phen)SO4].2H2O (20)
%T
80
75
70
[Mn(phen)SO4].7H2O (21)
%T
80
70
60
4000
3000
2000
1000
Wavenumbers (cm-1)

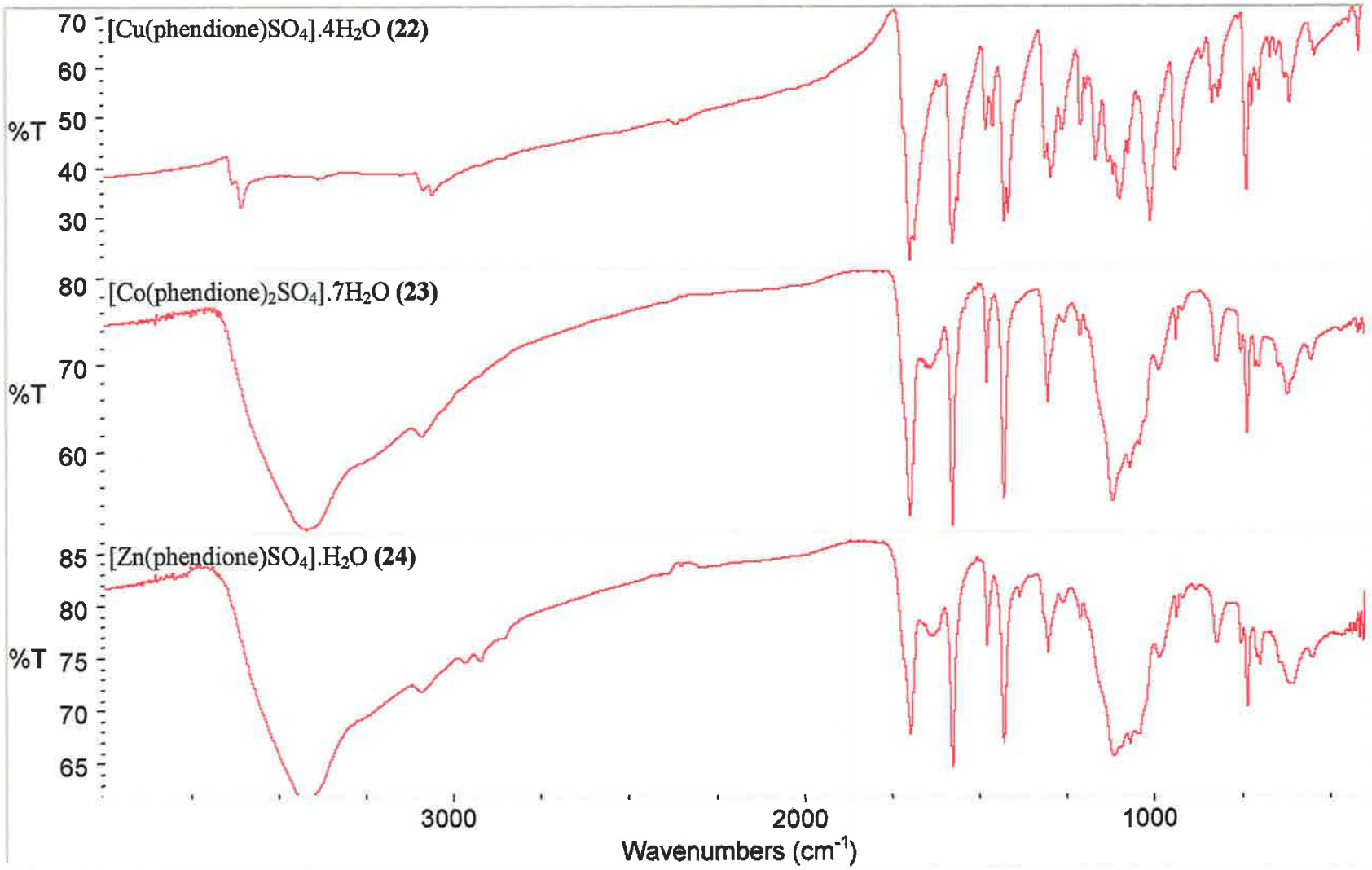
[Cu(phendione)SO4].4H2O (22)
%T
70
60
50
40
30
[Co(phendione)2SO4].7H2O (23)
%T
80
70
60
[Zn(phendione)SO4].H2O (24)
%T
85
80
75
70
65
3000
2000
1000
Wavenumbers (cm-1)

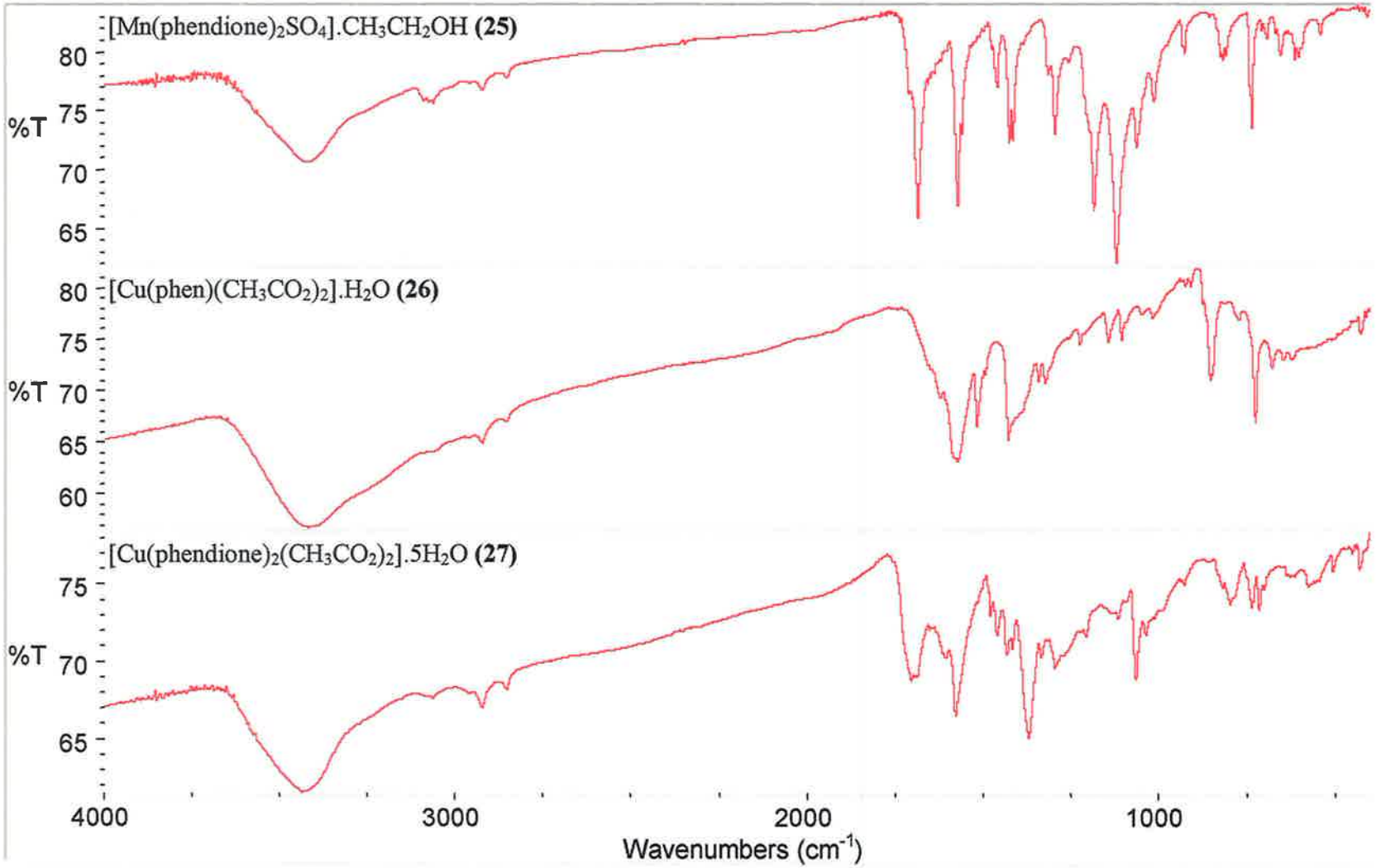
[Mn(phendione)2SO4].CH3CH2OH (25)
%T
80
75
70
65
[Cu(phen)(CH3CO2)2].H2O (26)
%T
80
75
70
65
60
[Cu(phendione)2(CH3CO2)2].5H2O (27)
%T
75
70
65
4000
3000
2000
1000
Wavenumbers (cm-1)

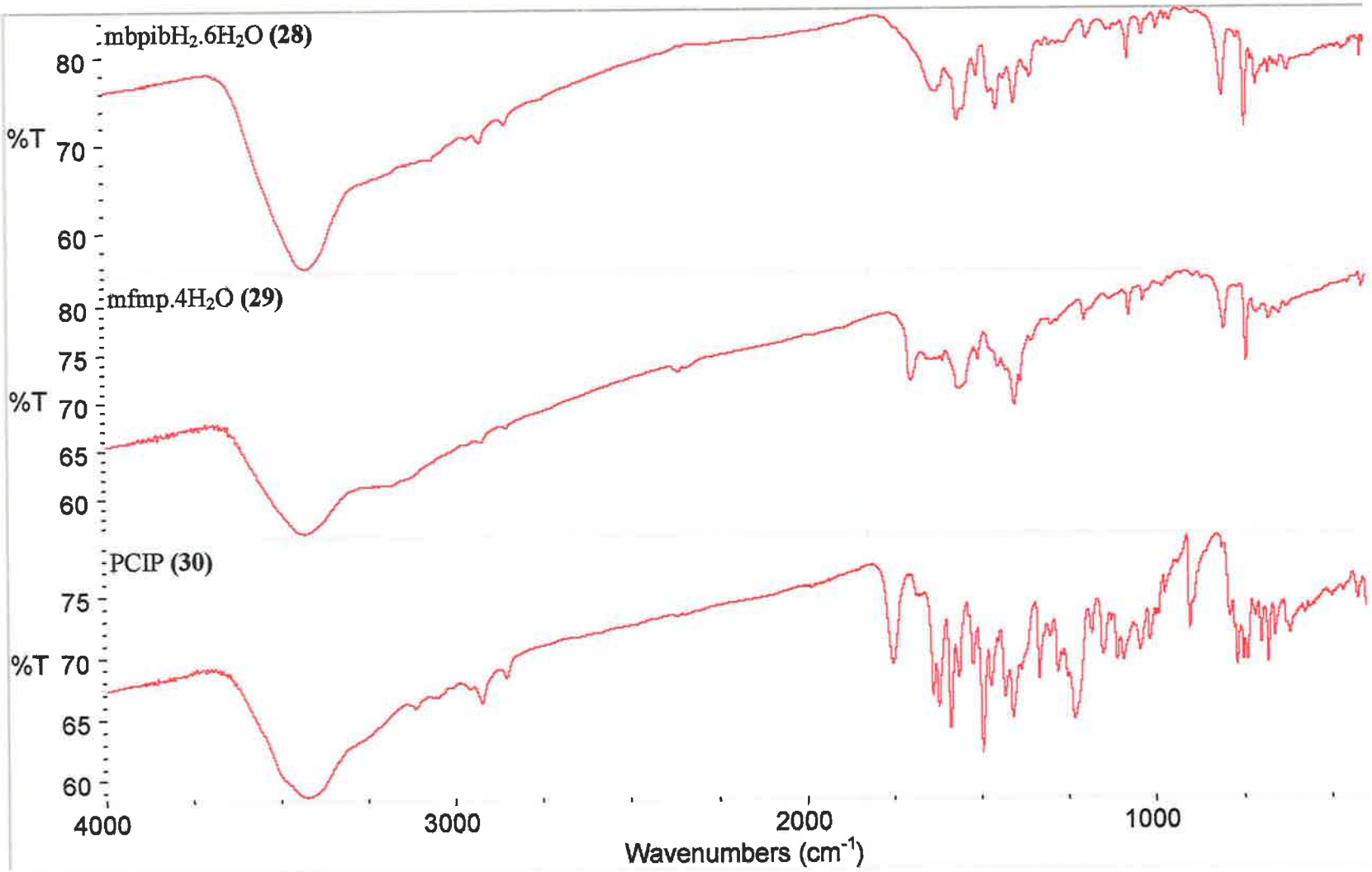
mbpibH2.6H2O (28)
%T
80
70
60
mfmp.4H2O (29)
%T
80
75
70
65
60
PCIP (30)
%T
75
70
65
60
4000
3000
2000
1000
Wavenumbers (cm-1)

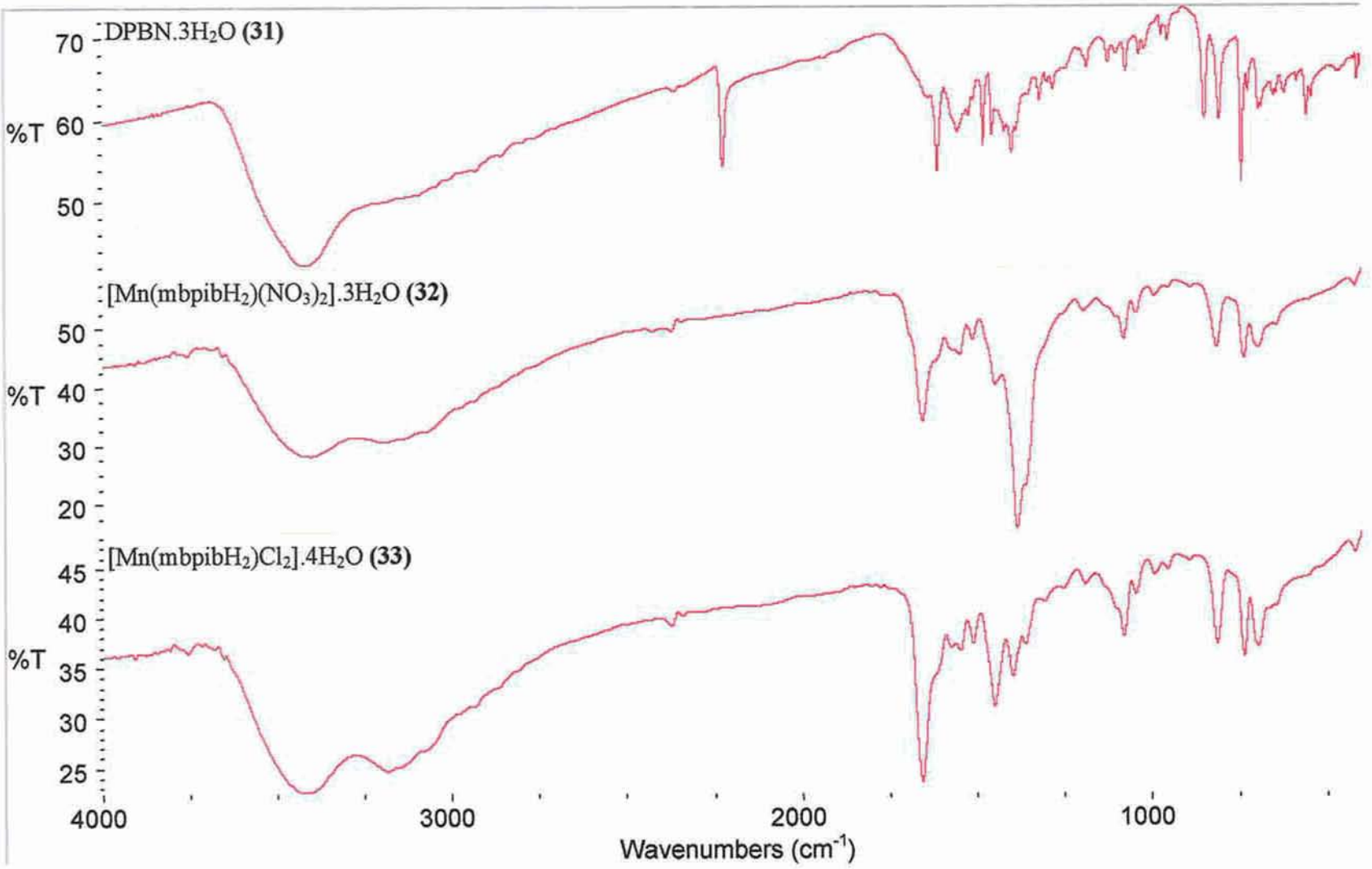
DPBN.3H2O (31)
%T
70
60
50
[Mn(mbpibH2)(NO3)2].3H2O (32)
%T
50
40
30
20
[Mn(mbpibH2)Cl2].4H2O (33)
%T
45
40
35
30
25
4000
3000
2000
1000
Wavenumbers (cm-1)

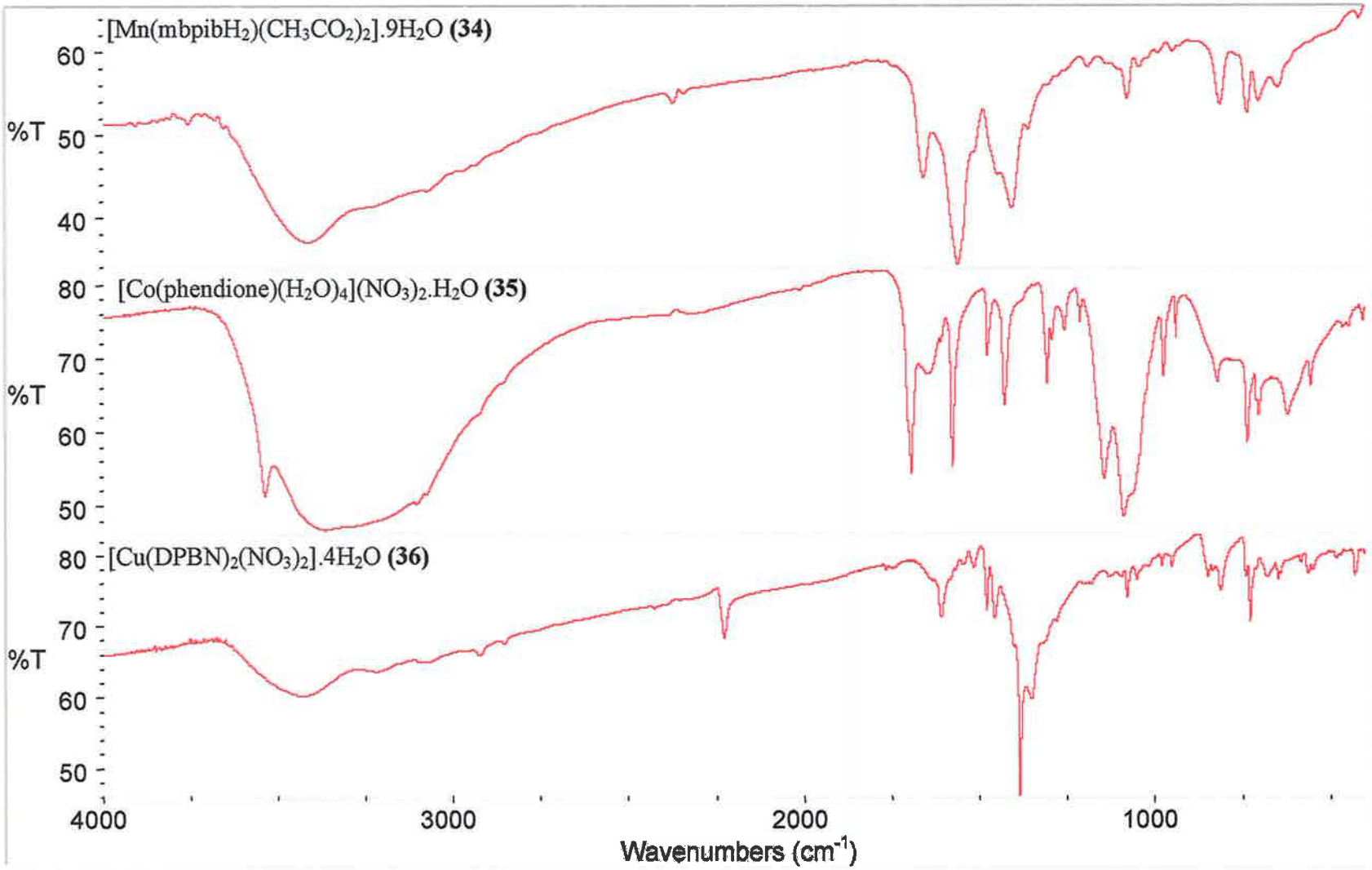
[Mn(mbpibH2)(CH3CO2)2].9H2O (34)
%T
60
50
40
[Co(phendione)(H2O)4](NO3)2.H2O (35)
%T
80
70
60
50
[Cu(DPBN)2(NO3)2].4H2O (36)
%T
80
70
60
50
4000
3000
2000
1000
Wavenumbers (cm-1)

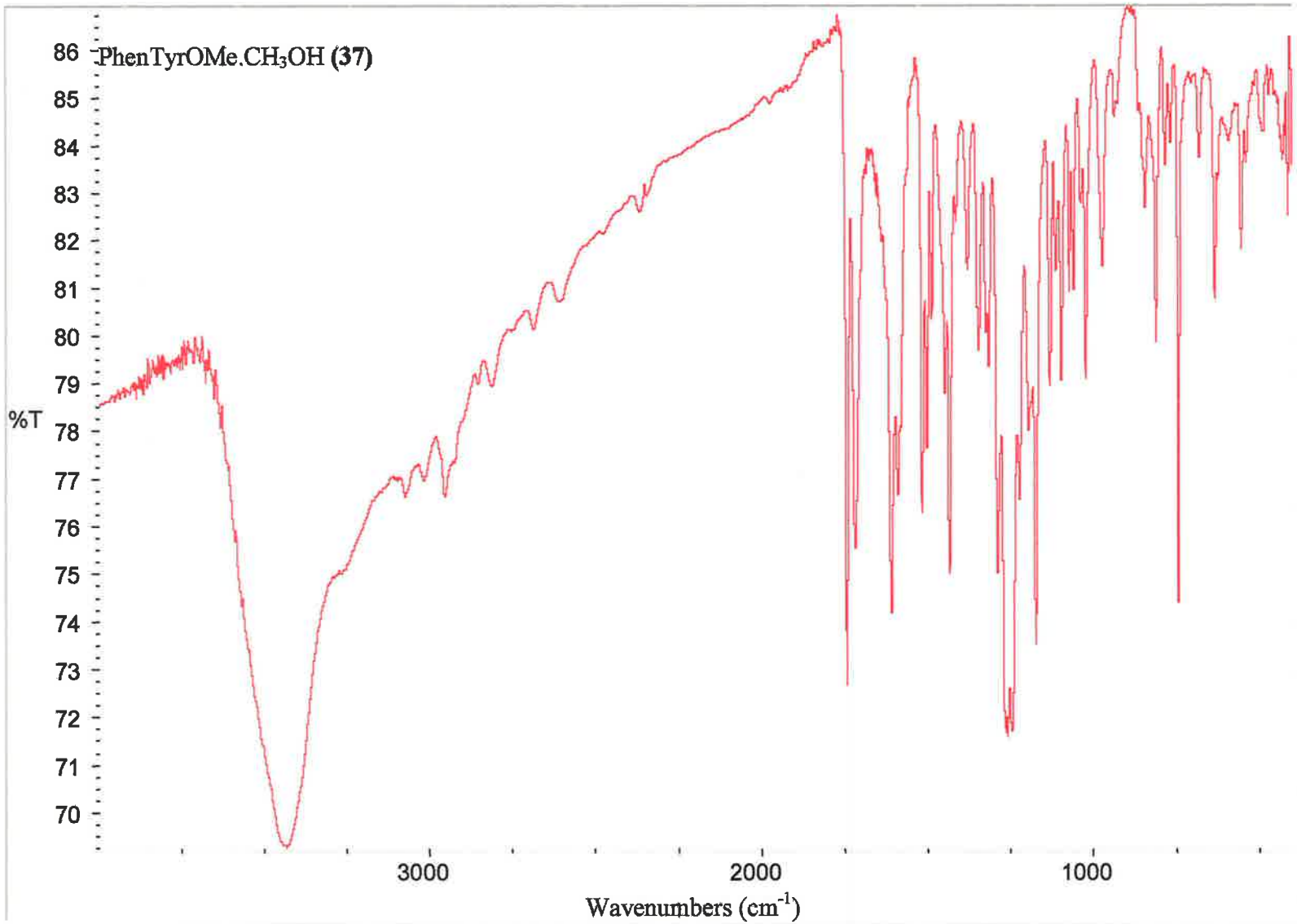
PhenTyrOMe.CH3OH (37)
86
85
84
83
82
81
80
79
%T
78
77
76
75
74
73
72
71
70
3000
2000
1000
Wavenumbers (cm-1)

APPENDIX 2 – ^{1}H NMR Spectra

Commercial Phendione

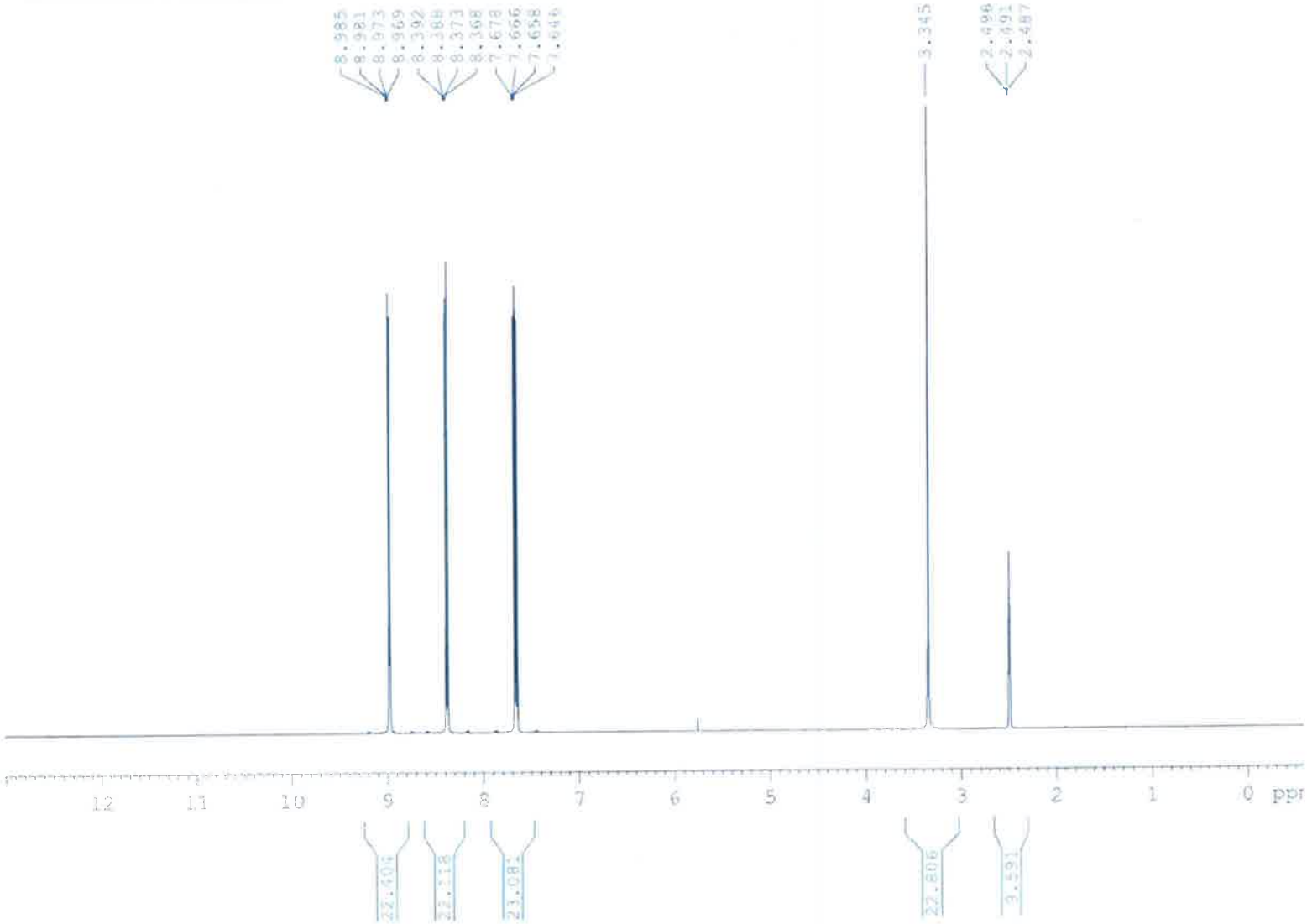

Phendione (1)

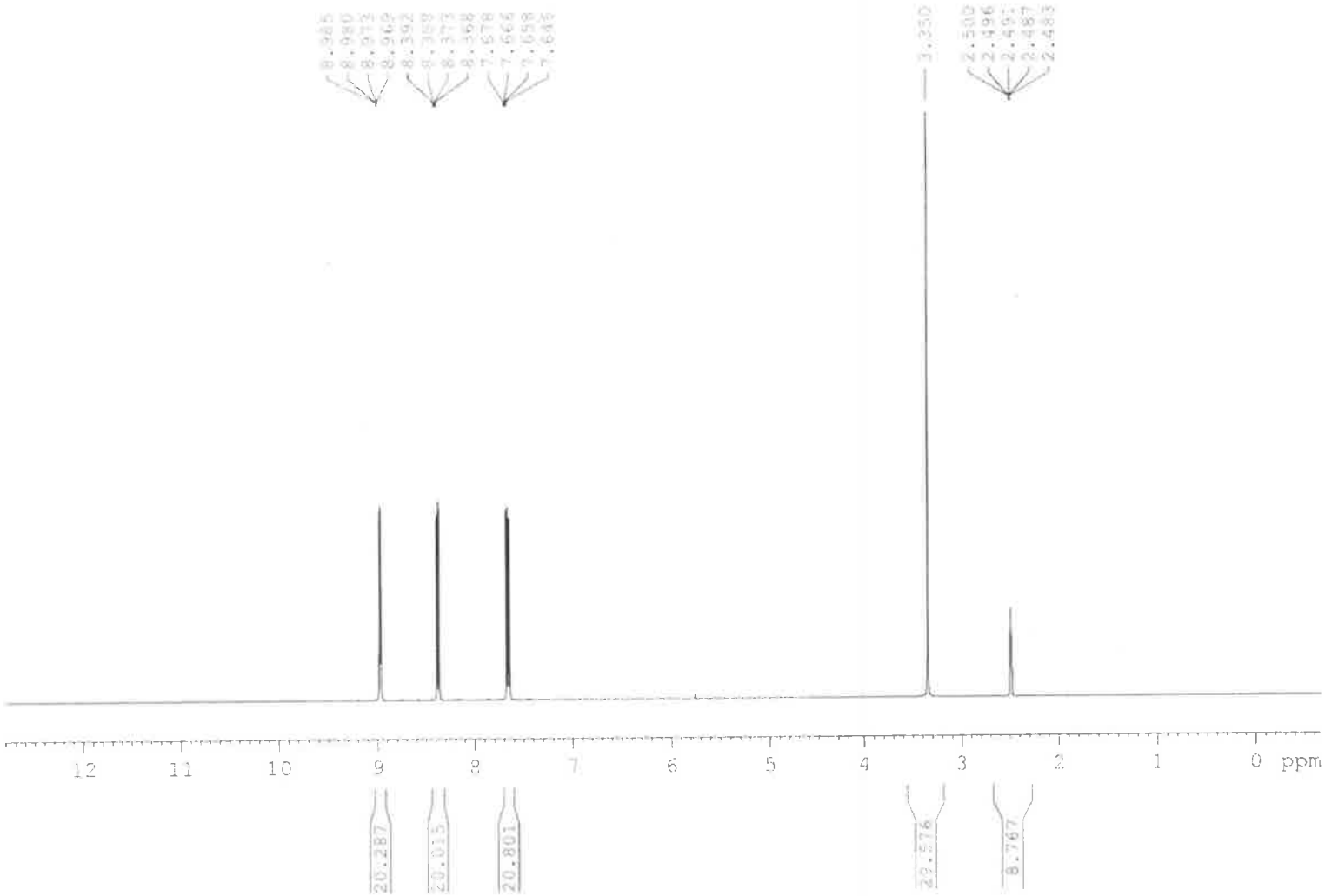
8.985
8.980
8.973
8.966
8.392
8.389
8.373
8.368
7.678
7.664
7.658
7.645
3.350
2.500
2.496
2.491
2.487
2.483
12
11
10
9
8
7
6
5
4
3
2
1
0 ppm
20.287
20.015
20.801
22.576
8.767

mbpibH_2.6H_2O (28)

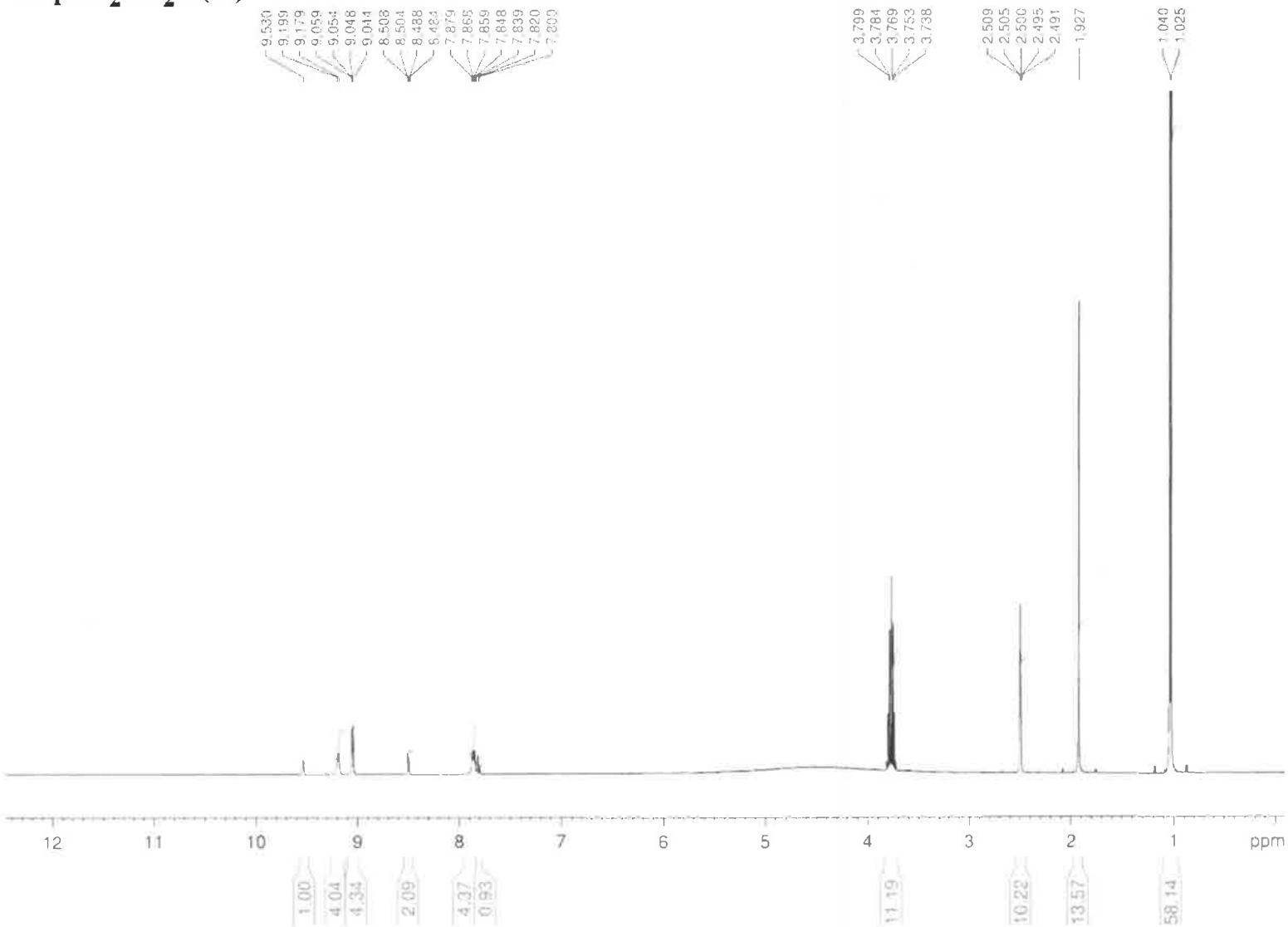

mfmp.4H_2O (29)

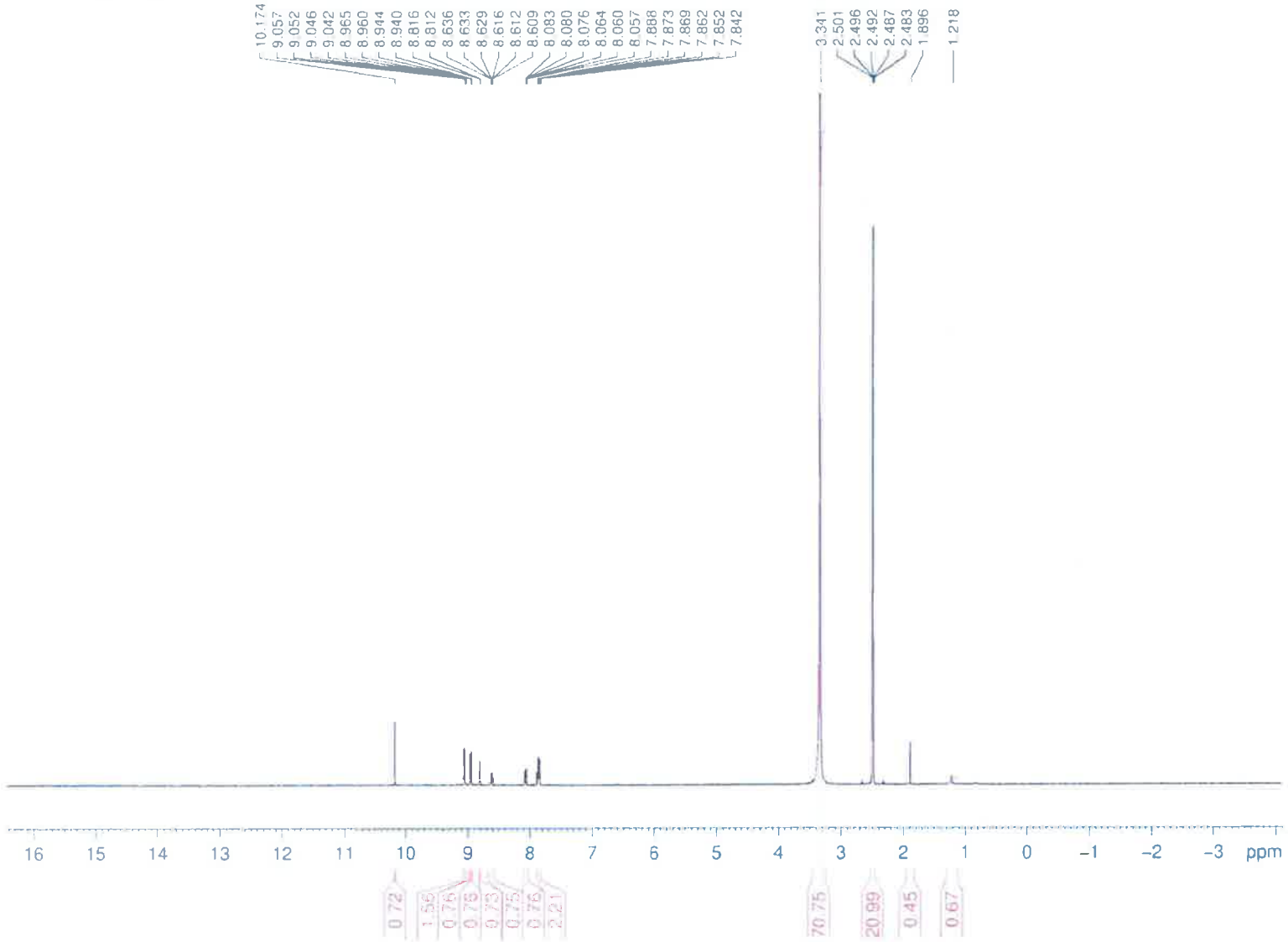
10.174
9.057
9.052
9.046
9.042
8.965
8.960
8.944
8.940
8.816
8.812
8.636
8.633
8.629
8.616
8.612
8.609
8.083
8.080
8.076
8.064
8.060
8.057
7.888
7.873
7.869
7.862
7.852
7.842
3.341
2.501
2.496
2.492
2.487
2.483
1.896
1.218
16 15 14 13 12 11 10 9 8 7 6 5 4 3 2 1 0 −1 −2 −3 ppm
0.72
1.56
0.76
0.76
0.73
0.75
0.76
2.21
70.75
20.99
0.45
0.67

PCIP (30)

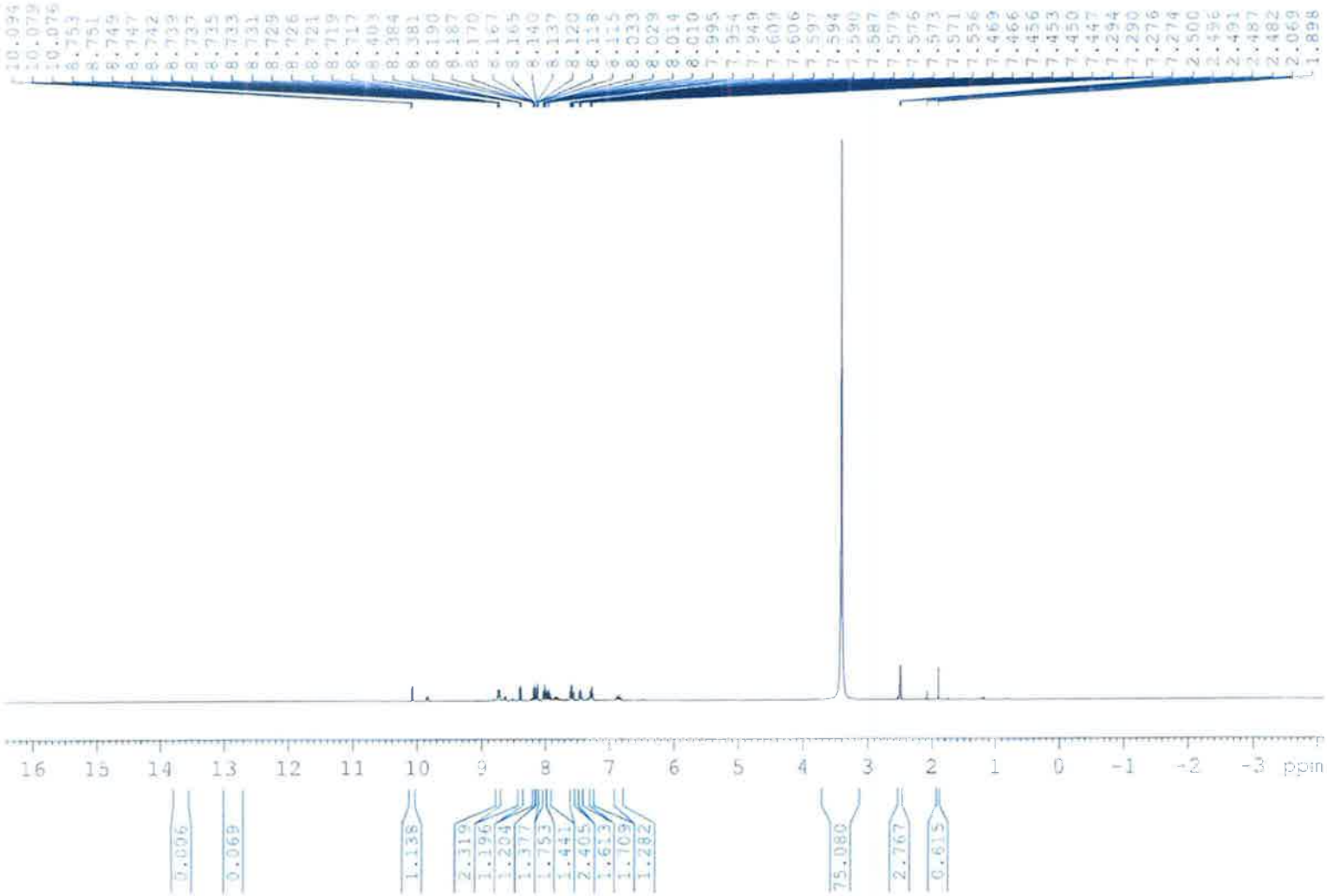
10.095
10.079
10.075
8.753
8.751
8.749
8.747
8.742
8.737
8.735
8.733
8.731
8.729
8.726
8.721
8.719
8.717
8.403
8.384
8.381
8.190
8.187
8.170
8.167
8.165
8.140
8.137
8.120
8.118
8.115
8.033
8.029
8.014
8.010
7.995
7.954
7.949
7.609
7.606
7.597
7.594
7.590
7.587
7.579
7.576
7.573
7.571
7.556
7.469
7.466
7.456
7.453
7.450
7.447
7.294
7.290
7.276
7.274
2.500
2.496
2.491
2.487
2.482
2.069
1.898
16 15 14 13 12 11 10 9 8 7 6 5 4 3 2 1 0 -1 -2 -3 ppm
0.006
0.069
1.138
2.319
1.196
1.204
1.377
1.753
1.441
2.405
1.613
1.709
1.282
75.080
2.767
0.615

DPBN.3H_2O (31)

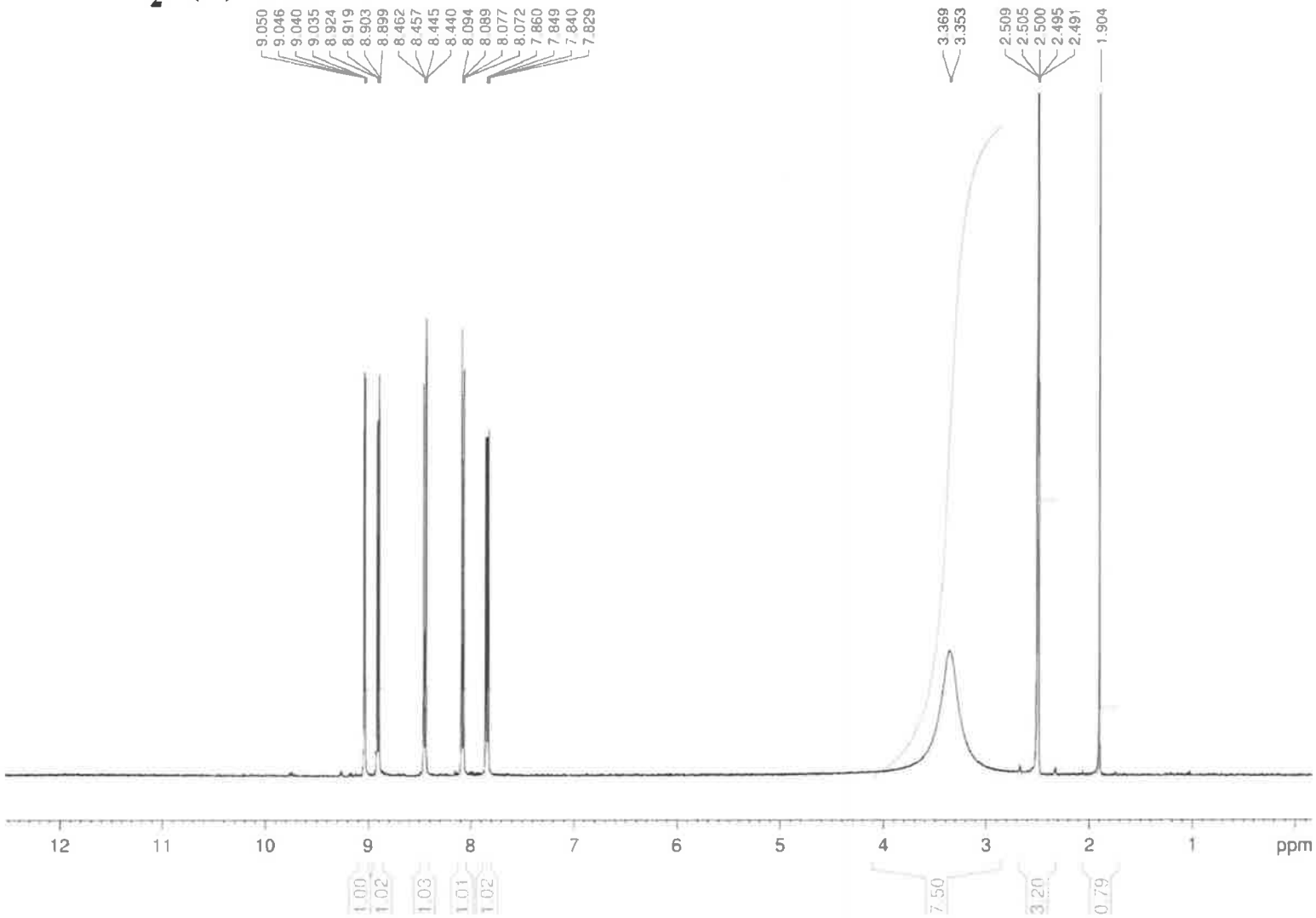
9.050
9.046
9.040
9.035
8.924
8.919
8.903
8.899
8.462
8.457
8.445
8.440
8.094
8.089
8.077
8.072
7.860
7.849
7.840
7.829
3.369
3.353
2.509
2.505
2.500
2.495
2.491
1.904
12
11
10
9
8
7
6
5
4
3
2
1
ppm
1.00
1.02
1.03
1.01
1.02
7.50
3.20
0.79

PhenTyrOMe.CH_3OH (37)

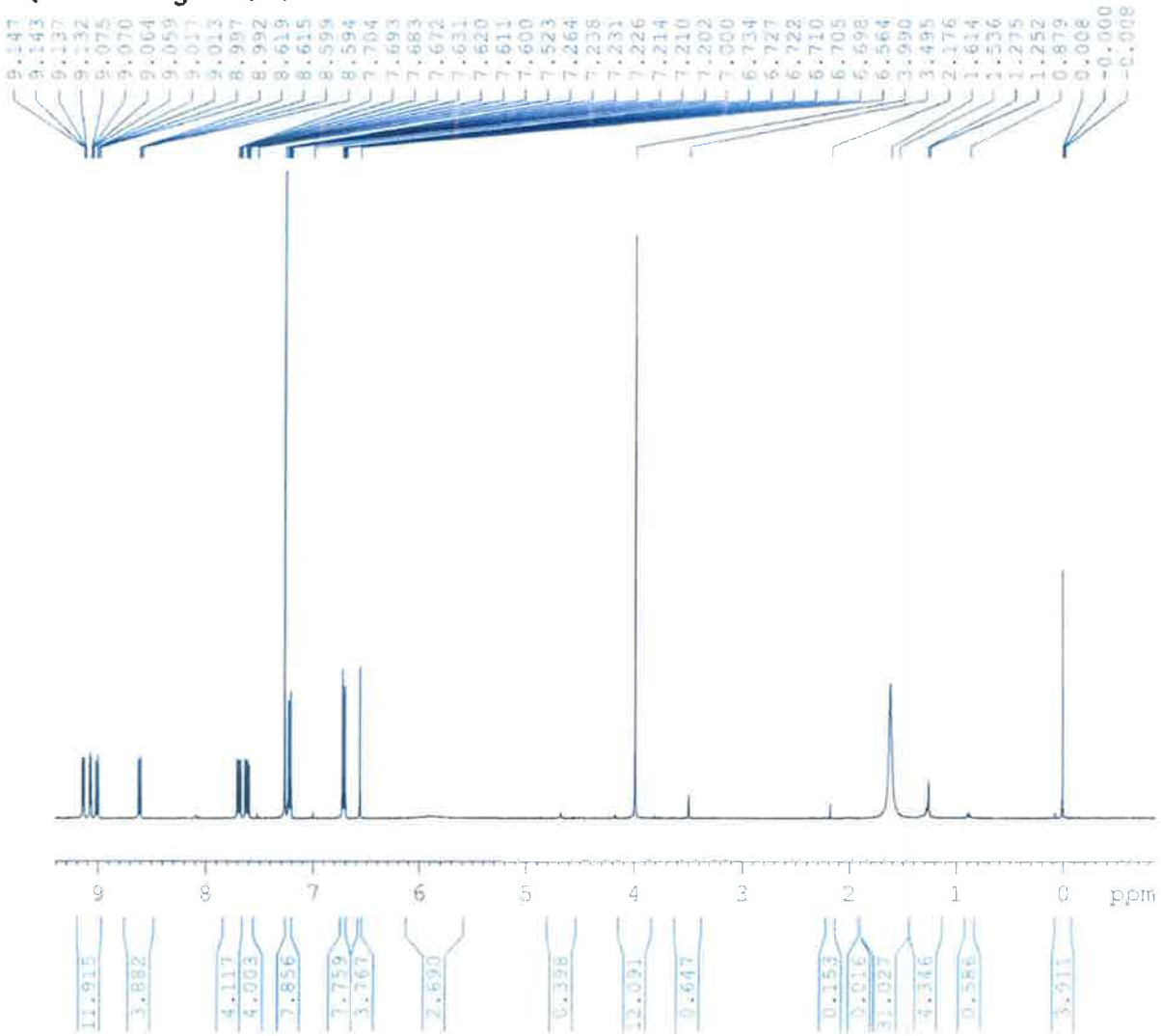

APPENDIX 3 – ^{13}C NMR Spectra

Phendione (1)

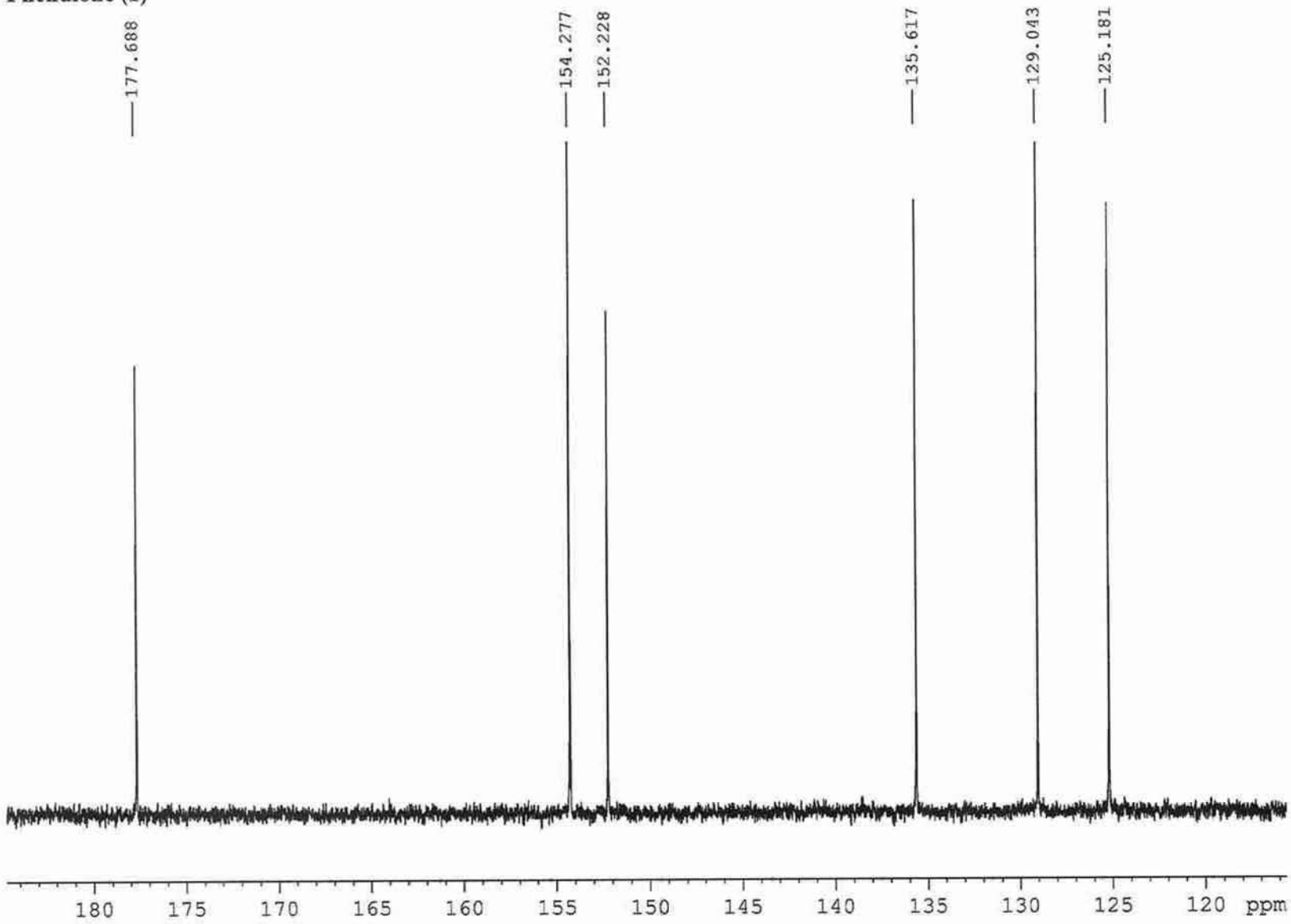
177.688
154.277
152.228
135.617
129.043
125.181
180
175
170
165
160
155
150
145
140
135
130
125
120
ppm

mfmp.4H_2O (29)

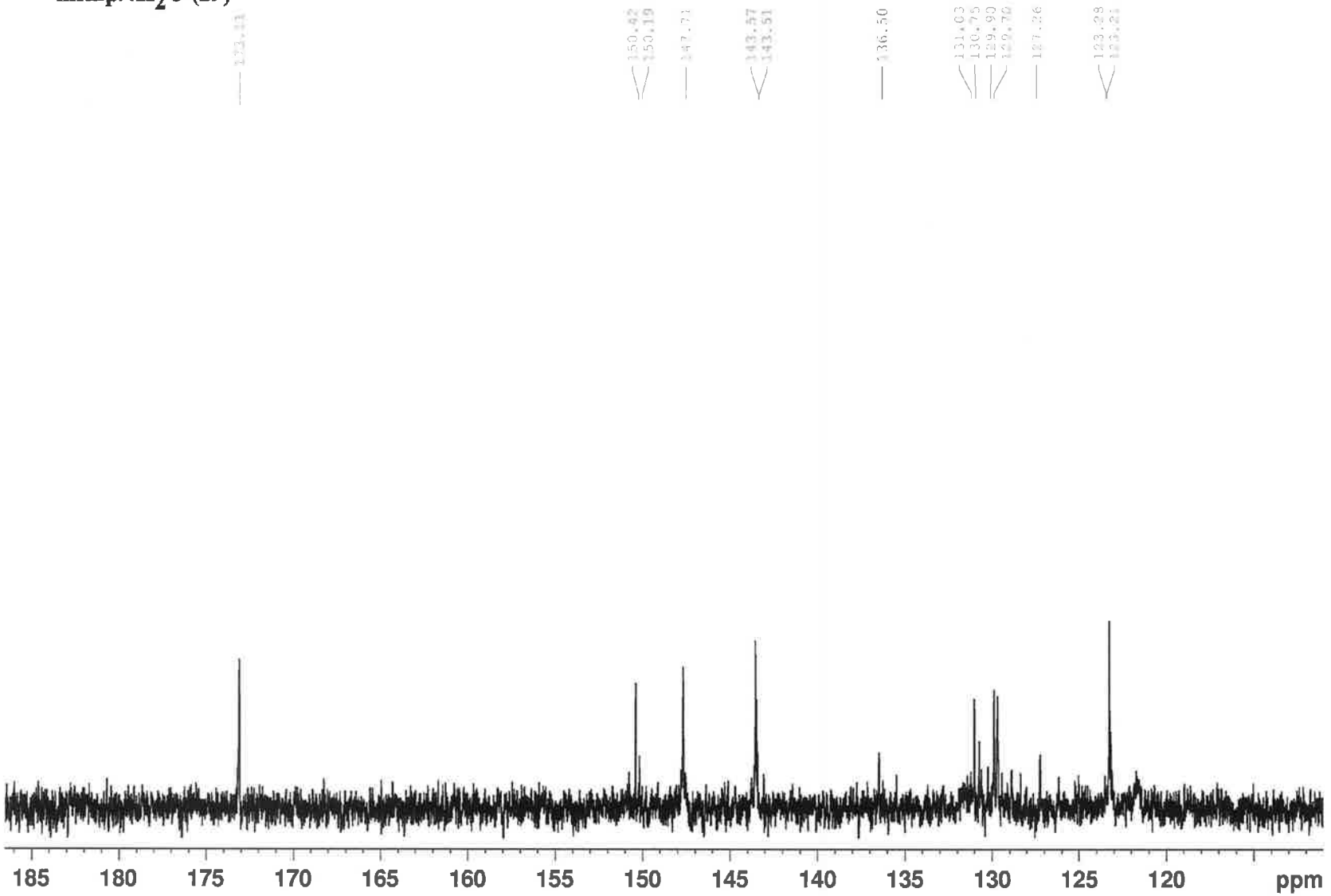
172.43
150.42
150.19
147.71
143.57
143.51
136.50
131.03
130.75
129.90
129.76
127.26
123.28
123.21
185
180
175
170
165
160
155
150
145
140
135
130
125
120
ppm

PCIP (30)

190
185
180
175
170
165
160
155
150
145
140
135
130
125
120
P
186.52
155.898
150.290
149.396
149.150
148.531
137.452
137.060
136.750
136.440
135.249
131.946
128.385
128.267
127.213
125.486
124.829
123.343
122.293
121.717
119.155
116.381